NADPH oxydase Nox4 : structure/fonction protéomique recombinante et approche immunologique

Leilei Zhang

UNIVERSITÉ DE GRENOBLE

THÈSE

Pour obtenir le grade de

DOCTEUR DE L'UNIVERSITÉ DE GRENOBLE

Spécialité : **Biologie cellulaire**

Arrêté ministériel : 7 août 2006

Présentée par

LEILEI ZHANG

Thèse dirigée par **Françoise MOREL**

préparée au sein du **Laboratoire d'Enzymologie**
dans **l'École Doctorale CHIMIE ET SCIENCES DU VIVANT**

NADPH oxydase Nox4: structure/fonction Protéomique recombinante et approche immunologique

Thèse soutenue publiquement le **30 Mai 2011**
devant le jury composé de :

Mme, Corinne, DUPUY
Fonction et lieu de la fonction, Rapporteur
Mr, Yves, GORIN
Fonction et lieu de la fonction, Rapporteur
Mr, Bernard, Lassegue
Fonction et lieu de la fonction, Membre
Mr, Bernard, LARDY
Fonction et lieu de la fonction, Membre
Mr, Christian, DROUET
Fonction et lieu de la fonction, Président
Mme, Françoise, MOREL
Fonction et lieu de la fonction, Membre

Remerciements

I would like to thank Pr. Françoise Morel, my dissertation advisor, for directing me through my Ph.D study. She spent a lot of time and energy on educating me, modifying the papers and the dissertation for me, helping me with my life in France. I am very grateful for having the opportunity to work with her and learn from her.

Special thanks go to the committee members Dr. Yves, Gorin, Dr. Bernard, Lassegue, Dr. Corinne, Dupuy, Dr. Christian, Drouet for serving on the committee and giving me good suggestions and comments on the dissertation.

I would like to thank Dr. Bernard Lardy, Dr. Chuong Nguyen, Dr. Marie-Hélène Paclet and sylvie Berthier for the encouragement and helpful advice through all of the technology challenges. They always give me a hand when I have difficulties and need help in daily life.

I thank Candice Trocme, Francis Rousset, Adam Baillet, Marie-claire Dagher for the help in learning the details of lab's life and French.

I thank all the members in the Laboratoire d'Enzymologie for everything. I do enjoy a memorial time staying with you guys in the past 3 years.

Thanks also go out to Alexei Grichine for the technique support in the use of confocal microscopy, TIRFM and to Pr. Algirdas J. Jesaitis for the phage display technique.

I am grateful to Prof. Guanxiang Qian and Prof. Shengfang Ge. They always give me a huge support and encouragement.

I am also thankful to Prof. Guy Vincendon for the help in scholarship application.

A special thanks to all my friends in China. And also friends in France, Samuel Degoul, Kelly Dilworth, Hai Huang, Rang Xu, Zhen Jiang, Yan Wang. They help me to adapt my life and study in France.

My very special thanks will also give to my parents Xudong Zhang and Chaofen Qian, my husband Aiping Ding. They use their broad mind and deep love to accept all my strengths and weaknesses. No matter what happens, They will always in there supportting me, encouraging me, helping me, and be my powerful support.

I appreciate the financial support from "the Region Rhône-Alpes, programme ARCUS", "the National Key Program for Basic Research of China (2010CB529902)", "the Science and Technology Commission of Shanghai (S30205, 06SR07110)", "the National Natural Science Foundation of China (30973663)", "L'Ambassade de France en Chine".

Finally, I would like to take the opportunity to thank everyone here.

FIGURES

TABLES

List of the abbreviations

AA: Arachidonic acid
AD: Activation domain
AIR: Autoinhibitory region
AFM: Atomic Force Microscopy
CGD: Chronic Granulomatous Disease
CDHD: Catalytic dehydrogenase domain
CMV: Cytomegalovirus
DAG: Diacylglycerol
DH: Dehydrogenase
DMEM: Dulbecco's Modification of Eagles Medium
DPI: Diphenyliodonium
EDTA: Ethylenediamine tetraacetic acid
ER: Endoplasmic reticulum
FAD: Flavin adenine dinucleotide
FNR: Ferredoxin NADP+ reductase
GFP: Green Fluorescent Protein
GSH/GSSG: Glutathione reduced/oxidized
HEK: Human embryonic kidney
HUVECs: Human umbilical endothelial cells
InsP3: Inositol 1,4,5-triphosphate
INT: Iodonitrotetrazolium
JNK: c-jun N-terminal kinase
LDL: Low density lipoproteins
MAPK: Mitogen activated protein kinase
MKP-1: MAPK phosphatase 1
NADPH: Nicotinamide adenine dinucleotide phosphate
NO: Nitric Oxide
8-OHdG: 8-hydroy-deoxyguanosine
PA: Phosphatidic acid
PAI-1: Plasminogen activator inhibitor 1
PB1: Phox and Bem 1
PC: Phosphatidylcholine
PhosR: Phosphorylation region
PKC: Protein kinase C
PLA2: Phospholipase A2
PLC: Phospholipase C
PLD: Phospholipase D
PMA: Phorbol-myristate acetate
Poldip2: Polymerase delta-interacting protein 2
PRR: Proline rich region
PX: Phagocyte oxidase (Phox)
REFBD: Regulatory EF-hand-binding domain

ROS: Reactive oxygen species
RTS: Rapid translation system
SDS: Sodium dodecyl sulfate
SH3: Src homology 3
SMC: Smooth muscle cells
SOD: Superoxide dismutase
TGF β : Transforming growth factor beta
TIRF: Total Internal Reflection Fluorescence
TLCK: N-alpha-p-tosyl-L-lysine chloromethyl ketone
TPR: Tetratricopeptide repeat
Ub: Ubiquitin
VEGF: Vascular endothelial growth factor

Summary in English

NADPH oxidase, Nox4, belongs to the Nox family which could generate reactive oxygen species by transferring an electron to molecular oxygen. Despite its wide distribution in tissues, Nox4 is still poorly understood. Unlike the other Noxes, Nox4 shows some unique characters: the constitutive activity, H_2O_2 formation. Nox4 involved ROS has been proposed to be implicated in several pathologies. Thus, to study the structure/function and the regulation of the activity of Nox4 will provide new ideas and new drug targets for the effective prevention and treatment of clinical diseases related with ROS.

To know more about Nox4, in this study, 5 novel monoclonal antibodies were raised against a truncated recombinant protein (AA: 206-578) of Nox4. The specificity of 3 mAbs (8E9, 5F9, 6B11) was confirmed by western blot analysis in HEK293 transfected cells and human kidney cortex. In FACS studies, only mAb 8E9 could react with intact tet-induced T-REx^{TM} Nox4 cells. Immunofluorescence confocal microscopy showed that Nox4 localized not only in the perinuclear and endoplasmic reticulum regions but also at the plasma membrane of the cells which was further confirmed by TIRF-microscopy. An interesting phenomena is that mAb 5F9 failed to detect Nox4 at the plasma membrane. Epitope determination showed that mAb 8E9 recognizes a region on the last extracellular loop of Nox4 (^{222}H-E^{241}), while mAb 6B11 (^{389}S-P^{416}) and 5F9 (^{392}D-F^{398}) are directed to its cytosolic tail. Cell-free oxidase assays showed a moderate but significant inhibition of constitutive Nox4 activity by mAb 5F9 and 6B11.

To study the protein region which is responsible for the unique ability of Nox4 of releasing H_2O_2 rather than O_2^-, chimeric proteins and mutants were used. E-loop of Nox4 is 28 amino acid longer than that of Nox1 or Nox2. Deletion of E-loop amino acids only present in Nox4 or change of the two cysteines in the E-loop switch Nox4 from H_2O_2 to O_2^- generation. In the presence of a NO donor, the O_2^--producing Nox4 mutants, but not widetype Nox4, generated peroxynitrite, excluding artifacts of the detection systems as the apparent origin of O_2^-. A second approach was used to confirm the responsibility of E-loop for the H_2O_2 formation. In Cos7 cells, which exhibit some plasma membrane expression of Nox4, addition of the mAb 8E9 decreased H_2O_2 production but increased O_2^- formation. Unlike Nox1 or Nox2, the E-loop of Nox4 contains a highly conserved histidine H222. Mutation of H222 also switched Nox4 from H_2O_2 to O_2^- formation. The structure of the E-loop might hinder O_2^- egress and/or provide a source for protons to accelerate dismutation to form H_2O_2.

Two bacterial protein expression approaches (in vitro RTS and bacterial induction) were used to produce Nox4 cytosolic tail for characterizing the electronic transfer property of Nox4. The presence of rare codons (^{1363}AGA AGA CUA^{1371}) and high level of hydrophobicity affects the production of soluble and active recombinant Nox4Aqc and Nox4Bqc. After optimization of the conditions, soluble and active recombinant proteins were obtained by RTS or by bacteria induction. The soluble proteins were produced in large scale, purified onto affinity chromatography and were tested for the diaphorase activity (INT and cytochrome c). Results showed that electronic acceptor cytochrome c gives a higher rate than INT. Nox4Aqc produced a lower specific activity by a cell-based system compared to the protein synthesized in cell-free technology. This activity is not stimulated by the addition of cytosolic factors.

A new method, topological determination by ubiquitin fusion assay (TDUFA), was used to investigate the topology of Nox4 and p22phox. ubGFP fusion proteins are used as tools to obtain details of membrane protein topology. This method was first validated by using two membrane proteins with known topology and then should get more topology information of Nox4 and p22phox further.

Key words: Nox4, monoclonal antibodies, subcellular localization, H_2O_2, diaphorase activity, topology

Part 1 Introduction

I. Reactive Oxygen Species

1 Introduction

Reactive oxygen species (ROS) is a generic collective term indicating a number of active and reactive partially reduced O_2 metabolites, including superoxide ($O_2^{\cdot -}$), hydroxyl ($^{\cdot}OH$), peroxyl ($RO_2^{\cdot}$), alkoxyl ($RO^{\cdot}$) and certain nonradicals that are either oxidizing agents and/or are easily converted into radicals, such as hypochlorous acid (HOCl), ozone (O_3), singlet oxygen ($^1O_2$), and hydrogen peroxide (H_2O_2) (Genestra, 2007). ROS generation is generally a cascade of reactions that starts with the production of superoxide. Two molecules of superoxide can react to generate hydrogen peroxide (H_2O_2) in a reaction known as dismutation, which is accelerated by the enzyme superoxide dismutase. In the presence of iron, superoxide and H_2O_2 react to generate hydroxyl radicals. In addition to superoxide, H_2O_2 and hydroxyl radical, other reactive oxygen species (ROS) occur in biological systems. In inflamed areas, these include hypochlorous acid (HOCl), formed in neutrophils from H_2O_2 and chloride by the phagocyte enzyme myeloperoxidase (MPO); singlet oxygen, which might be formed from oxygen in areas of inflammation through the action of Phox and MPO-catalysed oxidation of halide ions (Kanofsky, 1989); and ozone, which can be generated from singlet oxygen by antibody molecules (Nathan, 2002; Wentworth *et al.*, 2002) (Fig. 1).

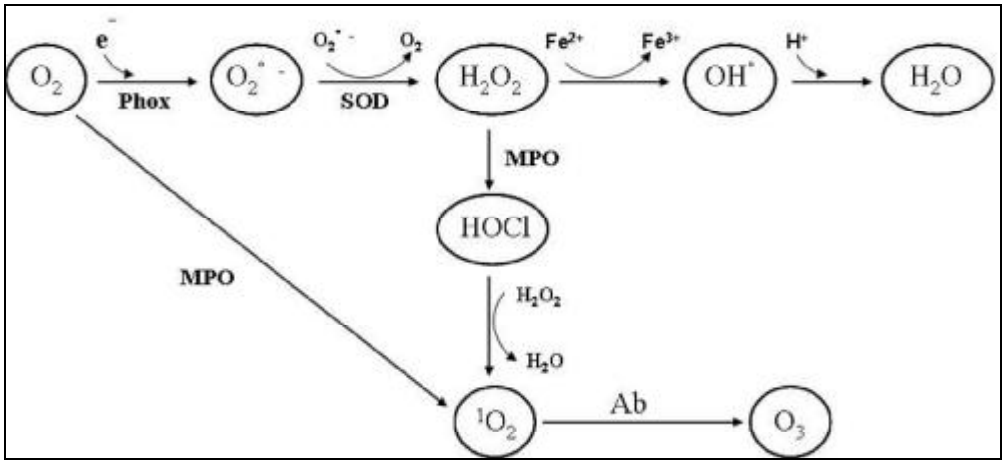

Figure 1. Reactive Oxygen Species. *Superoxide is generated from various sources, which include the NADPH oxidase enzymes such as the phagocyte Nox (Phox).*

ROS react non-specifically and rapidly with a large number of biomolecules, including DNA, proteins,

lipids, carbohydrates, and nucleic acids. Various investigations have elucidated roles for ROS in causing molecular damage such as DNA mutations, lipid peroxidation and protein oxidations. As a result of these investigations, ROS has historically been viewed as a harmful but unavoidable consequence of an aerobic lifestyle as major contributors to damage in biological organisms. In the first place, free radicals are present in living cells which was demonstrated in vivo by a paramagnetic resonance absorption method (Commoner ***et al.***, 1954). In 1956, Harmann observed that aging and degenerative diseases associated with it were attributed basically to the deleterious side attacks of free radicals on cell constituents and on the connective tissues (Harman, 1956). Since then, the free radical theory of aging has increasingly and widely been accepted (Beckman ***et al.***, 1998). However, it is better not to think of ROS as "bad". They are generated in a number of reactions essential to life, for example, phagocytic cells generate radicals to kill invading pathogens. Also, there are a large number of evidences indicating that oxygen radicals are involved in intercellular and intracellular signaling.

2 Sources of the Generation of ROS

There are many sources of the generation of ROS. ROS can be produced as a byproduct by mitochondria, peroxisomes, cytochrome P-450, lipoxygenase, xanthine oxidoreductase, etc (Gottlieb, 2003; Harrison, 2004; Schrader ***et al.***, 2004; Balaban ***et al.***, 2005; Gonzalez, 2005). However, the NADPH oxidase was the only enzyme whose primary function is to produce ROS. In living cells, without any doubt, the most relevant are those described as following (Novo et al., 2008).

2.1 Mitochondria

Mitochondrial electron generates superoxide as an inevitable by-product and primary ROS at two complexes, complexes I and III (Genova ***et al.***, 2003; Brand ***et al.***, 2004). Approximately 5% of electrons 'flowing' through the electron transport chain can be delivered to form $O_2^{\circ-}$ at the levels of complex I (NADPH/ubiquinone oxidoreductase) and complex III (ubiquinol/cytochrome c oxidoreductase). $O_2^{\circ-}$ is then usually converted by mitochondrial SOD into H_2O_2, which can cross mitochondrial membranes to reach the cytoplasm (Cadenas ***et al.***, 2000) (Figure 2). In mitochondria, Complex I releases superoxide into the matrix (also at hypoxia when superoxide is produced due to the reverse electron transport), whereas Complex III releases superoxide to both sides of the inner membrane. The sites of Complex I generating $O_2^{\circ-}$ are less precisely known (Raha ***et al.***, 2000; Brand ***et al.***, 2004). The lack of detailed knowledge is due to the great

complexity of this complex in mammalian mitochondria. The Complex III contribution to $O_2^{\cdot -}$ generation by autooxidation of the ubisemiquinone anion radical ($UQ^{\cdot -}$) is best understood. Within Complex III, the transfer of electrons from ubiquinol (UQH2) to cytochrome c is catalyzed in the so-called "Q cycle" (Jezek *et al.*, 2005).

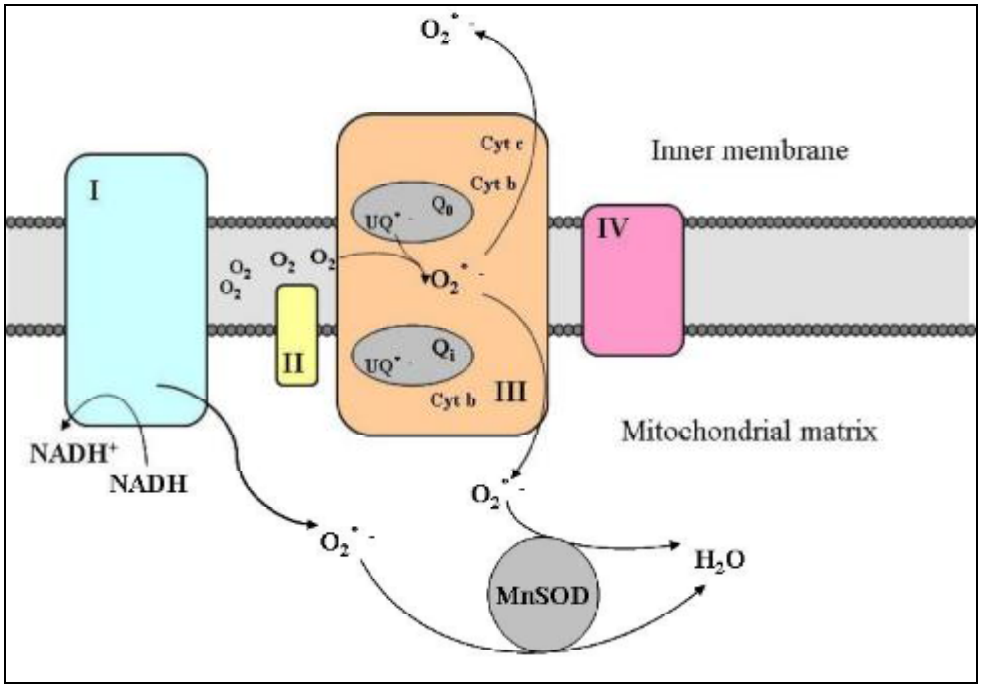

Figure 2. Mitochondria as Source of Reactive Oxygen Species. *Major mitochondrial ROS sources and ROS fluxes from mitochondria.Mitochondrial electron transport generates superoxide as an inevitable by-product and primary ROS at two complexes, Complexes I and III.Complex I releases superoxide into the matrix, whereas Complex III releases superoxide to both sides of the inner membrane.*

2.2 5-Lipoxygenase

5-Lipoxygenase (5-LOX) is a mixed function oxidase involved in the synthesis of leukotrienes from arachidonic acid in response to essentially the same stimuli that are able to stimulate Nox, particularly growth factors and cytokines. The latter mediators lead to membrane ruffling and the generation of superoxide, and then H_2O_2, through the intervention of the small GTPase Rac1 and a SOD isoform (Thannickal *et al.*, 2000; Droge, 2002; Chiarugi *et al.*, 2003; Soberman, 2003; Chiarugi *et al.*, 2007; D'Autreaux *et al.*, 2007) (Figure 3).

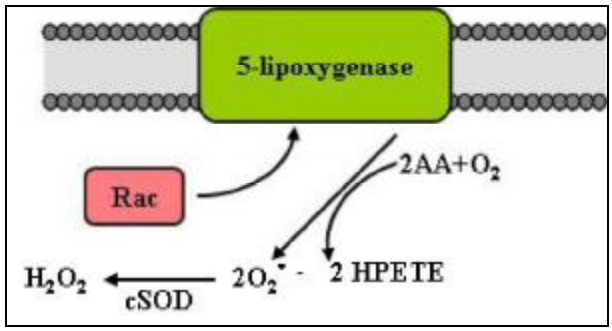

Figure 3. 5-Lipoxygenase as Source of Reactive Oxygen Species. *5-HPETE, acide 5-hydroperoxy-6-trans-8,11,14-cis-eicosatetraenoique.*

2.3 NADPH oxidase

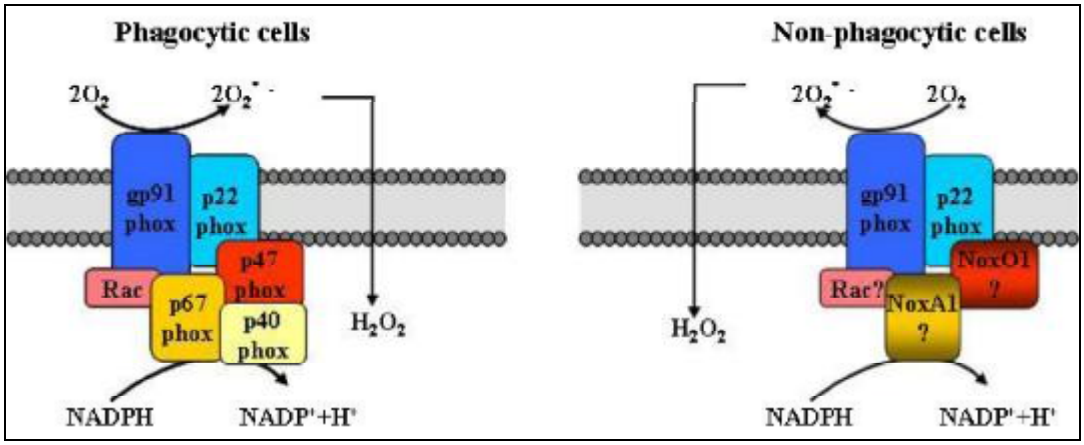

Figure 4. NADPH Oxidase as Source of Reactive Oxygen Species. *The phagocyte oxidase is agonist-dependent, exhibiting no detectable constitutive activity, and transfers electrons and consumes oxygen nearly instantaneously when stimulated. The regulation of its activity relies on p47phox, p67phox, p40phox and Rac. Regulation of other Nox family members in non-phagocytic cells is different, depending on the requirement of p22phox, cytosolic cofactors, the presence of EF-hands, and dependence on calcium. (see detail in 3.3)*

The phagocyte NADPH oxidase was the first identified example of a system that generates ROS not as a byproduct, but rather as the primary function of the enzyme system. The discovery of other members of the Nox family of NADPH oxidases demonstrated that enzymes with the primary function of ROS generation are not limited to phagocytes (Figure 4). Among the members of this family, gp91phox is best characterized. It is functional as an assembled complex following a stimulus. The complex includes a catalytic core (gp91phox and p22phox) and cytosolic regulatory factors (p40phox, p47phox, p67phox and Rac). The enzymes NADPH oxidase (Nox) and dual oxidase (Duox) are present in both professional phagocytic cells (macrophages, neutrophils and eosinophils) and non-phagocytic cells. They generate ROS in a regulated manner, producing

reactive oxygen in various cells and tissues in reponse to growth factors, cytokines and calcium signals. They play a crucial role in different diseases (Babior, 1999; Vignais, 2002; Lambeth, 2007).

2.3.1. Activation of the Phagocyte NADPH Oxidase (Morel et al., 1991)

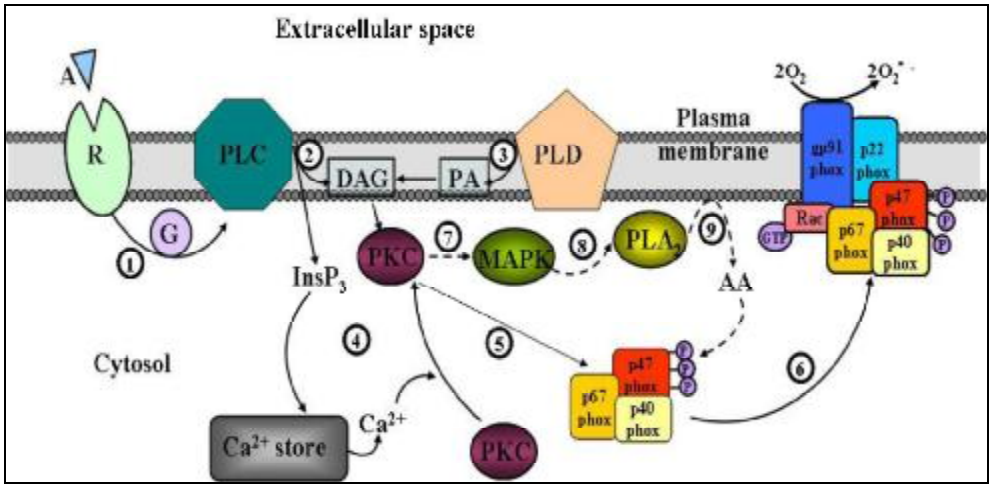

Figure 5. Signaling Pathway to Phagocyte NADPH Oxidase Activation. *A, agonists; R, receptors; G, G protein; PLC, phospholipase C; DAG, diacylglycerol; PA, phosphatidic acid; PLD, phospholipase D; PKC, protein kinase C; $InsP_3$, inositol 1,4,5-triphosphate; MAPK, mitogen activated protein kinase; PLA_2, phospholipase A_2, AA, arachidonic acid; P, phosphate. See text for detail explaination (2.3.1)*

Most studies on NADPH oxidase and the mechanism of its activation have been performed with neutrophils, which represent the most abundant cell type amongst the so-call professional phagocytes. There are several steps in the signaling pathway to oxidase activation in neutrophils (Figure 5). Upon binding of different agonists to specific receptors, agonists of the respiratory burst stimulate a phosphatidylinositol-4,5-bis phosphate-($PtdInsP_2$)-specific phospholipase C through a pertussis-toxin-sensitive G protein 1). Breakdown of $PtdInsP_2$ results in the rapid generation of diacylglycerol (DAG) and $InsP_3$, which are considered as second messengers 2). In addition to the phospholipase C signaling pathway, Hydrolysis of activated phospholipase D can produce phosphatidic acid, which is further degraded to diacylglycerol by a phosphatidic acid hydrolase 3). DAG can directly activate protein kinase C (PKC) while $InsP_3$ indirectly activates PKC by binding to Ca^{2+} stores to induce the release of Ca^{2+} to the cytosol 4). Activated PKC catalyses the phosphorylation of specific cytosolic proteins including p47phox 5), which is translocated to the membrane and there, interacts with the cytochrome b component of the oxidase 6). Activated PKC also can initiate a signaling cascade that results in the activation of MAPK 7). MAPK

phosphorylates phospholipase A_2 8). The effect of phospholipase A_2 is directed towards membrane phospholipids, it can release free fatty acids and most particularly arachidonic acid 9) which can interact with p47phox and activate oxidase. All these phenomena led to the activation of NADPH oxidase complex and the formation of superoxide ions.

II. A Historical Overview of ROS-Generating NADPH Oxidases (Bedard *et al.*, 2007)

Before the NADPH oxidase was identified, a respiratory burst by cells had already been described. The first description of a so-called respiratory burst dates back to 1908, when fertilization in sea urchin eggs was studied (Warburg, 1908). They found that a respiratory burst occurred after the fusion of spermatocytes with the egg. Then the "extra respiration of phagocytosis" was first described in 1932 (Baldridge *et al.*, 1932). They noticed that neutrophils demonstrated a dramatic increase in oxygen uptake when phagocytosing bacteria. It was assumed for many years that this "respiratory burst" was a response of the cell's mitochondria to provide the extra energy required to engulf the particles. It was only when the respiratory burst was shown to be insensitive to classic inhibitors of mitochondrial oxidative metabolism such as cyanide and azide that the unusual nature of this process was realized (Sbarra *et al.*, 1959). They demonstrated that the phagocyte respiratory burst was an energy-requiring process that depended on glucose metabolism. In 1961, Iyer et al. showed that the phagocyte respiratory burst results in the generation of hydrogen peroxide (Iyer *et al.*, 1961). There has been some controversy over the substrate specificity of this enzyme system, NADPH or NADH. In 1964, Rossi and Zatti correctly proposed that an NADPH oxidase was responsible for the respiratory burst (Rossi *et al.*, 1964). In 1967, it was found to be essential for the efficient killing of microbes that were adequately engulfed, but not killed, in the absence of oxygen (Selvaraj *et al.*, 1967). It gave a pointer as to the possible role of the respiratory burst. In 1970, Klebanoff found that azid and cyanide inhibit the microbicidal activity of myeloperoxidase and of intact normal leukocytes, but they have little or no effect on peroxidase-negative leukocytes. This demonstrated a contribution of myeloperoxidase to the respiratory burst-dependent antimicrobial activity of phagocytes (Klebanoff, 1970). In 1973, the circumstances under which O_2^- is produced in leukocytes suggest that superoxide as well as H_2O_2 may participate in bacterial killing. Superoxide instead of hydrogen peroxide was the initial product of the respiratory burst oxidase (Babior *et al.*, 1973).

Another important line of study that led to the discovery of the phagocyte NADPH oxidase came from clinical research. Chronic granulomatous disease (CGD) was first described in 1957 (Berendes *et al.*, 1957), but was not well-characterized until 1959 (Bridges *et al.*, 1959), when it was initially termed fatal granulomatous disease of childhood. In 1957, Berendes et al. recognized a new and relatively rare syndrome in young boys who suffered from recurrent pyogenic infections that was accompanied with granulomatous reaction, lymphadenopathy, and hypergammaglobulinemia. It is now simply referred to as CGD. Although originally thought to be only an X-linked disease that appeared exclusively in males, its recognition in girls in 1968 led to the determination of autosomal recessive forms as well (Azimi *et al.*, 1968). It was recognized that the respiratory burst was absent in the phagocytes of CGD patients. showed that diminished bactericidal capacity was a characteristic of CGD phagocytes, although they demonstrated nearly normal phagocytic capacity, such as chemotaxis, phagocytosis, and degranulation (Quie *et al.*, 1967).

Further characterization of ROS generation by phagocytes revealed that this enzyme system *1)* produced superoxide and its downstream metabolite hydrogen peroxide; *2)* was insensitive to cyanide, distinguishing it from mitochondria and myeloperoxidase; *3)* was present in phagocytes from MPO-deficient patients, but absent in those of CGD patient; and *4)* was selective for NADPH over NADH (Babior *et al.*, 1975).

A great deal of frustration could have been avoided if the observation in the early 1960s of a b-type cytochrome in neutrophils had been more widely recognized (Hattori, 1961; Shinagawa *et al.*, 1966). Until 1978 there was a breakthrough in the identification of proteins responsible for ROS production in phagocytes. The b-type cytochrome was rediscovered in human neutrophils and shown to be missing in the commonest (X-linked) form of CGD patients (Segal *et al.*, 1978; Segal *et al.*, 1978). When it was initially purified (Harper *et al.*, 1984), only a single protein that ran on SDS gels with a molecular mass of about 60-100 kDa (because of its heavy glycosylation (Harper *et al.*, 1985)) co-purified with the haem. This protein was initially called cytochrome b558 and its gene, commonly referred to as gp91phox, was found by positional cloning and shown to be abnormal in patients with X-GCD (Royer-Pokora *et al.*, 1986; Teahan *et al.*, 1987). In the novel Nox terminology, gp91phox is called Nox2.

However, it was rapidly understood that Nox2 was not the only component of the phagocyte enzyme. First, the cytochrome was shown to be a heterodimer, when a 22-kDa protein co-purified with the haem and the larger protein. Both subunits were shown to be missing in X-CGD (Segal, 1987; Parkos *et al.*, 1988). The smaller one was then called p22phox. Then the development of a cell-free system allowed activation of the phagocyte NADPH oxidase using purified cytosol and membrane fractions (Heyneman *et al.*, 1984; Bromberg

et al., 1985). This system provided the tools to discover the cytosolic subunits p47phox and p67phox (Nunoi *et al.*, 1988; Volpp *et al.*, 1988) and to define the roles of the small GTP-binding proteins Rac1 and Rac2 (Knaus *et al.*, 1991).

Development of more sensitive analytical systems for ROS detection revealed that some physiological and pathophysiological events in non-phagocytic cells were associated with ROS generation, although the subcellular source of oxidants remained uncertain. A series of observations suggested that similar enzyme systems exist in many other cell types, including fibroblasts (Meier *et al.*, 1991), various tumor cells (Szatrowski *et al.*, 1991), and vascular smooth muscle (Griendling *et al.*, 2000). The family of NADPH oxidase now consists of Nox1, Nox2, Nox3, Nox4, Nox5 as well as Duox1 and Duox2.

The poor production of ROS in cells that were transfected with Nox1 alone led to a search for homologues of p47phox and p67phox, and these have been recently cloned from colon epithelial cells, namely NoxO1 and NoxA1 (Banfi *et al.*, 2003; Geiszt *et al.*, 2003; Takeya *et al.*, 2003; Cheng *et al.*, 2004). Similarly, heterologous expression of Duox enzymes is only successfully achieved since the identification of the Duox maturation factors DuoxA1 and DuoxA2 (Grasberger *et al.*, 2006).

III. Structure, activity and function of NADPH oxidases

1 The Family of NADPH Oxidases

NADPH oxidases are membrane-bound enzymes that transport electrons across biological membranes to reduce oxygen to superoxide, and this is further converted to various reactive oxygen species. They exist in various supergroups of eukaryotes but not in prokaryotes, and play crucial roles in a variety of biological processes, such as host defense, signal transduction, and hormone synthesis. The first example of such enzymes is an NADPH oxidase expressed in mammalian professional phagocytes. In the mid-1990s, homologs of the flavocytochrome gp91phox were discovered in land plants; these have been designated respiratory burst oxidase homolog (Rboh) (Overmyer *et al.*, 2003; Torres *et al.*, 2005; Sagi *et al.*, 2006). Subsequent searches in genome databases led to the identification of novel homologs of gp91phox in animals, which are presently known as Nox (NADPH oxidase) or Duox (dual oxidase) (Geiszt *et al.*, 2004; Quinn *et al.*, 2004). The first one was identified by three separate groups. It is called Mox1 (mitogenic oxidase 1) because its overexpression in NIH3T3 cells leads to increased growth and cell transformation (Suh *et al.*, 1999). It is also known as the NOH-1 (Banfi *et al.*, 2000) or gp91-2 (Kikuchi *et al.*, 2000). The identification of Mox1

was quickly followed by the cloning of gp91-3in fetal kidney tissue (Kikuchi *et al.*, 2000; Cheng *et al.*, 2001), Renox in kidney cells (Geiszt *et al.*, 2000; Shiose *et al.*, 2001), and $p138^{Tox}$ (Dupuy *et al.*, 1999) or ThOx2 and ThOX1 (De Deken *et al.*, 2000) in the thyroid. Cloning of Nox5 (Banfi *et al.*, 2001; Cheng *et al.*, 2001) completes the family. In the new terminology, NADPH oxidases are known as Nox (NADPH oxidase) which Mox1 (NOH-1 or gp91-2) becomes Nox1; gp91phox, Nox2; gp91-3, Nox3; Renox, Nox4; $p138^{Tox}$ (ThOx2), Duox2 and ThOx1, Duox1 (Cheng *et al.*, 2001). There are two levels of tissue expression of these proteins. In most cases, these proteins were cloned from the type of tissue where they are predominantly expressed except Nox3 (Krause, 2004) (Table 1).

Proteins	Other names	Locus	Principle expression site
Nox1	Mox1, NOH-1, gp91-2	Xp21.1	colon
Nox2	gp91phox	Xq22	Phagocytes
Nox3	gp91-3	6q25.1-26	Inner ear
Nox4	Renox	11q14.2-q21	Kidney and blood vessels
Nox5	-	15q22.31	Lymphoid organs and testes
Duox1/2	ThOx1/p138Tox, ThOx2	15q21/15q15.3-q21	Thyroid

Table 1. Tissue distribution and main locus of NADPH oxidases

Nox2 is most abundant in phagocytes, but also found in cells of the vascular system, neurons, fibroblasts, and a variety of other cell types (Cheng *et al.*, 2001; Krause, 2004). In phagocytes, Nox2 localizes to both intracellular and plasma membrane in close association with the membrane protein p22phox (Borregaard *et al.*, 1983; Huang *et al.*, 1995). In cells other than phagocytes, the subcellular distribution varies depending on the specific cell type. In smooth muscle cells, Nox2 is found to localize with the perinuclear cytoskeleton (Li *et al.*, 2002). In hippocampal neurons, Nox2 is suggested to be localized in the membranes of synaptic sites (Tejada-Simon *et al.*, 2005). Nox1 is most abundant in the colon (Banfi *et al.*, 2003; Szanto *et al.*, 2005), but also expressed in a variety of other cell types, including vascular smooth muscle cells, endothelial cells, fibroblasts, prostate, uterus, and osteoblast precursors (Suh *et al.*, 1999; Banfi *et al.*, 2000; Cheng *et al.*, 2001; Lee *et al.*, 2005). Nox3 is the isoform that has the probably most specific and restricted tissue expression. It is essentially found in the inner ear, both the vestibular and the auditive part (Banfi *et al.*, 2004). Also, low levels of Nox3 can be detected in other tissues, including fetal spleen (Kikuchi *et al.*, 2000), fetal kidney (Cheng *et al.*, 2001), skull bone and brain (Banfi *et al.*, 2004). Nox5 is mostly expressed in testis, spleen and lymph nodes, and was also identified in endothelial cells and smooth muscle cells (Banfi *et al.*, 2001; Ha *et al.*, 2005;

Cheng *et al.*, 2006; BelAiba *et al.*, 2007). Dual oxidases were identified from thyroid glands (Dupuy *et al.*, 1999; De Deken *et al.*, 2000). In addition, they have been described on epithelial surfaces of the airways, salivary gland ducts, and along the digestive tract of the human body (Gerson *et al.*, 2000).

Light on Nox4: **tissue distribution and subcellular localization**

Nox4 was originally identified as an NADPH oxidase homolog highly expressed in the kidney (Geiszt *et al.*, 2000; Shiose *et al.*, 2001). Nox4 is more distant, sharing only ~39% identity to Nox2, comparing to Nox1 and Nox3. In addition to its strong expression in the kidney, Nox4 is also found in many other tissues and cell types of the human body such as osteoclasts (Yang *et al.*, 2001; Yang *et al.*, 2004), endothelial cells (Ago *et al.*, 2004; Hu *et al.*, 2005; Kuroda *et al.*, 2005; Van Buul *et al.*, 2005), fetal tissues (Cheng *et al.*, 2001), smooth muscle cells (Wingler *et al.*, 2001; Touyz *et al.*, 2002; Hoidal *et al.*, 2003; Pedruzzi *et al.*, 2004; Ellmark *et al.*, 2005; Clempus *et al.*, 2007), hematopoietic stem cells (Piccoli *et al.*, 2005), fibroblasts (Dhaunsi *et al.*, 2004; Cucoranu *et al.*, 2005; Park *et al.*, 2005; Rossary *et al.*, 2007), keratinocytes (Chamulitrat *et al.*, 2004), melanoma cells (Brar *et al.*, 2002; Govindarajan *et al.*, 2007), pancreas cells (Vaquero *et al.*, 2004; Edderkaoui *et al.*, 2005; Mochizuki *et al.*, 2006), renal cells (Maranchie *et al.*, 2005), adipocytes (Mahadev *et al.*, 2004; Mouche *et al.*, 2007), and neurons (Vallet *et al.*, 2005; Dai *et al.*, 2006). The wide tissue distribution of Nox4 suggests very diverse functions of this enzyme ranging from oxygen sensing to fibrotic processes. To clarify the mechanisms of constitutive and ubiquitous expression of Nox4, the promoter activities of the human Nox4 gene were analyzed by reporter assays (Katsuyama *et al.*, 2011). The 5'-flanking and non-coding regions of the human *Nox4* gene are known to contain multiple GC bases. Three of them containing putative Sp/Klf-binding sites, which were not found in rodent genes, were suggested to be essential for the basal expression of the *Nox4* gene in SH-SY5Y and HEK293 cells. The reduced promoter activity of the *Nox4* gene in SH-SY5Y and HEK293 cells after transfection of an anti-Sp3 short hairpin RNA-expression plasmid suggest that Sp3 plays a key role in the expression of Nox4 in various cell lineages in humans.

Unlike the other Noxs which seem to localize at the plasma membrane, more uncertainties exist regarding the subcellular localization of Nox4. Nox4 has been detected in several cellular compartments: In transfected cells, Nox4 was localized in the ER (Chen *et al.*, 2008) or plasma membrane (Lee *et al.*, 2006); in endothelial cells (Kuroda *et al.*, 2005), human hepatoma cells (de Mochel *et al.*, 2010) and smooth muscle cells (Hilenski *et al.*, 2004), the localization of Nox4 was reported within the nucleus; in vascular smooth muscle

cells, a localization close to focal adhesion was reported (Hilenski *et al.*, 2004). Moreover, in somatic cells, Nox4 was detected in mitochondria in mesangial cells (Block *et al.*, 2009) and cardiomyocytes (Ago *et al.*, 2010). It is uncertain whether these contradicting findings are a consequence of so-far unknown partner of Nox4 changing the localization of Nox4 or of potential problems arising from the overexpression of a membrane protein per se or of the specifity of the different Nox4 antibodies used. It is also possible that the localization of Nox4 changes with the functional or pathological state of the cells (Weyemi *et al.*, 2010). In fact, in vascular smooth muscle cells, Nox4 relocates from focal adhesions to stress fibers during differentiation (Clempus *et al.*, 2007). This also reflects the cell-specific targeting of Nox4 or the different specificity of Nox4 antibodies (Goettsch *et al.*, 2009). Different subcellular localization of NADPH oxidase 4 may be as a mechanism of localizing ROS and activation of downstream redox signalling events that mediate various cell functions.

2 Structure and Topology of NADPH Oxidases

Much of what is known about the structure and topography of the Nox isoforms is derived from studies on Nox2.

2.1 Conserved Structural Properties of NADPH Oxidases

The sequence analysis showed homology between the Nox2 and ferredoxin $NADP^+$ reductase (FNR) family, suggesting that the cytosolic part of Nox2 contains binding sites for FAD and NADPH (Rotrosen *et al.*, 1992; Segal *et al.*, 1992). Experiments have shown photo-affinity binding of NADPH and the FAD on the Nox2 (Doussiere *et al.*, 1986; Doussiere *et al.*, 1995). Directed mutagenesis showed that histidines in the third (H101 and H115) and 5th transmembrane (H209 and H222) are responsible for anchoring the two hemes: one is located near the cytosolic side coordinated by histidines H101 and H209 and the other is near the outer extracellular coordinated by histidines H115 and H222 (Biberstine-Kinkade *et al.*, 2001) (Fig. 7). Thus, the electron path from NADPH to oxygen is mediated by several redox centers: one domain containing FAD (cytosolic tail) and one containing two histidine residues that anchor two heme prosthetic groups. These histidine residues are well conserved in all Nox family members and are essential for trans-membrane electron transport.

Nox1 and Nox3 are the closest homologs of Nox2, sharing 60% (Suh *et al.*, 1999) and 56% (Kikuchi *et*

al., 2000; Cheng *et al.*, 2001) sequence identity respectively. Nox5 is more distantly with an overall homology to Nox2 of 27% (Banfi *et al.*, 2001). It consists of 737 amino acids and contains an additional N-terminal extension comprising four EF-hand motifs.

Duox proteins have a seventh trans-membrane domain at the NH_2 terminus with an ecto-facing peroxidase like domain, in addition to a Nox1-4 homology domain and a EF-hand region. The peroxidase-like domains of Duox proteins are unusual in that they lack conserved histidine residues found in all other peroxidases, considered essential for heme binding (Daiyasu *et al.*, 2000). Within the Nox backbone, Duox isoforms share ~50% identity with Nox2 (De Deken *et al.*, 2000).

Therefore, all Nox/Duox share a common backbone that contains the entire transmembrane redox machinery and a cytoplasmic dehydrogenase domain with FAD and NADPH binding sites. The Nox have not been crystallized but hydropathy plots and secondary structure prediction programs point to a structure with 6 transmembrane domains that are connected by 5 loops. 2 non-identical hemes are coordinated on the 3rd and the 5th alpha helices through 2 pairs of His residues separated by 13 or 14 AA. One of the hemes is positioned in membrane close to the cytosolic space; the second one is on the opposite side. The alignment of primary sequences revealed that the length of some regions connecting the transmembrane domains or FAD and NADPH binding domains vary differently among Nox members. These variations may influence the structure and regulation of NADPH oxidase activity of different Nox (Figure 6).

By analyzing the sequence of 107 Nox enzymes, conserved regions were identified to have important functions in Nox structure or activation. One such region is the cytosolic B-loop, which in Nox1-4 contains a conserved polybasic region. The Nox2 B-loop shares considerable homology, suggesting a general role for this loop in Nox function. In earlier studies of Nox2, this loop was proposed as a binding site for p47phox. Furthermore, both mutagenesis of arginine residues in the Nox2 B-loop and peptides corresponding to the Nox2 B-loop inhibited Nox2 activity and prevented p47phox/p67phox translocation to the membrane (DeLeo *et al.*, 1995; Park *et al.*, 1997; Biberstine-Kinkade *et al.*, 1999). Recent study proposed that the B-loop provides the interface between the transmembrane and dehydrogenase domains of Nox enzymes by binding to the dehydrogenase domain (Jackson *et al.*, 2010).

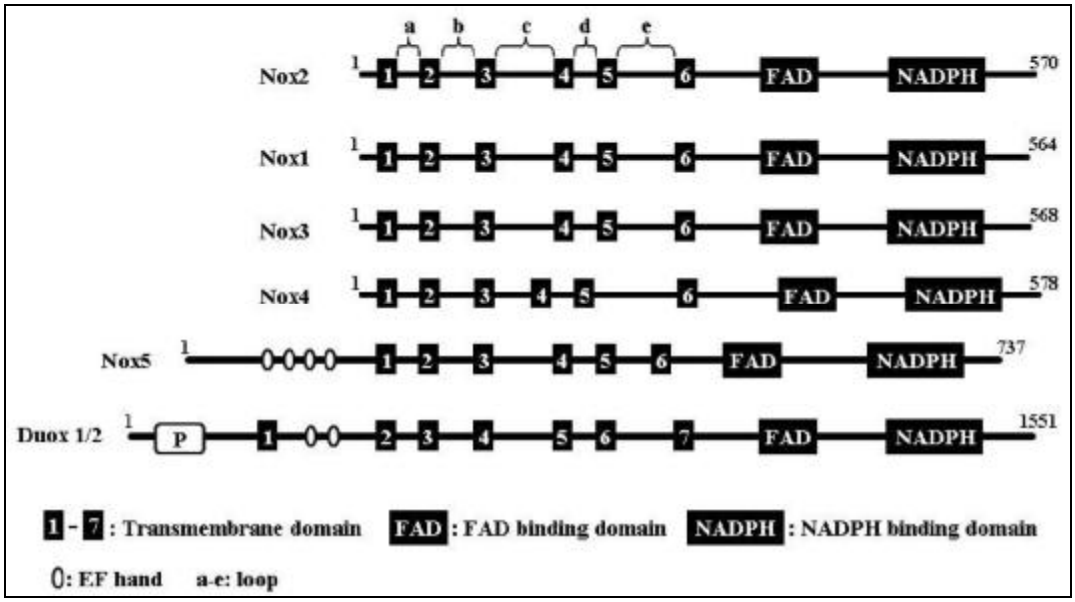

Figure 6. Linear Representation of the Protein Sequence of NADPH Oxidases. *Nox family members have six putative transmembrane helices, binding sites for NADPH and FAD. Nox5 has 4 EF-hand motifs. Duox proteins have a sequence highly homologous to that of the peroxidase (P), another transmembrane domain and 2 EF-hand motifs at the NH_2 terminus.*

In terms of structure related to the Nox activity, whatever the mechanism is involved, structural changes are linked to 3 regulation types: (a). An allosteric transition between two conformation states upon activation which has been illustrated by AFM (Paclet *et al.*, 2000; Paclet *et al.*, 2007); (b). A continuous phosphorylation for sustained activity has been shown for all Nox; (c). Calcium binding either directly as with Nox5 and the Duox, or indirectly through S100A8/A9 proteins or calmodulins as shown with Nox2 and Nox5 (Berthier *et al.*, 2003; Benedyk *et al.*, 2007; Paclet *et al.*, 2007).

Light on Nox4: Structural Properties

The structure of Nox4 has the same overall organization as Nox2 with 6 transmembrane domains, four highly conserved heme-binding histidines, two in the 3rd and two in the 5th transmembrane domains, a FAD-binding region in proximity of the most COOH-terminal transmembrane domain and a NADPH-binding region site at the very COOH terminus. Two extracellular regions of Nox4 are different with other Nox members: loop C is shorter while loop E is longer. Given that most studies report that Nox4 generate H_2O_2 instead of O_2^-, the differences in the extracellular loops might be responsible for the unique ability of Nox4. B-loop is critical for Nox4 function. Fluorescence polarization detected binding between Nox4 B-loop peptide

and dehydrogenase domain. This interaction was weakened with Nox4R96E B-loop corresponding to a mutation that also markedly decreased the activity of Nox4 (Jackson *et al.*, 2010).

2.2 Topology of NADPH oxidases

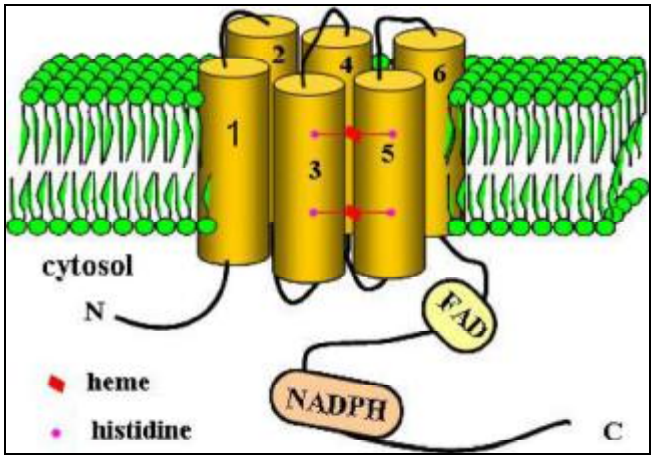

Figure 7. Topology of Nox2. *Nox2 has six transmembrane domains and its NH_2 terminus and its COOH terminus are facing the cytoplasm.*

The structure of Nox2 was not resolved yet, the data concerning the topology derived from experimental and predictive data. Computational analysis of the primary sequence of Nox2, as well as data from epitope mapping point to a structure with 6 transmembrane domains connected by 5 loops, termed A-E (Imajoh-Ohmi *et al.*, 1992; Burritt *et al.*, 2001). Antibody mapping studies demonstrate a cytoplasmic localization of the COOH terminus (Rotrosen *et al.*, 1990; Burritt *et al.*, 2003). Sequencing data and antibody mapping confirm a cytoplasmic NH_2 terminus. The N- as well as C-terminal part of Nox reside in the cytosol, giving rise to two intracellular loops (B- and D-loop) and three loops oriented away from the cytosol and towards the extracellular space or intracellular compartments (A-, C-, and E-loop). Phage display library screening also provides experimental data defining the extracellular domains (Nakamura *et al.*, 1987; Imajoh-Ohmi *et al.*, 1992; Burritt *et al.*, 2001). Loop C and E were identified as extracelluar part by identifying the epitopes of monoclonal antibodies specific to Nox2 (Burritt *et al.*, 2001; Yamauchi *et al.*, 2001; Campion *et al.*, 2007). Loop B is involved in the interaction with the cytosolic factor p47phox and therefore intracellular localization (DeLeo *et al.*, 1995; Biberstine-Kinkade *et al.*, 1999). Taken together, the available data suggest that Nox2 has six transmembrane domains and its NH_2 terminus and its COOH terminus are facing the cytoplasm (Paclet *et*

al., 2004) (Figure 7).

Light on Nox4: **Topology**

The topology information of Nox4 most comes from the computational analysis of Nox4 sequence and the comparison with Nox2. The current model to study the structure-function of Nox4 is based on it.

2.3 Post-translational Modification of NADPH Oxidases

Nox2 protein was synthesized in an immature form in the endoplasmic reticulum which has a molecular weight of 65kDa. It then undergoes maturation by high glycosylation that appears as a broad smear on SDS-PAGE reflecting the heterogeneity of glycosylation. The fully glycosylated form runs with an apparent molecular mass of ~70-90kDa. Removal of the carbohydrates by endoglycosidase F leaves a protein that runs at 55kDa, demonstrating the extent of glycosylation (Harper *et al.*, 1985). Mutagenesis approach shows that the extracellular loops II and III contain N-linked glycosylation sites (Wallach *et al.*, 1997). Through amino acid analysis of the new Noxes, we can find consensus sequences of potential *N*-glycosylation (Asn-X-Ser/Thr, X is any amino acid) (Table 2). In the case of Nox1, most studies suggest a molecular mass of Nox1 in a range of 55-60 kDa by Western blot (Ambasta *et al.*, 2004; Janiszewski *et al.*, 2005; Cui *et al.*, 2006). If these values are correct, Nox1 is most likely not *N*-glycosylated, despite the presence of two NXT/S consensus glycosylation sites in the extracellular domains. However, this fact remains to be confirmed given the lack of truly specific antibodies directed against Nox1. Nox3 and Duox1/2 are glycosylated due to a decrease in molecular weight by deglycosylation (De Deken *et al.*, 2002; Nakano *et al.*, 2007). Both Duox1 and Duox2 have two N-glycosylation states: the high mannose glycosylated form found in the ER, and a fully glycosylated form found at the plasma membrane (De Deken *et al.*, 2002). Nox5 has no predicted N-glycosylation site.

***Light on Nox4: N*-glycosylation**

Few studies concerned the post-translational modification of Nox4 by *N*-glycosylation. The theoretical size of Nox4 is 66.9kDa. Since now, it has been reported that Nox4 antibody recognize two kinds of bands: one of 75-80KDa and a second of 55-65KDa from both endogenous Nox4 expressing cells and/or Nox4-overexpressing cells (Shiose *et al.*, 2001; Hilenski *et al.*, 2004; Gorin *et al.*, 2005; Martyn *et al.*, 2006;

von Lohneysen *et al.*, 2008). The subcellular distribution of the two bands was distinct (Hilenski *et al.*, 2004). The fact that two molecular masses are detected and that Nox4 contains four putative N-glycosylation sites might suggest that Nox4 is glycosylated, although treatment with N-glycosidase F failed to reduce the protein to a single band (Shiose *et al.*, 2001).

Proteins	Potential N-glycosylation sites			Glycosylation	MW kDa
	N terminal	Loop c	Loop d		
Nox1	-	Asn162	Asn236	-	55/60
Nox2	-	Asn132/149	Asn240	+	65→91
Nox3	-	Asn163	Asn238	+	50→55
Nox4	-	Asn130/133	Asn230/236	+/-?	65→75-80
Nox5	-	-	-	-	75
Duox1	Asn94/342/354/461/534	-	-	+	160→190
Duox2	Asn100/348/382/455/537	-	-	+	160→190

Table 2. NADPH oxidases and glycosylation. *Asparagines corresponding to the potential sites of N-glycosylation.*

2.4 Isoforms of NADPH oxidases

Nox1 has another 2 isoforms. This isoform Nox1v lacks entire exon 11 which contains a domain predicted binding of NADPH (Geiszt *et al.*, 2004). It appears that this splice variant encodes a protein incapable of producing superoxide. Two other Nox1 mRNA (c-type and f-type) have been described in mouse due to the use of alternative promoter. These two mRNAs encode the same protein Nox1 (c/f-type) lying on the N terminal capable of having an activity equivalent to Nox1 NADPH oxidase (Arakawa *et al.*, 2006). Besides, a very short isoform of Nox1 had been suggested, but it proved to be an experimental artifact due to the formation of a stable loop in the Nox1 mRNA (Banfi *et al.*, 2000; Geiszt *et al.*, 2004; Harper *et al.*, 2005).

In regard to Nox2, a truncated isoform of Nox-2S has been described (Heidari *et al.*, 2004). It includes a previously unidentified exon (IIIa) and encodes an in-frame stop codon. Nox-2S displays a widespread pattern of expression in mouse tissues and human cells, with high levels present in the myeloid cell line HL-60. The function of Nox-2S awaits elucidation.

Nox5 (Nox5α) has another four isoforms (Nox5β, -γ, -δ, -ε). Nox5 isoforms (Nox5α-δ) described by Banfi et al. distinguish themselves from Nox1-4 enzymes by the presence of a long intracellular NH_2 terminus containing a Ca^{2+}-binding EF-hand domain (Banfi *et al.*, 2001; Banfi *et al.*, 2004). Nox5ε lacks the EF-hand region and therefore has an overall structure more similar to Nox1-4 (Cheng *et al.*, 2001).

Light on Nox4: **isoforms**

It has been suggested that Nox4 has another 4 isoforms except the prototype Nox4A (Goyal *et al.*, 2005) (Fig. 8). Nox4B differs from Nox4A by splicing of exon 14 that causes a deletion of the first binding domain of NADPH, therefore results in the lack of the first NADPH binding site in the protein. Nox4C is a result of a splicing of exon 9-11, which generates a frame shift in mRNA, and hence a new stop codon in the beginning of exon 12. Consequently, Nox4C lacks the complete C-terminus including FAD and NADPH binding domains in protein. Both variants B and C acted as dominant-negative molecules, since A549 cells transfected with these variants had lower ROS concentration as compared to control plasmid transfected cells. Meanwhile, the similar inhibitory effect on ROS generation between variant B and C indicated that the first NADPH binding site seems to have a strong impact on NADPH oxidase activity and cannot be fully compensated by the other NADPH and FADH binding sites. Nox4D and Nox4E are both a consequence of splicing of exons 3-11 whereas variant E has an additional splicing of exon 14. Therefore, Nox4D has only the first transmembrane domain and contains all FADH and NADPH binding sites while Nox4E has only the first transmembrane domain and additionally lacks one NADPH binding site similar to variant B. Interestingly, Nox4D was shown to have NADPH oxidase activity comparable to that of Nox4A brings into question of the necessity of conserved histidines distributed within the transmembrane containing N-terminus for enzymatic activity. These histidines are postulated to bind iron in complex with the heme group that is required for electron transfer to oxygen (Lambeth, 2000). Both Nox4D and Nox4E appear as glycosylated forms. As both of them lack the hydrophobic putative transmembrane domains, they are hence considered as soluble variants.

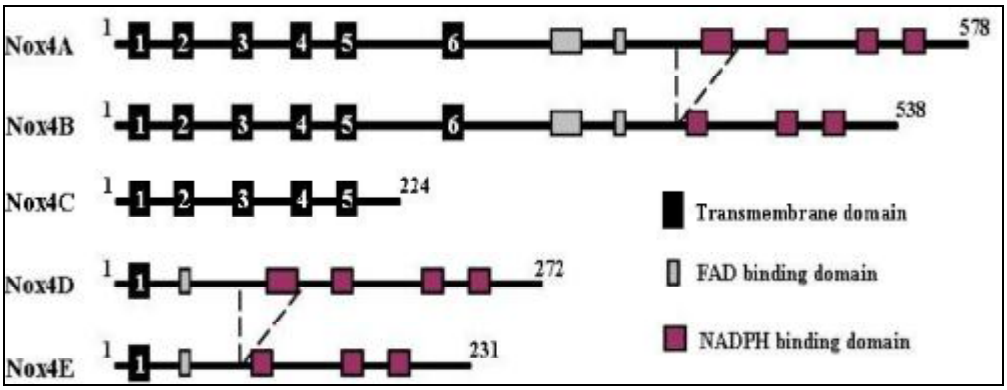

Figure 8. Schematic representastion of Nox4 isoforms

3 Regulation of the NADPH Oxidase Activity

3.1 Electron Transfer Mechanism of NADPH Oxidase Nox2 (Cross et al., 2004)

The NADPH oxidase catalyzes the production of superoxide by electron transfer from NADPH to molecular oxygen. The central component of the complex is the flavocytochrome b558, a membrane-bound heterodimeric protein consisting of two subunits: a larger glycoprotein (gp91phox) and a smaller nonglycosylated protein (p22phox). These two subunits are in a 1:1 stoichiometry. The mechanism of electron transfer is well documented for the Nox2 protein. gp91phox possesses the entire electron transport machinery (Geiszt *et al.*, 2004; Lambeth, 2004; Bedard *et al.*, 2007). It is the catalytic center of this enzyme. There are seven separate steps of electron transfer during a single turnover of NADPH oxidase, as illustrated in Figure. 9. The first step is the transfer of two electrons from NADPH to oxidized FAD. The second electron transfer step is from reduced FAD ($FADH_2$) to the inner haem, generating the FAD semiquinone (FAD°). In the third and fourth steps, the electron is passed from the inner to the outer haem and then to oxygen forming superoxide. The fifth, sixth and seventh steps recapitulate the third, fourth and fifth, the exception being in the fifth step, where it is the flavin semiquinone that is the donor to the inner haem.

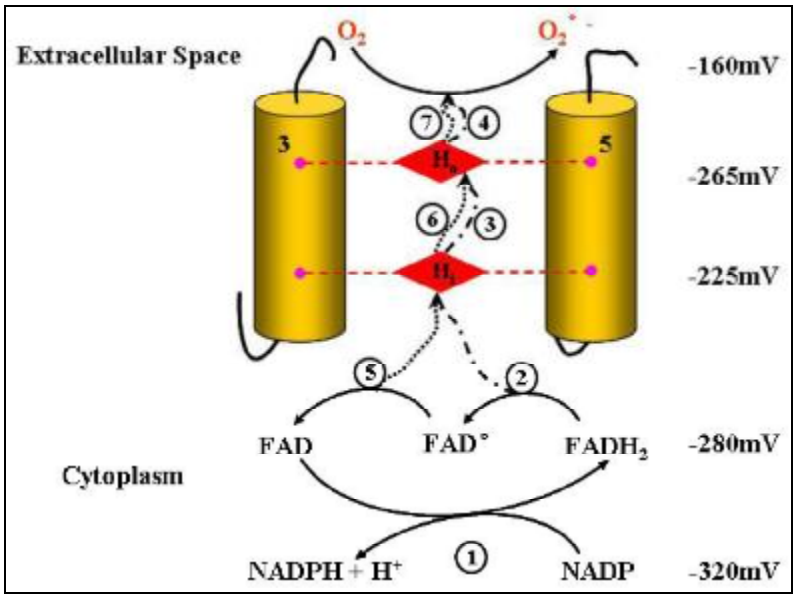

Figure 9. Electron transfer pathways within flavocytochrome b558 (Cross et al., 2004). *The seven electron transfer steps are numbered. The transfer of two electrons takes place from NADPH (step 1). The first electron transport is from FADH2 (step 2,3,4) and the second electron transport is from FAD° (step 5,6,7).*

Recent studies showed that cytosolic tail of Nox2 is sufficient to support diaphorase activity. This activity

can be distinguished from the NADPH oxidase activity by using INT (iodonitrotetrazolium) as a direct FAD electron acceptor, in PLB985 cells expressing the whole protein (Pessach *et al.*, 2001) and truncated protein containing only cytosolic part (Pessach *et al.*, 2006). Experiments with Nox2 truncated forms produced by bacteria were able to determine the region responsible for this activity, which corresponds to amino acids 221 to 570. The diaphorase activity is intrinsic and does not require the presence of cytosolic factors. However, these cytosolic factors (p67phox and Rac1) are capable of stimulating the activity (Han *et al.*, 2001; Nisimoto *et al.*, 2004).

Light on Nox4: **Diaphorase Activity**

Recently, the cytosol-facing dehydrogenase (DH) domain (AA: 298-578) containing a binding site for NADPH and one for FAD (Rotrosen *et al.*, 1992; Segal *et al.*, 1992; Sumimoto *et al.*, 1992) from Nox4 was expressed and purified to measure the electron transferase activity toward several artificial electron acceptors (Nisimoto *et al.*, 2010). In these experiments, the Nox4 DH domain showed significant rates of electron transfer (65-470 min^{-1} depending on the electron acceptor), and these activities were inhibited by DPI.

3.2 Nox Subunits and Regulation Proteins

Despite their similar structure and enzymatic function, Nox family differs in their mechanism of activation. The components involved in Nox activation include the membrane-bound p22phox, the cytosolic proteins p47phox, p67phox, the small GTPase Rac, and the modulatory p40phox, which together lead to the activation of the Nox enzyme.

3.2.1. p22phox: Indispensible Partner of NADPH Oxidases

p22phox is a membrane protein, which closely associates with Nox2 in a 1:1 complex (Huang *et al.*, 1995). This protein is encoded by the gene CYBA located on chromosome 16 (locus 16q24), it appears as a band at 22kDa by western blot and seems not glycosylated (Parkos *et al.*, 1987). At the moment, the topology and functional domains within p22phox are not clearly characterized. The membrane topology of p22phox is difficult to predict based on hydropathy plots, computational analysis of primary sequence of p22phox suggests that p22phox contains 2-4 membrane-spanning segments (Taylor *et al.*, 2004). However, the weight of experimental evidence obtained with both specific antibodies directed against the cytosolic parts of

p22phox and cytochrome b558 proteolytic digestion favors the presence of 2 transmembrane domains (Taylor *et al.*, 2004) and the cytosolic localization of the N- and C-terminal regions of the protein (Imajoh-Ohmi *et al.*, 1992; Burritt *et al.*, 1998). p22phox has a proline-rich region (amino acids 151-160) that serves as an anchor for cytosolic factors during oxidase activation. Moreover, the absence of antibodies and the protease sensitive sites against an extracellular portion of p22phox indicates that a very small portion of the protein is exposed to the extracellular surface.

The association of p22phox with Nox2 contributes to its maturation and stabilization. Nox2 or p22phox alone is degraded by the proteasome (DeLeo *et al.*, 2000; Block *et al.*, 2007). The interaction with p22phox and incorporation of heme are necessary for Nox2 maturation through the N-glycosylation (Yu *et al.*, 1999).

Studies in the subcellular distribution of p22phox show that p22phox localization is a function of the Nox isoform coexpressed with p22phox in a given cell type. The p22phox subunit has 2 major functions. It binds and stabilizes Nox proteins, and serves as a membrane anchor for cytosolic regulatory factors by binding organizer subunits. It was recently shown that p22phox also associates with Nox1 and Nox3 (Ambasta et al., 2004; Ueno et al., 2005), suggesting a central role of p22phox in the cellular production of reactive oxygen species. p22phox was also essential for the maturation of Nox3 (Nakano *et al.*, 2007) and would be stabilized by interaction with Nox1 (Ambasta *et al.*, 2004; Martyn *et al.*, 2006). The association of p22phox with Nox1-3 suggests that Nox proteins and the p22phox protein are stable only as a heterodimer, while monomers are degraded by the proteasome (DeLeo *et al.*, 2000). Consistent with this concept, Nox2-deficient CGD patients do not have detectable p22phox protein within phagocytes, and p22phox-deficient CGD patients do not have detectable Nox2 protein (Parkos *et al.*, 1989). Nox5 does not require p22phox for activity, as demonstrated by siRNA suppression of p22phox leading to a decrease in the activity of Nox1-3, but not of Nox5 (Kawahara *et al.*, 2005; Martyn *et al.*, 2006). Human Duox2 protein reportedly coimmunoprecipitates with p22phox (Ameziane-El-Hassani *et al.*, 2005), but there is little or no effect of p22phox on Duox enzymatic activity.

Light on Nox4: **Interaction between Nox4 and p22phox**

Nox4 is also a p22phox dependent enzyme. siRNA-mediated p22phox down-regulation leads to a decrease function of Nox4. Nox4 colocalizes and coimmunoprecipitates with p22phox. It also stabilizes the p22phox protein (Ambasta *et al.*, 2004). Truncation of p22phox or mutation within the COOH-terminal

domain leads to a loss of activation of Nox1, Nox2, and Nox3 (Leusen *et al.*, 1994; Kawahara *et al.*, 2005) but not Nox4 in agreement with the concept that Nox4 activation does not need cytosolic organizer subunits. Interestingly, a p22phox mutant (p22phox Y121H) is capable of distinguishing between Nox1-3 and Nox4 by forming a functional complex only with Nox4, further suggesting the unique structural features in Nox4 (von Lohneysen et al., 2008).

Recent structure-function analyses of complexes between Nox2 or Nox4 and the subunit p22phox documented specific regions and amino acid residues in p22phox necessary for complex formation and oxidase activity (Zhu et al., 2006; von Lohneysen et al., 2008; Helmcke et al., 2009). Extensive structure-function analysis of the oxidase complex showed that B-loop was crucial for the activity (Jackson et al., 2010; von Lohneysen et al., 2010) of both Nox enzymes and Nox4 D-loop is part of structural elements required in bridging dimerization of Nox4 with p22phox Y121H mutant (Helmcke et al., 2009; von Lohneysen et al., 2010).

3.2.2. p47phox, p67phox, p40phox and Rac: Cytosolic Regulatory Protein of Phagocyte NADPH Oxidase

3.2.2.1 Organizer Subunits: p47phox, NoxO1

Organizer subunits p47phox and NoxO1 shares ~25% sequence identity. p47phox contains a phagocyte oxidase (PX) domain, tandem SH3 domains, an autoinhibitory region (AIR) and a PRR (Figure. 10). The two SH3 domains cooperatively interact with the PRR in the C-terminal cytoplasmic region of p22phox, which is essential for both membrane translocation of p47phox and oxidase activation (Leto *et al.*, 1994; Sumimoto *et al.*, 1994). In the resting state, the two SH3 domains of p47phox are masked via an intramolecular interaction with AIR (Groemping *et al.*, 2003; Yuzawa *et al.*, 2004; Yuzawa *et al.*, 2004). During phagocytosis of invading microbes or with soluble stimuli such as N-formyl chemotactic peptide and PMA, p47phox undergoes phosphorylation at multiple Ser residues, several of which are present in the AIR (el Benna *et al.*, 1994; Inanami *et al.*, 1998), induces unmasking of the SH3 domains (Shiose *et al.*, 2000), therefore interacts with the PRR of p22phox. NoxO1 exhibits a domain architecture similar to that of p47phox, except that it lacks an AIR (Figure. 10), suggesting that NoxO1 is constitutively active. NoxO1 plays an essential role in Nox1 activation which functions via its PRR by interacting with NoxA1 and via its SH3 domains by binding to p22phox (Takeya *et al.*, 2003; Miyano *et al.*, 2006; Ueyama *et al.*, 2006; Yamamoto *et al.*, 2007).

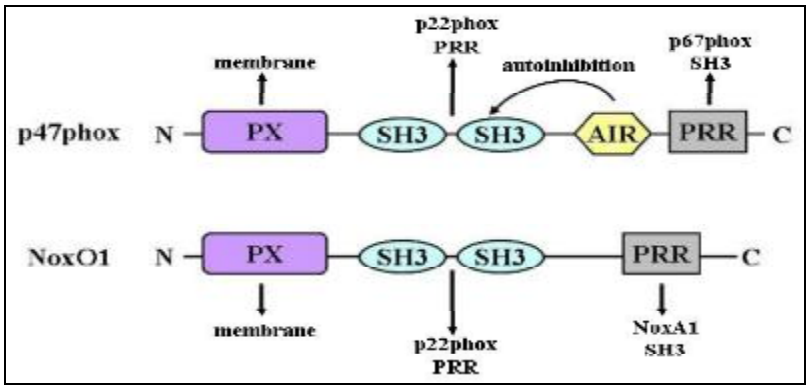

Figure 10. The two organizer homologs, p47phox and NoxO1, share a similar set of motifs. *PX, phagocyte oxidase domain; SH3, Src homology 3 domain; AIR, autoinhibitory region; PRR, proline rich region. See the detail of interaction of p47phox or NoxO1 with other protein in text (3.2.2.1).*

3.2.2.2 Activator Subunits: p67phox and NoxA1

Activator subunits p67phox and NoxA1 share ~28% amino acid identity and their overall domain structure is similar (Figure. 11). Both contain an NH_2-terminal tetratricopeptide repeat (TPR, interact with Rac) (Koga *et al.*, 1999; Lapouge *et al.*, 2000; Grizot *et al.*, 2001), a highly conserved activation domain (AD, interact with Nox proteins) (Han *et al.*, 1998; Nisimoto *et al.*, 1999; Geiszt *et al.*, 2004), a less conserved "Phox and Bem 1" domain (PB1, interact with the PC domain of p40phox) and a COOH-terminal SH3 domain (binding to the C-terminal PRR of p47phox) (Finan *et al.*, 1994; Leusen *et al.*, 1995). However, there are some differences between two activator subunits: the PB1 domain of NoxA1 has important differences from that of p67phox, thus fails to interact with p40phox (Takeya *et al.*, 2003). It also lacks the central SH3 domain found in p67phox (Banfi *et al.*, 2003; Geiszt *et al.*, 2003). Although the first SH3 domain is the most conserved region in p67phox (Mizuki *et al.*, 1998), its function is still unknown.

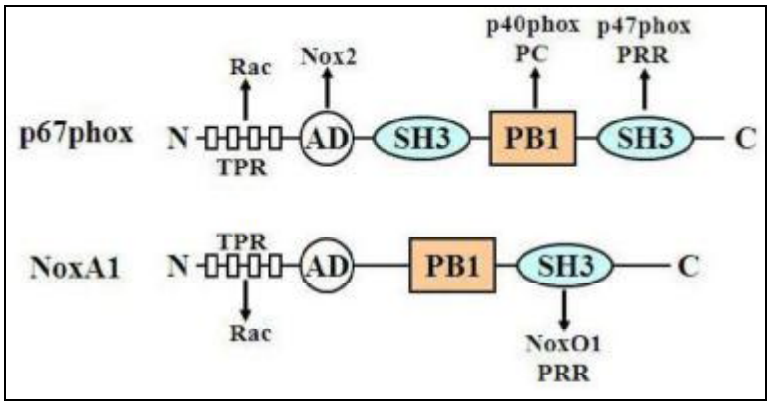

Figure 11. The two activator homologs, p67phox and NoxA1, share a similar overall domain structure. *TPR,*

tetratricopeptide repeat; AD, activation domain; SH3, Src homology 3 domain; PB1, Phox and Bem1 domain; PRR, proline rich region. See the detail of interaction of p67phox or NoxA1 with other protein in text (3.2.2.2).

3.2.2.3 p40phox

p40phox protein was discovered when it was co-purified with p67phox (Someya *et al.*, 1993; Wientjes *et al.*, 1993). It is stable only upon binding to p67phox, as it is absent from CGD patients who lack p67phox (Tsunawaki *et al.*, 1994). The structure domains of p40phox include a PX domain which is strongly homologous with p47phox, an SH3 domain, and a PC (Phox and cdc) domain which seems to be involved in the binding of p40phox to p67phox (Nakamura *et al.*, 1998) (Figure. 12). p40phox interacts with p47phox and p67phox with a 1:1:1 stoichiometry (Lapouge *et al.*, 2002).

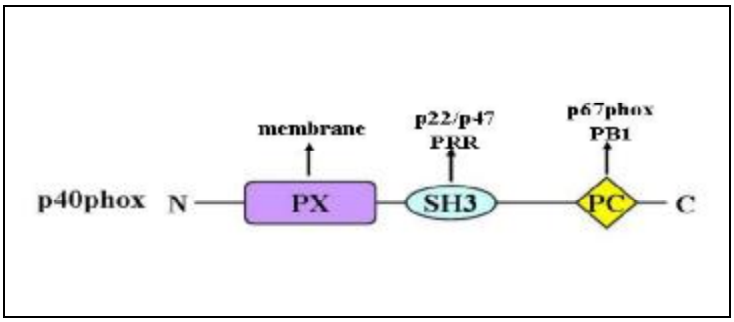

Figure 12. Regions of p40phox involved in protein/protein interactions. *PX, phagocyte oxidase domain; SH3, Src homology 3 domain; PC, Phox and cdc domain; PRR, proline rich region; PB1, Phox and Bem1 domain. See the detail of interaction of p40phox with other protein in text (3.2.2.3).*

3.2.2.4 Rac GTPase

Rac, a member of the Rho-family small GTPase, plays an essential role in Nox2 activation (Abo *et al.*, 1991; Knaus *et al.*, 1991; Mizuno *et al.*, 1992). There is no doubt that Rac GTPase are important activators of Nox1(Miyano *et al.*, 2006). However, the involvement of Rac GTPase in other Nox isoforms is still a matter of debate (Gorin *et al.*, 2003; Inoguchi *et al.*, 2003; Ueno *et al.*, 2005; Martyn *et al.*, 2006).

3.3 Assembly of the Phagocyte NADPH oxidase Nox2

The activation of Nox2 occurs through a complex series of protein/protein interactions (Nauseef, 2004; Groemping *et al.*, 2005; Sumimoto *et al.*, 2005). In resting neutrophil granulocytes, Nox2 and p22phox are found primarily in the membrane of intracellular vesicles. They exist in close association, co-stabilizing one

another. Indeed, the Nox2 protein is unstable in the absence of p22phox, and phagocytes from p22phox-deficient patients have not detectable Nox2 protein (Parkos *et al.*, 1989; Dinauer *et al.*, 1990; Stasia *et al.*, 2002). Under resting conditions, Rac is coupled to another protein, GDP dissociation inhibitor (Ottaviani *et al.*), which maintains it in the inactive form bound to GDP (Pick *et al.*, 1993). Upon activation, Rac is recruited to the membrane which requires geranylgeranylation of Cys189 at the C-terminus. At the membrane, Rac is converted to the GTP-bound active form via the function of guanine nucleotide-releasing factors (Kreck *et al.*, 1996). The GTPase Rac interacts with Nox2 via a two-step mechanism involving an initial direct interaction with Nox2 (Diebold *et al.*, 2001), followed by a subsequent interaction with the TPR domain of p67phox (Koga *et al.*, 1999; Lapouge *et al.*, 2000; Lapouge *et al.*, 2002). Phosphorylation of the cytosolic p47phox subunit leads to conformational changes allowing interaction with p22phox (Sumimoto *et al.*, 1996; Groemping *et al.*, 2003). The movement of p47phox brings with it the other cytoplasmic subunits, p67phox and p40phox, to form the active Nox2 enzyme complex (Han *et al.*, 1998). Recently available data show that p40phox is specific for Nox2 and most evidence indicates that it enhances the oxidase function (Cross, 2000; Kuribayashi *et al.*, 2002). Once activated, there is a fusion of Nox2-containing vesicles with the plasma membrane or the phagosomal membrane. The active enzyme complex transports electrons from cytoplasmic NADPH to extracellular or phagosomal oxygen to generate superoxide on the lumen or extracellular space (Figure. 13). Research on the genetic causes of the immune defect called chronic granulomatous disease (CGD) (Thrasher *et al.*, 1994) has advanced the understanding of the function of the Nox2 system. CGD is a rare inherited disorder characterized by the absence of NADPH oxidase (Nox2) activity. It results from mutations in the genes encoding in any one of four essential subunits of the complex (Segal *et al.*, 2000). Phagocytes lacking NADPH oxidase activity are unable to kill bacteria and fungi efficiently, with the predicted consequence that these patients are profoundly immunodeficient, demonstrating frequent, severe, acute and chronic, often fatal, infections.

In addition to their structural similarities, Nox1 shows the striking functional similarities as Nox2. Like Nox2, Nox1 requires p22phox (Ambasta *et al.*, 2004; Kawahara *et al.*, 2005) and Rac1 (Cheng *et al.*, 2006; Miyano *et al.*, 2006; Ueyama *et al.*, 2006) for complete activity (Figure. 14). Besides, superoxide generation by Nox1 also depends on cytosolic subunits NoxO1 and NoxA1 (Geiszt *et al.*, 2003; Takeya *et al.*, 2003). Nox1 is also able to use the p47phox and p67phox subunits, suggesting that cytosolic subunits are not specific for a given Nox protein (Banfi *et al.*, 2003). As the most significant structural difference between NoxO1 and p47phox is that NoxO1 lacks sequence homologous to the autoinhibitory region of p47phox that becomes

hyperphosphorylated and allows binding to p22phox and membrane phospholipids. The superoxide generation by Nox1 without stimulants such as PMA appears to be partially due to the absence of AIR in NoxO1 (Takeya *et al.*, 2003; Cheng *et al.*, 2004). Thus, the Nox1/NoxO1/NoxA1 system differs from the Nox2/p47phox/p67phox system in that it is less subject to tight controls and exhibits significant constitutive activity, which is further enhanced by PMA.

Nox3 is also a p22phox-dependent enzyme. Nox3 has a high, basal activity when expressed alone in heterologous systems, which can be further enhanced by expressing either one or both of the Nox1 or Nox2 supportive cytosolic partners (Figure. 14). In the presence of NoxO1, Nox3 activity was enhanced in all studies (Banfi *et al.*, 2004; Cheng *et al.*, 2004), while the requirement for NoxA1 is contradictory: some studies found enhancement of Nox3 activity through NoxA1 (Banfi *et al.*, 2004; Cheng *et al.*, 2004), others did not (Banfi *et al.*, 2004; Cheng *et al.*, 2004). The Rac dependence of Nox3 is also still debatable. Two studies suggest a Rac independence (Ueno *et al.*, 2005; Cheng *et al.*, 2006), while the results of a third study suggest an effect (Ueyama *et al.*, 2006).

Nox5 does not require p22phox for activity (Figure. 14), although Nox5 is able to bind p22phox (BelAiba *et al.*, 2007). Nox5 does not require cytosolic organizer or activator subunits and has shown to function in a cell-free system without the requirements of any cytosolic proteins. As predicted by the presence of EF hands, Nox5 seems to be mainly regulated in a Ca^{2+}-dependent manner (Banfi *et al.*, 2004). The binding of Ca^{2+} to the EF hands induces a structural rearrangement leading to the interaction of N-terminal EF-hand domain with the catalytic C-terminal catalytic dehydrogenase domain (CDHD) of the enzyme, and activates Nox5. Recent study showed that the interaction site for the regulatory Nox5-EF in the catalytic CDHD of Nox5 is composed of two short segments: the 637−660 segment, referred to as the regulatory EF-hand-binding domain (REFBD), and the 489−505 segment, previously identified as the phosphorylation region (PhosR) (Tirone *et al.*, 2010).

Like Nox5, Duox enzymes do not require activator or organizer subunits but can be activated by Ca^{2+} directly (Figure. 14); however, the p22phox requirement is still a matter of debate. Duox enzymes coimmunoprecipitate with p22phox, but there is no evidence for enhanced Duox function upon coexpression of p22phox (Wang *et al.*, 2005). Heterologous Duox expression in several mammalian cell lines fails to reconstitute ROS release, and superoxide generation can be measured only in broken cell preparations (Ameziane-El-Hassani *et al.*, 2005). Duox enzymes tend to be retained in the ER, suggesting other tissue-specific oxidase components are needed for Duox activity (De Deken *et al.*, 2002). This observation led

to the discovery of essential Duox maturation factors, which are ER proteins termed DuoxA1 and DuoxA2, required for full processing of Duox to the plasma membrane (Grasberger *et al.*, 2006).

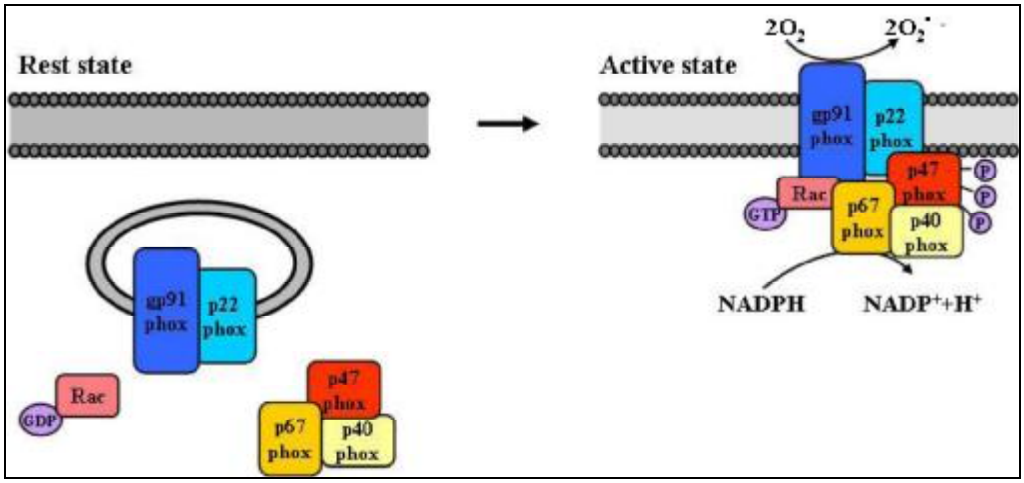

Figure 13. Assembly of the phagocyte NADPH oxidase Nox2. *In resting neutrophil granulocytes, heterodimeric gp91phox-p22phox resides primarily in the membrane of intracellular vesicles, whereas the complex of p47phox-p67phox-p40phox is cytosolic. Upon activation, the movement of p47phox brings with it the other cytoplasmic subunits, p67phox and p40phox, to form the active Nox2 enzyme complex at the plasma membrane. See text for additional details.*

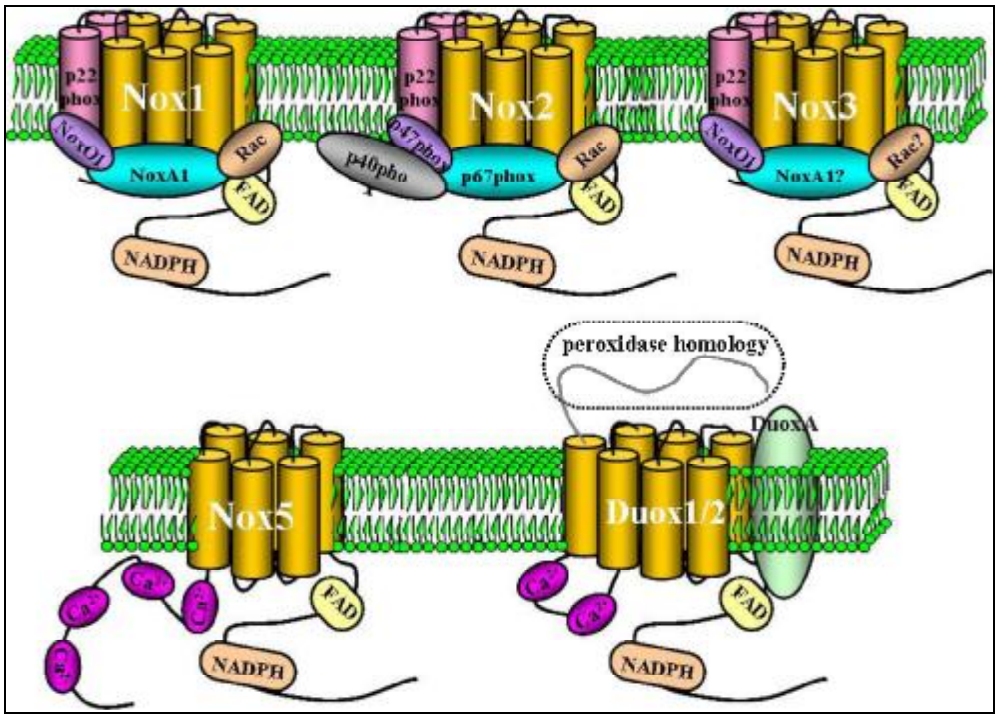

Figure 14. Activation of the NADPH oxidase isoforms. *Despite their similar structure and enzymatic function,*

Nox family enzymes differ in their mechanism of activation. Nox1, the activity requires p22phox, NoxO1, NoxA1, and the small GTPase Rac; Nox2, the activity requires p22phox, p47phox, p67phox, p40phox and Rac; Nox3, the activity requires p22phox and NoxO1, the requirement for NoxA1 may be species dependent, and the requirement of Rac is still debated; Nox5, the activity seems to be mainly regulated in a Ca^{2+}-dependent manner. It does not require p22phox and other cytosolic proteins; Duox, the activity can be activated by Ca^{2+} directly and Duox maturation factors are required for full processing of Duox to the plasma membrane.

Light on Nox4: **the Regulation of Activity**

Unlike all the other Nox family members, Nox4 is constitutively active and is independent of cytosolic activator proteins or regulatory domains (Geiszt *et al.*, 2000; Ambasta *et al.*, 2004) (Figure. 15). Upon heterologous expression, it is active without the need for cell stimulation (Martyn *et al.*, 2006). p22phox is the only known partner that interacts with Nox4, they colocalize with each other (Ambasta *et al.*, 2004). Functional studies demonstrate a p22phox requirement for Nox4-dependent ROS generation. Recently, Lyle et al. significantly advanced the understanding of NADPH oxidase regulation by identifying polymerase delta-interacting protein 2 (Poldip2) (Lyle *et al.*, 2009). Very little is known regarding Poldip2, which was originally described to bind to DNA polymerase delta and proliferating cell nuclear antigen (Liu *et al.*, 2003). Poldip2 associates with Nox4 via p22phox and colocalizes with p22phox at sites of Nox4 in SMCs. It was introduced as a positive regulator of Nox4 activity. However, the mechanism by which Poldip2 regulates Nox4 activity is still unknown. As no associated change in Nox4 protein level with changes in Poldip2 expression, Poldip2 may function to emulate the cytosolic subunits in activating Nox4. Through the redox-dependent activation of RhoA, Nox4-Poldip2 affects the cytoskeletal rearrangement necessary for cell migration, since either the overexpression or the depletion of Poldip2 inhibits migration of cultured SMCs. Furthermore, the observation of the association of Poldip2 with Nox4 in the nucleus may probably solve the previous question that how a membrane-associated Nox4 can be found in a membrane-free space. They proposed a potential role for Nox4 in regulation of the redox environment within the nucleus, resulting in redox modification of DNA or associated proteins, therefore the extending of the understanding of NADPH oxidase in diverse areas of redox biology (Miller, 2009).

Nox4 is consistently upregulated and acutely activated by transforming growth factor-beta in all cell types tested (Brown *et al.*, 2009; Lassegue *et al.*, 2010). In fact, TGF β is responsible for Nox4 activation in response to other stimuli, such as hypoxia (Ismail *et al.*, 2009; Jaulmes *et al.*, 2009). Investigations of downstream signaling pathways suggest that p38MAPK is a target of Nox4 (Goettsch *et al.*, 2009). Nox4 also

activates the Ras/ERK pathway, JNK, and Akt (Chen *et al.*, 2008). In addition to tyrosine kinase signaling pathways, Nox4 has been implicated in the activation of Rho in VSMC, consistent with its effects on the cytoskeleton (Lyle *et al.*, 2009).

Structure-function analyses of complexes showed that the constitutive activity of Nox4 is mediated by the cytosolic tail since Nox4/2 chimera or Nox4/1 chimera is inactive in the basal state but is activated by subunits with or without PMA. In contrast, the reverse chimera Nox2/4 or Nox1/4 shows constitutive activity independent of regulatory subunits (Helmcke *et al.*, 2009; Nisimoto *et al.*, 2010). Besides, Nox4 B-loop containing a polybasic sequence binds to the DH domain especially the NADPH-binding subdomain, provides the interface between the transmembrane and DH domain, thus to affect the electron transfer between electron centers residing in both domains (Jackson *et al.*, 2010; von Lohneysen *et al.*, 2010).

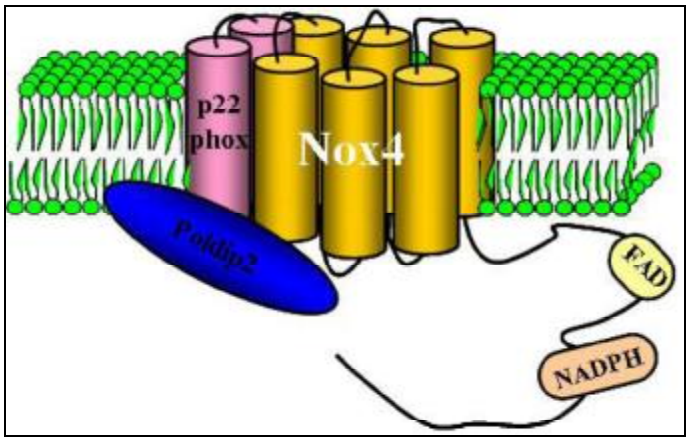

Figure 15. Activation of Nox4. *The activity of Nox4 requires p22phox and recent study indicated that Poldip2 could regulate its activity.*

3.4 Characteristic of NADPH Oxidases Dependent ROS Generation

NADPH oxidases including Nox1, Nox2, Nox3 and Nox5 produce primarily O_2^- while many studies have shown a generation of hydrogen peroxide by Duox enzymes (Geiszt *et al.*, 2003; Forteza *et al.*, 2005). In a recent study, the immature, partially glycosylated form of Duox2 generated superoxide, while the mature form generated hydrogen peroxide (Ameziane-El-Hassani *et al.*, 2005). It was speculated that posttranslational modifications favor intramolecular dismutation of superoxide to hydrogen peroxide. Thus it is likely that the primary product of Duox enzymes is superoxide and that a rapid dismutation precludes in many instances the detection of a superoxide intermediate.

Light on Nox4: Characteristic of Nox4-dependent ROS Generation

Most studies showed that H_2O_2 is the principal source of ROS detected outside of cells (Martyn *et al.*, 2006; Chen *et al.*, 2008; Hecker *et al.*, 2009). This should not, however, be taken as a proof of direct hydrogen peroxide generation by the enzyme. It has been suggested that the failure to detect O_2^- formation by Nox4 is a consequence of its intracellular location, resulting in the release of superoxide into the lumen of the organelles where it rapidly dismutates into the freely diffusible hydrogen peroxide. However Nox4 in some cells resides in part in the plasma membrane, but unexpectedly still produces H_2O_2 without any detectable O_2^- (von Lohneysen *et al.*, 2010). In contrast, Boudreau et al. recently reported that O_2^- is synthesized in the extracellular medium of hepatocytes (Boudreau *et al.*, 2009).

IV. Physiological Function of NADPH Oxidases

Nox2 is beyond any doubt an enzyme of the host defense, as evidenced by the clinical presentation of the patients with chronic granulomatous disease. Patients with this congenital disease lack either Nox2 or one of its subunits and suffer from severe infections. As ROS do have a microbicidal action, the host defense function of Nox2 is in general attributed to a direct killing of microorganisms by the ROS, or the interaction of ROS with the myeloperoxidase system. There is also increasing evidence that Nox2 is involved in a variety of pathological processes, including the development of cardiovascular disease; neurodegeneration, and HIV pathogenesis.

Basically two major physiological functions of Nox1 have been discussed: host defense function (Kawahara *et al.*, 2001; Kawahara *et al.*, 2004), through ROS-dependent bacterial killing, and stimulation of cell division through activation of redox-sensitive intracellular signaling mechanism. In early work exploring the function of Nox1, heterologous overexpression of Nox1 in NIH-3T3 cells was associated with increased cell proliferation and resulted in tumor formation when these cells were injected into nude mice (Suh *et al.*, 1999). ROS produced by Nox1 is also responsible for the increased mitogenesis (Szatrowski *et al.*, 1991; Sundaresan *et al.*, 1995; Irani *et al.*, 1997; Arnold *et al.*, 2001). Besides, some findings suggest that Nox1 serves some other specialized function in differentiated colon epithelium unrelated to mitogenesis (Geiszt *et al.*, 2003). A role for Nox1 in innate immunity was also suggested by experiments showing that Nox1 could replace Nox2 (gp91phox) in the regulated production of superoxide, thereby partially rescuing the deficiency

in superoxide production observed in chronic granulomatous disease neutrophils (Geiszt *et al.*, 2003). Whether Nox1 has a primary role in maintaining colon epithelial integrity or in host defense will require further investigation.

A unique role for Nox3 within the inner ear was revealed by positional cloning studies that mapped genetic lesions causing the *head tilt* (*het*) phenotype in mice (Paffenholz *et al.*, 2004). Mice with *Nox3* mutations exhibit impaired otoconial morphogenesis and defects in perception of gravity and balance. It was proposed that this oxidase mediates ROS-dependent conformation changes in otoconin 90 involved in the nucleation of calcite crystal formation during the development of otoconia, while the reason for its expression in the auditive system is not yet understood.

Little is known about the physiological function of Nox5, but its absence in rodents makes it the "least essential" Nox isoform in mammals. Nox5-related proteins in non-mammalian organisms have been linked to cell growth, differentiation, and signalling (Brar *et al.*, 2003; Lardy *et al.*, 2005; Torres *et al.*, 2005).

In mammals, both Duox1 and Duox2 are thought to be involved in the thyroid hormone synthesis (Moreno *et al.*, 2002). Duox mutants of C. elegant have an abnormal extracellular matrix and a role of Duox enzymes in cross-linking of the extracellular matrix proteins has been proposed (Edens *et al.*, 2001). The extra-thyroid function in mammals remains poorly understood, however based on their localization on respiratory and gastrointestinal epithelia, a host defense function is conceivable (Geiszt *et al.*, 2003).

Light on Nox4: **Physiological Function**

Despite its ubiquitous expression and activity, the primary physiological function of Nox4 is not clear. It is perhaps not wise to pursue one specific role, since it appears that the function Nox4 may depend on its expression site. The most popular working hypothesis is a role in oxygen sensing in the kidney cortex (Geiszt *et al.*, 2000; Gerald *et al.*, 2004; Maranchie *et al.*, 2005; Lee *et al.*, 2006). Also it has been proposed to have role in cell migration, growth, and SMC differentiation, etc.

Nox4-dependent ROS have an important role in the pathogenesis of diabetic nephropathy. Etoh et al. showed increased expression of Nox4 and p22phox in the kidney of streptozotocin-induced diabetic rats (Etoh *et al.*, 2003). They also showed that Nox4 and p22phox co-localized with 8-hydroy-deoxyguanosine (8-OHdG), which is a marker for ROS-induced DNA damage. A causative relationship between Nox4-derived ROS and diabetic nephropathy was shown by Gorin et al., who used antisense oligonucleotides to inhibit

Nox4 expression (Gorin *et al.*, 2005). This treatment effectively reduced ROS production and prevented the development of hypertrophy and increases in fibronectin expression.

Nox4 may have important roles in the cardiovascular system. According to expression studies performed on vascular endothelial cells, Nox4 seems to be the dominant ROS source in endothelial cells (Sorescu *et al.*, 2002; Kuroda *et al.*, 2005). In human umbilical endothelial cells (HUVECs), Nox4 was reported to detect in nuclear fraction and the nuclear fraction of HUVEC cells produced superoxide in an NADPH-dependent manner. In blood vessels, Nox4 is also present in smooth muscle cells and 7-Ketocholesterol, a major oxysterol component in LDL, stimulates its expression. ROS production by Nox4 may be responsible for the oxidative stress induced by 7-ketocholesterol (Pedruzzi *et al.*, 2004). Nox4 is also present in the heart, where cardiac fibroblasts express the enzyme (Szocs *et al.*, 2002). TGF-beta stimulates the conversion of cardiac fibroblasts into myofibroblasts in a ROS-dependent manner. Nox4 is the likely source of oxidants in this process, since downregulation of Nox4 expression by siRNA inhibited both ROS production and the TGF-beta induced expression of smooth muscle actin. Furthermore, many redox-sensitive mitochondrial proteins, including aconitase and components of Complex I and the MPTP, are significantly more oxidized in the mouse heart overexpressing Nox4, and less in the cardiac-specific Nox4 KO heart (Kuroda *et al.*, 2010). It indicated that Nox4 is an important source of oxidative stress in mitochondria during cardiac hypertrophy and failure. In addition, Zhang et al. observed a Nox4-dependent preservation of myocardial capillary density after pressure overload, since Nox4-null animals developed exaggerated contractile dysfunction, hypertrophy, and cardiac dilatation during exposure to chronic overload whereas Nox4-transgenic mice were protected (Zhang *et al.*, 2010). The results showed that cardiomyocyte Nox4 is a unique inducible regulator of myocardial angiogenesis, a key determinant of cardiac adaptation to overload stress.

The involvement of Nox4 in TGF-beta signaling was also described in various cell types, such as pulmonary artery smooth muscle cells (Sturrock *et al.*, 2006; Hecker *et al.*, 2009), HUVECs (Hu *et al.*, 2005; Sturrock *et al.*, 2006) and stem cells (Xiao *et al.*, 2009), which mediates many of the effects of TGF-beta. However, the molecular mechanisms remain poorly defined. It has been reported an increased generation of ROS by Nox4 mediates TGF-β1-induced plasminogen activator inhibitor 1 (PAI-1) gene expression at least in part through oxidative modification and inhibition of MKP-1 leading to a sustained activation of JNK and p38 MAPKs in murine embryo fibroblasts (Liu *et al.*, 2010). PAI-1 is a TGF-β-responsive gene involved in the pathogenesis of many diseases. A similar mechanism may exist in human lung fibroblasts. TGFβ1-mediated fibroblast-to-myofibroblast differentiation of primary human prostatic stromal cells (PrSCs) is

driven via induction of Nox4/ROS signaling (Sampson *et al.*, 2011). Nox4/ROS induce the phosphorylation of c-jun N-terminal kinase (JNK), which subsequently activates the downstream transcriptional program of differentiation.

Nox4 was suggested as a participant in insulin receptor signal transduction (Mahadev *et al.*, 2004). In many cells growth factors and insulin stimulates low-level hydrogen peroxide production. Hydrogen peroxide then inhibits tyrosine phosphatases, thus enhancing the tyrosine phosphorylation induced by the receptor agonists (Rhee *et al.*, 2003). Recently it was shown that Nox4 would be involved in insulin-induced H_2O_2 production in 3T3-L1 adipocytes.

V. Cellular Models

1 HEK293 cells

HEK293 cells were generated by transformation of human embryonic kidney cell cultures (hence HEK) with sheared adenovirus 5 DNA and subsequently demonstrated to be a useful cell type to produce adenovirus, other viral vectors (Graham *et al.*, 1977). HEK 293 cells are very easy to grow and to be transfected. It has been widely used in cell biology research for many years. This cell line expresses endogenous p22phox (Maturana *et al.*, 2001; Ambasta *et al.*, 2004).

This cellular system has been used to study the interaction of Nox proteins with p22phox (Maturana *et al.*, 2001; Ambasta *et al.*, 2004). Immunoprecipitation from transfected HEK293 cells revealed co-precipitation of native p22phox with cyan fluorescent protein-tagged Nox1, Nox2, Nox4 suggesting that there is a direct interaction of the Nox proteins with p22phox.

2 HEK293 T-REx™ Nox4 cells

HEK293 T-REx™ Nox4 cells are HEK293 (human embryonic kidney) cells overexpressing a tet receptor (T-REx™) following transfected with the Nox4-containing tet-on vector (Nox4-pDEST30). Because Nox4 is constitutively active upon heterologous expression, here we used a tet-inducible system that allowed controlled Nox4 expression. T-REx™ is based on the expression of a tet repressor that binds to a modified CMV promoter and thereby maintains the latter in an inactive state. Tet binds to the tet repressor removing it from the promoter, thereby permitting transcription (Figure. 16).

Given the fact that Nox4 generates substantial amounts of ROS without a need for cell stimulation, a stable expression system has some inherent dangers which may lead to an accumulation of DNA mutations, increased mitochondrial ROS generation, and difficult to distinguish the acute Nox4 effects from a long-term antioxidant response. Thus an inducible Nox4 system is preferable to cells stably expressing Nox4.

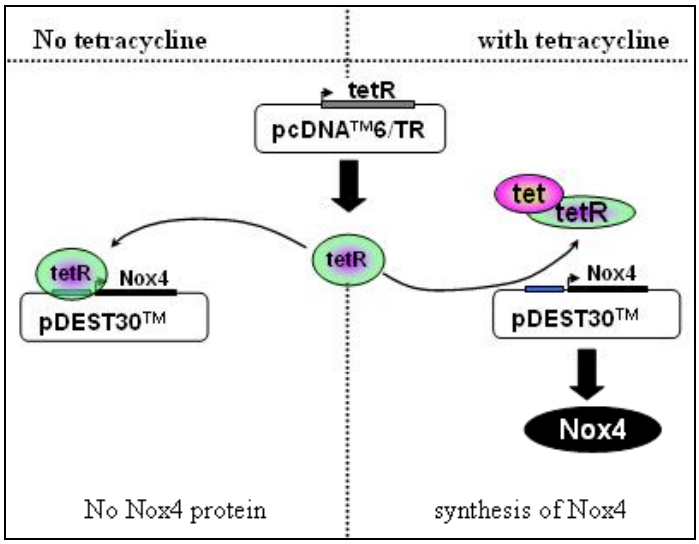

Figure 16. Principle of T-REx™ system. *Tet, tetracycline; See text for additional details.*

3 C-20/A4 chondrocyte cell lines

C-20/A4 chondrocyte cell lines are human chondrocyte cell lines derived from juvenile costal chondrocytes by immortalization with origin-defective simian virus 40 large T antigen (Moulton *et al.*, 1998). Nox4 mRNA is found in chondrocytes (Grange *et al.*, 2006). In the C-20/A4 chondrocyte cell lines, Nox4 constitutes the dominant catalytic subunit and oxidase activity is very low. The C-20/A4 cells have been used in several laboratories to study a variety of general and specific chondrocyte functions, including the expression of MMPs, which are a major component of cartilage degradation during osteoarthritis (Finger *et al.*, 2004). Moreover, the expression of caspases associated with apoptosis (Nuttall *et al.*, 2000), vascular endothelial cell growth factor (VEGF) and VEGF receptors (Pufe *et al.*, 2004) has been reported. Nuttal et al. demonstrated the ability of caspase inhibitors to prevent the C-20/A4 cells and primary human chondrocytes from undergoing apoptosis. They have also been used to evaluate a number of cellular functions that are important for normal chondrocyte physiology (Lee *et al.*, 2000; Browning *et al.*, 2002; Richardson *et al.*, 2003).

VI. The Objectives of Our Work

Nox4 was discovered in the kidney cortex where it is abundantly expressed. It is also found in many other tissues. Because of the extent of its presence, this enzyme may be implicated in several pathologies such as atherosclerosis, hypertension, diabetes, pancreatic cancer, or in oxygen sensing. Thus, to study the structure, the function and the regulation of the activity of Nox4 will provide new ideas and new drug targets for the effective prevention and treatment of clinical diseases related with ROS.

Although knowledge of Nox4 gene expression and its association with biological systems and pathologies is rapidly growing, little is known about the role of Nox4 in the production of reactive oxygen species and the regulation mechanism of oxidase activity. By comparing with other NADPH oxidase family members, Nox4 shows some unique characters.

Our studies are based on the following questions:

1) Are there any other partners to participate in the activation and regulation of Nox4?
2) Does Nox4 exist at the plasma membrane?
3) Since most studies showed that hydrogen peroxide, rather than superoxide, is detected, who is responsible for this unique ability of Nox4?
4) What is the relationship between the structure and function of Nox4?

These questions are hindered by the lack of monoclonal antibodies specific to Nox4. To answer these questions, we tried to produce and use a good tool for Nox4 to further study its function, membrane topology and analyze its interaction with p22phox or other possible partners. Therefore, the object of this work includes:

1) Production, validation and characterization of the monoclonal antibodies specific to Nox4;
2) Possible mechanism involved in the intrinsic hydrogen peroxide formation of Nox4;
3) Characterization of the diaphorase activity of Nox4 in an acellular model based on purified recombinant proteins;
4) Develop a new manner to study the topology information of the membrane protein: Nox4 and p22phox.

Part 2 Research Work

Chapter 1: Validation and characterization of the first monoclonal antibodies against NADPH oxidase Nox4: essential tools for the structural and immunochemical investigations.

Résumé en français

1 Introduction

Les dérivés réactifs de l'oxygène (ROS) produits à bas niveau sont impliqués dans de multiples voies de signalisation aboutissant à des processus cellulaires tels que la prolifération, l'apoptose, la sénescence ou le cancer. Ces dérivés sont essentiellement produits par une famille d'enzymes: Les NADPH oxydases. Cette famille est composée de cinq membres, dont fait partie l'oxydase des phagocytes Nox2 qui est étudiée depuis plus 20 ans. A l'inverse, l'oxydase Nox4 malgré une expression très largement distribuée au niveau tissulaire est très mal connue. Beaucoup de questions restent encore sans réponse en particulier: la localisation sub-cellulaire de cette enzyme, les modifications post-traductionnelles, son activation, ses partenaires.

Les seuls outils, actuellement non disponibles et nécessaires pour pouvoir répondre à ces questions sont des anticorps monoclonaux spécifiques de Nox4.

2 Objectifs et méthodes

L'objectif de ce travail est ciblé sur la préparation d'anticorps monoclonaux (ACm) dirigés contre Nox4 et leur caractérisation avec successivement:

- La production d'anticorps monoclonaux dirigés contre une construction de Nox4 recombinant;
- L'étude de leur spécificité;
- L'analyse des caractéristiques moléculaires des 5 clones sélectionnés.

A terme, à l'aide de ces ACm, on cherchera à étudier la localisation subcellulaire de Nox4 dans les cellules HEK293, par différentes approches: immunochimie et imagerie.

Les anticorps monoclonaux ont été produits par la société Biotem à partir de protéine recombinante

correspondant à la partie C-terminale de Nox4 (AA: 207-578) synthétisée et purifiée au laboratoire. La validation des anticorps a été faite par western blot sur des constructions de Nox4 recombinant, en cellule entière, par FACS ou western blot sur les HEK293 surexprimant ou non Nox4, soit de façon stable (HEK293Nox4GFP) soit de façon inductible après addition de tétracycline (TRex-Nox4).

Les épitopes des différents anticorps ont été identifiés par technique de phage display et sur différentes constructions de la protéine recombinante Nox4 tronquée.

La localisation subcellulaire de Nox4 à été analysée par microscopie confocale, par la technique TIRF (Total Internal Reflection Fluorescence) et par FACS.

3 Résultats

- L'antigène est la protéine tronquée Nox4 recombinante (résidus 206 à 578): elle contient la partie cytosolique, le 6ème passage transmembranaire, la dernière boucle extracellulaire comprise entre le 5ème et le 6ème passage transmembranaire ainsi qu'une étiquette poly-histidine et un S tag en position N terminale. Cette protéine purifiée est utilisée pour la préparation des anticorps monoclonaux (société Biotem).
- Cinq anticorps monoclonaux (5F9, 6B11, 8E9, 10B4, 7C9) ont été obtenus: leur spécificité a été validée d'une part sur l'antigène NHS-Nox4A-1TM par ELISA (société Biotem) et par western blot (notre laboratoire), d'autre part par western blot et FACS en cellule entière surexprimant Nox4 (HEK-Nox4, TRex-Nox4) .Les résultats démontrent la spécificité de 3 anticorps (5F9, 6B11, 8E9) pour Nox4. L'analyse par FACS des cellules TRex-Nox4, révèle que l'anticorps 8E9 est le seul à permettre un marquage des cellules sans perméabilisation. Ce résultat suggère une localisation de Nox4 à la membrane plasmique. Les résultats de microscopie confocale ainsi que ceux obtenus par la technique de TIRF confirment la localisation de Nox4 non seulement au niveau du réticulum endoplasmique mais aussi à la membrane plasmique.
- Par technique de phage display et sur différentes constructions de la protéine recombinante Nox4 tronquée, les épitopes des différents anticorps ont été identifies. L'épitope de 8E9 est ^{222}H-E^{241}, l'épitope de 5F9 est ^{392}D-F^{398}, l'épitope de 6B11 est ^{389}S-P^{416}.
- La présence de l'anticorps 5F9 ou 6B11 a entraîné une inhibition modérée mais significative de l'activité oxydase en système acellulaire. Par contre, l'anticorps 8E9 n'a pas d'effet sur l'activité oxydase de Nox4. Ce qui indique que les anticorps 5F9 et 6B11 interagissent avec une région importante pour le transfert

d’électron.

Summary in English

1 Background

Reactive oxygen species (ROS) are involved in multiple signaling pathways leading to cellular processes such as proliferation, apoptosis, senescence or cancer. Therefore, it is of great importance to identify the molecular sources for the production of ROS and understand their regulation. As we know now, these derivatives are primarily produced by a family of enzyme: the NADPH oxidase, or Nox. Nox2, the prototype, phagocytic oxidase, has been well studied, while the oxidase Nox4 is still poorly understood despite its wide distribution in tissues. The activity of Nox4 is constitutive and Nox4 involved ROS may be implicated in several pathologies. Thus, the study of structure, function and regulation of the activity of Nox4 will provide new ideas and new drug targets for the effective prevention and treatment of clinical diseases related with ROS. Many questions remain unanswered: the subcellular localization of this enzyme, the post-translational modifications, its activation and its partners, the topology of Nox4, etc. One tool, currently unavailable, is needed to answer these questions: specific monoclonal antibodies to Nox4.

This study emphasizes the production, validation and characterization of 5 monoclonal antibodies raised against Nox4. These antibodies were also used to clarify the subcellular localization of Nox4 in HEK293 cell lines. Due to their respective properties, these reported mAbs will be useful tools in studying subcellular localization/structure/function relationship of Nox4 and the regulation of Nox4 activity.

2 Generation and validation of monoclonal antibodies raised against recombinant Nox4

5 novel monoclonal antibodies, named 5F9, 6B11, 8E9, 10B4, 7C9, were developed. The antigen used for the immunization of the mice corresponded to a Nox4 truncated protein from the amino acid 206 to 578 and named NHS-Nox4-1TM. This truncated protein contained the cytosolic part of Nox4 plus the 6th potential transmembrane helix, the last extracellular loop between the 5th and 6th transmembrane helices and a poly-histidine tag at the N terminal position.

The specificity of these antibodies was first validated by Elisa (Biothem Co.) and western blot using the antigen NHS-Nox4-1TM (Fig. 1). Then, the ability of the 5 purified mAbs to bind the full length Nox4 *ex vivo* were investigated by using 2 cell lines (HEK293 cells overexpressing Nox4 fused with a GFP tag at the C terminus and HEK293 T-REx^{TM} Nox4 cells which overexpress Nox4 upon tetracycline induction) and kidney cortex by western blot (Fig. 2). Finally, the binding of the purified mAbs to native antigen was further investigated by FACS on intact and Triton X-100 permeabilized T-REx^{TM} Nox4 cells (Fig. 3).

- ✓ The results showed that among 5 mAbs, 3 of them (8E9, 5F9, 6B11) specifically recognized Nox4 protein in HEK293 transfected cells or human kidney cortex;
- ✓ 58 kDa, instead of 66.9 kDa, is the size of Nox4 detected in two different cell lines over-expressing Nox4. 68 kDa is the size of Nox4 detected in kidney;
- ✓ The different sizes of Nox4 obtained from different denaturation protocol in western blot experiment suggested a high sensitivity of Nox4 to heat degradation (Fig. S3);
- ✓ The immunoreactivity of mAb 8E9 on non-permeabilized cells suggested that Nox4 might be expressed at the plasma membrane of tet-induced T- REx^{TM} Nox4 cells.

3 Subcellular localization of NADPH oxidase 4

Nox4 has been detected in several cellular compartments and it has been proposed that the biological function of Nox4 links to its subcellular localization (Chen ***et al.***, 2008). As reported recently (Martyn ***et al.***, 2006; Helmcke ***et al.***, 2009), Nox4 was shown to be located in the ER of HEK293 transfected cells. In our study, subcellular localization of Nox4 in HEK293 transfected cells was investigated with 3 mAbs (8E9, 5F9, 6B11) by confocal microscopy and Total Internal Reflection Fluorescence (TIRF) microscopy, in which the plasma membrane close to the glass surface is visualized preferentially.

- ✓ When cells were not permeabilized, Nox4 was observed only at the plasma membrane of tet-induced T- REx^{TM} Nox4 cells with mAb 8E9 by confocal microscopy (Fig. 7A). This result was further confirmed by TIRF microscopy (Fig. 8);
- ✓ When cells were permeabilized, Nox4 was detected as well at the plasma membrane than in the perinuclear and endoplasmic reticulum regions of tet-induced T- REx^{TM} Nox4 cells (Fig. 7B). This multi-cellular distribution was also found in the same fluorescence localization of Nox4GFP in HEK293Nox4GFP cells (Fig. 7C);
- ✓ An interesting phenomenon is that the labeling of mAb 5F9 was mainly intracellular and no clear signal could be observed at the plasma membrane.

4 Characterization of monoclonal antibodies raised against recombinant Nox4

To identify specific inhibitor of Nox4 activity, the effect of mAbs on the NADPH oxidase activity in a cell-free system was analyzed using chemiluminescence. Total lysates of tet-induced T- REx^{TM} Nox4 cells were pre-incubated with an excess of mAb for 30min on ice before adding reaction mixture. The data

demonstrated a moderate but significant inhibition of constitutive Nox4 activity by mAbs 5F9 and 6B11 compared to the activity measured in the presence of an irrelevant mAb (Fig. 9). To understand which region was important for the electron transfer, a phage-display experiment was applied to define the antibody epitopes (Fig. 6) combined to the use of different recombinant constructions of truncated Nox4 (Fig. 5).

- ✓ Phage display analysis showed that 10B4 recognizes an epitope on the last extracellular loop of Nox4 (^{210}G-L^{219}), while mAb 5F9 is directed to cytosolic tail of Nox4 (^{392}D-F^{398});
- ✓ Immunoblotting analysis of different Nox4 truncated forms suggested that the epitope region of mAb 8E9 was on the extracellular E loop of Nox4 (^{222}H-E^{241}), mAb 6B11 bound a region at the C-terminal part of Nox4 (^{389}S-P^{416}) and mAb 7C9 was also directed to cytosolic tail of Nox4 (^{362}E-S^{389});
- ✓ The region of Nox4 (^{389}S-P^{416}), especially the region of Nox4 (^{392}D-F^{398}) might be important for the electron transfer.

My contribution to this work was 1) to validate and characterize 5 mAbs raised against recombinant Nox4 by western blot and FACS, 2) to study the subcellular localization of Nox4 in HEK293 transfected cells by confocal microscopy and TIRF; 3) to analyze the effect of Nox4 mAbs on the constitutive NADPH oxidase activity and 4) to determine the epitope region of these mAbs.

Article 1:

New insight into the Nox4 subcellular localization in HEK293 cells: First monoclonal antibodies against Nox4. ***Leilei Zhang****, Minh Vu Chuong Nguyen, Bernard Lardy, Algirdas J. Jesaitis, Alexei Grichine, Francis Rousset, Monique Talbot, Marie-Hélène Paclet, GuanXiang Qian and Françoise Morel*

Biochimie 93 (2011) 457–468

Contents lists available at ScienceDirect

Biochimie

journal homepage: www.elsevier.com/locate/biochi

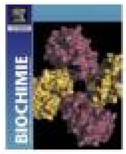

Research paper

New insight into the Nox4 subcellular localization in HEK293 cells: First monoclonal antibodies against Nox4

Leilei Zhang [a,b], Minh Vu Chuong Nguyen [a], Bernard Lardy [a], Algirdas J. Jesaitis [c], Alexei Grichine [d], Francis Rousset [a], Monique Talbot [e], Marie-Hélène Paclet [a], GuanXiang Qian [b], Françoise Morel [a,*]

[a] GREPI TIMC-Imag UMR-CNRS 5525, Enzymologie/CHU Albert Michallon, BP 217, 38043 Grenoble, France
[b] Department of Biochemistry and Molecular Biology, Research Center for Human Gene Therapy, School of Medicine, Shanghai Jiao Tong University, Shanghai 200025, PR China
[c] Department of Microbiology, Montana State University, Bozeman, MT 59717, USA
[d] Plateforme 'Optical Microscopy – Cell Imaging' – UJF, Inserm U823, Institut Albert Bonniot, 38076 La Tronche, France
[e] UMR-CNRS 8200, Institut de cancérologie Gustave Roussy, 94805 Villejuif, France

A R T I C L E I N F O

Article history:
Received 7 June 2010
Accepted 3 November 2010
Available online 12 November 2010

Keywords:
NADPH oxidase 4
Monoclonal antibodies
Subcellular localization
O_2

A B S T R A C T

Nox4, a member of Nox family of NADPH oxidase expressed in nonphagocytic cells, is a major source of reactive oxygen species in many cell types. But understanding of the role of Nox4 in the production of ROS and of regulation mechanism of oxidase activity is largely unknown. This study reports for the first time the generation and characterization of 5 mAbs against a recombinant Nox4 protein (AA: 206–578). Among 5 novel mAbs, 3 mAbs (8E9, 5F9, 6B11) specifically recognized Nox4 protein in HEK293 transfected cells or human kidney cortex by western blot analysis; mAb 8E9 reacted with intact tet-induced T-REx™ Nox4 cells in FACS studies. The other 2 mAbs 10B4 and 7C5 were shown to have a very weak reactivity after purification. Immunofluorescence confocal microscopy showed that Nox4 localized not only in the perinuclear and endoplasmic reticulum regions but also at the plasma membrane of the cells which was further confirmed by TIRF microscopy. Epitope determination showed that mAb 8E9 recognizes a region on the last extracellular loop of Nox4, while mAbs 6B11 and 5F9 are directed to its cytosolic tail. Contrary to mAb 6B11, mAb 5F9 failed to detect Nox4 at the plasma membrane. Cell-free oxidase assays demonstrated a moderate but significant inhibition of constitutive Nox4 activity by mAbs 5F9 and 6B11. In conclusion, 5 mAbs raised against Nox4 were generated for the first time. 3 of them will provide powerful tools for a structure/function relationship of Nox4 and for physiopathological investigations in humans.

1. Introduction

NADPH oxidase, Nox4, belongs to the Nox family which could generate reactive oxygen species (ROS) by transferring an electron to molecular oxygen. All these members contain six putative transmembrane helices, conserved binding sites for FAD and NADPH, and four heme-binding histidines in the third and fifth transmembrane domain [1]. Nox2 is the prototype of the Nox family [2]: it is essentially present in phagocytes and a well studied characterized source for ROS production. By interacting with the membrane-bound $p22^{phox}$, it becomes the heterodimer flavocytochrome b_{558}. This core unit assembles with various cytosolic regulating and activating factors $p47^{phox}$, $p67^{phox}$, $p40^{phox}$, and Rac 1/2 being recruited upon activation, at the membrane level from cytosol [3–5].

Nox4 is a ubiquitous protein with 39% identity to Nox2 [6–8]. Although originally identified and highly expressed in the kidney, Nox4 mRNA was also reported in many human and murine tissues [6,8,9]. Nox4 is a $p22^{phox}$-dependent enzyme which co-immunoprecipates with $p22^{phox}$, and stabilizes the $p22^{phox}$ protein [10]; Contrary to Nox2, the activity of Nox4, is constitutive: it is active without the need for cell stimulation [6,7,11,12] and does not require the assembly of cytosolic factors. $P22^{phox}$ is the only component necessary for its activity. Recently, Poldip2 (polymerase

Abbreviations: IPTG, Isopropyl β-d-1-thiogalactopyranoside; ER, endoplasmic reticulum; ROS, reactive oxygen species; DFP, Diisopropylfluoro-phosphate; eGFP, enhanced Green Fluorescent Protein; SOD, Superoxide dismutases; CAT, catalase; TIRF, Total Internal Reflection Fluorescence; HEK, human embryonic kidney; VSMC, vascular smooth muscle cell; FAD, flavin adenine dinucleotide.

* Corresponding author. Tel.: +33 (0) 4 76 76 57 52; fax: +33 (0) 4 76 76 56 08.
E-mail addresses: zll1981@hotmail.com (L. Zhang), mvchuong@yahoo.fr (M.V.C. Nguyen), blardy@chu-grenoble.fr (B. Lardy), umbaj@montana.edu (A.J. Jesaitis), alexei.grichine@ujf-grenoble.fr (A. Grichine), francisrousset@yahoo.fr (F. Rousset), Talbot@igr.fr (M. Talbot), MHPaclet@chu-grenoble.fr (M.-H. Paclet), qiangx@shsmu.edu.cn (GuanXiang Qian), FrMorel.enzymo@chu-grenoble.fr (F. Morel).

0300-9084/$ – see front matter
doi:10.1016/j.biochi.2010.11.001

DNA-directed delta-interacting protein 2) was introduced as a novel Nox4/p22^{phox}-interacting protein: it is a potent positive regulator of Nox4 activity in VSMC [13].

Despite its ubiquitous expression and activity, the primary function of Nox4 derived ROS is not clear. It has been proposed to have a role in oxygen sensing, growth, senescence and differentiation [14]. The abnormal expression and activation of Nox4 may induce tumorigenesis, tumor angiogenesis [15], and be related with the occurrence and development of other diseases, such as hypertension [16,17], atherosclerosis [18], fibrosis [19] and osteoarthritis [20]. Although the reasons for these differences are not quite clear, an important clue to the biological function of Nox4 links to its subcellular localization [21]. Localization studies of Nox4 remain controversial. Nox4 was shown primarily to be located in perinuclear and endoplasmic reticulum regions of COS7, HEK293 and endothelial cells [11], but it was also detected at the plasma membrane [22], focal adhesion and within the nucleus [8]. It may not be surprising that the same protein displays distinct localization in different cell types. However, different Nox4 localization was also reported in human vascular endothelial cells [21,23]. It will be interesting to know whether these different localizations could be due to the specificity between different Nox4 antibodies used. It may also come from the different physiological and pathological state of cells, as different intracellular localization of Nox4 was reported in normal and pathological human thyroid tissues [24].

Although the knowledge of gene expression and Nox4 association with pathologies is rapidly growing, understanding of the role of Nox4 in the production of reactive oxygen species and of regulation mechanism of oxidase activity has been hindered by the lack of specific monoclonal antibodies which are also essential tools to provide direct evidence to topology models and to identify structural features of heterodimer with p22^{phox}.

In this present study, we report for the first time the generation and characterization of 5 novel monoclonal antibodies raised against a truncated recombinant protein (residues 206–578) of Nox4, which were then used to clarify the subcellular localization of Nox4 in human embryonic kidney cell lines. These Nox4-reactive mAbs were epitope mapped by phage-display analysis or by immunodetection of recombinant Nox4 truncated constructions and were examined for effects on Nox4 oxidase activity. Due to their respective properties, these mAbs reported in this study will be valuable in characterizing the regulation of Nox4 activity, the subcellular localization/function relationship of Nox4, therefore to provide new drug targets for the effective prevention of diseases related to ROS.

2. Materials and methods

2.1. Materials

DMEM, fetal bovine serum, neomycin (G418, geneticin) were purchased from GIBCO; Alexa Fluor 488 F(ab') fragment of goat anti-mouse IgG(H + L) was purchased from Invitrogen; ECL Western Blotting Detection reagents were purchased from Amersham Biosciences; complete mini EDTA-free protease inhibitor EASYpack, Atto-565-concanavalin A, $Na_4P_2O_7$, Na_2VO_4, PMSF, luminol, isoluminol, Triton X-100, Chaps, Isopropyl β-D-1-thio-galactopyranoside(IPTG) and monoclonal antibody anti-poly-Histidine-peroxidase were purchased from SIGMA; okadaic acid, leupeptin, pepstatin, trypsin inhibitor, TLCK, and protein G Agarose were purchased from Roche; Hoechst 33258 was purchased from Molecular Probes; DTP was purchased from Acros Organics; GFP mAb and isotype antibodies were purchased from Santa Cruz; Lab-Tek II chamber slide and Lab-Tek chambered coverglass were purchased from Thermo; Goat anti-Mouse IgG-HRP was purchased from GE healthcare; HiPerFect Transfection Reagent was purchased from QIAGEN; HEK293 T-REx™ Nox4 cells, siRNA a and c were generous gifts from PATIM laboratory, Pr KH. Krause, Geneve university, Switzerland; pET15b ΔT/Stop ZEBRA/MD4-eGFP plasmid was obtained from TheREx laboratory, Pr JL. Lenormand (TIMC-Imag, UMR-CNRS 5525, Grenoble, France).

2.2. Cell culture

All cells were cultured in DMEM containing 4.5 g/L glucose and 0.11 g/L sodium pyruvate, supplemented with 10% (v/v) fetal bovine serum and 100 units/ml penicillin and 100 μg/ml streptomycin and 2 mM glutamine at 37 °C in air with 5% CO_2. Selecting antibiotics, blasticidin (5 μg/ml) and neomycin (400 μg/ml) were used with HEK293 T-REx™ Nox4 cells, while neomycin (500 μg/ml) was used with HEK293 Nox4GFP cells.

2.3. Generation of plasmids for the expression of recombinant Nox4 proteins

2.3.1. Truncated Nox4 proteins coupled with a His-tag at the N terminus

pET30b plasmid (Novagen) was used to express NHS-Nox4-1TM protein corresponding to the amino acid 206–578 of Nox4. PCR fragments corresponding to the Nox4 (206–578)-truncated form were obtained by using pEF/Nox4 plasmid as a matrix with the forward primer 5'-GGA ATT CTC CAT GCT CTT GCA TGT TTC AGG AGG GCT GC-3'including a *Not*I site (underlined) and the reverse primer 5'-CCG TTA CTC GAG TCA GCT GAA AGA CTC TTT ATT GTA TTC-3'. The *Xho*I restriction site of the reverse primers is underlined. The purified PCR product was digested with *Not*I and *Xho*I and ligated into linearized pET30b plasmid to obtain a plasmid encoding for NHS-Nox4-1TM protein. PCR fragments corresponding to the other various Nox4 truncated forms 1–10 (Table S1) were obtained by using pET30b Nox4-1TM as a matrix with each forward primers and reverse primers (Table S1) including a *Not*I and *Xho*I restriction site (underlined). The purified PCR products were digested with *Not*I and *Xho*I and ligated into linearized pET30b plasmid to obtain plasmids encoding for various Nox4 truncated forms (Table S1).

2.3.2. Truncated Nox4 proteins coupled with a His-tag at the C-terminus

pIVEX2.3MCS plasmid (Roche) was used to express Nox4-1TM-CH (AA: 206–578) and Nox4$_{loc}$-CH (AA: 309–578). PCR fragments corresponding to the Nox4 (206–578) or (309–578)-truncated forms were obtained by using pEF/Nox4 plasmid as a matrix with the forward primer 5'-GGA TGA GCG GCC GCG GCT TGC ATG TTT CAG CAG CCC TGC-3' for Nox4 (206–578) or with the forward primer 5'-GGA TGA GCG GCC GCC AGT CCA TCA TTT CGG TC-3' for Nox4 (309–578) including a *Not*I site (underlined) and the reverse primer 5'-GCG TTA CTC GAG TTG CTG AAA GAC TCT TTA TTG TAT TC-3'. The *Xho*I restriction site of the reverse primers is underlined. The purified PCR product was digested with *Not*I and *Xho*I and ligated into linearized pIVEX2.3MCS plasmid.

2.4. Nox4 truncated proteins produced by in vitro translation (RTS, rapid translation system)

Expression for each protein was performed using the RTS^{100} HY100 (Roche Applied Science) according to the manufacturer's instructions. 5 μl of the reaction was used for western blot experiments [25,26].

2.5. Generation of monoclonal antibodies raised against Nox4 truncated protein (AA: 266–578)

Mice immunization and monoclonal antibody production were carried out by Biotem Co. Briefly, Balb/c mice were immunized by three intraperitoneal injections of 50 μg NHS-Nox4-1TM (AA: 266–578) used as antigen and diluted with adjuvant. 12 days later, mice received a last injection of antigen. Three days after the last injection, the spleen cells were fused with myeloma cells. Hybrids producing specific monoclonal antibodies which were positive for the antigen and negative for ZEBRA/MD4-GFP protein by ELISA were selected. ELISA-positive hybridoma clones (Biotem Co) were cloned twice. Monoclonal antibodies were produced in the ascite of nude mice. Monoclonal antibodies were purified from ascitic fluid after isotype identification. The isotype for 8E9 and 7C9 is IgM, the isotype for 10B4 is IgG1, the one for 5F9 and 6B11 is IgG2a and IgG2b respectively (Biotem Co.).

2.6. Purification of immunoglobulins from ascitic fluids

Ascitic fluids were centrifuged at 10,000*g* for 30 min at 4 °C. IgG were purified from the supernatant of centrifugation on protein G Sepharose. Depending on the Ig isotype, protein G Sepharose was equilibrated with 100 mM H_3BO_3 pH8.9 containing 3M NaCl for IgG1 purification or 20 mM Na_2HPO_4 pH7 for IgG2 purification. After extensive washes, IgG were eluted with 0.1 M glycine pH3 [27]. Purified Ig were dialyzed against PBS and stored at −20 °C. IgG purification was controlled by SDS-PAGE. IgM was purified on Sephacryl S300 by gel filtration [28]. Purified antibodies were dialyzed against PBS and stored at −20 °C.

2.7. Expression of various Nox4 truncated forms 1–10 (Table S1)

BL21(λDE3) Codon Plus-RIL bacteria (Stratagen) transformed with different recombinant plasmids were grown in LB medium supplemented with Kanamycin (50 μg/ml) and Chloramphenicol (40 μg/ml) and allowed to grow to reach an OD_{600} of 0.7–1. then bacteria were induced by IPTG at a final concentration of 1 mM at 16 °C overnight. Bacteria pellets were lysed by sonication in lysis buffer (50 mM Tris pH7.5, 100 mM NaCl, 15 mM DTT, 0.1% Chaps, 2 μg/ml leupeptin, 2 μg/ml pepstatin, 10 μM TLCK) and the lysates were centrifuged at 30,000*g* at 4 °C for 30 min to obtain total protein. Supernatant was collected and stored at −80 °C until further use.

2.8. Cell-free oxidase assay

Whole cell extracts were prepared using the Chaps lysis buffer. Cells were treated with 3 mM DFP and then lysed in Chaps lysis buffer containing 20 mM Tris–HCl pH7.4, 1% (v/v) Chaps, 150 mM NaCl, 1 mM EDTA, 10 mM $Na_4P_2O_7$, 10 nM okadaic acid, 2 mM Na_3VO_4, 2 μg/ml leupeptin, 2 μg/ml pepstatin, 10 μg/ml trypsin inhibitor, 44 μg/ml PMSF, 10 μM TLCK and complete mini EDTA-free protease inhibitor. After 10 min incubation on ice, the mixture was centrifuged at 10,000*g* for 30 min at 4 °C and the supernatant was collected. An appropriate amount of cell lysates (50 μg of protein) were pre-incubated with Nox4-specific or irrelevant mAb (40 μg) for 30 min on ice. Then 10 μM FAD was added to the cell lysates in a final volume of 50 μl. After 5 min incubation on ice, cell lysates were transferred to the Corning Costar 96 well Assay Plate. The reaction was initiated by addition of 200 μl PBS containing 20 μM luminol, 10 units/ml horseradish peroxidase, 10 μM FAD and 150 μM NADPH. Photon emission was recorded at 37 °C for 1 h with a luminescan (Labsystem, Pontoise, France).

2.9. SDS/PAGE and Western Blotting

2.9.1. In vitro experiments

Mammalian cells were treated with 3 mM DFP and then lysed in Triton lysis buffer containing 20 mM Tris–HCl pH7.4, 1% (v/v) Triton X-100, 150 mM NaCl, 1 mM EDTA, 10 mM $Na_4P_2O_7$, 10 nM okadaic acid, 2 mM Na_3VO_4, 2 μg/ml leupeptin, 2 μg/ml pepstatin, 10 μg/ml trypsin inhibitor, 50 mM NaF, 20 μg/ml aprotinin, 44 μg/ml PMSF, 10 μM TLCK and complete mini EDTA-free protease inhibitor. After 10 min incubation on ice, the mixture was centrifuged at 10,000*g* for 30 min at 4 °C. Supernatant was collected and stored at −80 °C until further use.

2.9.2. In vivo experiments

Homogenate from human renal cortex was prepared in the following Triton lysis buffer containing 20 mM Tris–HCl pH7.4, 1% (v/v) Triton X-100, 150 mM NaCl, 5 mM EDTA, 2 mM Na_3VO_4, 10 mM

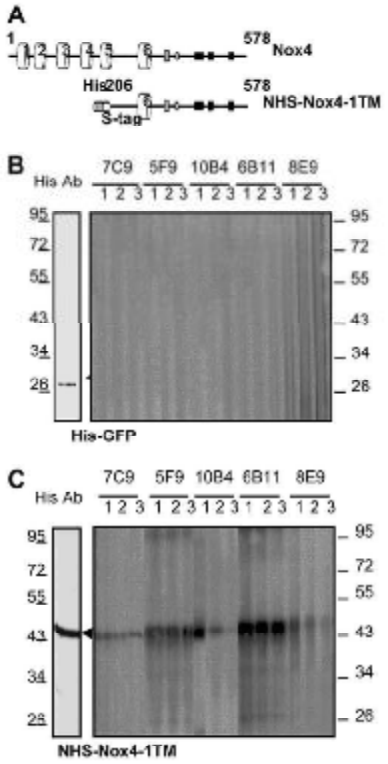

Fig. 1. Specificity of novel mAbs directed against the antigen. (A) Schematic representation of the antigen used to develop Nox4 mAbs. Full-length Nox4 is presented at the top of the diagram. Transmembrane domains (1–6) are shown. Its cytoplasmic FAD and NADPH binding sites are represented by rectangles, filled gray and black, respectively. The antigen NHS-Nox4-1TM (AA: 266–578, 44 kDa) is a Nox4 truncated form expressed as an N-terminal His-tagged protein; (B) Specificity of Nox4 mAbs to the antigen. NHS-Nox4-1TM was produced by IPTG induction and a His-tagged GFP (His-GFP) was synthesized by in vitro translation assay (RTS); they were used to evaluate the specificity of novel mAbs against Nox4. Asterisk indicates the position of His-GFP and arrow indicates the position of NHS-Nox4-1TM added as 1 μl from 2 ml elution fraction. The dilution of the antibodies (ascite) in PBS is indicated as follows: 1, 1/100; 2, 1/500 and 3, 1/1000. Immune complexes were detected by ECL after binding with peroxidase. These pictures are representative of 2 experiments.

$Na_4P_2O_7$, 10 mM okadaic acid, 20 μg/ml leupeptin, 2 μg/ml pepstatin, 10 μg/ml trypsin inhibitor, 50 mM NaF, 1 mM PMSF, 10 μM TLCK and 20 μg/ml aprotinin using a Dounce homogenizer (Kontes Glass Co., Vineland, N. J.). Homogenate was incubated for 1 h on ice and centrifuged at 10,000g for 15 min at 4 °C. Supernatant was collected and stored at −80 °C until further use.

A fraction aliquot of 10,000g soluble extracts supernatant of HEK293 Nox4GFP cells (200 μg) or of T-REx™ Nox4 cells (200 μg) or of human kidney homogenates (60 μg) or of bacteria (5 μg) was denatured at 60 °C for 1 h or 4 °C overnight or 95 °C for 5 min and loaded on a 10% or 12.5% (p/v) SDS-PAGE for migration and then electro-transfered to nitrocellulose, as previously described [29]. Immunodetection was performed using primary monoclonal antibodies against Nox4 (dilution 1:500) or monoclonal antibody directed against the cytosolic domain of $p22^{phox}$ (16G7) (dilution 1:5000) [30] or monoclonal GFP antibody (dilution 1:1000). The immune complexes were detected with a secondary antibody combined with peroxidase (1:5000). The bound peroxidase activity was detected using ECL reagents.

Human kidney sections (5 μm thick) were prepared from paraffin embedded tissues. Briefly, sections were deparaffined with xylene, dehydrated by ethanol and rehydrated with water. After pretreatment, antigen retrieval was done by EDTA pH8 at 98 °C for 40 min. Sections were incubated for 10 min with 3% (v/v) H_2O_2 in water to quench the endogenous peroxidase activity. Primary antibodies were diluted 1/100, incubated for 60 min at room temperature and thereafter rinsed with PBS. The EnVision (K4007, Dako) signal enhancement system was used to develop the bound antibodies. Sections were counterstained with Mayers haematoxylin, dehydrated, mounted and examined by light microscope (Leica DMRXA).

3.10. Flow cytometry

HEK293 T-REx™ Nox4 cells suspended in PBS/BSA/$CaCl_2$ (PBS containing 0.2% (w/v) BSA and 0.5 mM $CaCl_2$) were neither fixed nor permeabilized, or cells suspended in PBS were fixed with 1% (w/v) paraformaldehyde for 15 min on ice and resuspended at the concentration of 10^7 cells/ml in PBS/BSA/$CaCl_2$ containing 0.1% (v/v) Triton X-100 for the permeabilization. 10^6 cells were then incubated on ice for 30 min with 5 μg of mouse monoclonal Ig (irrelevant Ig or specific Ig) diluted in 100 μl of PBS/BSA/$CaCl_2$ buffer. Cells were washed twice and resuspended in 150 μl of the Alexa Fluor 488 goat anti-mouse antibody diluted 1:200 in PBS/BSA/$CaCl_2$ buffer. After 30 min incubation on ice, cells were washed. Fluorescence intensity (FL1) of the cells was measured on a FACScalibur (Becton Dickinson) cytometer [31].

2.11. Phage-display epitope mapping

Monoclonal antibodies 5F9 and 10B4 were epitope mapped by selecting peptide sequences from J404 nonapeptide library [32] by 3 successive rounds of affinity purification on antibodies covalently coupled to Sepharose followed by amplification on bacterial lawns on nutrient media, as previously described [33]. After selection, high affinity mAb-binding clones were identified after replica-plating on nitrocellulose and immunoblot analysis, then purified and sequenced. 24 to 33 nonapeptide sequences were obtained for the 2 mAbs selections and were aligned visually as well as by the EPIMAP algorithm [34].

2.12. Confocal microscopy

3×10^4 HEK293 T-REx™ Nox4 cells were seeded on chamber slide. When the cells reached ~60% confluence, they were

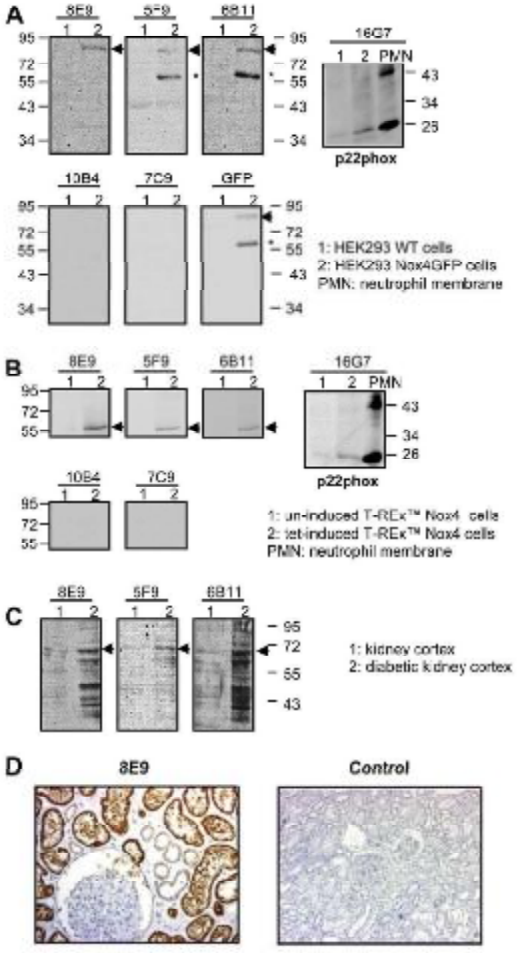

Fig. 2. Immunodetection of Nox4 expression in human embryonic kidney cell lines and human kidney cortex. (A) Immunodetection of Nox4GFP or $p22^{phox}$ in HEK293 Nox4GFP cells. Total lysates of HEK293 WT cells and HEK293 Nox4GFP cells (200 μg/lane) were analyzed by Western blot to evaluate the capacity of Nox4 mAbs (1:500) to bind to Nox4GFP. Proteins were denatured at 4 °C overnight. Control of expression was performed with anti-GFP mAb (1:500). The expression of $p22^{phox}$ was detected by monoclonal antibody anti-p22 (16G7, 1:5000). 1: HEK293 WT cells, 2: HEK293 Nox4GFP cells, PMN: Neutrophil membrane. Arrow indicates full-length Nox4GFP protein (85 KDa), asterisk indicates degraded Nox4GFP protein (58 KDa); (B) Immunodetection of Nox4 or $p22^{phox}$ in tet-induced HEK293 T-REx™ Nox4 cells. Total lysates of un-induced and tet-induced HEK293 T-REx™ Nox4 cells (200 μg/lane) were analyzed by western blot using 5 Nox4 mAbs (1:500) or monoclonal antibody anti-p22 (16G7, 1:5000). Arrow indicates full-length Nox4 protein (58 KDa). 1: un-induced T-REx™ Nox4 cells, 2: tet-induced T-REx™ Nox4 cells. PMN: Neutrophil membrane fractions complexes were detected by ECL after binding with peroxidase. These pictures are representative of at least 5 experiments; (C) Immunodetection of Nox4 in human kidney cortex. Homogenates were prepared in Triton X-100 lysis buffer using a Dounce homogenizer from human renal cortex as described in materials and methods: they were incubated for 1 h on ice and centrifuged at 10,000g for 15 min at 4 °C. Proteins presented in the soluble fraction (supernatant) were denatured at 4 °C overnight and analyzed by western blot (60 μg/lane). Expression of Nox4 was checked by 3 purified Nox4 mAbs (8E9(1:500), 5F9(1:500), 6B11(1:500); 1: normal kidney cortex, 2: diabetic kidney cortex. Immune complexes were detected by ECL after binding with peroxidase. Immunodetection of Nox4 by mAbs 8E9 and 5F9 was repeated twice. (D) Immunohistochemical detection of Nox4 on human kidney sections by purified mAb 8E9 (1:100 overnight). DAB reaction. Photographed and printed to a total magnification of ×100 for the left picture, and ×50 for the right (control).

incubated for 16 h with tetracycline to induce Nox4 expression. Un-induced and induced HEK293 T-REx™ Nox4 cells were fixed with 4% (w/v) paraformaldehyde for 10 min at room temperature. Paraformaldehyde fluorescence was then quenched by 50 mM NH_4Cl for 10 min at room temperature. After two washes with PBS, cells were unpermeabilized or permeabilized with 0.1% (v/v) Triton X-100 for 5 min at room temperature, followed by two washes with PBS containing 1% (w/v) BSA; Then cells were incubated for 1 h at room temperature with 5 μg of mouse monoclonal Ig (irrelevant Ig or specific Ig) diluted in 200 μl of PBS/BSA/$CaCl_2$ buffer. Following washes, a secondary Alexa Fluor 488 goat anti-mouse antibody (1:1000 in PBS containing 1% (w/v) BSA) were added. After a 1 h-incubation, cells were then washed with PBS containing 1% (w/v) BSA.

1×10^5 HEK293 Nox4GFP cells were seeded on chamber slide. When the cells reached ~80% confluence, they were fixed with 4% (w/v) paraformaldehyde for 10 min at room temperature. Paraformaldehyde fluorescence was quenched by 50 mM NH_4Cl for 10 min at room temperature. Cells were then washed with PBS.

Cell nuclei were stained with Hoechst 33258 (0.5 μg/ml). Samples were then mounted in DABCO solution, sealed, and stored at 4 °C in the dark. Confocal microscopy was carried out by using the Zeiss LSM 510 NLO META. In the green channel, the pinhole was adjusted to 1 Airy unit resulting in 0.7 μm thick slices. Hoechst fluorescence was visualised using a 2P excitation.

2.13. Total internal reflection fluorescence microscopy TIRF

2×10^4 HEK293 T-REx™ Nox4 cells were seeded on chambered coverglass. When the cells reached ~60% confluence, they were incubated for 16 h with tetracycline to induce Nox4 expression. Un-induced and induced HEK293 T-REx™ Nox4 cells were fixed with 4% (w/v) paraformaldehyde for 10 min at room temperature. Paraformaldehyde fluorescence was then quenched by 50 mM NH_4Cl for 10 min at room temperature. After two washes with PBS, cells were incubated with concanavalin A atto-565 conjugated (6 μg/ml) for 30 min. After washing with PBS once, cells were unpermeabilized or permeabilized with 0.1% (v/v) Triton X-100 for 5 min at room temperature, followed by two washes with PBS containing 1% (w/v) BSA; Then following with the incubation of primary antibodies against Calnexin (1:500) or Nox4 (5 μg) and 2nd antibodies (1:1000) as confocal microscopy. Samples were incubated with PBS containing 1% (w/v) BSA and stored at 4 °C in the dark, then observed with a TIRF microscope Axiovert 200M (Carl Zeiss) equipped with the 100×/1.46 plan-apochromat objective. The evanescent field was excited with 488

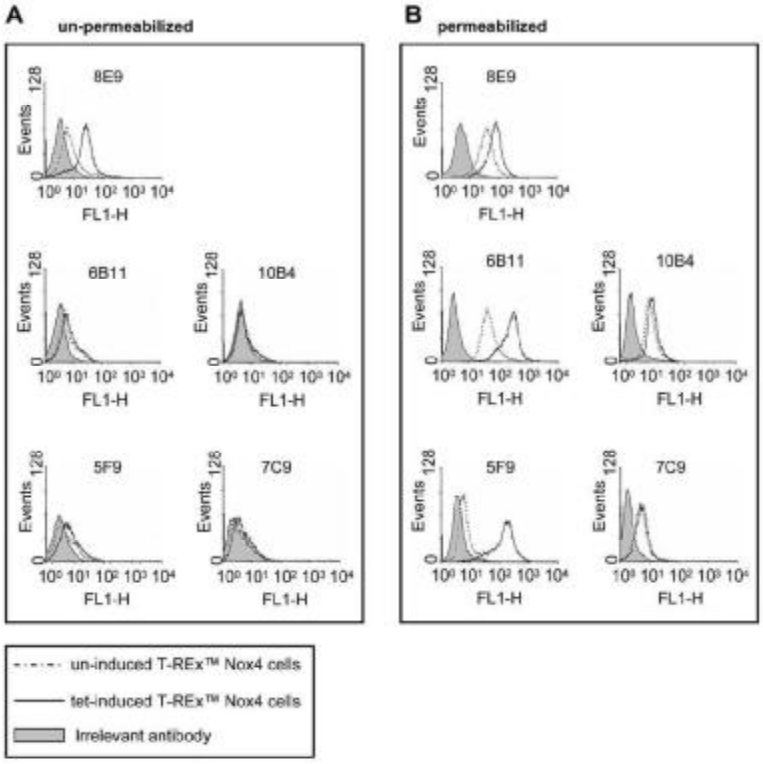

Fig. 3. Flow-cytometry analysis of Nox4 expression in tet-induced T-REx™ Nox4 cells. Un-induced (dotted line) and tet-induced (solid line) T-REx™ Nox4 cells (10^6 cells) were unpermeabilized (A) or fixed with 1%(w/v) paraformaldehyde and permeabilized (B) with 0.1% Triton X-100 and labelled with specific and purified Nox4 mAbs (5 μg) (white area) or irrelevant (IR) mAb (5 μg) (gray area) for 30 min on ice as described in materials and methods. The antibody-labelled cells were stained with the second antibody (Alexa Fluor 488 goat anti-mouse, 1:200), and the fluorescence (FL1) was measured by FACS. These pictures are representative of at least 3 experiments.

or 514 nm Ar laser lines and fluorescence was detected in green or red channel respectively.

2.14. Statistical data

Data are presented as means ± S.D., significance levels are assessed using Student's t-test. A p-value of 0.05 or less between groups is considered to indicate a statistically significant difference.

3. Results

3.1. Production of a recombinant NADPH oxidase truncated Nox4

In order to investigate subcellular localization and topology of Nox4, 5 novel monoclonal antibodies, named 5F9, 6B11, 8E9, 10B4, 7C9, were developed. The antigen used for the immunization of the mice corresponds to a Nox4 truncated protein from the amino acid 206 to 578 and named NHS-Nox4-1TM (Fig. 1A). This truncated protein contained the cytosolic part of Nox4 plus the 6th potential transmembrane helix, the last extracellular loop between the 5th and 6th transmembrane helices and a poly-histidine tag at the N terminal position. BL21(λDE3) Codon Plus-RIL bacteria were transformed with the plasmid encoding for NHS-Nox4-1TM protein and the protein was produced upon IPTG induction. The overexpressed protein was mainly insoluble (Fig. S1A, lane 3). Denatured protein (urea 8 M) was purified from inclusion bodies and partially refolded in column by a decreasing gradient of urea (from 8 M to 2 M) (Fig. S1B). In order to avoid the selection of antibody directed against the histidine tag, a negative control antigen, ZEBRA/MD4-eGFP protein which contains the same poly-histidine tag, was expressed (Fig. S1B, right panel). After immunization, sera and hybridoma supernatants were both controlled and shown to be positive with the antigen and negative with ZEBRA/MD4-GFP by ELISA (Biotem company).

3.2. Validation and characterization of 5 novel monoclonal antibodies raised against recombinant Nox4

The specificity of these antibodies was first validated by western blot using the antigen NHS-Nox4-1TM and a recombinant eGFP protein containing a histidine tag. All of the ascitic fluids of mAbs recognized the antigen (Fig. 1B, lower panel) by western blot but did not bind to the histidine tagged eGFP at different concentrations (Fig. 1B, upper panel), excluding the possibility of the recognition of mAbs to the histidine tag.

Next, we investigated the ability of the 5 purified mAbs to bind the full-length Nox4 ex vivo by using 2 cell lines: HEK293 cells overexpressing Nox4 fused with a GFP tag at the C-terminus and HEK293 T-REx™ Nox4 cells which overexpress Nox4 upon tetracycline (tet) induction. In both models, Nox4 protein expressed upon tet-induction or fused with a GFP tag were fully functional, an O_2 generating, SOD-sensitive Nox4 activity was detected compared to HEK293 WT cells and to un-induced HEK293 T-REx™ Nox4 cells (Fig. S2). First, GFP mAb was used as a positive control to detect Nox4GFP in HEK293 Nox4GFP cells (Fig. S3). The protein denaturation at 4 °C overnight allowed the detection of two forms: an 85 kDa form (arrows), corresponding to the predicted molecular weight of the full-length Nox4GFP (58 kDa plus 27 kDa for GFP) and a 58 kDa form (asterisk) that may be a degraded form of Nox4GFP (31 kDa for the degraded Nox4 plus 27 kDa for GFP). In contrast, the 60 °C denaturation protocol leads to the only detection of the 58 kDa form suggesting a high sensitivity of Nox4 to heat degradation. Therefore, all samples were treated at 4 °C for further western blot experiments. The intact Nox4GFP protein was recognized by only three purified Nox4 mAbs (8E9, 5F9, 6B11) and GFP mAb in HEK293 Nox4GFP cell lysates compared to the wild type cell lysates (Fig. 2A, arrows). To confirm the specificity of the signal observed, we used a RNA interference (RNAi) approach with small interfering RNA (siRNA) targeting Nox4 mRNA (Nox4 siRNA) (Fig. S4). One of the two siRNAs, siRNA a decreased the expression of Nox4GFP by ~80% compared to the cells transfected with scrambled siRNA (Fig. S4A). This is consistent with the decrease tendency of the NADPH oxidase activity observed with these siRNAs (Fig. S4B). Similar results were observed by using HEK293 T-REx™ Nox4 cells. Upon tet-induction, a band at about 58 kDa was recognized by the same three purified Nox4 mAbs 8E9, 5F9 and 6B11 compared to un-induced T-REx™ Nox4 cells (Fig. 2B). Furthermore, Nox4 proteins were also able to interact with $p22^{phox}$ and stabilized its expression as shown by the increase of $p22^{phox}$ expression in HEK293 Nox4GFP cells and tet-induced HEK293

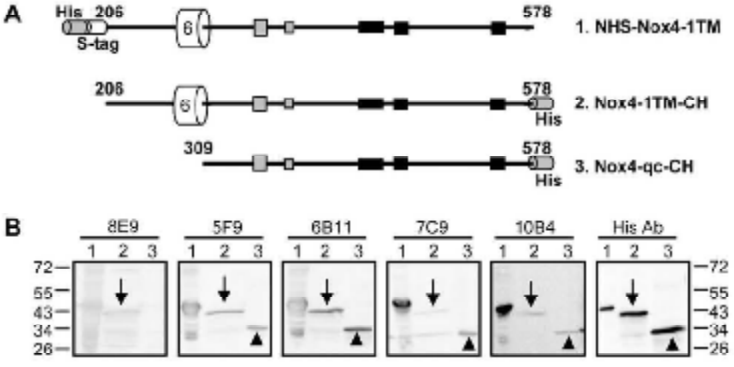

Fig. 4. Evaluation of novel mAbs binding to Nox4 truncated recombinant proteins. (A) Schematic representation of Nox4 truncated recombinant proteins. NHS-Nox4-1TM: residue 206–578 with His-tag and S-tag at N terminal (48 KDa) was expressed in bacteria by IPTG induction; Nox4-1TM-CH (residue 206–578 with His-tag at C-terminal (45 KDa)) and Nox4qc-CH (residue 309–578 with His-tag at C-terminal (32 KDa)) were synthesized by in vitro translation assay (RTS); (B) Western blot analysis of Nox4 truncated recombinant proteins. (1): NHS-Nox4-1TM (1 μl from 1 ml of elution fraction); (2): Nox4-1TM-CH; (3): Nox4qc-CH; 5 μl from 30 μl of reaction medium for (2) and (3). Expression of all truncated recombinant proteins was checked by using the monoclonal antibody anti-polyhistidine (1:5000). The binding of the 5 mAbs (1:500), ascite except for 8E9, to Nox4 truncated forms was analyzed to determine their epitope regions. Immune complexes were detected by ECL after binding with peroxidase. Arrow indicates the position of truncated form Nox4-1TM-His, arrow head indicates the position of truncated form Nox4qc-CH. These pictures are representative of 3 or 5 experiments.

T-REX™ Nox4 cells compared to their respective negative controls by western blot (Fig. 2A and B). Since Nox4 is widely expressed in kidney, we investigated the expression of Nox4 in human kidney cortex by using the 3 functional purified Nox4 monoclonal antibodies. A positive band at about 68 kDa was detected both in diabetic and non-diabetic kidney cortex. Moreover, the expression of Nox4 was increased in diabetic kidney cortex compared with non-diabetic controls (Fig. 2C, arrows) as described by Gorin et al. [35]. Meanwhile, commassie blue staining of the gel was used to assess the loading quantity of each well (data not shown). We confirmed the presence of Nox4 in kidney tissues by immunohistochemistry (Fig. 2D).

The specificity of these mAbs raised against Nox4 was tested against purified cytochrome b_{558}. The results show no cross reaction with Nox2 (data not shown).

The binding of the 5 purified mAbs to native antigen was further investigated by flow cytometry on intact and Triton X-100 permeabilized T-REX™ Nox4 cells. The results showed that 3 purified mAbs (5F9, 6B11 and 8E9) bound to Nox4 upon permeabilization (Fig. 3B) while only mAb 8E9 recognized Nox4 in intact cells (Fig. 3A). These data suggested that 8E9 recognized an extracellular epitope on Nox4 whereas 5F9 and 6B11 bound to an intracellular domain.

3.3. Determination of mAb epitope regions using different truncated forms of Nox4

Protein alignments of different NADPH oxidases revealed that the last extracellular loop of Nox4 (E loop) contains a more extended amino acid sequence than the other Nox family members. To determine if some of these mAbs could recognize the E loop, we evaluated the immunoreactivity of these mAbs against the cytosolic tail of Nox4, Nox4qc-CH (Fig. 4A). As we can see in Fig. 4B, the ascites of 5F9, 6B11, 7C9 and 10B4 recognized Nox4qc-CH suggesting a cytosolic epitope on Nox4 while mAb 8E9 did not. The data favor a localization of the mAb 8E9 epitope on the extracellular E loop, consistent with the results of FACS (Fig. 3A). Furthermore, since NHS-Nox4-1TM possesses an S-tag sequence, by using a recombinant protein (Nox4-1TM-CH) sharing the same amino acid sequence of Nox4 (amino acid 205–578) but without S-tag, we ruled out the possibility that mAbs could be directed against this sequence and demonstrated their specificity towards Nox4 (Fig. 4B).

Then, different Nox4 truncated forms containing a poly-histidine tag at the N-terminal position (Fig. 5A, Table. S1) were used to further determine the epitope regions of these novel purified Nox4 mAbs. As results shown by Fig. 5C, mAb 8E9 could recognize the Nox4 truncated form 10 but not 7 and 3; combined with previous results that mAb 8E9 failed to recognize Nox4qc-CH (Fig. 4B), these data together showed that its epitope region was on the extracellular E loop of Nox4 (^{222}I–^{241}F). Both mAbs 6B11 and 5F9 recognized the Nox4 truncated form 6 but no. 7, which suggested that these 2 mAbs bound a region at the C-terminal part of Nox4 (^{389}S–^{435}F). As mAbs 10B4 and 7C9 could not label Nox4 in two cell lines by western blot and FACS, the reactivity difference between ascite and mAb was studied. By using the same recombinant proteins (NHS-Nox4-1TM and Nox4-1TM-CH), we found that neither mAb 10B4 nor mAb 7C9 could bind these two recombinant proteins when using the same dilution of their ascites (Fig. S5A). This is contrary to what is obtained with both mAb 5F9 and its ascite (Fig. S5). The binding of mAb 10B4 to NHS-Nox4-1TM but not to NHS-Nox4qc was observed only when its concentration was increased up to 1:50. For mAb 7C9, different concentrations of this antibody were used to detect the recombinant protein NHS-Nox4-1TM. As seen in Fig. S5B, the signal of specific band (NHS-Nox4-1TM, arrow) recognized by mAb 7C9 was stronger than unspecific band (asterisk) until the dilution was increased up to 1:25. Due to the weak reactivity of mAbs 10B4 and 7C9, mAb 10B4

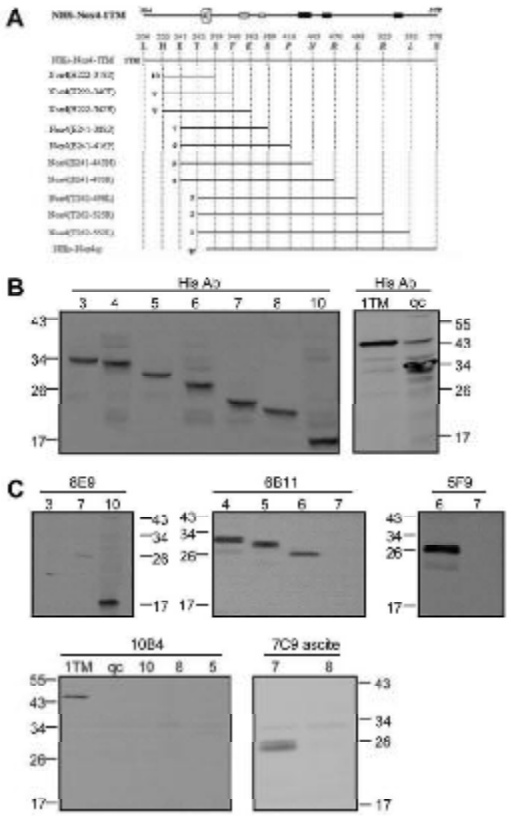

Fig. 5. Determination of mAb epitope regions by using Nox4 truncated recombinant proteins. (A) Schematic representation of Nox4 truncated recombinant proteins expressed in bacteria by IPTG induction. 1–10 indicate the number of each different truncated recombinant protein, the letters in non-italic and italic indicate the beginning and ending AA of each truncated recombinant protein, respectively; (B) Western blot analysis of Nox4 truncated recombinant proteins. Expression of the truncated recombinant proteins (1 μl from 1 ml of elution fraction) was checked by using the monoclonal antibody anti-polyhistidine (1:5000); (C) Determination of mAb epitope regions by using different truncated Nox4 recombinant proteins. 8E9(1:500), 5F9 (1:500), 6B11(1:500) and 10B4(1:50) used here were purified mAbs, while 7C9(1:500) used here was ascite. Immune complexes were detected by ECL after binding with peroxidase. These pictures are representative of 2 or 3 experiments.

(dilution: 1:50) and ascite 7C9 were used to study their epitope regions. As seen in Fig. 5C, mAb 10B4 recognized only Nox4-1TM but neither Nox4qc nor Nox4 truncated form 10, this result suggesting that its epitope region was on the extracellular E loop of Nox4 (^{205}I–^{222}I); for the ascite 7C9 which could recognize the Nox4 truncated form 7 but not 8, the result showed that it bound a region at the C-terminal part of Nox4 (^{362}E–^{389}). The expression of all these Nox4 truncated forms used was confirmed by histidine antibody at each right size (Fig. 5B).

3.4. Determination of mAb epitopes by phage display

To define the antibody epitopes, phage-display analysis was applied as previously reported [27,30]. After immunopurification

on mAb affinity matrices, several unique peptide sequences were identified for mAbs 5F9 and 10B4 (Fig. 6). Alignments of the peptide sequences recognized by mAbs 5F9 and 10B4 revealed the amino acid residues ^{352}DSEILPF^{358} which are present in the cytosolic tail of Nox4 and ^{210}GGLLKYQTNL^{219} which are present on the extracellular E loop of Nox4, respectively (Fig. 6A and B, lower panel). To gain a more comprehensive understanding of the mAbs 5F9 and 10B4 epitopes, an extensive analysis of the peptide sequences obtained by phage display was performed by using the computer program EPIMAP in order to map the epitopes to discontinuous segments of the protein that are distant in the primary sequence, but are in close spatial proximity in the structure. Histograms resulting from EPI-MAP software analysis confirmed a matching of the mAbs 5F9 and 10B4 consensus sequences on the region of Nox4 ^{352}DSEILPF^{358} and ^{210}GGLLKYQTNL^{219} (Fig. 6A and B, upper panel).

3.5. Subcellular localization of Nox4

The immunoreactivity of mAb 5F9 on non-permeabilized cells (Fig. 3A) suggests that Nox4 could be expressed at the plasma membrane of tet-induced T-REx™ Nox4 cells. To provide a direct evidence of this specific subcellular localization, we looked at Nox4 subcellular distribution by confocal microscopy. As 5F9 recognized an extracellular epitope on Nox4 whereas 5F9 and 6B11 bound to an intracellular domain (Fig. 3), 8E9 or 5F9 and 6B11 were used to observe the localization of Nox4 in intact or permeabilized cells respectively. When cells were not permeabilized, by using mAb 8E9, Nox4 was observed only at the plasma membrane of tet-induced T-REx™ Nox4 cells compared to un-induced T-REx™ Nox4 cells (Fig. 7A). After permeabilization, Nox4 was detected as well at the plasma membrane than in the perinuclear and endoplasmic reticulum regions (Fig. 7B, lower panel) by mAb 6B11. This multi-cellular distribution was confirmed by the same fluorescence localization of Nox4GFP protein (Fig. 7C). Interestingly, the labelling of mAb 5F9 was mainly intracellular and no clear signal could be observed at the plasma membrane (Fig. 7B, upper panel).

The localization of Nox4 at the plasma membrane in tet-induced T-REx^{TX} Nox4 cells was further confirmed by Total Internal Reflection Fluorescence (TIRF) microscopy, in which the plasma membrane close to the glass surface is visualised preferentially due to the small penetration depth of the evanescent excitation field (<150 nm). Concanavalin A, a plasma membrane marker and calnexin, an endoplasmic reticulum marker, were used as a positive and a negative control respectively. Thus, only the fluorescence signal of concanavalin A at the plasma membrane could be seen but not that of calnexin by TIRF (Fig. 8A). As shown in the Fig. 8B, a positive signal was obtained by using mAbs 8E9 and 6B11 only in tet-induced HEK293 T-REx™ Nox4 indicating a localization of Nox4 at the plasma membrane. On the contrary, no fluorescence could be observed by TIRF with mAb 5F9 showing that this antibody is unable to bind to Nox4 at the plasma membrane (Fig. 8B). This result is consistent with the absence of fluorescence observed with

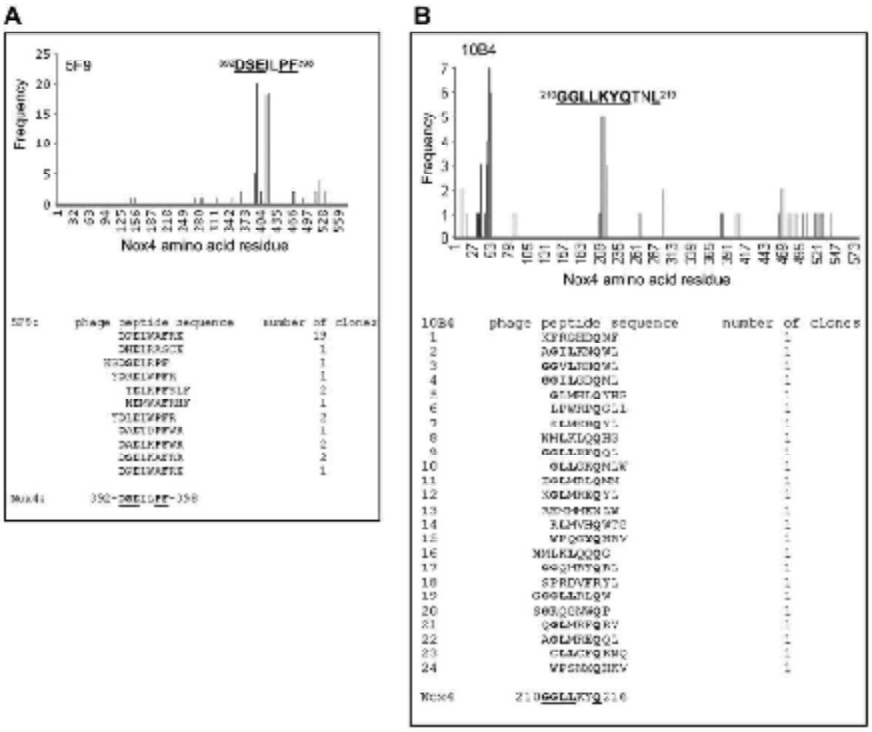

Fig. 6. EPIMAP analysis for mAbs 5F9 and 10B4. Alignment of phage sequences of mAbs 5F9 (A) and 10B4 (B) to discontinuous protein regions of Nox4 by using the program EPIMAP. Histograms presented the frequency of phage peptide amino acids recovered in the large protein sequence (upper panel). The potential epitope is presented in frame with amino acids belonging to Nox4 (lower panel).

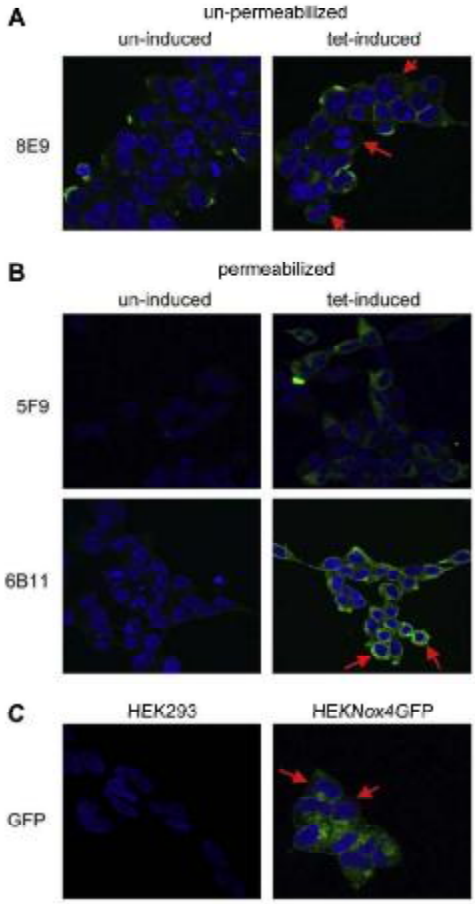

Fig. 7. Subcellular localization of Nox4 by confocal microscopy. Un-induced and tet-induced HEK293 T-REx™ Nox4 cells (1×10^5 cells) were fixed, unpermeabilized(A) or permeabilized(B) with 0.1% Triton X-100 and labelled with Nox4 mAbs 8E9, 5F9, 6B11 (5 μg) for 1 h at room temperature as described in Methods. The second antibody (Alexa Fluor 488 goat anti-mouse, 1:1000) was used to detect mAb binding by confocal microscopy. (C) HEK293 wild type cells and HEK293 Nox4GFP were fixed. GFP fluorescence was detected by confocal microscopy. Arrows indicated the plasma membrane of the cells. These pictures are representative of 2 or 3 experiments.

the same antibody at the plasma membrane by confocal microscopy (Fig. 7B, upper panel).

3.6. Effect of Nox4 mAbs on the constitutive NADPH oxidase activity in vitro

In order to identify specific inhibitors of Nox4 activity, the effect of mAbs on the NADPH oxidase activity in a cell-free system was analyzed. In this experiment, total lysates of tet-induced T-REx™ Nox4 cells were pre-incubated with an excess of mAb for 30 min on ice before adding reaction mixture which contained 20 μM luminol, 10 units/ml horseradish peroxidase, 10 μM FAD and 150 μM NADPH. A control experiment was performed with an irrelevant antibody. Contrary to 8E9, the presence of mAb 6B11 or 5F9 in the assay resulted in a moderate but significant inhibition of the NADPH oxidase activity of ~25% compared to the activity measured in the presence of an irrelevant mAb (Fig. 9).

4. Discussion

Five monoclonal antibodies specific to Nox4 were raised for the first time and characterized in the present work. Among these mAbs, 3 of them, 8E9, 6B11 and 5F9, could recognize native overexpressed Nox4 in HEK293 cells, tet-induced T-REx™ Nox4 cells and C20/A-4 human chondrocyte cell lines (unpublished data). The current findings focus on distinct properties of these mAbs referring to identification and subcellular localization of Nox4 as NADPH oxidase activity.

The theoretical size of Nox4 is 66.9 kDa (expasy, proteomic server), as shown for the first time by Shiose et al. [7]. By consequence, the fused protein Nox4–GFP should appear at a size of 93.9 kDa. It has been reported that Nox4 antibodies recognize two kinds of bands: one of 75–80 kDa and a second of 55–65 kDa from endogenous Nox4 expressing cells and/or Nox4-overexpressing cells by Martyn et al. [11], Kawahara et al. [12], and Hilenski et al. [36]. As for us, Nox4 was detected using two different cell lines (HEK293 overexpressing Nox4GFP and the Tet-induction model HEK293 T-RexNox4) at the size of 58 kDa instead of 66.9 kDa. This size, for Nox4 was also observed by Ambasta et al. [10], Martyn et al. [11], Kawahara et al. [12], and Von Löhneysen et al. [22]. 68 kDa is the size of Nox4 detected in kidney cortex, which has also been reported by [35,37,38]. Immunohistochemical experiments highlighted the presence of Nox4 in kidney (Fig. 2D) as well as in thyroid tissues (data not shown). The difference of size of Nox4 might suggest that the protein is more glycosylated in the tissues or less degraded. The degradation process of Nox4 may depend on the modalities of storage and freezing and thawing, and on the procedure of cell homogenization and protein extraction. In this paper we emphasized also (Fig. S3) the great sensitivity of Nox4 to the temperature and the necessary addition to sample fraction not only of an anti-protease cocktail but also of vanadate and okadaic acid reagents that inhibit phosphatases; moreover the SDS solubilisation procedure has to be carried out at 4 °C.

As reported recently [11,39], Nox4 was shown to be located in the ER of HEK293 transfected cells. In our study, the binding of mAb 8E9 to intact tet-induced T-REx™ Nox4 cells in FACS analysis favors a plasma membrane localization of Nox4 (Fig. 3A). By confocal microscopy, we confirmed its localization in ER, but we demonstrated that Nox4 is also present in the plasma membrane of tet-induced T-REx™ Nox4 cells (Fig. 7) and C20/A-4 human chondrocyte cells (unpublished data) by using mAbs 8E9 and 6B11. The data were further confirmed by total internal reflection fluorescence microscopy (TIRF) (Fig. 8). Nox4 has been detected in several cellular compartments: in transfected cells, Nox4 was localized in the ER [11,21] or plasma membrane [22,40]; in endothelial cells [23] and smooth muscle cells [36], the localization of Nox4 was reported within the nucleus; in vascular smooth muscle cells, a localization close to focal adhesion was reported [36]. Moreover, in somatic cells, Nox4 was detected in mitochondria [41]. It is uncertain whether these contradicting findings are a consequence of so-far unknown partner of Nox4 changing the localization of Nox4 or of potential problems arising from the overexpression of a membrane protein per se or of the specificity of the different Nox4 antibodies used. It is also possible that the localization of Nox4 changes with the functional or pathological state of the cells [24]. In fact, in vascular smooth muscle cells, Nox4 relocates from focal adhesions to stress fibers during differentiation [42]. This also reflects the cell-specific targeting of Nox4 or the different

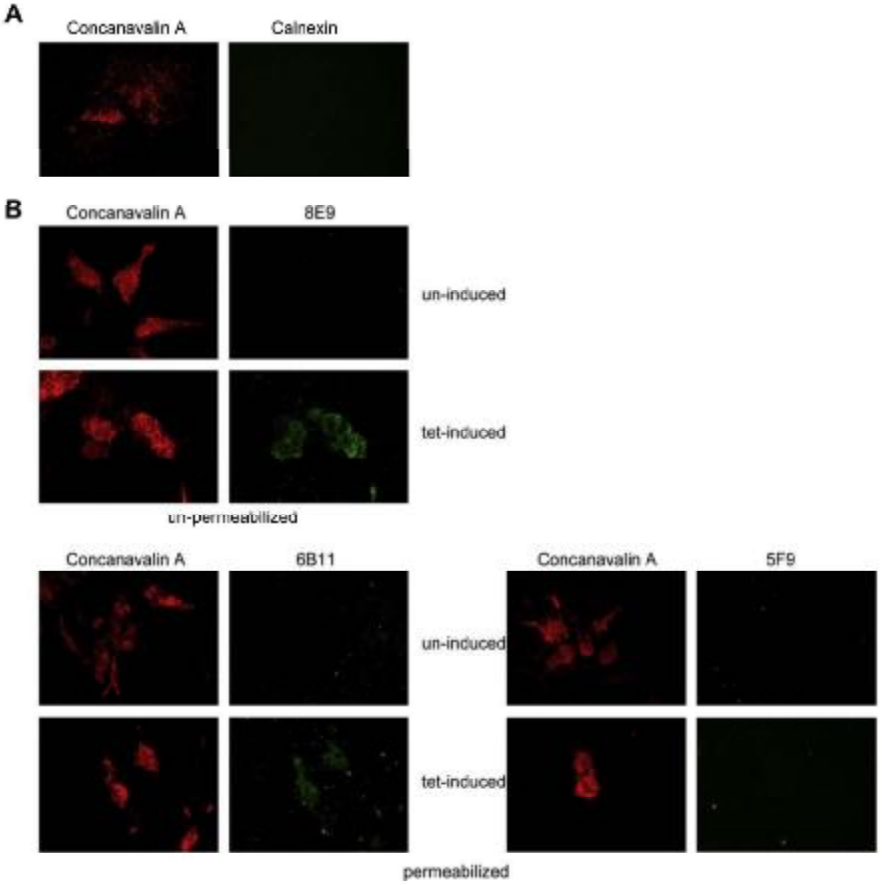

Fig. 8. Subcellular localization of Nox4 by total internal reflection fluorescence microscopy. (A) TIRF signals of plasma membrane and 8E in permeabilized, un-induced HEK293 T-REx™ Nox4 cells. Cells were labelled with concanavalin A-Alexa 568 conjugated (plasma membrane marker, red) (6 μg/ml) and mouse anti-calnexin monoclonal antibody (ER marker 1:500) followed with Alexa Fluor 488 goat anti-mouse (green) (1:1000). (B) TIRF signals of concanavalin A and Nox4 in un-induced and tet-induced HEK293 T-REx™ Nox4 cells (unpermeabilized (upper panel) or permeabilized (lower panel). Red indicates the concanavalin A (6 μg/ml) on the plasma membrane, green indicates the Nox4 expression detected by Nox4 mAbs (5 μg). These pictures are representative of 2 experiments. (For interpretation of the references to colour in this figure legend, the reader is referred to the web version of this article.)

specificity of Nox4 antibodies [43]. Plasma membrane localization of Nox4 is in favor of a ROS production directly in the extracellular medium. Most studies showed that H_2O_2 is the principal source of ROS detected outside of cells [11,21,37]; However, Boudreau et al. [19] recently reported that O_2 is synthesized in the extracellular medium of hepatocytes. We also detected the O_2 release from tet-induced T-REx™ Nox4 cells and HEK293 Nox4GFP cells (Fig. S2).

Surprisingly, mAb 5F9 was not able to label Nox4 at the plasma membrane. Phage-display epitope mapping suggested that mAb 5F9 interacts with (^{397}D–F^{398}) region of Nox4. Three possibilities could explain such a result: (1) Nox4 may change its conformation once transferred to the plasma membrane and therefore could hide the epitope of 5F9; (2) additional Nox4 partner such as Foldip2 [13] which influence Nox4 subcellular localization in VSMC may bind to this epitope region, (3) the permeabilization process could alter the epitope of 5F9. We are working on directed mutagenesis in this region to study strategic AA residues referring to the localization and activity of Nox4.

The inability of mAbs against Nox4 (except mAb 8E9) to bind intact tet-induced T-REx™ Nox4 cells in FACS analysis provides support for topology models localizing these respective regions to the cytoplasmic portion of Nox4, while the epitope of mAb 8E9 is accessible on the E loop. But this could not completely rule out the possibility of extracellular regions of Nox4 being masked on the cell surface. In fact, the epitope determination by using different truncated forms of Nox4 and by phage display showed that the epitope of 10B4 was on the E loop of Nox4 (^{210}GGLLKYQTNL^{219}), although the frequency of consensus sequence is low (Fig. 6B). The failing of 10B4 and 7C9 mAbs to recognize Nox4 in native cells may be due to a low sensitivity of mAbs; interaction forces between mAbs and native or recombinant antigen remain to be addressed.

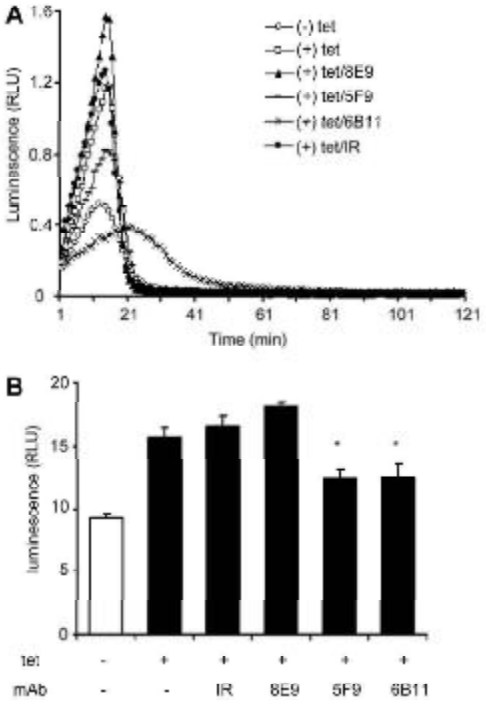

Fig. 9. Effect of Nox4 mAbs on the NADPH oxidase activity in a cell free system. Cell lysates (50 μg) of tet-induced HEK293 T-REx™ Nox4 cells were pre-incubated with Nox4 specific mAbs (8E9, 5F9, 6B11) (40 μg) or irrelevant antibody (40 μg) for 30 min on ice. Then 10 μM FAD was added to the cell lysates at a final volume of 60 μl. After 5 min incubation on ice, cell lysates were transferred to the Corning Costar 96 well Assay Plate. The reaction was initiated by addition of 200 μl PBS containing 20 μM luminol, 10 units/ml horseradish peroxidase, 10 μM FAD and 150 μM NADPH. (A) Representative traces from each treatment. (B) Means ± S.D. from accumulated signals after 1 h. Values are presented as the average of three experiments ± S.D. * indicates $P < 0.05$.

For mAbs 8E9 and 6B11, the epitope region was not clearly determined. However, immunodetection of Nox4 truncated forms suggested that the epitope of mAb 8E9 was on the extracellular E loop of Nox4 (^{222}H–E^{241}) and mAb 6B11 bound a region at the C-terminal part of Nox4 (^{387}S–P^{418}). Pre-incubation of total lysates of tet-induced T-REx™ Nox4 cells with either mAb 6B11 or mAb 5F9 leads to a moderate but significant inhibition of Nox4 activity, indicating that they interact with a region important for the electron transfer. Furthermore, this result also suggested that the cytosolic tail of Nox4 could be responsible for its constitutive activity. In fact, as previously reported by Lambeth team [38], the constitutive activity of Nox4 resides in the dehydrogenase domain. This domain is located immediately C-terminal to the TM domain. It is constitutively "turned on" compared with the DH domain of other Nox 1–3. Of note, we have produced and purified a recombinant protein NHS-Nox4qc (AA: 309–578); a constitutive activity was measured at 550 nm as the SOD-sensitive reduction of cytochrome c (*unpublished data*).

Table 1
Summary of characteristics of monoclonal antibodies directed against Nox4.

Nox4 mAbs	Reactivity of mAbs against Nox4	Epitope	Localization of Nox4	Effect on NADPH oxidase activity
8E9	+	^{222}H–E^{241}	Plasma membrane	No effect
5F9	+	^{386}D–P^{398}	Perinuclear and endoplasmic reticulum regions	Inhibition
6B11	+	^{387}S–P^{418}	Plasma membrane, perinuclear and endoplasmic reticulum regions	Inhibition
10B4	–	^{211}G–L^{219}	NH	NH
7C9	–	^{434}E–S^{444}	ND	ND

ND: non determined.

Unlike Nox2, p22^{phox} is the only known partner that interacts with Nox4 [10–12]. In our study, results obtained by flow cytometry (data not shown) and western blot confirmed that Nox4 is a p22^{phox}-dependent enzyme. Both in tet-induced T-REx™ Nox4 cells and HEK293 Nox4GFP cells, the expression of Nox4 is consistent with the increase of p22^{phox} (Fig. 2). Recently, Lyle et al. [13] reported in VSMC the association of Poldip2 (polymerase, DNA-directed, delta-interacting protein 2) with heterodimer Nox4/p22^{phox} and Poldip2 was introduced as a positive regulator of Nox4. The isolation of Nox4 with additional partners such as Poldip2 as a complex from HEK293 cells and the capacity of 5F9 to specifically map this putative complex should be addressed further.

In conclusion, among 5 novel mAbs described in this study, 3 mAbs (8E9, 5F9, 6B11) could specifically recognize Nox4 protein in human kidney cortex and HEK293 cell lines and chondrocytes cell line (Table 1). These mAbs display distinct and specific properties: mAb 8E9 recognizes an epitope on the last extracellular loop of Nox4 (^{222}H–E^{241}), while mAb 6B11 and mAb 5F9 are directed to cytosolic tail of Nox4 (^{387}S–P^{418}) and both of them interact with a region involved in Nox4 constitutive activity, but mAb 5F9 could not detect Nox4 at the plasma membrane. More work is necessary to further determine the epitope of mAbs 8E9 and 6B11. Monoclonal antibodies developed against Nox4 described in this study will be a valuable set of probes specific to Nox4 and will provide powerful tools for a structure/function relationship investigation and physiopathological studies.

Acknowledgments

We greatly appreciate the gift of human renal cortex from Dr. Nicole Pinel (Département d'Anatomie et Cytologie Pathologiques, CHU Albert Michallon; BP 217, 38043 Grenoble, France). We would like to give our thanks to Hedia Ramara (Department of Computer Science, Montana State University) for running the EPIMAP programs and to Sylvie Berthier (DRDPI Timc-Imag UMR-CNRS 5525, Enzymologie;CHU Albert Michallon, BP 217, 38043 Grenoble, France) for technical assistance. We thank Pr Karl-Heinz Krause (Department of Pathology and Immunology, Geneva Medical Faculty and University Hospital) for providing Nox4 siRNAs and for the helpful advice or comments on the results. We also thank Dr Bernard Caillou (Department of Pathology, Institut Gustave Roussy, Villejuif, France) for immunohistochemical experiments.

This work was supported by grants from the "ministère de l'Enseignement Supérieur de la Recherche et Technologie, Paris", the "UFR de Médecine, Université Joseph Fourier, Grenoble", the "Region Rhône-Alpes, programme Emergence 2003", the "association nationale de défense contre l'Arthrite Rhûmatoïde, délégation de l'Isère, ANDAR", the "Groupement des Entreprises Françaises dans la Lutte contre le Cancer, GEFLUC, délégation de Grenoble", the "Société Française de Rhûmatologie", and the "Délégation Régionale de la Recherche Clinique, DRRC" CHU Grenoble.

Leilei Zhang was supported by "the Region Rhône-Alpes, programme ARCUS", "the National Key Program for Basic Research of China (2010CB529902)", "the Science and Technology Commission of Shanghai (S30205, 06SR07110)", "the National Natural Science Foundation of China (30973663)", "L'Ambassade de France en Chine". Algirdas J. Jesaitis was supported by USPHS grant R01-AI26711.

Appendix. Supplementary material

Supplementary material related to this article can be found at doi:10.1016/j.biochi.2010.11.001.

References

[1] G. Cheng, Z. Cao, X. Xu, E.G.V. Meir, J.D. Lambeth, Homologs of gp91phox: cloning and tissue expression of Nox3, Nox4, and Nox5, Gene 269 (2001) 131–140.

[2] D. Rotrosen, C.L. Yeung, J.P. Katkin, Production of recombinant cytochrome b558 allows reconstitution of the phagocyte NADPH oxidase solely from recombinant proteins, Journal of Biological Chemistry 268 (1993) 14256–14260.

[3] W.M. Nauseef, Assembly of the phagocyte NADPH oxidase, Histochemistry and Cell Biology 122 (2004) 277–291.

[4] S. Berthier, M.H. Paclet, S. Lerouge, F. Roux, S. Vergnaud, A.W. Coleman, F. Morel, Changing the conformation state of cytochrome b558 initiates NADPH oxidase activation, Journal of Biological Chemistry 278 (2003) 25499–25508.

[5] M.H. Paclet, S. Berthier, L. Kuhn, J. Garin, F. Morel, Regulation of phagocyte NADPH oxidase activity: identification of two cytochrome b558 activation states, FASEB Journal 21 (2007) 1244–1255.

[6] M. Geiszt, J.B. Kopp, P. Várnai, T.L. Leto, Identification of Renox, an NAD(P)H oxidase in kidney, Proceedings of the National Academy of Sciences of the United States of America 97 (2000) 8010–8014.

[7] A. Shiose, J. Kuroda, K. Tsuruya, M. Hirai, H. Hirakata, S. Naito, M. Hattori, Y. Sakaki, H. Sumimoto, A novel superoxide-producing NAD(P)H oxidase in kidney, Journal of Biological Chemistry 276 (2001) 1417–1423.

[8] K. Bedard, K.H. Krause, The NOX family of ROS-generating NADPH oxidases: physiology and pathophysiology, Physiological Reviews 87 (2007) 245–313.

[9] M. Geiszt, T.L. Leto, The Nox family of NAD(P)H oxidases: host defense and beyond, Journal of Biological Chemistry 279 (2004) 51715–51718.

[10] R.K. Ambasta, P. Kumar, K.K. Griendling, H.H.H.W. Schmidt, R. Busse, R.P. Brandes, Direct interaction of the novel Nox proteins with p22phox is required for the formation of a functionally active NADPH oxidase, Journal of Biological Chemistry 279 (2004) 45935–45941.

[11] K.D. Martyn, L.M. Frederick, K. von Loehneysen, M.C. Dinauer, U.G. Knaus, Functional analysis of Nox4 reveals unique characteristics compared to other NADPH oxidases, Cellular Signalling 18 (2006) 69–82.

[12] T. Kawahara, D. Ritsick, G. Cheng, J.D. Lambeth, Point mutations in the proline-rich region of p22phox are dominant inhibitors of Nox1- and Nox2-dependent reactive oxygen generation, Journal of Biological Chemistry 280 (2005) 31859–31869.

[13] A.N. Lyle, N.N. Deshpande, Y. Taniyama, B. Seidel-Rogol, L. Pounkova, P. Du, C. Papaharalambus, B. Lassegue, K.K. Griendling, Poldip2, a novel regulator of Nox4 and cytoskeletal integrity in vascular smooth muscle cells, Circulation Research 105 (2009) 249–259.

[14] F.J. Miller Jr., NADPH oxidase 4: walking the walk with Poldip2, Circulation Research 105 (2009) 209–210.

[15] C. Xia, Q. Meng, L.Z. Liu, Y. Rojanasakul, X.R. Wang, B.H. Jiang, Reactive oxygen species regulate angiogenesis and tumor growth through vascular endothelial growth factor, Cancer Research 67 (2007) 10823–10830.

[16] T. Akasaki, Y. Ohya, J. Kuroda, K. Eto, I. Abe, H. Sumimoto, M. Iida, Increased expression of gp91phox Homologues of NAD(P)H oxidase in the Aortic media during chronic hypertension: involvement of the renin–angiotensin system, Hypertension Research 29 (2006) 813–820.

[17] M. Sedeek, R.L. Hébert, C.R. Kennedy, K.D. Burns, R.M. Touyz, Molecular mechanisms of hypertension: role of Nox family NADPH oxidases, Current Opinion in Nephrology and Hypertension 18 (2009) 122–127.

[18] D. Sorescu, D. Weiss, B. Lassegue, R.E. Clempus, K. Szocs, G.P. Sorescu, L. Valppu, M.T. Quinn, J.D. Lambeth, J.D. Vega, W.R. Taylor, K.K. Griendling, Superoxide production and expression of Nox family proteins in human atherosclerosis, Circulation 105 (2002) 1429–1435.

[19] H.E. Boudreau, S.U. Emerson, A. Korzeniowska, M.A. Jendrysik, T.L. Leto, Hepatitis C virus (HCV) proteins induce NADPH oxidase 4 expression in a transforming growth factor (beta)-dependent manner: a new contributor to HCV-induced oxidative stress, The Journal of Virology 83 (2009) 12934–12946.

[20] L. Grange, M.V.C. Nguyen, B. Lardy, M. Derouazi, Y. Campion, C. Trocme, M.H. Paclet, P. Gaudin, F. Morel, NAD(P)H oxidase activity of Nox4 in chondrocytes is both inducible and involved in collagenase expression, Antioxidants & Redox Signaling 8 (2006) 1485–1496.

[21] K. Chen, M.T. Kirber, H. Xiao, Y. Yang, J.F. Keaney, Regulation of ROS signal transduction by NADPH oxidase 4 localization, The Journal of Cell Biology 181 (2008) 1129–1139.

[22] K. von Lohneysen, D. Noack, A.J. Jesaitis, M.C. Dinauer, U.G. Knaus, Mutational analysis reveals distinct features of the Nox4–p22phox complex, Journal of Biological Chemistry 283 (2008) 35273–35282.

[23] J. Kuroda, K. Nakagawa, T. Yamasaki, K.I. Nakamura, R. Takeya, F. Kuribayashi, S. Imajoh-Ohmi, K. Igarashi, Y. Shibata, K. Sueishi, H. Sumimoto, The superoxide-producing NAD(P)H oxidase Nox4 in the nucleus of human vascular endothelial cells, Genes to Cells 10 (2005) 1139–1151.

[24] U. Weyemi, B. Caillou, M. Talbot, R. Ameziane-El-Hassani, L. Lacroix, O. Lagent-Chevallier, A. Al Ghuzlan, D. Roos, J.M. Bidart, A. Virion, M. Schlumberger, C. Dupuy, Intracellular expression of reactive oxygen species-generating NADPH oxidase NOX4 in normal and cancer thyroid tissues, Endocrine-Related Cancer 17 (2010) 27–37.

[25] B. Marques, L. Liguori, M.H. Paclet, A. Villegas-Mendéz, R. Rothe, F. Morel, J.L. Lenormand, Liposome-mediated cellular delivery of active gp91^{phox}, PloS ONE 2 (2007) e856.

[26] L. Liguori, B. Marques, A. Villegas-Méndez, R. Rothe, J.L. Lenormand, Production of membrane proteins using cell-free expression systems, Expert Review of Proteomics 4 (2007) 79–90.

[27] Y. Campion, M.H. Paclet, A.J. Jesaitis, B. Marques, A. Grichine, S. Berthier, J.L. Lenormand, B. Lardy, M.J. Stasia, F. Morel, New insights into the membrane topology of the phagocyte NADPH oxidase: characterization of an anti-gp91-phox conformational monoclonal antibody, Biochimie 89 (2007) 1145–1158.

[28] G. Batot, C. Martel, N. Capdeville, F. Wientjes, F. Morel, Characterization of neutrophil NADPH oxidase activity reconstituted in a cell-free assay using specific monoclonal antibodies raised against cytochrome b558, European Journal of Biochemistry 234 (1995) 208–215.

[29] H. Towbin, T. Staehelin, J. Gordon, Electrophoretic transfer of proteins from polyacrylamide gels to nitrocellulose sheets: procedure and some applications, Proceedings of National Academy of Sciences 9 (1979) 4350–4354.

[30] Y. Campion, A.J. Jesaitis, M.V.C. Nguyen, A. Grichine, Y. Herenger, A. Baillet, S. Berthier, F. Morel, M.H. Paclet, New p22-phox monoclonal antibodies: identification of a conformational probe for cytochrome b 558, Journal of Innate Immunity 1 (2009) 556–569.

[31] M.H. Paclet, L.M. Henderson, Y. Campion, F. Morel, M.C. Dagher, Localization of Nox2 N-terminus using polyclonal antipeptide antibodies, Biochemical Journal 382 (2004) 981–986.

[32] J.B. Burritt, C.W. Bond, K.W. Doss, A.J. Jesaitis, Filamentous phage display of oligopeptide libraries, Analytical Biochemistry 238 (1996) 1–13.

[33] J.B. Burritt, M.T. Quinn, M.A. Jutila, C.W. Bond, A.J. Jesaitis, Topological mapping of neutrophil cytochrome b epitopes with phage-display libraries, Journal of Biological Chemistry 270 (1995) 16974–16980.

[34] E.M. Mumey, B.W. Bailey, B. Kirkpatrick, A.J. Jesaitis, T. Angel, E.A. Dratz, A new method for mapping discontinuous antibody epitopes to reveal structural features of proteins, Journal of Computational Biology 10 (2003) 555–567.

[35] Y. Gorin, K. Block, J. Hernandez, B. Bhandari, B. Wagner, J.L. Barnes, H.E. Abboud, Nox4 NAD(P)H oxidase mediates hypertrophy and fibronectin expression in the diabetic kidney, Journal of Biological Chemistry 280 (2005) 39616–39626.

[36] L.L. Hilenski, R.E. Clempus, M.T. Quinn, J.D. Lambeth, K.K. Griendling, Distinct subcellular localizations of Nox1 and Nox4 in vascular smooth muscle cells, Arteriosclerosis, Thrombosis, and Vascular Biology 24 (2004) 677–683.

[37] L. Hecker, R. Vittal, T. Jones, R. Jagirdar, T.R. Luckhardt, J.C. Horowitz, S. Pennathur, F.J. Martinez, V.J. Thannickal, NADPH oxidase-4 mediates myofibroblast activation and fibrogenic responses to lung injury, Nat Med 15 (2009) 1077–1081.

[38] Y. Nisimoto, H.M. Jackson, H. Ogawa, T. Kawahara, J.D. Lambeth, Constitutive NADPH-dependent electron transferase activity of the Nox4 dehydrogenase domain, Biochemistry 49 (2010) 2433–2442.

[39] I. Helmcke, S. Heumüller, R. Tikkanen, K. Schröder, R.P. Brandes, Identification of structural elements in Nox1 and Nox4 controlling localization and activity, Antioxidants & Redox Signaling 11 (2009) 1279–1287.

[40] Y.M. Lee, B.J. Kim, Y.S. Chun, I. So, H. Choi, M.-S. Kim, J.W. Park, NOX4 as an oxygen sensor to regulate TASK-1 activity, Cellular Signalling 18 (2006) 499–507.

[41] K. Block, Y. Gorin, H.E. Abboud, Subcellular localization of Nox4 and regulation in diabetes, Proceedings of the National Academy of Sciences 106 (2009) 14385–14390.

[42] R.E. Clempus, D. Sorescu, A.E. Dikalova, L. Pounkova, P. Jo, G.P. Sorescu, B. Lassegue, K.K. Griendling, Nox4 is required for maintenance of the differentiated vascular smooth muscle cell phenotype, Arteriosclerosis, Thrombosis and Vascular Biology 27 (2007) 42–48.

[43] C. Goettsch, W. Goettsch, G. Muller, J. Seebach, H.J. Schnittler, H. Morawietz, Nox4 overexpression activates reactive oxygen species and p38 MAPK in human endothelial cells, Biochemical and Biophysical Research Communications 380 (2009) 355–360.

Supplement Data

Materials and Methods

S1. Production and purification of Nox4 antigen for mice immunization

BL21(λDE3) Codon Plus-RIL bacteria (Stratagen) transformed with pET30b NHS-Nox4-1TM or with pET15b ΔT/Stop ZEBRA/MD4-eGFP plasmid were allowed to grow to reach an OD600 of 0.7 and bacteria were induced by 0.5M IPTG at 4°C for 4h. Cell pellets were lysed by sonication in buffer A (50mM Tris pH7.5, 100mM NaCl, 1mM EDTA, 2mM MgCl2, 2µg/ml leupeptin, 2µg/ml pepstatin, 10µM TLCK) and the lysates were centrifuged at 100,000g at 4°C for 1h to obtain the insoluble protein. The pellets were resuspended in buffer A containing 2M NaCl and then centrifuged at 100,000g at 4°C for 1h. The recovered pellets were resuspended and denatured in buffer A containing 8M urea and 1mM glycine (buffer A-urea). The denatured proteins were centrifuged again at 100,000g at 4°C for 1h and the supernatants were used further for the protein purification step. Samples were equilibrated by dilution in order to obtain a final concentration of 10mM imidazole and then loaded onto a pre-equilibrated His Gravitrap™ column. The column was then washed extensively with 20 column volumes of buffer A-urea containing 40mM imidazole. The proteins were partially refolded by a progressive step of 8M decreasing concentration of urea until 2M. The proteins were then eluted with buffer A-2M urea containing 250mM imidazole. The recovered proteins were used for the mice immunization.

S2. Measurement of NADPH oxidase activity in intact HEK293 overexpressed Nox4 cells [20]

For each well in a 96-well plate, 5×10^5 cells suspended in 50µl PBS were added to 200µl PBS containing 20µM luminol and 10units/ml horseradish peroxidase. Reactive oxygen species were measured using chemiluminescence in the absence or presence of 10µg/ml superoxide dismutase (SOD) or 50U/ml catalase (CAT). Photon emission was recorded at 37°C for 1h with a luminoscan (Labsystem, Pontoise, France).

S3. Generation of a recombinant plasmid for the expression of Nox4 coupled with eGFP

pCDNA3.1-V5/HisB was used to express Nox4 fused with eGFP at the C-terminal part. Firstly, full-length eGFP was amplified with Pfu polymerase from the pTT3/eGFP plasmid with the following primers: 5'-GTT TCT CGA GAT GAT CGA TGT GAG CAA GGG CGA GGA

G-3' and 5'-GTT TGG GCC CTC ACT TGT ACA GCT CGT CCA TGC CG-3'. The nucleotides corresponding, respectively, to the restriction sites XhoI and ApaI are underlined. The purified PCR product was digested with XhoI and ApaI and ligated into linearized pCDNA3.1-V5/HisB vector to obtain the pCDNA/eGFP plasmid. Secondly, Nox4 was digested with KpnI and XhoI from the plasmid pEF/Nox4, the resulting fragment was inserted into linearized pCDNA/eGFP plasmid to obtain a plasmid encoding Nox4GFP.

S4. Stable transfection of mammalian expression plasmids

5×10^5 HEK293 cells were seeded in 6-well plates and allowed to grow for 24h to reach a 70% confluence in 2ml of culture medium. The cells were transfected with 3µg of vectors according to the manufacturing protocol (JetPEI, Polyplus transfection). After 24h, stable transfected cells were selected with 500µg/ml geneticin for 3 weeks before analysis.

S5. siRNA transfection

RNA interference process was performed as described previously [44] with minor modifications. 6×104 HEK293 Nox4GFP cells were seeded in 24-well plates. siRNA oligos (siRNAa, siRNAc) directed against human Nox4 mRNA were transfected into the cells by using HiPerFect transfection reagent (as recommended by the manufacturer). Nox4 siRNA-a sense oligo: 5'AAA GCA GGA CAU UCA UGG AGA GCC A 3'; Nox4 siRNA-a antisense oligo: 5'UGG CUC UCC AUG AAU GUC CUG GCU UU 3'; Nox4 siRNA-c sense oligo: 5'CCA GGA GAU UGU UGG AUA A 3'; Nox4 siRNA-c antisense oligo: 5'UUA UCC AAC AAU CUC CUG G 3'. All analyses of siRNA-treated cells, that is, ROS measurements, western blot, were done 24h after siRNA treatment.

[44] B. Li, K. Bedard, S. Sorce, B. Hinz, M. Dubois-Dauphin, K.H. Krause, NOX4 expression in human Microglia leads to constitutive generation of reactive oxygen species and to constitutive IL-6 expression, Journal of Innate Immunity 1 (2009) 570–581.

Supplement Data

Table and figure legends

Table S1. List of primers for Nox4 truncated forms used for the determination of mAb epitope regions

Fig. S1. Production and purification of NHS-Nox4-1TM. (A) NHS-Nox4-1TM solubility test. IPTG induced BL21(λDE3) bacteria containing the plasmid encoding for NHS-Nox4-1TM construction were lysed and the total lysate (1) was centrifuged at 14 000 g at 4°C for 30min to separate the soluble proteins (2) (supernatant) from the insoluble (3) (pellet). These 3 fractions were analysed by SDS-PAGE gel stained by Coomassie Blue. The arrows indicate NHS-Nox4-1TM protein. (B) ZEBRA/MD4-GFP (ZEBRA) and NHS-Nox4-1TM purifications. Bacteria were lysed by sonication. The inclusion bodies were denaturated with 8M urea and the soluble fraction after ultracentrifugation was loaded onto a His Gravitrap™ column. After partial renaturation to 2M urea, the proteins were eluted with 250mM imidazole. The eluted fractions (1µl from 1ml of elution fraction) were loaded into SDS-PAGE gel and revealed with Coomassie staining. The amount of the purified protein was estimated by a BSA standard curve. The arrows indicate purified NHS-Nox4-1TM and ZEBRA proteins. MW: molecular weight marker.

Fig. S2. $O_2^{\cdot-}$ is the major oxidative metabolite measured from tet-induced HEK293 T-REx™ Nox4 cells and HEK293 Nox4GFP cells. Un-induced and tet-induced HEK293 T-REx™ Nox4 cells (5×10^5 cells/well) (A) or HEK293 WT and HEK293Nox4GFP cells (5×10^5 cells/well) (B) were added to the luminol detection mixture. Signals were recorded for 60min, in the presence or absence of SOD or catalase (CAT) as described in materials and methods. Results are expressed as the sum of RLU measurements. Values are presented as the average of at least three experiments ± S.D. * indicates $P<0.05$.

Fig. S3. The sensitivity of Nox4 to the temperature. The expression of Nox4GFP in total lysates of HEK293 WT cells (1) and HEK293 Nox4GFP cells (2) (200µg/lane) were detected by anti-GFP mAb. Proteins were denatured at 4°C overnight or 60°C for 1h. Full-length Nox4GFP: 85KDa (arrow), degraded Nox4GFP: 58KDa (asterisk). 1: HEK293 WT cells, 2: HEK293

Nox4GFP cells. Immune complexes were detected by ECL after binding with peroxidase. These pictures are representative of 3 experiments.

Fig. S4. Inhibition of Nox4 expression in HEK293 Nox4GFP cells by RNAi. HEK293Nox4GFP cells were transfected with scrambled siRNA or siRNA targeting Nox4 (siRNAa, siRNAc, siRNAac) using HiPerfect transfection reagent. (A) Inhibition of Nox4 expression in HEK293Nox4GFP cells transfected with siRNA determined by western-blot with anti-GFP mAb, β-actin was used as the internal control for normalization, the value of Nox4GFP control was set as 100%. These pictures are representative of 2 experiments; (B) inhibition of Nox4 expression in HEK293 Nox4GFP cells transfected with siRNA determined by NADPH oxidase activity. Cells (5×10^5 cells/well) were added to the detection mixtures for luminol. Signals were recorded for 60min as described in materials and methods. Results are expressed as the sum of RLU measurements and are reported as a percentage of ROS produced by untransfected HEK293 Nox4GFP cells. Values represent the mean ± S.D. of triplicate determinations. * indicates $P<0.05$.

Fig. S5. Weak reactivity of purified mAbs 10B4 and 7C9. (A) Reactivity comparison between ascite and purified mAb. Western blot were carried out by using truncated recombinant proteins (Nox41TM and Nox4qc, 5μg each) and ascite or purified mAb of 5F9 (upper panel), 10B4 (lower panel, left) or 7C9 (lower panel, right) as the primary antibody respectively; (B) The capacity of purified mAb 7C9 to bind to the antigen (NHS-Nox4-1TM, 1μl from 1ml of elution fraction) was checked with different concentrations. Arrow indicates the position of NHS-Nox4-1TM, asterisk indicates the unspecific signal. Immune complexes were detected by ECL after binding with peroxidase. These pictures are representative of 2 experiments.

Figure S1.

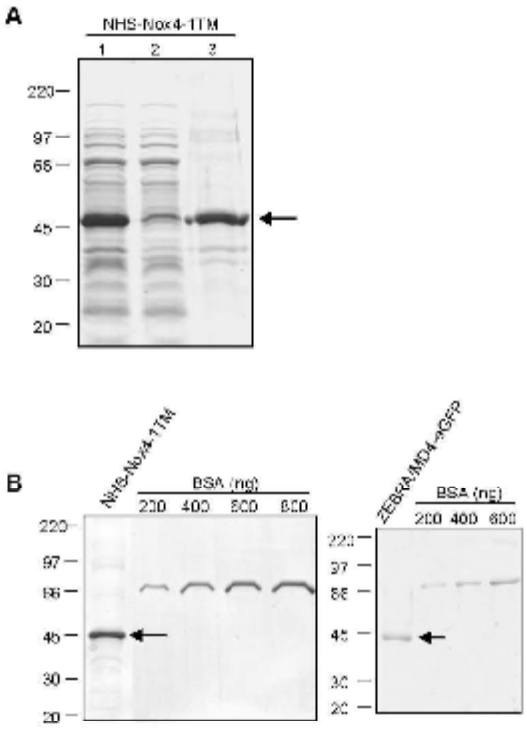
A
NHS-Nox4-1TM
1
2
3
220
97
66
45
30
20
B
NHS-Nox4-1TM
BSA (ng)
200 400 600 800
220
97
66
45
30
20
ZEB8KA/MD4-eGFP
BSA (ng)
200 400 600

Figure S2.

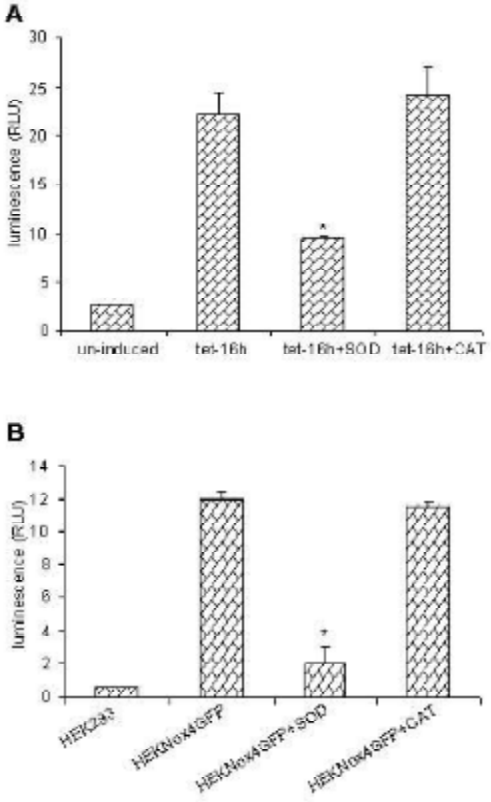
A
luminescence (RLU)
30
25
20
15
10
5
0
un-induced
tet-16h
tet-16h+SOD
tet-16h+CAT
B
luminescence (RLU)
14
12
10
8
6
4
2
0
HEK293
HEKNox4GFP
HEKNox4GFP+SOD
HEKNox4GFP+CAT

Figure S3.

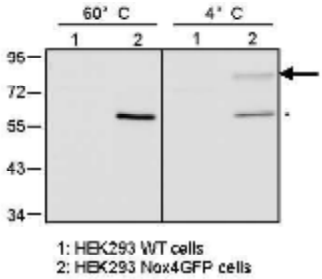
60° C
4° C
1
2
1
2
96
72
55
43
34
1: HEK293 WT cells
2: HEK293 Nox4GFP cells

Figure S4.

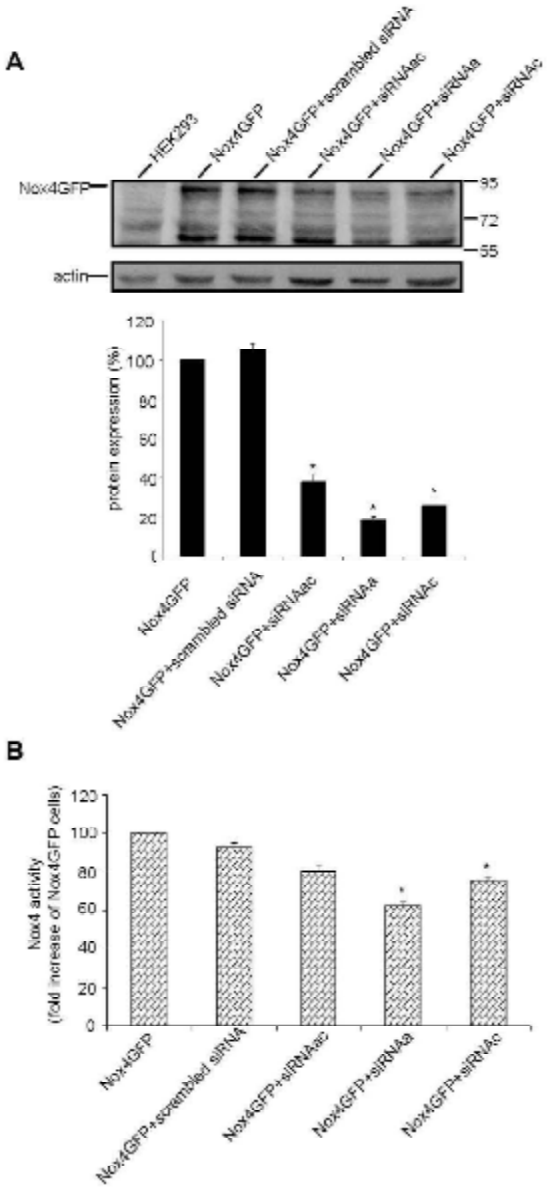
A
HEK293
Nox4GFP
Nox4GFP+scrambled siRNA
Nox4GFP+siRNAac
Nox4GFP+siRNAa
Nox4GFP+siRNAc
Nox4GFP
actin
95
72
55
protein expression (%)
120
100
80
60
40
20
0
Nox4GFP
Nox4GFP+scrambled siRNA
Nox4GFP+siRNAac
Nox4GFP+siRNAa
Nox4GFP+siRNAc
B
Nox4 activity
(fold increase of Nox4GFP cells)
120
100
80
60
40
20
0
Nox4GFP
Nox4GFP+scrambled siRNA
Nox4GFP+siRNAac
Nox4GFP+siRNAa
Nox4GFP+siRNAc

Figure S5.

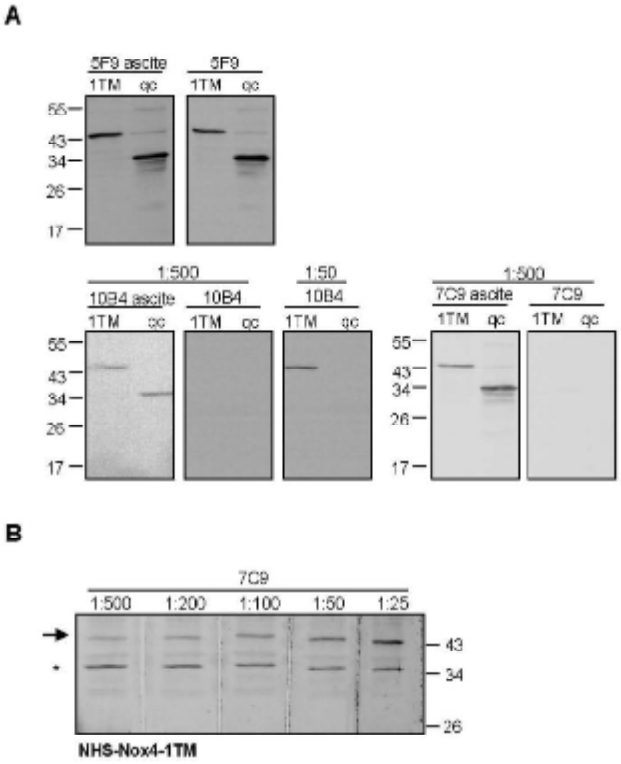
A
5F9 ascite
5F9
1TM
qc
55
43
34
26
17
1:500
10B4 ascite
10B4
1:50
7C9 ascite
7C9
B
7C9
1:500
1:200
1:100
1:50
1:25
NHS-Nox4-1TM

Chapter 2: The E-loop is involved in the hydrogen peroxide formation of Nox4

Résumé en français

1 Introduction

Même si les caractéristiques structurelles des protéines Nox sont très conservées, leurs modes d'activation diffèrent d'une oxydase à l'autre. Contrairement aux autres Nox, l'activité NADPH oxydase de Nox4 est constitutive et semble indépendante de la présence des facteurs cytosoliques dédiés à l'activation de Nox1, Nox2 et Nox3. Une autre différence importante entre les Nox1 et 2 et Nox4 est que les oxydases produisent essentiellement O_2^-, alors que la plupart des études suggèrent que Nox4 produit H_2O_2. L'expression de la protéine Nox4 a été retrouvée dans la mitochondrie, le noyau, le cytosquelette ainsi que le réticulum endoplasmique. C'est pourquoi, la quantification de la formation de O_2^- par Nox4 est délicate à mettre en évidence et que le seul dérivé réactif de l'oxygène révélé est H_2O_2 qui diffuse librement à travers les membranes. Bien que Nox4 soit exprimé à la membrane plasmique dans certaines cellules, la mise en évidence de l'ion superoxyde O_2^- par Nox4 est toujours difficile alors que celle de H_2O_2 est quantifiable. La question d'une production directe de H_2O_2 par Nox4 est posée, mais aucune évidence expérimentale n'a encore été apportée et les bases moléculaires restent à démontrer.

2 Objectifs et méthodes

Les objectifs de ce travail sont:

- De prouver que la production de H_2O_2 est une caractéristique intrinsèque de Nox4;
- D'étudier les bases structurelles expliquant la formation de H_2O_2 par Nox4 et ses conséquences biologiques.

La comparaison des séquences protéiques des Nox montre une différence importante de la boucle E de Nox4 par rapport à celle des autres Nox ce qui pourrait expliquer une différence dans la nature des ROS produits. Dans ce travail, la boucle E de Nox4 à été mutée et l'on a analysé les conséquences de cette mutation en terme de production de ROS. L'approche expérimentale à été ciblée sur plusieurs techniques de mesure des ROS: la chimiluminescence en présence ou non d'un donneur de monoxyde d'azote, la fluorescence par oxydation de l'Amplex Red, et la réduction du cytochrome c. On a également analysé les conséquences de

l'interaction entre deux composés, l'anticorps monoclonal dirigé contre un épitope présent sur la boucle E, et le bis sulfosuccinimidyl suberate (BS3) avec la protéine Nox4 sauvage présente à la surface des cellules COS7.

3 Résultats

- Un alignement de séquence d'acides aminés de Nox1, Nox2 et Nox4 a révélé que la boucle E de Nox4 présente deux régions absentes dans les oxydases Nox1 et Nox2: la première région va de l'acide aminé 218 à l'acide aminé 235, la deuxième région de l'acide aminé 264 à l'acide aminé 273. La délétion de ces deux régions n'affecte pas la localisation de Nox4 dans le réticulum endoplasmique (Fig. 1C). Par contre, contrairement à Nox4 sauvage, les deux mutants de la boucle E produisent principalement l'ion superoxyde O_2^- et non pas le peroxyde d'hydrogène (Fig. 1D et E). En présence d'un donneur de NO, les données obtenues par chimioluminescence montrent que seuls les mutants de la boucle E de Nox4 produisent le peroxynitrite $ONOO^-$, confirmant ainsi que les mutants de Nox4 produisent bien l'ion superoxyde (Fig. 3A).
- Les deux régions de la boucle E spécifique de Nox4 contiennent deux cystéines qui ont été mutées en valine Nox4 Cys226Val ou Nox4 Cys270Val. Les cellules HEK293 transfectées transitoirement par les deux mutants Nox4 Cys226Val ou Nox4 Cys270Val ont produit O_2^- au lieu de H_2O_2 (Fig. 2A et B). Ces données ont montré que les modifications, même mineures, des régions de la boucle E de Nox4, sont capables de modifier la nature des dérivés réactifs de l'oxygène produit par Nox4.
- Les cellules Cos7 sont capables après transfection d'exprimer Nox4 à la surface de la membrane plasmique. Ce modèle cellulaire permet donc d'intervenir directement sur la boucle E de Nox4 sauvage qui se trouve exposé de façon extracellulaire. Dans ces cellules, Nox4 produit également H_2O_2. Au contact de l'anticorps monoclonal 8E9 dirigé contre la boucle E, Nox4 diminue la production de H_2O_2 (Fig. 4B). Ce résultat est comparable à l'effet du composé BS3, qui détruit l'activité de Nox4 en formant des liaisons covalentes à la surface de la membrane plasmique. Ainsi, la structure de Nox4 au niveau de la boucle E semble jouer un rôle essentiel dans la formation de H_2O_2.
- Cinq histidines hautement conservées entre les oxydases Nox4 de différents organismes ont été mutées en glutamine et la formation ainsi que la nature des ROS produits par ces mutants a été étudiée. Seul le mutant His222Gln localisé dans la boucle E de Nox4 augmente de façon significative la production de O_2^- et diminue la production de H_2O_2 (Fig. 5B). Cette histidine nécessaire à la formation de H_2O_2 pourrait

servir de source de proton ou de site de fixation à un ion métallique et avoir ainsi un rôle de type « superoxyde dismutase ».

- Contrairement aux oxydases Nox1 et Nox2, l'activité de Nox4 à été montrée comme étant impliquée dans la phosphorylation des protéines Erk1/2. Cette propriété a été vérifiée dans les cellules HEK transfectées transitoirement par Nox4 sauvage. Par contre, les cellules HEK transfectées avec les mutants de Nox4 Cys226Val ou Cys270Val présentent une diminution de près de 80% du taux de phosphorylation des protéines Erk1/2 (Fig. 6). Les résultats suggèrent que le type de ROS produit a des conséquences biologiques importantes dans la transduction du signal dépendant de Nox4.

Summary in English

1 Background

Despite the highly conserved structural features, Nox proteins differ in their mode of activation, the interaction with p22phox and the requirement for additional maturation and activation factors. Unlike all the other Noxs, Nox4 is constitutively active and is independent of cytosolic activator proteins or regulatory domains. Recent studies (Helmcke *et al.*, 2009; Nisimoto *et al.* 2010) showed that the constitutive activity of Nox4 resides in its dehydrogenase (DH) domain that contains the binding sites for both FAD and NADPH (Segal *et al.*, 1992; Helmcke *et al.*, 2009; Nisimoto *et al.*, 2010). Complex interactions between the cytosolic tail and the intracellular loops of the individual Nox homologues have been demonstrated with the aid of chimeric proteins and mutants (Carrichon *et al.*, 2010; Jackson *et al.*, 2010; von Lohneysen *et al.*, 2010), but a molecular explanation of the differences between Nox1/2 and Nox4 is not yet clear. Another interesting difference between Nox1/2 and Nox4 is that Nox1 and Nox2 produce primarily O_2^-, whereas most studies report that Nox4 generates H_2O_2.

The failure to detect O_2^- formation by Nox4 has been proposed due to its intracellular location and dismutation to the freely diffusible H_2O_2 to pass through the membrane. However Nox4 in some cells exists at the plasma membrane still produces H_2O_2. This work focused on the studying the structural basis for H_2O_2 formation by Nox4.

2 H_2O_2 production is an intrinsic feature of Nox4

The alignment of the amino acid sequences of human and mouse Nox1, Nox2 and Nox4 revealed that the E-loop of Nox4 is longer than the loop of Nox1 and Nox2 as a consequence of 2 insertions. The sequence within the two insertions is similar among Nox4's different species, suggesting a conserved Nox4-specific function. To exclude the failure of detected O_2^- formation of Nox4 is a consequence of its intracellular location or some artifact of the detection system, Nox4 E-loop mutants were used to study the relationship between the type of ROS formed by Nox4 and its localization. Also, ROS formation was studied in the presence of NO donor, which can react with O_2^- at a near diffusion controlled rate. ROS was determined by using chemiluminescence measurement and subcellular localization of Nox4 mutants was observed by confocal microscopy.

- ✓ Immunofluorescence data showed that deletion of these Nox4-specific E-loop regions did not affect the ER localization of Nox4 (Fig. 1C), but these mutants produced very little H_2O_2 compared to

native Nox4 and instead release O_2^- (Fig. 1D&E). In the presence of NO, luminol chemiluminescence data showed that only Nox4 E-loop mutants but not native Nox4 yield $ONOO^-$ (Fig. 3A), the H_2O_2 formation occurs via free intermediate formation of O_2^-. These results indicated that H_2O_2 production is an intrinsic feature of Nox4.

3 Structural basis for H_2O_2 formation of Nox4 and its biological consequence

The E-loop of Nox4 as well as Nox1 and Nox2 both contain two conserved cysteines. In Nox4, both are lost upon the construction of the deletion mutants of Nox4. As the cysteines might form a disulfide bridge to maintain the intergrity of the E-loop, their role for the function of Nox4 was studied. As Nox4 activity has previously been linked to Erk1/2 phosphorylation, the biological consequence of the type of ROS released by Nox4 was investigated.

Since local mutation in structure may affect the function of an enzyme at a remote site by some allosteric modulations, mAb 8E9 was used to confirm the role of E-loop of Nox4. As this antibody was directed against the E-loop of Nox4, this study was carried out in Cos7 cells, which Nox4 exhibits at the plasma membrane.

Activity was measured by chemiluminescence measurement, Amplex Red measurement and cytochrome c-reduction measurement. The protein expression was analyzed by western blot.

- ✓ HEK293 cells transiently transfected with Nox4 Cys226Val or Nox4 Cys270Val produce O_2^- instead of H_2O_2 (Fig. 2A&B). These data showed that even minor alterations of the E-loop of Nox4 switch the protein from H_2O_2 to O_2^-. These mutants significant decreased the expression of the phosphorylated Erk1/2 (Fig. 6), indicating that the direct formation of H_2O_2 by Nox4 has important biological consequences for Nox-dependent signal transduction;
- ✓ In Cos7 cells transiently transfected with Nox4, mAb 8E9 was used to interfere with the E-loop. Addition of mAb 8E9 decreased H_2O_2 production (Fig. 4B). This result has equally effective as BS3, which should destroy the Nox4 activity at the plasma membrane, in reducing H_2O_2 formation by Nox4.

4 Identification of a molecular explanation for H_2O_2 formation by Nox4

Structural alignment revealed that, in addition to those that are directly involved in heme ligation, Nox4 contains five additional highly conserved histidines in transmembrane domain. Three of these are located in the E-loop. Role of these histidine mutants for H_2O_2 production by Nox4 was investigated. Activity was

measured by chemiluminescence measurement and the protein expression was analyzed by western blot.

- ✓ Western blot analysis showed that the expression of the histidine mutants were similar to that of native Nox4. Activity results showed that only one mutant, Nox4-His222Gln, produced O_2^- instead of H_2O_2. This observation suggested that His222 might play a role in generating H_2O_2 by serving as a source for protons need to form H_2O_2, or by binding a metal.

My contribution to this work was to provide a well validated and characterized monoclonal antibody 8E9 specific to Nox4. The epitope region of mAb 8E9 was on the extracellular E- loop of Nox4 (^{222}H-E^{241}). It was well used in studying the role of E-loop of Nox4 in its intrinsic feature.

Article 2:

The E-loop is involved in hydrogen peroxide formation by the NADPH oxidase Nox4. *Ina Takac, Katrin Schröder, **Leilei Zhang**, Bernard Lardy, Narayana Anilkumar, J. David*

Lambeth, Ajay M. Shah, Francoise Morel, Ralf P. Brandes.

THE JOURNAL OF BIOLOGICAL CHEMISTRY VOL. 286, NO. 15, pp. 13304–13313, April 15, 2011

The E-loop Is Involved in Hydrogen Peroxide Formation by the NADPH Oxidase Nox4*

Received for publication, October 5, 2010, and in revised form, January 6, 2011 Published, JBC Papers in Press, February 22, 2011, DOI 10.1074/jbc.M110.192138

Ina Takac[‡], Katrin Schröder[‡], Leilei Zhang[§], Bernard Lardy[§], Narayana Anilkumar[¶], J. David Lambeth[‖], Ajay M. Shah[¶], Francoise Morel[§], and Ralf P. Brandes[‡1]

From the [‡]Institut für Kardiovaskuläre Physiologie, Goethe-Universität, 60596 Frankfurt am Main, Germany, the [§]Groupe de Recherche et d'Etude du Processes Inflammatoire, TIMC-Imag UMR-CNRS 5525, Joseph Fourier University, 38041 Grenoble Cedex 09, France, the [¶]Cardiovascular Division, King's College London British Heart Foundation Centre, London SE5 9NU, United Kingdom, and the [‖]Department of Pathology and Laboratory Medicine, Emory University Medical School, Atlanta, Georgia 30322

In contrast to the NADPH oxidases Nox1 and Nox2, which generate superoxide (O_2^-), Nox4 produces hydrogen peroxide (H_2O_2). We constructed chimeric proteins and mutants to address the protein region that specifies which reactive oxygen species is produced. Reactive oxygen species were measured with luminol/horseradish peroxidase and Amplex Red for H_2O_2 *versus* L-012 and cytochrome *c* for O_2^-. The third extracytosolic loop (E-loop) of Nox4 is 28 amino acids longer than that of Nox1 or Nox2. Deletion of E-loop amino acids only present in Nox4 or exchange of the two cysteines in these stretches switched Nox4 from H_2O_2 to O_2^- generation while preserving expression and intracellular localization. In the presence of an NO donor, the O_2^--producing Nox4 mutants, but not wild-type Nox4, generated peroxynitrite, excluding artifacts of the detection system as the apparent origin of O_2^-. In Cos7 cells, in which Nox4 partially localizes to the plasma membrane, an antibody directed against the E-loop decreased H_2O_2 but increased O_2^- formation by Nox4 without affecting Nox1-dependent O_2^- formation. The E-loop of Nox4 but not Nox1 and Nox2 contains a highly conserved histidine that could serve as a source for protons to accelerate spontaneous dismutation of superoxide to form H_2O_2. Mutation of this but not of four other conserved histidines also switched Nox4 from H_2O_2 to O_2^- formation. Thus, H_2O_2 formation is an intrinsic property of Nox4 that involves its E-loop. The structure of the E-loop may hinder O_2^- egress and/or provide a source for protons, allowing dismutation to form H_2O_2.

The class of Nox protein NADPH oxidases is a group of enzymes whose sole known function is the production of reactive oxygen species (ROS).[2] The enzyme family is named for the enzymatically active transmembrane protein Nox. All seven Nox proteins share highly conserved structural features; the C-terminal dehydrogenase domain contains binding sites for FAD and NADPH. The N-terminal transmembrane region consists of six α-helical transmembrane domains that contain four conserved histidine residues, located in the third and fifth transmembrane helices that coordinate two hemes. Electron transfer occurs from NADPH to oxygen via FAD and the two heme groups, with the second heme group reducing molecular oxygen (1, 2). Because heme is an obligate 1-electron donor, it is generally accepted that the superoxide anion (O_2^-) is the initial reduction product of oxygen, although the latter can also react with a second O_2^- to form hydrogen peroxide (H_2O_2) plus oxygen.

Despite these similarities, Nox proteins differ in their mode of activation, their interaction with the small transmembrane protein $p22^{phox}$, and the requirement for additional maturation and activation factors. The most extensively studied NADPH oxidase isoform is the phagocyte Nox2 (previously termed $gp91^{phox}$), which depends on $p22^{phox}$ and whose activation requires assembly with the cytosolic regulatory subunits $p47^{phox}$ and $p67^{phox}$ (3), along with GTP-loaded Rac1 or Rac2. Similar to Nox2, the homologue Nox1 requires regulatory subunits. Unlike all the other Nox proteins, Nox4 is constitutively active and is independent of cytosolic activator proteins or regulatory domains (4, 5). Another interesting difference between Nox1/2 and Nox4 is that Nox1 and Nox2 produce primarily O_2^-, whereas most studies report that Nox4 generates H_2O_2 (4, 6, 7).

Given that the prosthetic groups are identical and the core protein structures are very similar among the Nox proteins, it has been suggested that the failure to detect O_2^- formation by Nox4 is a consequence of its intracellular location, resulting in problems detecting O_2^- within the cell and the inability of this ion to pass freely through the membrane. Indeed, although a significant fraction of Nox1 and Nox2 is located at the plasma membrane and thus would reduce extracellular oxygen, Nox4 is localized predominantly to intracellular membranes where any generated O_2^- might be cryptic. In fact, Nox4 protein has been reported in mitochondria (8), the nucleus (9), the cytoskeleton (10), and the endoplasmic reticulum (11). Thus, it was plausible to propose that O_2^- generated in these compartments must undergo dismutation to leave the cell as the freely diffusible H_2O_2. However, Nox4 in some cells resides in part in the plasma membrane but unexpectedly still produces H_2O_2 without any detectable O_2^- (12). Moreover, a careful analysis of intracellular ROS formation using overexpressed Nox4 failed to

* This work was supported, in whole or in part, by National Institutes of Health Grant RO1 CA084138, RO1 CA105114, and RO1 HL071162 (to J. D. L.) and the Leducq Foundation and the British Heart Foundation (to A. M. S.). This work was also supported by grants from the Deutsche Forschungsgemeinschaft (SFB815/TP1 and SFB834/TPA2) and the Excellence Cluster Cardio-pulmonary System (ECCPS).

[1] To whom correspondence should be addressed: Institut für Kardiovaskuläre Physiologie, Goethe Universität, Theodor Stern Kai 7, 60590 Frankfurt am Main, Germany. Tel.: 49-69-6301-6905; Fax: 49-69-6301-7568; E-mail: r.brandes@em.uni-frankfurt.de.

[2] The abbreviation used is: ROS, reactive oxygen species.

detect Nox4-mediated $O_2^{\cdot-}$ production using ESR spin traps and the dihydroethidium method (13). In contrast, Nox4 was able to reduce nitro blue tetrazolium. However, the site of the electron efflux from Nox4 to nitro blue tetrazolium has not yet been determined but is potentially via the FAD-containing dehydrogenase domain, which is known to catalyze the direct reduction of various dyes (14). Based on the above, it has to be concluded that although mechanistically, heme reduction of oxygen must initially generate $O_2^{\cdot-}$, Nox4 releases H_2O_2 without releasing free $O_2^{\cdot-}$. The molecular basis for this potentially physiologically important difference is unclear.

Based on the presence of six transmembrane α-helical domains, the current model for NADPH oxidases predicts that the N- as well as C-terminal parts of the protein reside in the cytosol, giving rise to two intracellular loops (B- and D-loop) and three loops oriented away from the cytosol and toward the extracellular space or intracellular compartments (A-, C-, and E-loop). So far, little work has been devoted to the extracellular loops. Although asparagines within these regions are glycosylated in Nox2, to our knowledge, no mutations leading to chronic granulomatous disease have been reported for these loops. Also, the functional significance of glycosylation is somewhat uncertain as unlike human Nox2, the murine enzyme does not undergo this modification and glycosylation has not been reported for Nox1. Based upon their proximity to the site of oxygen reduction by the B heme, we hypothesized that differences in the extracEular loops are responsible for the unique ability of Nox4 to release H_2O_2 rather than $O_2^{\cdot-}$.

EXPERIMENTAL PROCEDURES

Sequence Alignment—Nox sequences were aligned using the online program ClustalW2 from the European Molecular Biology Laboratory-European Bioinformatics Institute (EMBL-EBI) (15).

Generation and Transfection of Mutant Nox Constructs—Plasmids encoding human full-length Nox1, Nox4, and $p22^{phox}$ were kindly provided by T. Leto (National Institutes of Health, Bethesda, MD). The plasmids coding for mouse Noxa1 and Noxo1 were generous gifts of B. Banfi (Iowa University, Iowa City, IA). The plasmids coding for the Nox4 deletion mutants were generated by overlap extension PCR. The plasmids coding for the cysteine and histidine mutants of Nox1 and Nox4 were generated by site-directed mutagenesis using the QuikChange mutagenesis kit (Stratagene, La Jolla, CA) according to the manufacturer's instructions. All cloned plasmids were confirmed with DNA sequencing. Transient transfection of HEK293 or Cos7 cells (ATCC, Manassas, VA) was performed with Lipofectamine 2000 (Invitrogen, Paisley, UK) according to the manufacturer's instructions. HEK293 cells stably expressing Nox4 Δ218–235 + Δ264–273 were generated by transfection with linearized plasmid with Lipofectamine 2000 and subsequent antibiotic selection.

Determination of ROS by Chemiluminescence Measurement—HEK293 or Cos7 cells were seeded on 3.5-cm dishes and transiently transfected. After 24 h, EDTA-detached cells were suspended in 500 μl of HEPES-modified Tyrode's solution containing the appropriate chemiluminescence enhancer. As enhancer for H_2O_2, luminol (Sigma; 100 μM) in combination with horseradish peroxidase (HRP; Sigma; 1 units/ml) were used. As enhancer for $O_2^{\cdot-}$, L-012 (WAKO Chemicals, Richmond, VA, 200 μM) was used. As enhancer for peroxynitrite ($ONOO^-$), luminol without HRP was used, and DetaNONOate (Enco Life Sciences, Plymouth Meeting, PA; 100 μM) was added as NO donor to facilitate the formation of $ONOO^-$ from $O_2^{\cdot-}$.

Determination of ROS by Amplex Red Measurement—HEK293 cells were grown on 12-well plates and transiently transfected. 24 h later, cells were washed once with phosphate-buffered saline (PBS) and subsequently incubated in PBS containing 100 μM Amplex Red and 0.25 units/ml HRP. After 30 min, the supernatant was transferred to a 96-well plate, and H_2O_2-dependent oxidation of Amplex Red was measured in a microplate fluorometer (excitation 540 nm, emission 580 nm). H_2O_2 formation was quantified by a standard curve of known H_2O_2 concentrations.

Determination of Reactive Oxygen Species by Cytochrome c Reduction—HEK293 cells were seeded on 12-well plates and transiently transfected. 24 h later, cells were washed once in HEPES-modified Tyrode's solution containing cytochrome *c* (from horse heart; Sigma; 1 mg/ml) and then incubated in this solution in the presence or absence of superoxide dismutase (Sigma, 100 units/ml) at 37 °C. After 30–60 min, supernatants were transferred to fresh tubes on ice, and the superoxide dismutase-inhibitable reduction of cytochrome *c* was quantified in a spectrophotometer (Uvikon, Kontron Instruments). Data were normalized to the isosbestic points at 542 and 558 nm, and $O_2^{\cdot-}$ formation was calculated with the aid of the molar extinction coefficient of 21 mM^{-1} cm^{-1}.

Western Blot Analysis—24 h after transfection, cells were incubated for 8 h with the proteasome inhibitor MG132 (10 μM, Calbiochem) to stabilize and increase the Nox expression. Cell lysis, SDS-PAGE, and Western blot were carried out (16). The following antibodies were used: anti-Nox1 (Santa Cruz Biotechnology: Mox-1 H-15); anti-Nox4 (generated by us (17)); anti-β-actin (Sigma); and anti-Erk1/2 and anti-phosphorylated Erk1/2 (Cell Signaling).

Confocal Fluorescence Microscopy—HEK293 cells stably expressing Nox4 Δ218–235 + Δ264–273 were seeded on μ-dishes (Ibidi, Martinsried, Germany). When the cells reached ~80% confluence, they were incubated for 8 h with the translation inhibitor anisomycin (Calbiochem; 20 μM) to reduce potential localization of the protein to the endoplasmic reticulum due to *de novo* synthesis. Imaging was carried out as described (16) with the following antibodies: anti-Nox4 (generated by us) and anti-GRP78 (Santa Cruz Biotechnology) for endoplasmic reticulum staining.

Statistical Analysis—Unless otherwise stated, all data shown are mean ± S.E. Statistical significance was determined by one-way analysis of variance followed by Newman-Keuls post hoc test or by paired or unpaired *t* test, if appropriate.

RESULTS

Role of the Length of the E-loop of Nox4—To identify a structural basis for the H_2O_2 formation of Nox4, we compared this protein with Nox1 and Nox2. An alignment of the amino acid sequences of human and mouse Nox1, Nox2, and Nox4 revealed that the E-loop of Nox4 is 28 amino acids longer than

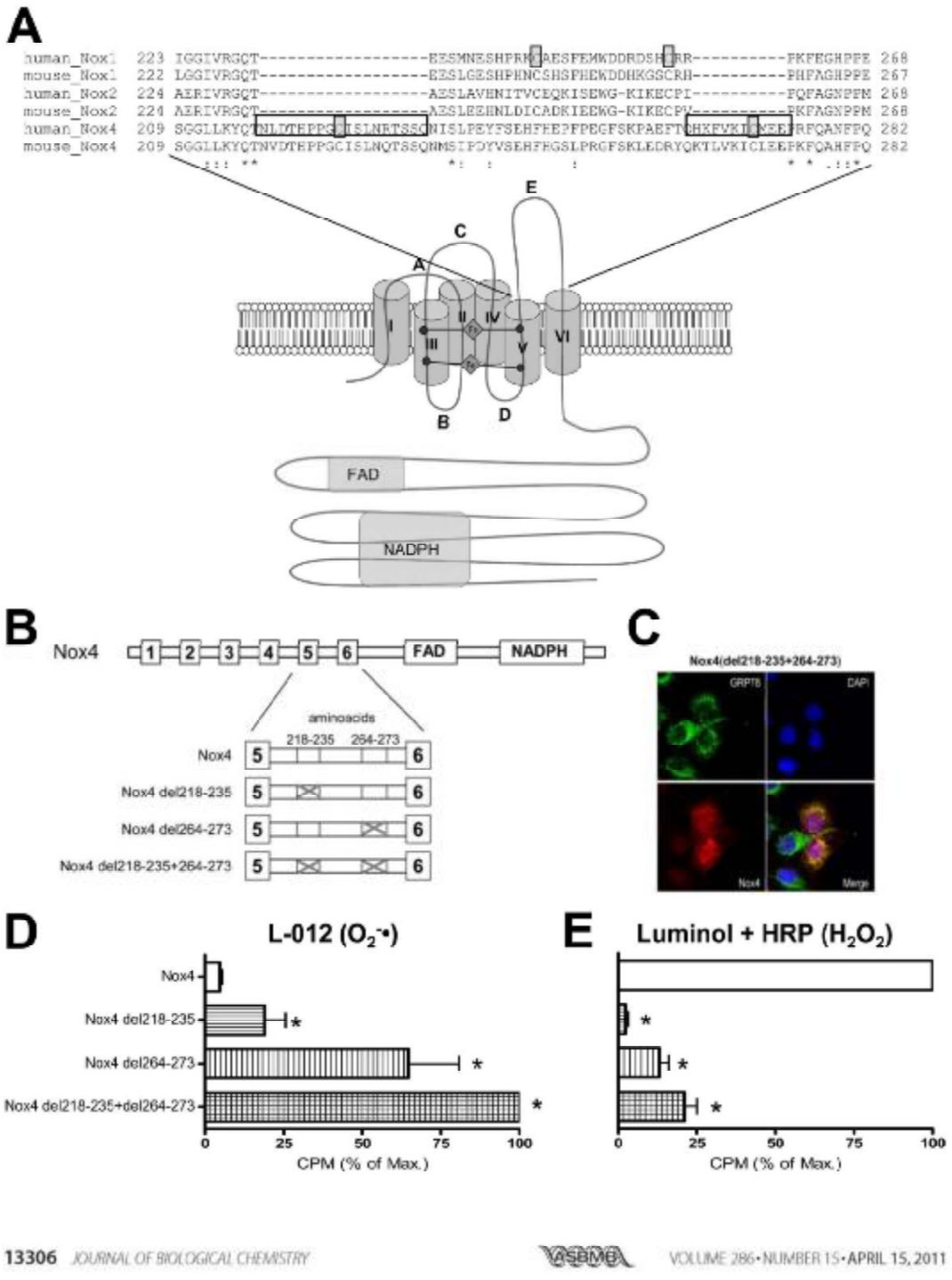

the E-loop of Nox1 and Nox2 (Fig. 1*A*) as a consequence of two insertions of 18 and 10 amino acids, respectively. The sequence within the two insertions is similar among Nox4s from different species, suggesting a conserved Nox4-specific function. We deleted these Nox4-specific E-loop regions so as to approximate the length of the E-loop in Nox1 and Nox2 (Fig. 1*B*). These mutations, which did not affect the endoplasmic reticulum localization of Nox4 (Fig. 1*C*), had a strong effect on ROS production by Nox4; the mutants produced very little H_2O_2 when compared with native Nox4 and instead released $O_2^{\cdot-}$ (Fig. 1, *D* and *E*). The effect was more pronounced in the double deletion mutant, which lacked both sequence insertions, but deletion of amino acids 264–273 was almost equally effective. Although the Nox4 deletion mutants produced $O_2^{\cdot-}$, their $O_2^{\cdot-}$ formation rate was still lower than that of native Nox1 when equimolar amounts of the expression plasmid were transfected (data not shown). Given that Nox4 del218–235+264–273 colocalized with the heat-shock protein GRP78 (Fig. 1*C*) and thus is expressed in the endoplasmic reticulum-like native Nox4, we conclude that the type of ROS formed by Nox proteins is an intrinsic feature of the protein and not a consequence of the intracellular localization.

Role of the Cysteines in the E-loop of Nox Proteins—The E-loops of Nox4 as well as Nox1 and Nox2 both contain two conserved cysteines, although they are located in different positions in the two isoforms. In Nox4, both are lost upon the construction of the deletion mutants of Nox4. As the cysteines might form a disulfide bridge to maintain the integrity of the E-loop, we studied their role for the function of Nox4. Mutation of the cysteines to valines had a similar, although less pronounced, effect on ROS production by Nox4 as the deletion constructs (Fig. 2, *A* and *B*), as demonstrated by chemiluminescence as well as cytochrome *c* reduction and Amplex Red oxidation. A plasmid harboring the mutation of both Nox4 cysteines together showed a more pronounced effect on the switching of the ROS type generated than the single mutations (data not shown). Mutation of the two cysteines in Nox1 decreased the overall activity of the enzyme but did not change the type of ROS released (Fig. 2*C*). These data show that even minor alterations of the E-loop of Nox4 switch the protein from H_2O_2 to $O_2^{\cdot-}$ production and that the integrity of the E-loop is also essential for $O_2^{\cdot-}$ formation of Nox1.

Nox4 E-loop Mutants but Not Native Nox4 Form Peroxynitrite in the Presence of an NO Donor—To address whether the H_2O_2 formation of Nox4 occurs via free intermediate formation of $O_2^{\cdot-}$ and to further exclude that H_2O_2 formation is a consequence of some artifact of the detection system, we studied ROS formation in the presence of an NO donor using luminol chemiluminescence. We hypothesized that the failure to detect $O_2^{\cdot-}$ by various methods may have resulted from a combination of poor access to the site of formation of $O_2^{\cdot-}$ and/or relatively slow rates of reaction of the probe with $O_2^{\cdot-}$. NO, on the other hand, is known to react at a near diffusion controlled rate with $O_2^{\cdot-}$ to yield $ONOO^-$, and its small size should allow better access to the site of ROS generation when compared with larger probes. Therefore, if any free $O_2^{\cdot-}$ is formed by Nox4, it should react rapidly with NO to yield $ONOO^-$, which is able to oxidize luminol in the absence of HRP. Indeed, for overexpressed Nox1, the DetaNONOate-induced luminol signal was easily detected, whereas overexpressed Nox4 failed to produce any luminol signal. These data exclude that significant amounts of $O_2^{\cdot-}$ are released by Nox4. Importantly, similar to the other assays that detected $O_2^{\cdot-}$ (above), the E-loop mutants of Nox4 produced $ONOO^-$ (Fig. 3).

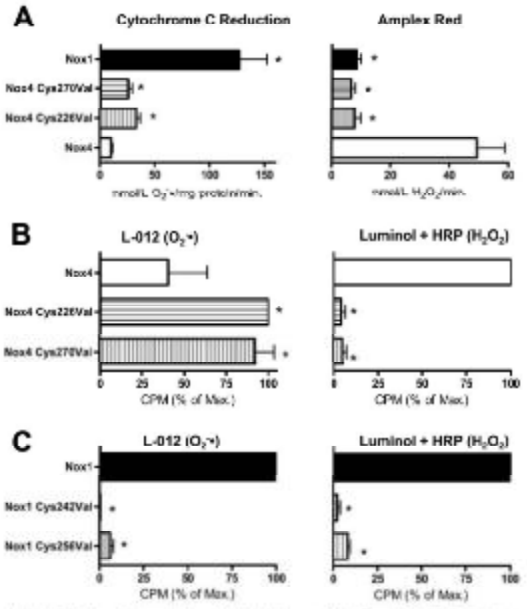

FIGURE 2. **Role of the cysteines in the E-loop of Nox4 and Nox1.** *A–C*, determination of ROS production of HEK293 cells transiently transfected with the plasmids indicated. $O_2^{\cdot-}$ generation was determined by superoxide dismutase-sensitive cytochrome *c* reduction (*A*, *left*) or by L-012 chemiluminescence (*B* and *C*, *left*). H_2O_2 formation was determined by Amplex Red oxidation (*A*, *right*) or luminol + HRP chemiluminescence (*B* and *C*, *right*). The Nox1 plasmid was cotransfected with Noxo1 and Noxa1. Normalization was as in Fig. 1, $n \geq 3$, mean ± S.E. *, $p < 0.05$ *versus* wild-type construct. 100% corresponds to mean 35,800 and 711,785 cpm (*B*, *left* and *right*) and to mean 734,017 and 59,462 cpm (*C*, *left* and *right*). % *of Max.*, percentage of maximum.

Binding of an Antibody to the E-loop Affects H_2O_2 Production of Nox4—A general problem with mutational analyses is that local changes in structure may affect the function of an enzyme

FIGURE 1. **Function of the E-loop of Nox4.** *A*, schematic illustration of the Nox protein and alignment of the amino acid sequence of the E-loop of human and murine Nox1, Nox2, and Nox4. *B*, schematic illustration of Nox4 and the deletion constructs generated. *Boxes* represent transmembrane domains (I–6), FAD binding site (*FAD*), and NADPH binding site (*NADPH*). Illustrations are not to scale. *C*, confocal microscopic fluorescent image of Nox4 del218–235+264–273 (*red*) stably expressed in HEK293 cells counterstained with GRP78 (*green*) and DAPI. *D* and *E*, determination of ROS production of HEK293 cells transiently transfected with the plasmids indicated. $O_2^{\cdot-}$ generation was determined by L-012 (*D*), and H_2O_2 formation was determined by luminol + HRP chemiluminescence (*E*). ROS production was normalized against Nox protein expression determined by Western blot analysis. To facilitate better comparison of the constructs, the ROS formation of the most active construct was set to 100% (corresponding to mean 271,217 cpm (*D*) and 426,172 cpm (*E*)) $n \geq 3$, mean ± S.E., *, $p < 0.05$ versus wild-type construct. % *of Max.*, percentage of maximum.

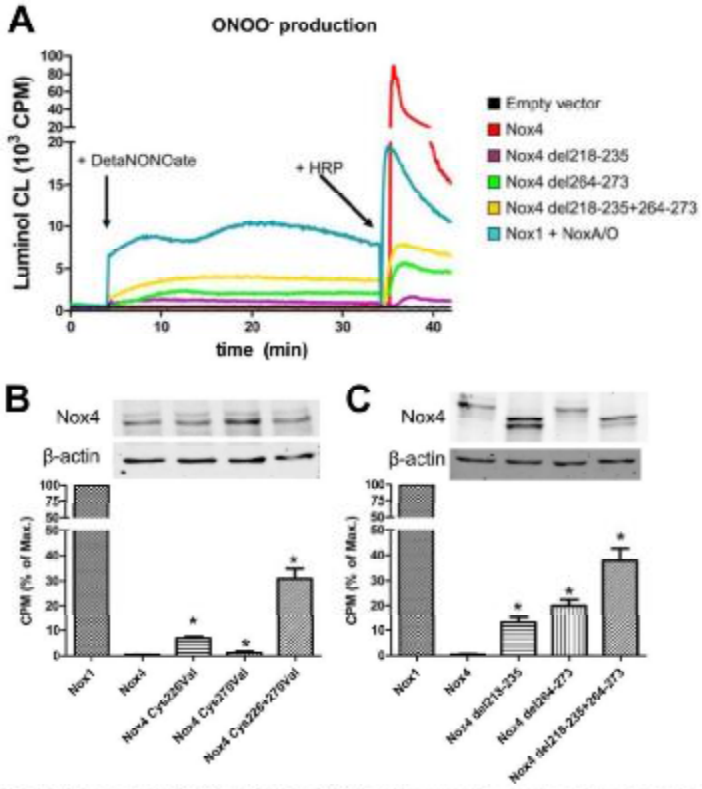

FIGURE 3. **Effect of mutations in the E-loop on the $ONOO^-$ production of Nox4.** *A–C*, representative recording (*A*) and statistical analysis (*B* and *C*) of $ONOO^-$ production of HEK293 cells transiently transfected with the plasmids indicated as well as protein expression of the constructs. ROS formation was determined by luminol chemiluminescence. After reading the cells in the absence of NO, the NO donor DetaNONOate (100 μmol/liter) was administered (*first arrow*). The subsequent signal was considered to arise from $ONOO^-$ formation. At the end of the experiment, horseradish peroxidase (+*HRP*) was added (*second arrow*) to determine H_2O_2 formation. The Nox1 plasmid was cotransfected with Noxo1 and Noxa1. Normalization was as in Fig. 1. Exemplary Western blots of the construct are shown in *B* and *C*. $n \geq 3$, mean ± S.E., *, $p < 0.05$ *versus* wild-type construct. 100% corresponds to mean 7625 and 7818 cpm (*B* and *C*, respectively). *% of Max.*, percentage of maximum.

at a remote site by some allosteric modulations. We therefore sought a second approach to interfere with the E-loop. Recently, a monoclonal antibody directed against this part of the protein was generated (mAb8E9) (18). When compared with an antibody that binds in the NADPH binding site (Fig. 3*C*), Western blot analysis confirmed that the antibody mAb8E9 binds the E-loop as labeling was lost in the Nox4 mutants (Fig. 4). As the antibody can only directly interact with extracellular portions of Nox4, this part of the study was carried out in Cos7 cells, which exhibit some plasma membrane expression of this NADPH oxidase (12).

The addition of the mAb8E9 decreased H_2O_2 production by Nox4-transfected Cos7 cells by ~20% (Fig. 4), and in a pilot study, mAb8E9 also increased the O_2^- formation of Nox4 ($-28 \pm 11\%$, $n = 2$). Importantly, a nonspecific mouse IgG control at the same concentration had no effect on ROS formation by Nox4, and also, mAb8E9 did not alter O_2^- production in Nox1-overexpressing cells. The interpretation of the signaling is, however, difficult as the fraction of plasma membrane-localized Nox4 to total Nox4 is unknown. To estimate the amount of Nox4 accessible by this approach, we treated the cells with the non-cell-permeable cross-linker bis-sulfosuccinimidyl suberate (1 mM), assuming that this should destroy the Nox4 activity at the plasma membrane, and indeed, Nox4 protein became undetectable by Western blot after cross-linking (data not shown). With respect to ROS production, bis-sulfosuccinimidyl suberate was equally effective as mAb8E9 in reducing H_2O_2 formation by Nox4. Surprisingly, the compound increased O_2^- produced by Nox1, suggesting that indeed alterations of the extracytosolic loop directly affect the efficacy of O_2^- formation (Fig. 4).

Western blot analysis of the Nox4 deletion constructs (Fig. 3*C*) indicated that the protein Nox4 del218–235 might be unstable as it was detected with a molecular mass of 6 kDa less than the calculated mass. As, however, ROS measurements of the other deletion constructs and the cysteine mutants in the same region yielded similar results, the reduced stability of this single construct might be of lesser importance for the interpretation of the data.

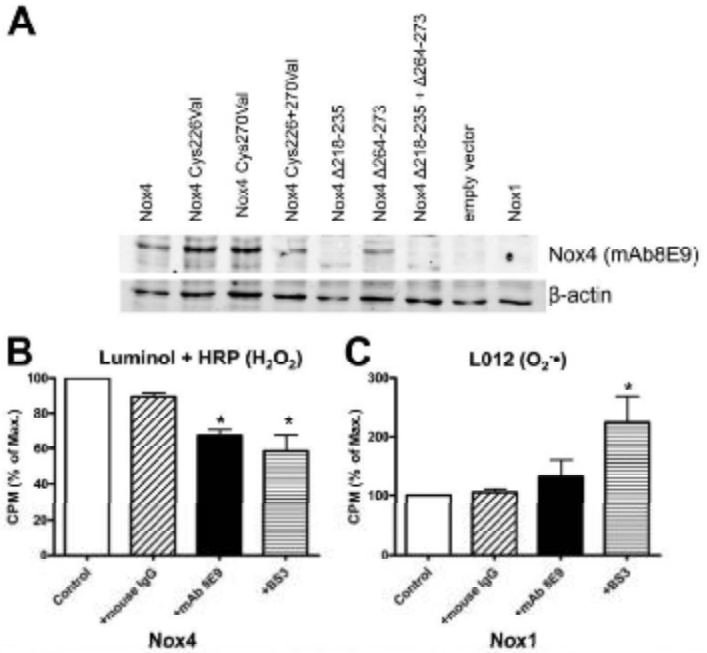

FIGURE 4. **Effect of an antibody directed against the E-loop on the H_2O_2 formation of Nox1 and Nox4.** *A*, representative Western blot of HEK293 cells transfected with the plasmids indicated probed with the antibody mAB8E9, which is directed against the E-loop of Nox4. *B* and *C*, determination of H_2O_2 production by luminol + HRP chemiluminescence and $O_2^{\cdot-}$ production in Cos7 cells transiently transfected with wild-type Nox4 or Nox1 (cotransfected with Noxo1 and Noxa1). The following substances indicated were added to the cells prior to measurements: monoclonal antibody directed against the E-loop (mAb8E9; 1 μg/ml), normal control mouse IgG (1 μg/ml), and the surface cross-linker bis-sulfosuccinimidyl suberate (*BS3*, 1 mmol/liter). Normalization was as in Fig. 1. $n \geq 3$, mean ± S.E., *, $p < 0.05$ *versus* control. 100% corresponds to mean 1390 and 1355 cpm (*B* and *C*, respectively). *% of Max.*, percentage of maximum.

Role of Extracytoplasmic Histidines for H_2O_2 Production by Nox4—Our data so far suggest that Nox4 directly generates H_2O_2 without the formation of significant amounts of a free $O_2^{\cdot-}$ intermediate. To generate H_2O_2, Nox4 either has to act as a dioxygenase (which could not occur from the heme itself) or has to facilitate the transfer of an electron from one $O_2^{\cdot-}$ to a second, in effect acting as a superoxide dismutase. We speculate that histidine residues might play a role in generating H_2O_2 by serving as a source for protons or by binding a metal, as is needed for catalysis by all known superoxide dismutase enzymes.

Structure alignment revealed that in addition to those that are directly involved in heme ligation, Nox4 contains five additional highly conserved histidines in its membrane integrated part (Fig. 5*A*), and interestingly, three of these are located in the E-loop. We mutated these five histidines to glutamine and studied protein expression and ROS formation by the mutants. The mutations of His-47, His-246, and His-248 had no effect on ROS production, whereas H16Q reduced H_2O_2 formation by Nox4 by ~50% without affecting $O_2^{\cdot-}$ formation. In contrast, Nox4-H222Q, which carries the mutation at the beginning of the E-loop, produced almost no H_2O_2 and instead released $O_2^{\cdot-}$ (Fig. 5*B*). The expression of the histidine mutants was similar to that of native Nox4 as determined by Western blot analysis (Fig. 5*C*). These observations not only confirm that the E-loop is central for H_2O_2 formation but also indicate that specific features of the E-loop are required for the process.

Mutation of the Cysteines in the E-loop Prevents Nox4-induced Erk1/2 Phosphorylation—In the final step, we sought to demonstrate that the type of ROS released by Nox4 is physiologically relevant. Unlike Nox2 and Nox1, Nox4 activity has previously been linked to Erk1/2 phosphorylation (17). We therefore investigated the activation of this MAP kinase in response to the overexpression of Nox4 *versus* Nox4 cysteine mutants. Although overexpression of native Nox4 induced a robust Erk1/2 phosphorylation in HEK293 cells, this effect was not observed with the cysteine mutants, although they were expressed to a similar level and total Erk1/2 expression was not affected by this approach (Fig. 6). These data indicate that the direct formation of H_2O_2 by Nox4 has important biological consequences for Nox-dependent signal transduction.

DISCUSSION

In this work, we studied the structural basis for H_2O_2 formation by Nox4. We identified the extended E-loop of the protein as an essential structural feature for this process and showed that alterations of the E-loop switch Nox4 from an H_2O_2 into an $O_2^{\cdot-}$-producing enzyme. The ROS product generated appears to be sensitive to minor structural perturbations in the E-loop because binding by a monoclonal antibody or cross-linking at

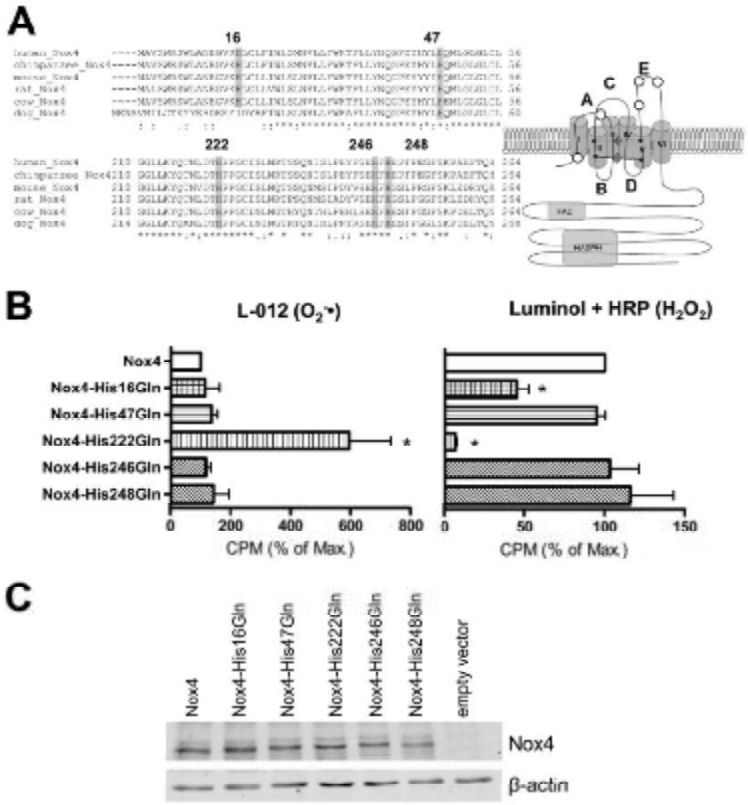

FIGURE 5. **Role of conserved histidines on the ROS formation of Nox4.** *A*, sequence alignment of Nox4 proteins from different species for conserved histidines on the extracytoplasmic side of the protein and schematic representation of the localization of the conserved histidines within the proteins (*white circles*). *B*, ROS production of HEK293 cells transiently transfected with the plasmids indicated. $O_2^{\cdot-}$ generation was determined by L-012 chemiluminescence (*left panel*), and H_2O_2 formation was assessed by luminol + HRP chemiluminescence (*right panel*). Normalization was as in Fig. 1, $n \geq 3$, mean ± S.E. *, $p < 0.05$ versus wild-type construct. 100% corresponds to mean 7647 (*left*) and 82,425 cpm (*right*). *C*, Western blot analysis of the expression of the different histidine mutants in HEK293 cells.

the cell surface impaired H_2O_2 formation by Nox4 but not $O_2^{\cdot-}$ formation by Nox1. H_2O_2 formation appeared to be an intrinsic function of Nox4 as we could not detect $O_2^{\cdot-}$ formation, based on the formation of $ONOO^-$ in the presence of an NO donor. In agreement with such a scenario, we identified a highly conserved histidine in the E-loop, which might serve as source of protons or as a binding site for metals to provide superoxide dismutase activity to Nox4.

Based on their similarity to Nox2 and the obligate 1-electron transfer from heme iron, all Nox NADPH oxidases should primarily produce $O_2^{\cdot-}$ (1). The H_2O_2 formation by Nox4 was therefore initially interpreted as artifact but occurring as a result of the use of reagents that detected exclusively extracellular ROS generated by an intracellular enzyme. Mutational analysis (16), intracellular probes for ROS detection (13), and comparative expression studies in cells exhibiting different localizations of Nox4 (12), however, demonstrated that the type of ROS produced by the enzyme is independent of its localization. This suggests that Nox NADPH oxidases can directly release either $O_2^{\cdot-}$ or H_2O_2 and that this feature is dependent on structural properties of the individual Nox enzyme.

Nox4, indeed, is not the only Nox homologue that primarily produces H_2O_2. Under physiological conditions, the Duox enzymes also generate H_2O_2 exclusively (19, 20). The molecular mechanisms leading to Duox-dependent H_2O_2 formation are not clear but appear to be distinct from that of Nox4. Based on homologue searches, it was suggested that Duox enzymes might bear an intrinsic superoxide dismutase activity localized to the peroxidase homology domain of these proteins (21), but recently, it was shown that although structurally similar to peroxidases, mammalian Duox enzymes are not able to directly dismutate $O_2^{\cdot-}$ (22). Rather, the type of ROS generated appears to depend on the maturation state of the Duox enzymes. In the absence of the maturation factors Duoxa1 or Duoxa2, the Duox enzymes generate $O_2^{\cdot-}$, and only after interaction with the Duoxa proteins does H_2O_2 formation becomes apparent (23). This process also involves relocalization of the Duox-Duoxa complex from the endoplasmic reticulum to the plasma membrane,

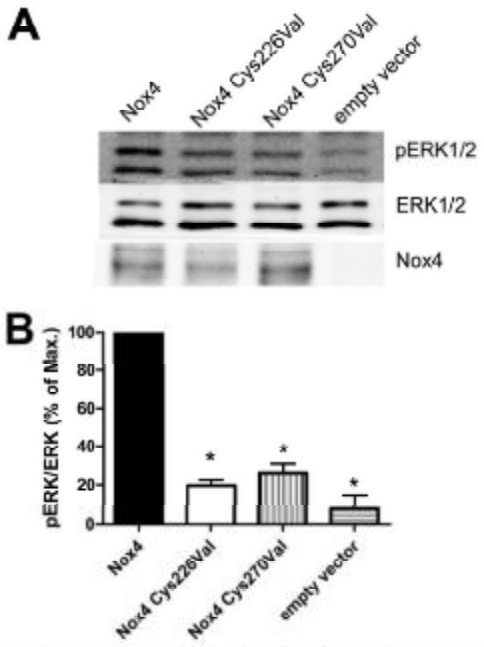

FIGURE 6. **Effect of mutations in the E-loop of Nox4 on Erk1/2 phosphorylation.** HEK293 cells were transiently transfected with the plasmids indicated and subsequently subjected to SDS-PAGE and Western blot analysis with the antibodies indicated. *A* and *B*, representative blots (*A*) and statistical analysis (*B*) of the ratio of phosphorylated to non-phosphorylated Erk1/2 (*pERK1/2*). To allow better comparison, the signal of wild-type Nox4 was set to 100%. $n \geq 3$, mean ± S.E. *, $p < 0.05$ *versus* Nox4 construct. *% of Max.*, percentage of maximum.

and it is not clear whether localization impacts the observed reduced oxygen species (24). The enzymatic activity of the Duox enzymes is independent of $p22^{phox}$, whereas the maturation of Nox2 (25) as well as the activity of most of the Nox proteins (with the exception of Nox5) is dependent on $p22^{phox}$ (7). Thus, it is not an understatement that, by analogy with the Duox-Duoxa proteins, $p22^{phox}$ was referred to as a maturation factor for the Nox proteins (24). Divergent from this concept, it was observed that alteration of the maturation factors for the Duox proteins switch them from H_2O_2 to $O_2^{\cdot-}$ formation (24), whereas so far no mutation in $p22^{phox}$ was reported to induce such a transition for Nox4 (7). Interestingly, based on truncation experiments, it can be concluded that at least some different regions of $p22^{phox}$ interact with Nox1/2 when compared with Nox4 (7), but an in-depth molecular analysis has not yet been carried out.

As for Nox4, a molecular explanation for H_2O_2 formation by Duox is unclear. The lack of superoxide dismutase activity in the peroxidase domain may suggest that the enzymes can produce H_2O_2 directly like dioxygenases or that whatever $O_2^{\cdot-}$ is produced remains cryptic and inaccessible to assay reagents prior to its dismutation to form H_2O_2, for example, due to either spontaneous dismutation or transfer to a second, so far unidentified, interacting protein like a superoxide dismutase. Obviously, these mechanisms could also account for the H_2O_2 formation of Nox4. The localization of Nox4 differs among cell types, which is suggestive of the presence of interacting proteins directing the protein to different destinations, but so far, little has been published to support this view. The $p22^{phox}$-interacting protein Poldip2 has been shown to affect Nox4 expression and activity, but it has not been reported that it alters the type of ROS formed by Nox4 (26). A direct interaction of Nox4 with one of the superoxide dismutase isoforms seems unlikely due to the orientation of the $O_2^{\cdot-}$ exit site to the extracytosolic compartment. Indeed, by co-immunoprecipitation experiments, we found no evidence for such an interaction.[3]

On the basis of the present data, we suggest that H_2O_2 formation is an intrinsic function of Nox4. Thus, either the enzyme has endogenous superoxide dismutase activity or it acts as a dioxygenase and directly forms H_2O_2. For both processes, histidines and cysteines could be important. Superoxide dismutase activity requires the presence of metal cofactors such as zinc, manganese, or iron, which are coordinated by these amino acids. Indeed, zinc in CuZn-superoxide dismutase is coordinated by three histidines (27), and the zinc in zinc finger proteins is coordinated by two histidines and two cysteines. However, at least two coordinating histidines are likely to be required to form a metal binding site, and our mutational analysis of Nox4 provided evidence for only a single histidine (His-222) of importance. Such a scenario might, however, be viable if Nox4 forms a homodimer in the membrane, as has been suggested for Nox5 (35). According to this scenario, the metal binding site would be formed at the interface between the subunits. Interestingly, also $p22^{phox}$ contains a single histidine, and this is not required for the function of Nox2 (28). This histidine is located in a region important for Nox4-$p22^{phox}$ interaction (7) but appears to be located in the transmembrane region of the protein directed more toward the cytosolic side. Thus, it seems unlikely that this amino acid of $p22^{phox}$ has a specific function for ROS formation by Nox4. Interestingly, His-222 of Nox4 is embedded in the sequence THPPGC, and deletion of this stretch or mutation of the Cys-226 also switched Nox4 from H_2O_2 to $O_2^{\cdot-}$ formation. Given that the two prolines in this sequence should force a 90° deviation in the secondary structure of the sequence, the Cys-226 is likely to be in close proximity to His-222 and therefore might contribute to metal coordination. Unfortunately, we are currently unable to purify sufficient amounts of Nox4 to test whether it indeed contains such metals. To our knowledge, no specific chelators are available that are compatible with living cells and that might deplete the metal from the E-loop without extracting the heme iron. With EDTA, at least, we were unable to switch Nox4 from H_2O_2 to $O_2^{\cdot-}$ generation.[4]

Despite this speculation about metal coordination, histidine might also directly accelerate the formation of H_2O_2 in the absence of a metal. This amino acid is frequently involved in enzyme catalysis, where it acts as a proton donor (29). The spontaneous rate of dismutation of superoxide is high, provided that the reaction is between $O_2^{\cdot-}$ and its protonated form $HO_2^{\cdot}$

[3] I. Takac, unpublished observation.
[4] R. Brandes, unpublished observation.

(pK_a 4.9). The reported rate constant for the process is ~1 × 10^8 M^{-1} s^{-1}, 7 orders of magnitude higher than the spontaneous dismutation rate for two superoxide anions (30). Thus, we suggest that His-222 could serve as a proton donor for a superoxide anion to form the perhydroxyl radical, which would accelerate spontaneous $O_2^{\cdot-}$ dismutation by many orders of magnitude. Although this rate is still at least 100-fold less than that catalyzed by superoxide dismutases, it is likely to be more than sufficient to keep up with the turnover rate of Nox4, which has been reported to be around 200 min^{-1} (14).

Another possible role for the E-loop (not mutually exclusive with the above) is to form a physical structure that slows the egress of $O_2^{\cdot-}$ and/or $HO_2^{\cdot}$ from its site of formation at the heme, allowing it to accumulate and accelerating the spontaneous dismutation by virtue of increasing the local concentration of $O_2^{\cdot-}$. Because the rate of spontaneous dismutation of superoxide is a function of the square of its concentration, creation of a "cage" at the site of generation would be expected to accelerate the spontaneous dismutation rate, particularly in the presence of a proton donor. Such a mechanism would extend the retention time of $O_2^{\cdot-}$ and potentially allow for the collision of two $O_2^{\cdot-}$ molecules before $O_2^{\cdot-}$ can be released into solution. Relative to Nox1 and Nox2, Nox4 shows significantly increased length of the extended E-loop, consistent with this concept. The cysteines Cys-226 and Cys-270 might form a disulfide bridge to stabilize such a structure. According to such a model, any manipulation at the E-loop (e.g. the truncation experiments, the cysteine, and the His-222 mutations) would affect the conformation of the E-loop, thereby accelerating the exit of $O_2^{\cdot-}$. The data obtained with the antibody mAb81G9 appear to support this concept. Although the exact effect of the antibody binding to the E-loop is unknown, it was able to decrease H_2O_2 to the same extent as an extracytoplasmic cross-linking agent, which should also interfere with the structure of the E-loop. Our observation of an inability of Nox4 to form peroxynitrite in the presence of an NO donor would argue that if $O_2^{\cdot-}$ is formed as an intermediate, either its half-life has to be unusually short or its access to the NO donor must be impeded by the native protein structure. Thus, according to the "caged superoxide" scenario, $O_2^{\cdot-}$ is not released free into solution, where it can react with NO.

Structurally, H_2O_2- and $O_2^{\cdot-}$-forming enzymes are usually quite different, and xanthine oxidase is one of the few examples of an enzyme capable of producing both types of ROS (31). The enzymatic mechanisms underlying this function are, however, completely different from the Nox proteins. Recently, a mutant of xanthine oxidase was constructed with increased $O_2^{\cdot-}$ and decreased H_2O_2 formation (32), which was achieved by increasing the redox potential of FAD so that the rate constant of electron transfer from $FADH^{\cdot}$ onto dioxygen was increased (32). Usually, dioxygen is reduced by $FADH_2$ in xanthine oxidase, and as this reaction in the native enzyme is much faster than the single electron transfer from $FADH^{\cdot}$, native xanthine oxidase produces much less $O_2^{\cdot-}$ than H_2O_2 (33). In this context, it is important to emphasize that H_2O_2 formation indeed usually occurs at FAD sites and does not require the heme present in Nox proteins. Heme proteins such as cytochrome P450 monooxygenases, the NO synthase enzymes, and also the Nox enzymes in contrast produce $O_2^{\cdot-}$. Thus, one could speculate that H_2O_2 formation by Nox4 occurs at the FAD site. Up to now, no evidence has been presented to suggest that the FAD in Nox enzymes is able to directly reduce oxygen. Expression of the isolated dehydrogenase domain of Nox4 demonstrated that this domain of Nox4 is able to reduce cytochrome *c* and several dye electron acceptors (14) but does not form H_2O_2 directly.[5]

From the physiological point of view, the functional role of Nox4 is still incompletely understood, and thus, it is also unclear whether the type of ROS generated by Nox4 impacts function. In overexpression experiments, Nox4 activated a different set of MAP kinases than Nox2, with a particularly strong activation of the Erk1/2 pathway (17). As Erk1/2 phosphorylation was attenuated in the present study by switching Nox4 from H_2O_2 to $O_2^{\cdot-}$, it could be inferred that this action is indeed predominately mediated by H_2O_2. In line with this concept, it was recently shown that Nox4-derived H_2O_2 oxidizes Ras (34), which would subsequently activate the Erk1/2 pathway.

In conclusion, we have demonstrated that Nox4 directly produces H_2O_2 by a mechanism involving the relatively large E-loop of the enzyme and that the mechanism requires Cys-226 and Cys-270 as well as His-222 of this loop. Functionally, Erk1/2 activation by Nox4 required H_2O_2 formation and was not observed with $O_2^{\cdot-}$-generating Nox4 mutants. Structural information on the transmembrane region of Nox4, however, will be needed to ultimately clarify the exact mechanism of H_2O_2 formation.

REFERENCES

1. Bedard, K., and Krause, K. H. (2007) *Physiol. Rev.* **87**, 245–313
2. Vignais, P. V. (2002) *Cell. Mol. Life Sci.* **59**, 1428–1459
3. Nauseef, W. M. (2004) *Histochem. Cell Biol.* **122**, 277–291
4. Ambasta, R. K., Kumar, P., Griendling, K. K., Schmidt, H. H., Busse, R., and Brandes, R. P. (2004) *J. Biol. Chem.* **279**, 45935–45941
5. Geiszt, M., Kopp, J. B., Varnai, P., and Leto, T. L. (2000) *Proc. Natl. Acad. Sci. U.S.A.* **97**, 8010–8014
6. Martyn, K. D., Frederick, L. M., von Loehneysen, K., Dinauer, M. C., and Knaus, U. G. (2006) *Cell. Signal.* **18**, 69–82
7. von Löhneysen, K., Noack, D., Jesaitis, A. J., Dinauer, M. C., and Knaus, U. G. (2008) *J. Biol. Chem.* **283**, 35273–35282
8. Block, K., Gorin, Y., and Abboud, H. E. (2009) *Proc. Natl. Acad. Sci. U.S.A.* **106**, 14385–14390
9. Kuroda, J., Nakagawa, K., Yamasaki, T., Nakamura, K., Takeya, R., Kuribayashi, F., Imajoh-Ohmi, S., Iyanagi, K., Shibata, Y., Sueishi, K., and Sumimoto, H. (2005) *Genes Cells* **10**, 1139–1151
10. Hilenski, L. L., Clempus, R. E., Quinn, M. T., Lambeth, J. D., and Griendling, K. K. (2004) *Arterioscler. Thromb. Vasc. Biol.* **24**, 677–683
11. Chen, X., Kirber, M. T., Xiao, H., Yang, Y., and Keaney, J. F., Jr. (2008) *J. Cell Biol.* **181**, 1129–1139
12. von Löhneysen, K., Noack, D., Wood, M. R., Friedman, J. S., and Knaus, U. G. (2010) *Mol. Cell. Biol.* **30**, 961–975
13. Serrander, L., Cartier, L., Bedard, K., Banfi, B., Lardy, B., Plastre, O., Sienkiewicz, A., Fórró, L., Schlegel, W., and Krause, K. H. (2007) *Biochem. J.* **406**, 105–114
14. Nisimoto, Y., Jackson, H. M., Ogawa, H., Kawahara, T., and Lambeth, J. D. (2010) *Biochemistry* **49**, 2433–2442
15. Larkin, M. A., Blackshields, G., Brown, N. P., Chenna, R., McGettigan, P. A., McWilliam, H., Valentin, F., Wallace, I. M., Wilm, A., Lopez, R., Thompson, J. D., Gibson, T. J., and Higgins, D. G. (2007) *Bioinformatics* **23**, 2947–2948
16. Helmcke, I., Heumüller, S., Tikkanen, R., Schröder, K., and Brandes, R. P. (2009) *Antioxid. Redox Signal.* **11**, 1279–1287

[5] Y. Nishimoto and J. D. Lambeth, unpublished observation.

17. Anilkumar, N., Weber, R., Zhang, M., Brewer, A., and Shah, A. M. (2008) *Arterioscler. Thromb. Vasc. Biol.* **28**, 1347–1354
18. Zhang, L., Nguyen, M. V., Lardy, B., Jesaitis, A. J., Grichine, A., Rousset, F., Talbot, M., Paclet, M. H., Qian, C., and Morel, F. (2011) *Biochimie* **93**, 457–468
19. Geiszt, M., Witta, J., Baffi, J., Lekstrom, K., and Leto, T. L. (2003) *FASEB J.* **17**, 1502–1504
20. Fortea, R., Salathe, M., Miot, F., Fortea, R., and Conner, G. E. (2005) *Am. J. Respir. Cell Mol. Biol.* **32**, 462–469
21. Leto, T. L., and Geiszt, M. (2006) *Antioxid. Redox Signal.* **8**, 1549–1561
22. Meitzler, J. L., and Ortiz de Montellano, P. R. (2009) *J. Biol. Chem.* **284**, 18634–18643
23. Ameziane-El-Hassani, R., Morand, S., Boucher, J. L., Frapart, Y. M., Apostolou, D., Agnandji, D., Gnidehou, S., Ohayon, R., Noel-Hudson, M. S., Francon, J., Lalaoui, K., Virion, A., and Dupuy, C. (2005) *J. Biol. Chem.* **280**, 30046–30054
24. Morand, S., Ueyama, T., Tsujibe, S., Saito, N., Korzeniowska, A., and Leto, T. L. (2009) *FASEB J.* **23**, 1205–1218
25. DeLeo, F. R., Burritt, J. B., Yu, L., Jesaitis, A. J., Dinauer, M. C., and Nauseef, W. M. (2000) *J. Biol. Chem.* **275**, 13986–13993
26. Lyle, A. N., Deshpande, N. N., Taniyama, Y., Seidel-Rogol, B., Pounkova, L., Du, P., Papaharalambus, C., Lassègue, B., and Griendling, K. K. (2009) *Circ. Res.* **105**, 249–259
27. Strange, R. W., Antonyuk, S., Hough, M. A., Doucette, P. A., Rodriguez, J. A., Hart, P. J., Hayward, L. J., Valentine, J. S., and Hasnain, S. S. (2003) *J. Mol. Biol.* **328**, 877–891
28. Yu, L., Quinn, M. T., Cross, A. R., and Dinauer, M. C. (1998) *Proc. Natl. Acad. Sci. U.S.A.* **95**, 7993–7998
29. Holliday, G. L., Mitchell, J. B., and Thornton, J. M. (2009) *J. Mol. Biol.* **390**, 560–577
30. Marklund, S. (1976) *J. Biol. Chem.* **251**, 7504–7507
31. Nishino, T., Okamoto, K., Eger, B. T., Pai, E. F., and Nishino, T. (2008) *FEBS J.* **275**, 3278–3289
32. Asai, R., Nishino, T., Matsumura, T., Okamoto, K., Igarashi, K., Pai, E. F., and Nishino, T. (2007) *J. Biochem.* **141**, 525–534
33. Harris, C. M., and Massey, V. (1997) *J. Biol. Chem.* **272**, 8370–8379
34. Wu, R. F., Ma, Z., Liu, Z., and Terada, L. S. (2010) *Mol. Cell. Biol.* **30**, 3553–3568
35. Kawahara, T., Jackson, H. M., Smith, S. M., Simpson, S. M., and Lambeth, J. D. (2011) *Biochemistry*, in press

Chapter 3: The study of constitutive diaphorase activity of Nox4 and topological study of the transmembrane heterodimer Nox4/p22phox.

Les résultats concernant le chapitre 3 sont introduits en deux parties:

Une première partie avec un article soumis (**article 3**) ciblé sur l'expression des différentes constructions de Nox4 recombinant à partir de 2 approches expérimentales: une expression dans ***E. Coli*** et une expression à l'aide d'un système de transcription/traduction ***in vitro*** (RTS, rapid translation system).

Ces deux approches méthodologiques sont comparées au plan quantitatif et en ce qui concerne le rendement et la solubilité. L'activité diaphorase des formes recombinantes synthétisées est évaluée.

Une deuxième partie avec un article qui est actuellement en préparation (article 4) et qui fait l'objet d'un partenariat avec Chuong Nguyen. Il s'intéresse à la topologie membranaire de Nox4 et p22phox. Il consiste à appliquer une nouvelle approche expérimentale: «Topological Determination by Ubiquitine Fusion Assay, TDUFA».

The study of constitutive diaphorase activity of Nox4 (article 3)

Résumé en français

1 Introduction

Le mécanisme de transfert d'électrons est bien documenté pour la protéine Nox2. L'activité diaphorase correspond à un transfert d'électron depuis NADPH jusqu'au centre redox du FAD (portion en C terminale de Nox2). Cette activité peut être distinguée de l'activité NADPH oxydase par utilisation d'un accepteur d'électron directement à partir du FAD, l'INT (**I**odo**n**itrote**t**razolium); cette activité est mesurée soit à partir de la protéine entière soit sur la protéine tronquée ne contenant que la partie cytosolique. La protéine Nox4 n'a encore jamais pu être isolée sous forme native probablement compte tenu des très faibles quantités de protéine exprimées mais aussi parce que la localisation subcellulaire n'est pas parfaitement définie. Peu de données existent à l'heure actuelle, concernant les sites impliqués dans l'activité diaphorase de Nox4. Une étude récente a indiqué que l'activité constitutive de Nox4 réside dans le domaine catalytique, flavodeshydrogénase, qui contient un site de liaison du NADPH et un autre pour le FAD.

2 Expression de différentes constructions de Nox4 recombinant par RTS

Résultats:

- La présence de groupements de codons rares (^{1363}AGA AGA CUA^{1371}) de Nox4 affectent la synthèse des protéines Nox4 par RTS et la position de l'étiquette (N terminale ou C terminale) influence le niveau de production protéique.
- L'expression et la solubilisation des protéines Nox4-2TM-CH, Nox4-1TM-CH, Nox4Aqc-CH et Nox4Bqc-CH sont optimisées en présence de 0.1mM de DDM, de la protéine chaperonne GroE et 0.1mM/4mM de GSH/GSSG par RTS.

3 Expression de Nox4 recombinant dans les bactéries

Résultats:

- La production de ces protéines par les bactéries BL21(λDE3) aboutit à l'apparition de formes tronquées. L'apparition des protéines est également la conséquence de la présence de groupements de codons rares (^{1363}AGA AGA CUA^{1371}) de Nox4. Là encore on a utilisé la souche d'expression bactérienne BL21(λDE3) CodonPlus RIL.
- L'expression et la solubilisation de la protein NH-Nox4Aqc est optimisée en présence de 50mM de Tris-HCl pH 7,6, 500mM de NaCl, 1% de Chaps, 10mM de DTT, 2µg/ml de pepstatin, 2µg/ml de leupetin et 10µM de TLCK par les bactéries.

4 Activité diaphorase

Résultats:

- Pour les deux protéines Nox4Aqc-CH et NH-Nox4Aqc, le cytochrome c, accepteur d'électron, présente une activité supérieure à celle de l'INT. En plus la protéine Aqc produit en système bactérien possède une activité spécifique plus faible comparée à la protéine synthétisée en milieu acellulaire.
- L'activité diaphorase de Nox4 n'est pas stimulée par l'addition de cytosol provenant de cellules exprimant naturellement Nox4.

Summary in English

1 Background

The mechanism of electron transfer is well documented for the Nox2 protein. Diaphorase activity is the electron transfer from FAD to redox center and is located at the cytosolic tail of Nox2. This activity can be distinguished from the NADPH oxidase activity by using INT (iodonitrotetrazolium) as a direct FAD electron acceptor, in PLB985 cells expressing the whole protein (Pessach *et al.*, 2001) and truncated protein containing only cytosolic part (Pessach *et al.*, 2006). Experiments with Nox2 truncated forms produced by bacteria were able to determine the region responsible for this activity, which corresponds to amino acids 221 to 570. The diaphorase activity is intrinsic and does not require the presence of cytosolic factors.

Few data exist at present on the diaphorase activity of Nox4. Nox4 protein has not been isolated probably due to the very low amounts of expression and also because its subcellular localization is not well defined. In order to characterize the molecular mechanism involved in the establishment of the electron transfer through Nox4, a series of truncated Nox4 proteins containing the NADPH and FAD domain were generated by two methods (in vitro RTS and bacteria induction) to study its diaphorase activity.

2 In vitro expression of Nox4 truncated proteins by RTS

4 truncated Nox4 proteins (2-TM, 1-TM, Aqc, Bqc) were synthesized in vitro by RTS system. Each protein contains a poly-histidine tag either at the C terminus or at the N terminus. The protein expression was analyzed by western blot using an anti-histidine antibody. As different predictive softwares reveals a high hydrophobic domain surrounding the first NADPH binding site, the solubility of these proteins were optimized under different conditions to facilitate the correct folding of the proteins during its synthesis.

- ✓ The presence of rare codons (^{1363}AGA AGA CUA^{1371}) affects the synthesis of Nox4 by RTS and the position of the poly-histidine tag influences the expression level of 2-TM and 1-TM, therefore, C terminal tagged proteins was chosen to use in RTS study;
- ✓ The solubility of these proteins are optimized in the presence of 0.1mM DDM, GroE and 0.1mM/4mM of GSH/GSSG.

3 Expression of Nox4 truncated proteins by bacterial induction

Constructs were transformed into BL21(λDE3) CodonPlus RIL bacteria and the expression of the proteins was induced by the addition of IPTG. The expression of these proteins was analyzed by western blot.

Then an extensive screening of refolding conditions was performed to obtain soluble proteins.

- ✓ As rare codons (^{1363}AGA AGA CUA^{1371}) also affects the synthesis of Nox4 by bacterial induction, BL21(λDE3) CodonPlus RIL bacteria strain was used. NH-Nox4-2TM was unable to be synthesized;
- ✓ The solubility of these proteins are optimized in lysis buffer containing the detergent chaps (50mM Tris pH7.6, 500mM NaCl, 10mM DTT, 1% Chaps, 2µg/ml pepstatin, 2µg/ml leupetin et 10µM TLCK).

4 Diaphorase activity of recombinant truncated Nox4 truncated constructions

Large scale of truncated Nox4Aqc and Nox4Bqc were produced using optimized conditions for the RTS system and bacterial induction approach. Then soluble proteins were purified onto chromatography and were tested for the diaphorase activity (INT and cytochrome c).

- ✓ For both proteins Nox4Aqc-CH and NH Nox4Aqc, electronic acceptor cytochrome c gives a higher rate than INT. And Nox4Aqc produced a lower specific activity by a cell-based system compared to the protein synthesized in cell-free technology;
- ✓ The diaphorase activity of Nox4 is not stimulated by the addition of cytosolic factors.

My contribution to this work includes over-expression the truncated Aqc proteins in large scale by bacterial induction approach, optimization of the recombinant proteins and purification; study the diaphorase activity of NH-Nox4Aqc (INT and cytochrome c).

Article 3:

Nox4 cytosolic domain generates a constitutive diaphorase activity. *Chuong Nguyen, Leilei Zhang, Nicolas Mouz, Jean Luc Lenormand, Bernard Lardy, and Françoise Morel* (submitted)

Nox4 cytosolic domain generates a constitutive diaphorase activity

Abstract:

NADPH oxidase Nox4 is a membrane protein that generates reactive oxygen species in a constitutive manner differing from the activity of other NADPH oxidases particularly Nox2 which needs a stimulus to be active. The production of ROS by Nox2 results from a precise mechanism of electronic transfer throughout the protein. Our study was designed to investigate the initial electronic transfer step (diaphorase activity) of the cytosolic tail of Nox4 and was focussed on two different approaches to produce soluble and active truncated Nox4 proteins. After optimization, on one hand, soluble proteins were obtained by *in vitro* translation (RTS) in direct presence of 0.1mM of DDM, GroE and 0.1mM/4mM of GSH/GSSG during the protein synthesis process. On the other hand, the IPTG induced Nox4 bacteria were lysed in a buffer containing 1% chaps. The soluble proteins produced by both techniques showed a diaphorase activity in a cell free system with a turn-over about 26±2.6 nmol/min/nmol with INT and 48±20.2 nmol/min/nmol with cytochrome c for the protein obtained by RTS and about 4.4±1.7 nmol/min/nmol with INT and 20.5±2.8 nmol/min/nmol with cytochrome c. This activity was constitutive and did not need any stimulus. Furthermore, the cytosolic tail of the isoform Nox4B which lacks the first NADPH binding site was unable to show any diaphorase activity pointing out the importance of this domain.

Highlight

Two bacterial protein expression approaches (bacteria induction and in vitro translation) were used to produce Nox4 cytolosic tail. Production of a soluble and active recombinant truncated Nox4 protein is low due to a high level of hydrophobicity and the presence of rare codon sequences. Nox4 cytosolic tail displays a constitutive diaphorase activity which is independent of cytosolic fraction isolated from HEK293E cells. Findings contribute to the understanding of the NADPH oxidase activity mechanism of Nox4.

Introduction:

Reactive oxygen species (ROS), comprising superoxide anion and its derivatives, play an essential role both in the immune system to fight against bacteria invasion and also act as signaling molecules involved in critical cellular events such as signal transduction, oxygen sensing, proliferation, and apoptosis. NADPH

oxidases or Nox which are the major source of ROS production, are specifically dedicated to this aim. The Nox's family includes seven members and consists of 5 Nox (Nox1 to Nox5) and 2 dual oxidases (Duox1 and Duox2). All these members are expressed in different type of tissue and their function differs to each other. Nox2, also as known as gp91phox, is the most extensively studied and is mainly expressed phagocytic cells. Nox2 is fully functional in activated phagocytes generates high level of ROS (respiratory burst) which act as bactericides molecules. A dysfunction of Nox2 leads to a chronic granulomatose disease (CGD). In this pathology, oxidase activity is abolished and patients are submitted to severe and recurrent infections due to the absence of bactericidal tools (Morel, 2007; Nauseef, 2008). Nox2 forms a stable heterodimer called cytochrome b_{558} with a membrane associated catalytic partner p22phox. Upon activation, cytosolic factors such as p40phox, p47phox, p67phox and Rac1/2 translocate to the plasma membrane to interact with the cytochrome b_{558} (Morel *et al.*, 1991). The conformation of Nox2 switches to an active form (Paclet *et al.*, 2000). The mechanism of ROS production by Nox2 is well studied and implies electronic transfer throughout the protein from the NADPH to the oxygen molecule. Nox2 protein possesses a hydrophilic cytosolic C terminus that contains a binding site for FAD and for NADPH. The N terminus side of Nox2 is highly hydrophobic and consists of 6 transmembrane helices where reside 2 hemes stabilized by 4 histidines residues located in the 3rd and 5th transmembrane domains (Biberstine-Kinkade *et al.*, 2001). In an active state, electrons travel from the NADPH to the FAD then through the 2 hemes molecules in order to finally reduce the oxygen leading to the generation of superoxide anion (Cross *et al.*, 2004). The electronic transfer in the cytosolic tail of Nox2 from the NADPH to the FAD is also called diaphorase activity and have been described in PLB985 cells for the full length protein and the cytosolic truncated protein as well (Pessach *et al.*, 2001; Pessach *et al.*, 2006).

Nox4 is widely expressed but is primary source of ROS production in kidney tissue (Geiszt *et al.*, 2000; Shiose *et al.*, 2001; Gorin *et al.*, 2005; Maranchie *et al.*, 2005). Nox4 is also expressed in placenta and glioblastoma cells (Cheng *et al.*, 2001), vascular smooth muscle cells (Wingler *et al.*, 2001; Touyz *et al.*, 2002; Ellmark *et al.*, 2005; Clempus *et al.*, 2007), endothelial cells (Ago *et al.*, 2004; Kuroda *et al.*, 2005), skin (Park *et al.*, 2005; Rossary *et al.*, 2007) or cardiac (Colston *et al.*, 2005; Cucoranu *et al.*, 2005) fibroblast cells, keratinocytes (Chamulitrat *et al.*, 2004), adipocytes (Mahadev *et al.*, 2004; Mouche *et al.*, 2007), neurons (Vallet *et al.*, 2005; Dai *et al.*, 2006) and hematopoietic stem cells (Piccoli *et al.*, 2005). The dysfunction of Nox4 activity have been linked to the development of disease such as diabetes (Mahadev *et al.*, 2004), hypertension (Djordjevic *et al.*, 2005; Akasaki *et al.*, 2006; Sedeek *et al.*, 2009), atherosclerosis (Sorescu *et al.*,

2002), and osteoarthritis (Grange *et al.*, 2006). Similarly to Nox2, Nox1 and Nox3 activity is regulated by cytosolic subunit known as NoxO1 and NoxA1, homologues of p47phox and p67phox respectively (Banfi *et al.*, 2003; Geiszt *et al.*, 2003; Takeya *et al.*, 2003). In contrast, the presence of regulatory subunits is not necessary for Nox4 activity since the co-expression of Nox4 with different combination of cytosolic regulator (p47phox, p67phox, NoxO1 and NoxA1) (Martyn *et al.*, 2006). This independence could be explained by the fact that the poly-proline domain of p22phox does not modify Nox4 NADPH oxidase activity. Indeed this domain serves as a binding site for the cytosolic factors (Kawahara *et al.*, 2005). Furthermore, unlike the other member of Nox's family, Nox4 activity is constitutive (Geiszt *et al.*, 2000; Shiose *et al.*, 2001; Grange *et al.*, 2006; Serrander *et al.*, 2007; Zhang *et al.*, 2011). Nevertheless, the electron transfer mechanism of Nox4 is not well studied and only two recent publications described the diaphorase activity of the cytosolic domain of Nox4.

Since Nox4 activity is unique compared to other Noxes in term of regulation, we decided to characterize the diaphorase activity possibly located in the C terminus domain of Nox4 which contains the NADPH and FAD binding sites. For this purpose we first described the optimization of two approaches to produce soluble and active recombinant proteins. The first approach is base on an *in vitro* transcriptional-translational technique, Rapid Translation System (RTS) and second an *E.coli* based expression system. We were able therefore to observe a diaphorase activity for this portion of Nox4 and shown that this activity is constitutive. We also established that the first NADPH binding site which is absent in the isoform Nox4B is necessary to initiate the first electronic transfer step.

Material and method

Nox4 truncated constructs generation. The plasmids pIVEX 2.4NdeI and pET30b were used to add an N terminal his-tag whereas pIVEX2.3MCS allowed to add a C terminal his-tag. The different constructs of Nox4 were obtained by PCR and directly cloned into vectors. The forward primers (5' GGA ATT CTC CAT GGT TCA CCA TCA TTT CGG TCA TAA GTC 3' for N-Aqc and N-Bqc; 5' GGA TGA **GCG GCC GC**C CAG TCA CCA TCA TTT CGG TC 3' for Aqc-C and Bqc-C; 5' GGA ATT CTC CAT GGT CTT GCA TGT TTC AGG AGG GCT GC 3' for N-1TM; 5' GGA TGA **GCG GCC GC**G CCT TGC ATG TTT CAG GAG GGC TGC 3' for 1TM-C; 5' GGA ATT CTC CAT GGC CTC TAC ATA TGC AAT AAG AG 3' for N-2TM and 5'

GGA TGA **GCG GCC GC**G CCT CTA CAT ATG CAA TAA GAG 3' for 2TM-C) were designed to introduce a NcoI site (underlined) or a NotI site (boldface). The reverse primers (5' GCG TTA **CTC GAG** TCA GCT GAA AGA CTC TTT ATT GTA TTC 3' for all the N terminal his-tag constructs or 5' GCG TTA **CTC GAG** TTG CTG AAA GAC TCT TTA TTG TAT TC 3' for all the C terminal his-tag position) possess a XhoI site and a stop codon (underline) for the N terminal his-tag construct.

Protein extraction. Transformed BL21(λDE3) or BL21(λDE3) Codon Plus-RIL bacteria (Stratagen) were grown in LB medium supplemented with adequate antibiotics (Kanamycin (50µg/ml) or Chloramphenicol (40µg/ml) or Ampicilin (100ug/mL)) and allowed to reach an OD_{600} of 0.7-1, then bacteria were induced by 1mM IPTG at 16°C overnight. Bacteria pellets were lyzed by sonication in lysis buffer (50mM Tris pH7.5, 100mM NaCl, 2mM MgCl2, 2µg/ml leupeptin, 2µg/ml pepstatin, 10µM TLCK or 50mM Tris pH7.6, 500mM NaCl, 10mM DTT, 1% Chaps, 2µg/ml leupeptin, 2µg/ml pepstatin, 10µM TLCK) and the lysates were centrifuged at 10,000g at 4°C for 10min to obtain total protein fraction. Supernatant corresponding to the total protein content was collected and subsequently centrifuged at 46000g 4°C for 30min to separate the soluble (supernatant) from the insoluble fraction (Hadj-Slimane *et al.*). The protein expression and solubility were analyzed by SDS-PAGE, the gel being colored with Coomassie bleu dye or used for western blot with an anti-histidine antibody (Sigma).

Inclusion bodies purification. IPTG induced transformed BL21(λDE3) bacteria were sonicated in lysis buffer A (50mM Tris pH7.5, 100mM NaCl, 2mM MgCl2, 2µg/ml leupeptin, 2µg/ml pepstatin, 10µM TLCK) to extract the proteins. The homogenate was centrifuged at 10000g, 4°C for 10min and the subsequent supernatant was centrifuged at 46000g, 4°C for 10min. The resulting pellet was resuspended in buffer A containing 2M NaCl. The resuspended solution was then centrifuged again and the resulting pellet resuspended in buffer A supplemented with 2% triton X-100. A series of centrifugation and pellet resuspension were performed with different buffer compositions: first with buffer A containing 1M urea and finally with buffer A containing 8M urea and 1mM glycine. The solution was then centrifuged for a last time and the supernatant contains the inclusion bodies.

Cell-free expression of different Nox4 truncated forms by Rapid Translation System (Roche). Expression tests for each protein were performed using the RTS™ HY100 (Roche Applied Science) according to the manufacturer's instructions. Different compounds were used to optimize the expression and the solubility (5mM Nonidet P40 (NP40), 0.1mM n-Dodecyl-b-D-maltoside (DDM), 0.1mM/4mM GSH/GSSG, GroE chaperone (1 to 50 dilution). The reactions were performed during 20-24h at 20°C. At the end of the

incubation, the final reaction (total proteins) was centrifuged at 21400g, 4°C for 30min to separate the soluble (supernatant) from the insoluble protein fraction (Hadj-Slimane *et al.*). The different fractions were analyzed by western blot with anti-histidine antibody (Sigma) to estimate the level of expression and the solubility of the proteins. The expression of the proteins at large scale was performed with RTS™ HY500 ProteoMaster (Roche Applied Science) in the Proteomaster™ apparatus at 20°C for 24h with 990rpm shaking speed. The total protein fraction was then centrifuged (21400g at 4°C for 30min) and the supernatant was considered as the soluble fraction.

Purification of his-tag recombinant protein. The soluble fraction was equilibrated by the addition of 4 column volumes (CV) of buffer A and then loaded onto a column containing the adequate resin pre-equilibrated with 20 CV of buffer A. The column was washed extensively with 20 CV of buffer A+10mM imidazole and the proteins were eluted by a gradient of imidazole starting from 100mM to 1M. The composition of the buffer A and resin used for the different sources of soluble fractions are indicated below: 1) for inclusion bodies (buffer A: 50mM Tris pH7.5, 100mM NaCl, 2mM MgCl2, 2µg/ml leupeptin, 2µg/ml pepstatin, 10µM TLCK, 8M urea, 1mM glycine and resin: Ni Sepharose™ 6 Fast Flow (GE Healthcare), 2) for soluble fraction obtained from transformed BL21(λDE3) Codon Plus-RIL bacteria (buffer A: 50mM Tris pH7.6, 500mM NaCl, 10mM DTT, 1% chaps, 2µg/ml leupeptin, 2µg/ml pepstatin, 10µM TLCK and resin: Ni-NTA), 3) for soluble proteins obtained by RTS™ (buffer A: sodium phosphate 150mM pH 7.4, 300mM NaCl, 20mM d'imidazolee, 0,1mM de n-dodecyl-β-D-maltoside and resin: TALON® Polyhistidine-Tag Purification Resins).

Refolding protocol. Different compounds were used to optimize the refolding conditions (pH: from 6-9; Salts: 200mM KCl or 100mM NaCl; Cations: 2mM EDTA or mix cations (1mM $MgCl_2$, 20mM $CaCl_2$ and 10mM $ZnCl_2$); additive: 400mM sucrose; Detergents: 0.1% chaps or 0.1mM DDM; Redox: 4mM/8mM GSH/GSSG or 1mM DTT; Cofactors: 150uM FAD or 10uM NADPH; 0.5mM NV10). These compounds were randomly combined using the SAmBa software (http://www.igs.cnrs-mrs.fr/samba/) (Audic *et al.*, 1997) to generate the composition of different refolding buffer used in this study. The refolding of purified protein solubilized in 8M urea was realized by dilution method. 37.5uL of purified protein were diluted by 40 fold in 1.5ml of refolding buffer. The solution was mix 5 times by manual inversion and rotated for 2h at 4°C and then centrifuged at 21400g, 4°C for 30min to separate the soluble (supernatant) from the insoluble fraction (Hadj-Slimane *et al.*). 20ul soluble fractions were analyzed by SDS-PAGE colored with Coomassie bleu dye and the solubility was evaluated by densitometry analysis of the gel using Scion® programme (NIH, USA).

The solubility of the purified proteins, reflecting a possible correct refolding state, was estimated in comparison with the amount of proteins diluted with the same procedure in 8M urea buffer which corresponds to 100% of solubility. The score obtained for each compound was calculated as follow: the percentages of solubility in which the compound is present were summed and divided by the number of time this compound appears. A high score indicates a good solubilization capacity of the compound.

Cell-free system diaphorase activity assay. The capacity of electron transfer *in vitro* was evaluated using an adapted protocol previously described (Berthier ***et al.***, 2003). 10pmol of purified proteins were incubated for 5min at 4°C in PBS buffer containing 10uM FAD (with or without 300ug of cytosol isolated from HEK293E cells) and then added PBS reaction buffer containing 10uM FAD, 100uM INT (iodonitro tetrazolium chloride) or 100uM cytochrome c. When a stable base line was reached, the reaction was initiated by the addition of 150uM NADPH and the reduction of these compounds was followed during 30 minutes (at 500nm for INT, ε_{500nm}=11mM^{-1}.cm^{-1} or at 550nm for cytochrome c, ε_{550nm}=21.1mM^{-1}.cm^{-1}).

Results and discussion

As well described for Nox2, the first electronic transfer step takes place at the cytosolic part of gp91phox protein and is called diaphorase activity (Han ***et al.***, 2001; Pessach ***et al.***, 2001; Nisimoto ***et al.***, 2004; Pessach ***et al.***, 2006; Marques ***et al.***, 2007). This portion of gp91phox protein possesses specific domains dedicated to the binding of NADPH and FAD which are necessary to initiate the electron transfer. A comparison between Nox2 and Nox4 sequence reveals that the C terminal part of Nox4 also contains these two conserved domains (Fig.1A). We hypothesize then that Nox4 could share the same pattern of initiation of its activity. In order to characterize the molecular mechanism involved in the establishment of the electron transfer through Nox4, we generated a series of truncated Nox4 proteins containing the NADPH and the FAD domain. Those were: 2-TM (177-578), 1-TM (206-578) and Aqc (309-578) which derived from the variant Nox4A; Bqc (309-578) derived from the isoform Nox4B (Fig.1A). The isoform NoxB result from the translation of a splice Nox4 mRNA lacking one of the NADPH binding domains. This variant has been described as inactive (Goyal ***et al.***, 2005; Grange ***et al.***, 2006). Bqc proteins were used to investigate if the NADPH binding domain is in fact necessary for the diaphorase activity and if so it could be therefore used as negative control. We used two different approaches to express those proteins. First we used an *in vitro*

transcriptional-translational technique, Rapid Translation System (RTS) and second an *E.coli* based expression system.

In vitro expression of Nox4 truncated proteins by RTS

Constructs described in Fig1 were used for this study. Each protein contains a poly-histidine tag either at the C terminus or at the N terminus side. Truncated proteins were synthesized *in vitro* by a transcriptional-translational system based on an *E.coli* lysat and the protein expression was analyzed by western blot using an anti-histidine antibody. Using standard synthesis conditions provided by the manufacturer without additives, we were able to express all the truncated proteins at variable levels as shown in the Fig2. A slight effect of the position of the poly-histidine tag on the expression level of 2-TM and 1-TM proteins was noticeable. We observed also the presence of additional shorter protein bands by western blot only with the Nter tag for the proteins 2-TM and 1-TM but not for the Cter tag (Fig2B). This is due to the existence of rare codons in Nox4 nucleic acid sequence (Wada *et al.*, 1992). These codons are AGG AGA ACC AGG AGA and AGA AGA CUA and are located at nucleic acid 273 and 1363, respectively (Fig1). Rare codons interfere with the bacterial translational mechanism leading therefore to a premature stop of the synthesis of the protein (Varenne *et al.*, 1986; Spanjaard *et al.*, 1988). This is particularly noticeable during the synthesis of the full length Nox4 Nter tagged protein as well (Fig2A).

Since the solubility of the protein is a good indication of his potential correct folding state and therefore may increase its ability to be active, we next assessed and optimized conditions to obtain soluble proteins. An analysis of the hydrophobic properties of Nox4 protein by different softwares (TMHMM, PRED-TMR, DAS, PHD, SOSUI, TMPred, HMMTOP and TopPred) reveals that a majority of them predict a high hydrophobic domain surrounding the first NADPH binding site (Fig1). Interestingly, the predicted sixth transmembrane domain appears to be poorly hydrophobic. To counter balance the negative effect of the hydrophobic domain, we used the chaperone GroE, the redox couple GSH/GSSG and detergents like NP40 and DDM as additives in the *in vitro* translation reaction. The idea of this approach is to facilitate the correct folding of the proteins directly during its synthesis. Our results showed that all parameters play an important role to obtain soluble proteins. For example, the position of the poly-histidine influenced not only the amount of proteins produced but also its solubility in the presence of NP40 for the 1-TM construct (Fig2, condition E, F and G). Interestingly, the use of the detergent DDM favored toward a better solubility of all constructs contrasting

with the addition of NP40 which in some cases (Bqc and 2-TM proteins) annihilated the production of soluble proteins (Fig2, conditions E and G). Furthermore, the addition of GroE and GSH/GSSG to DDM increased even more the solubility of all of the truncated proteins (Fig2, condition C and D versus B). Nevertheless, a higher concentration of DDM has led to a loss of the solubility without affecting the total amount of proteins produced (SuppS1A). Although FAD is a natural substrate, it did not significantly increase the solubility (SuppS1B). Finally based on our results, we found a common optimized condition for the synthesis of all constructs: 0.1mM of DDM, GroE and 0.1mM/4mM of GSH/GSSG. The use of the C terminal tagged proteins was chosen to eliminate the interferences mediated by the rare codons.

Expression of Nox4 truncated proteins by bacterial induction

Constructs were transformed into BL21(λDE3) bacteria and the expression of the proteins was induced by the addition of IPTG. The analysis of the production of Aqc and Bqc by western blot showed as previously described the expression of shorter proteins (Fig3A). To exclude the interference of these additional proteins in our study, we used the BL21DE3 Codon+RIL bacterial strain. In these conditions, we were able to avoid the synthesis of these incomplete proteins and expressed 1-TM, Aqc and Bqc as shown by western blot in fig3B. However, we were unable to synthesize the 2-TM protein. This is likely due to the toxicity of the over-expression membrane proteins toward bacteria (Miroux *et al.*, 1996). We next checked if the produced protein could be expressed in a soluble form. Unfortunately no solubility was observed for the protein Aqc (Fig3C). Same observation was made concerning the expression of the cytosolic tail of Nox2 (Han *et al.*, 2001; Nisimoto *et al.*, 2004).

To obtain soluble proteins we designed an approach in two steps. We first decided to perform an extensive screening of refolding conditions of purified inclusion bodies of Aqc solubilized by 8M urea. For this purpose, we tested a series of combination of different compounds randomly generated by software (SAmBa) (Audic *et al.*, 1997). Denaturated Aqc proteins were refolded by dilution in specific buffer and the solubility was analyzed after centrifugation by SDS-PAGE, scanned and scored as stipulated in the method section. The conditions and compounds used are described in the table 1. A series of refolding experiments were necessary to find out the optimized conditions and an example of a screening is shown and described in the supplementary figure S2. The refolding experiments revealed that a basic pH above 9 by itself is important to solubilize the denaturated protein Aqc compared to pH 7.4. More interestingly, NV10 and chaps at pH7.4 have also a positive effect on the refolding (Fig3D). Based on these results, we decide then to lyse directly the

induced bacteria pellet in a buffer containing 1% chaps. With this condition we were able to obtain soluble proteins (Fig3E).

Diaphorase activity of Nox4 truncated proteins

In order to characterize the electronic transfer property of Nox4, it was necessary to generate enough soluble proteins compatible with the functional assays. We therefore over-expressed the truncated Aqc and Bqc proteins in large scale using the optimized conditions obtained previously for the cell-free expression system and for the bacterial induction approach. The soluble proteins were then purified onto affinity chromatography and were tested for the diaphorase activity. The figure 4A shows the purified protein on SDS-PAGE colored with Coomassie bleu. The amount of Aqc proteins obtained is 9µg/mL RTS reaction compared to 0.9ug/mL media culture.

The diaphorase activity of these proteins was estimated by two electron acceptors usually used to measure the transfer of electrons from NADPH to FAD through the cytosolic tail of Nox2 (Otsuka-Murakami *et al.*, 1995; Poinas *et al.*, 2002; Nisimoto *et al.*, 2004) : INT (p-Iodonitrotetrazolium) and cytochrome c. 10pmol of protein was used for each assay. The values of the specific diaphorase activity for the protein Aqc obtained by RTS are 26±2.6 nmol/min/nmol for INT and 48±20.2 nmol/min/nmol for cytochrome c (Fig4B). We next compared these results with the turnover rate of the protein Aqc purified from the IPTG induced bacteria which are 4.4±1.7 nmol/min/nmol for INT and 20.5±2.8 nmol/min/nmol for cytochrome c (Fig4C). First for both proteins, the electron acceptor cytochrome c gave a higher rate than INT. Second the protein Aqc produced by a cell based system possessed a lower specific activity compared to the protein synthesized by the cell-free technology. This difference may results from a distinct folding state of the protein. Indeed, in the case of the cell-free based system, the direct contact of the detergent DDM and the chaperone GroE during the protein synthesis process may have provided a better folding environment. We have shown in a previous work that the isoform Nox4B is inactive when it is over-expressed in chondrocyte cell line compared to the conventional variant Nox4A (Grange *et al.*, 2006). In order to determine if the absence of activity is due to the inability for the protein to initiate the first electronic transfer step, we submitted the purified truncated Bqc protein to the diaphorase assay. As expected, Bqc was unable to reduce any of the two electronic acceptors.

Unlike Nox2, the diaphorase activity of Aqc is constitutive and the addition of cytosolic factors was not necessary to reduce the electron acceptors (Nisimoto *et al.*, 2004; Marques *et al.*, 2007). This result is in

line with the observation that Nox4A possesses a constitutive NADPH oxidase activity measured in cell lines (Ambasta *et al.*, 2004; Grange *et al.*, 2006; Martyn *et al.*, 2006; Serrander *et al.*, 2007) and by cell-free system (Jackson *et al.*, 2010; Nisimoto *et al.*, 2010). Using two different method of protein synthesis, we demonstrated here that the cytosolic domain of Nox4 is responsible of Nox4 constitutive activity. Same observations were made by others authors using a very similar portion of the C-terminal part of Nox4 (Jackson *et al.*, 2010; Nisimoto *et al.*, 2010) nevertheless with disparity in the turnover activity value. A turnover of around 100 min^{-1} was observed by Jackson and al while Nisimoto and his colleagues found a diaphorase activity 160 min^{-1} when measured with the cytochrome c. The difference observed in each study may be due to different tags usage and also the buffer composition. To find out whether Nox4 diaphorase activity could be stimulated by unknown cytosolic components, we measured the turnover rate of Aqc in the presence of cytosol extracted from HEK293 cell. The choice of HEK293 cells was made because these cells express endogenously Nox4. As shown in figure 4D, the addition of the cytosol extract did not enhance Aqc activity.

In conclusion

In this work, the ability of the cytosolic tail of Nox4 to generate a diaphorase activity was investigated. We have demonstrated that the C terminal domain of Nox4 is capable of generating a diaphorase activity. Furthermore, this activity is constitutive due to a spontaneous transfer of electrons from NADPH to FAD and is independent of cytosolic factors isolated from HEK293 cells. We also showed that the isoform Nox4B is unable to initiate the first electronic transfer step.

We described in this work two different optimized methods to produce soluble and active truncated Nox4 proteins. We point out two critical parameters for the synthesis of functional proteins which are rare codons and high hydrophobicity in Nox4 sequence. Finally, this approach could be extended and be useful to characterize step by step the electronic transfer mechanism throughout Nox4 protein and other NADPH oxidase as well.

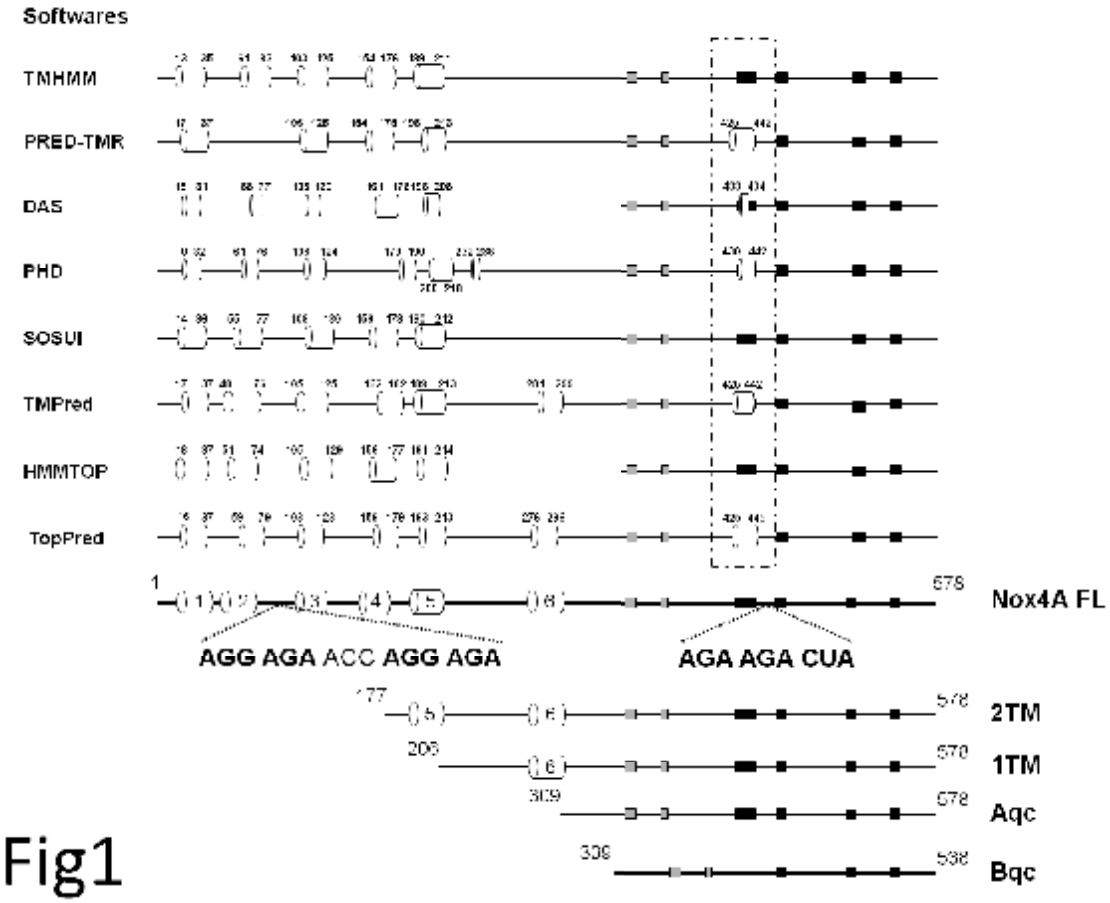

Fig1

Figure 1. Schematic representation of the NADPH oxydase Nox4 and truncated forms used in this study. The top of the diagram shows an alignment of predicted hydrophobic domains of Nox4 by using different softwares. Transmembrane domains are represented by white cylinder. FAD and NADPH binding-sites are represented in gray and black boxes, respectively. Rare codon sequences are highlighted at the bottom of the Nox4 full-length scheme.

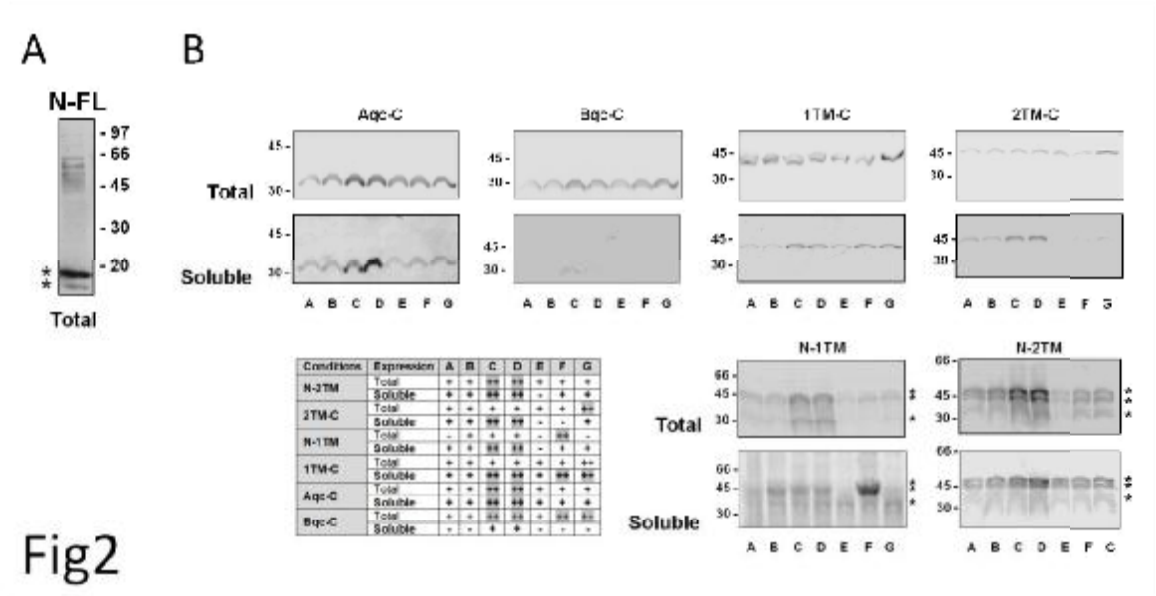

Figure 2. (A) Analysis of full length form of Nox4 protein by western blot, upon expression by cell-free translation system, using a monoclonal antibody anti-his. **(B)** Expression of truncated Nox4 proteins in a bacterial cell-free translation system. Optimization of the solubility of the Nox4 truncated proteins by western blot using a monoclonal antibody anti-his. The table summarizes the total and soluble expression of the proteins. A, no additives; B, DDM; C, DDM and GroE; D, DDM, GroE and GSH/GSSG; E, NP40; F, NP40 and GroE; G, NP40, GroE and GSH/GSSG. The concentration of each additive is mentioned in the material and methods section. Stars indicate different molecular sizes of the truncated proteins due to the presence of rare codons in Nox4 nucleic acid sequence. The position of the tag is noted on the name of the protein itself which C and N correspond respectively to the C and N terminal poly-histidine tag.

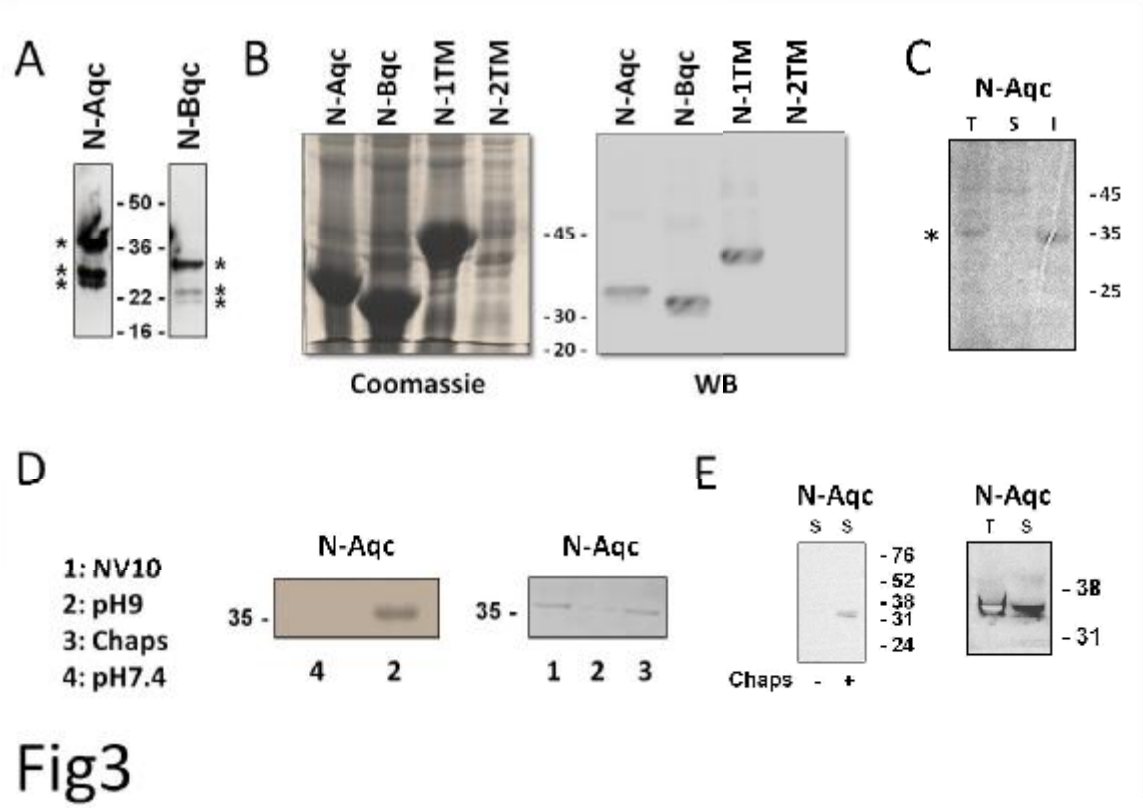

Fig3

Figure 3. Expression of truncated Nox4 proteins by bacterial IPTG induction. **(A)** Analysis of the expression of truncated forms of Nox4 protein expressed by BL21(DE3) IPTG induction by western blot using a monoclonal antibody anti-his. Stars indicate different molecular sizes of the truncated proteins due to the presence of rare codons in Nox4 nucleic sequence. **(B)** Expression tests of truncated Nox4 proteins produced by IPTG induction of BL21(DE3) codon+RIL bacteria. SDS-PAGES colored with Coomassie bleu dye or western blot using a monoclonal antibody anti-his. **(C)** Analysis of the soluble fraction containing of truncated Nox4 proteins by SDS-PAGE. T, total; S, soluble and I, insoluble. **(D)** Coomassie bleu gel showing soluble N-Aqc proteins using 4 determined refolding conditions: 1, with NV10 (0.5mM) at pH 7.4; 2, pH9; 3, with chaps at pH7.4 and 4, pH7.4. **(E)** Direct solubilization of N-Aqc proteins in the lysis buffer with chaps as detergent (50mM Tris pH7.6, 500mM NaCl, 10mM DTT, 1% Chaps, 2µg/ml leupeptin, 2µg/ml pepstatin, 10µM TLCK). IPTG induced BL21(DE3) codon+RIL transformed with plasmid encoding N-Aqc protein were directly lyzed by sonication in lysis buffer containing the detergent chaps. The soluble proteins were evidenced by western blot using a monoclonal anti-histidine antibody. T, total and S, soluble.

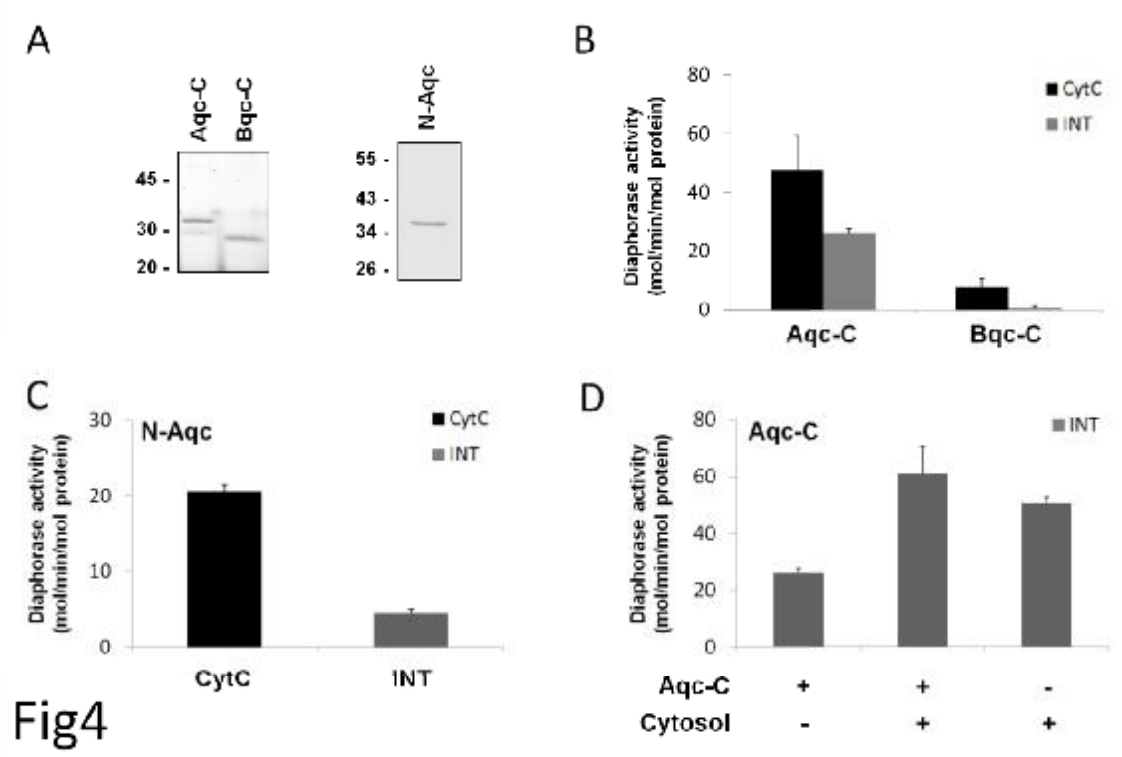

Figure 4. Diaphorase activity of purified truncated Nox4 proteins. **(A)** Coomassie bleu gel showing purified soluble Aqc-C and Bqc-C proteins expressed by a transcription/translation coupled system (left panel) and purified soluble N-Aqc expressed in BL21(DE3) codon+RIL bacteria (Right panel). Diaphorase activity measured by INT and cytochrome c of purified soluble Aqc-C and Bqc-C by a transcription/translation coupled system **(B)** or of purified soluble N-Aqc expressed in BL21(DE3) codon+RIL bacteria **(C)**. **(D)** Measurement of diaphorase activity of the purified soluble Aqc-C in the presence or not of 300ug of cytosolic proteins extracted from HEK293 cells.

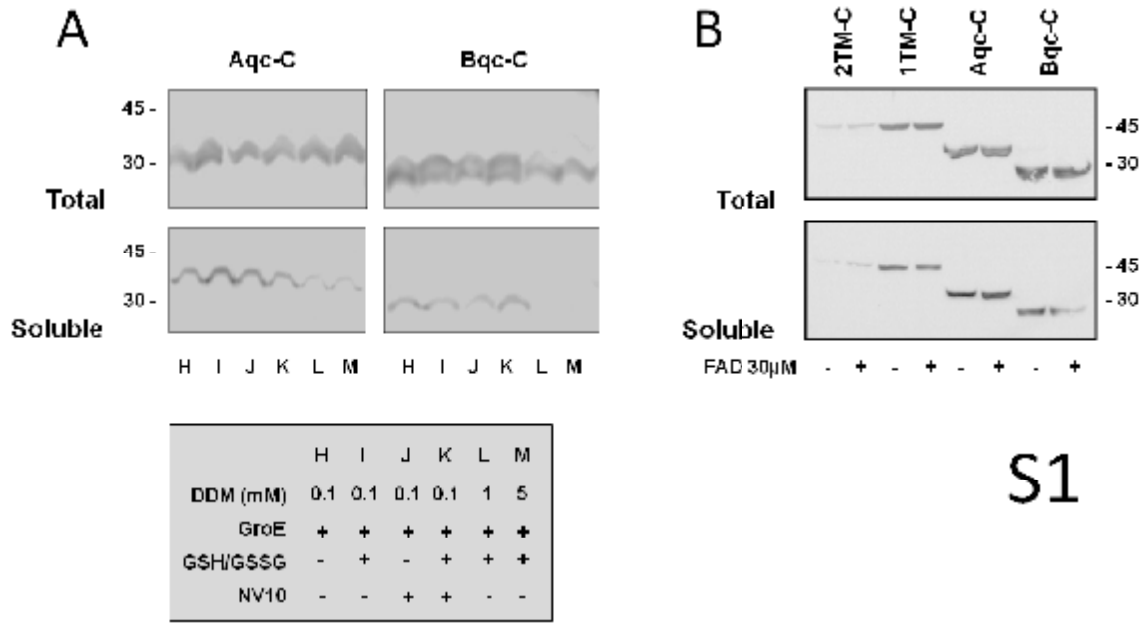

	H	I	J	K	L	M
DDM (mM)	0.1	0.1	0.1	0.1	1	5
GroE	+	+	+	+	+	+
GSH/GSSG	-	+	-	+	+	+
NV10	-	-	+	+	-	-

Supp1. Effect of concentration of DMM, NV10 and the cofactor FAD on the solubility of truncated Nox4 proteins expressed by a transcription/translation coupled system.

A

Conditions	pH	Salts	Cations	Additives	Detergents	Redox	Cofactors
1	7	KCl	None	None	DDM	None	None
2	8	NaCl	Mix	None	DDM	GSH/GSSG	NADPH
3	7	None	None	Sucrose	Chaps	GSH/GSSG	NADPH
4	8	KCl	EDTA	None	Chaps	None	NADPH
5	8	NaCl	EDTA	Sucrose	Chaps	DTT	FAD
6	8	KCl	EDTA	Sucrose	None	DTT	NADPH
7	8	None	None	Sucrose	None	DTT	None
8	9	NaCl	None	None	DDM	DTT	NADPH
9	9	KCl	None	None	Chaps	DTT	FAD
10	8	None	Mix	None	DDM	DTT	FAD
11	7	KCl	None	Sucrose	None	None	NADPH
12	9	NaCl	EDTA	None	None	None	FAD
13	7	None	EDTA	Sucrose	None	GSH/GSSG	FAD
14	7	KCl	EDTA	Sucrose	DDM	DTT	None
15	8	KCl	Mix	None	None	GSH/GSSG	None
16	9	None	EDTA	None	DDM	None	None
17	8	None	EDTA	Sucrose	Chaps	GSH/GSSG	None
18	7	NaCl	Mix	Sucrose	Chaps	None	FAD
19	7	NaCl	Mix	Sucrose	None	DTT	None
20	8	NaCl	None	Sucrose	None	None	None
21	8	None	None	Sucrose	DDM	None	FAD
22	6	NaCl	None	Sucrose	Chaps	GSH/GSSG	None
23	8	NaCl	EDTA	None	DDM	GSH/GSSG	NADPH
24	8	None	Mix	None	Chaps	DTT	NADPH
25	8	KCl	None	None	None	GSH/GSSG	FAD
26	9	KCl	Mix	None	DDM	GSH/GSSG	FAD
27	8	KCl	Mix	Sucrose	Chaps	None	None
28	9	None	Mix	None	None	None	NADPH

B

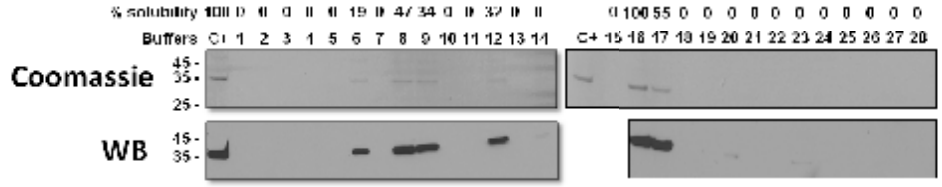

C

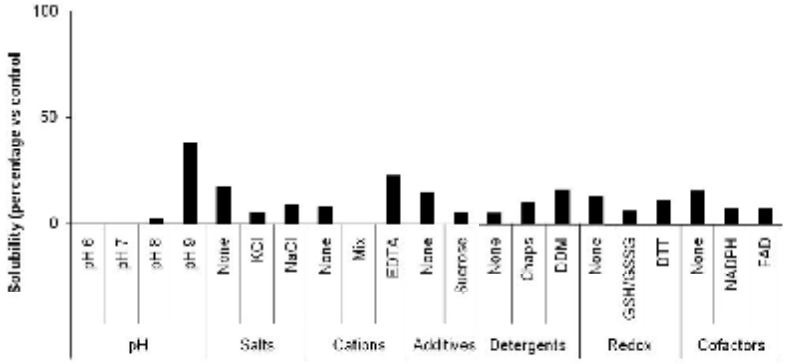

Supp2. Example of one refolding experiment of the purified N-Aqc proteins. **(A)** The table summarizes the different refolding condition used in this refolding experiment. **(B)** Purified N-Aqc in 8M urea buffer were refolded by dilution (40 fold) in different buffers. The soluble fractions (21400g at 4C for 30min) were analyzed by Coomassie bleu SDS-PAGE gel *(C)* and by western blot *(WB)* using a monoclonal anti-histidine antibody. The SDS-PAGE gel was scanned and the density of each band was evaluated by Scion® software

and expressed as percentage of the positive control. **(C)** The score reflecting the ability of each compound to solubilized N-Aqc protein was calculated as described in materials and methods section.

pH	Salts	Cations	Additives	Detergents	Redox	Cofactors
6	None	None	None	None	None	None
7	KCl 200mM	Mix	Sucrose 400mM	Chaps 1%	GSH/GSSG (4mM/8mM)	NADPH 150uM
7.4	NaCl 100mM	EDTA 2mM		DDM 0.1mM		FAD 10uM
8						
9						
9.5						
10						

Table 1. The table summarizes different compounds and conditions used in all refolding experiments. Cation mix: $MgCl_2$ 1mM, $CaCl_2$ 20mM and $ZnCl_2$ 10mM.

References:

[1] W.M. Nauseef, Biological roles for the Nox family NADPH oxidases, J Biol Chem 283 (2008) 16961-16965.

[2] F. Morel, [Molecular aspects of chronic granulomatous disease. "the NADPH oxidase complex"], Bull Acad Natl Med 191 (2007) 377-390; discussion 390-372.

[3] F. Morel, J. Doussiere, P.V. Vignais, The superoxide-generating oxidase of phagocytic cells. Physiological, molecular and pathological aspects, Eur J Biochem 201 (1991) 523-546.

[4] M.H. Paclet, A.W. Coleman, S. Vergnaud, F. Morel, P67-phox-mediated NADPH oxidase assembly: imaging of cytochrome b558 liposomes by atomic force microscopy, Biochemistry 39 (2000) 9302-9310.

[5] K.J. Biberstine-Kinkade, F.R. DeLeo, R.I. Epstein, B.A. LeRoy, W.M. Nauseef, M.C. Dinauer, Heme-ligating histidines in flavocytochrome b(558): identification of specific histidines in gp91(phox), J Biol Chem 276 (2001) 31105-31112.

[6] A.R. Cross, A.W. Segal, The NADPH oxidase of professional phagocytes--prototype of the Nox electron transport chain systems, Biochim Biophys Acta 1657 (2004) 1-22.

[7] I. Pessach, T.L. Leto, H.L. Malech, R. Levy, Essential requirement of cytosolic phospholipase A(2) for stimulation of NADPH oxidase-associated diaphorase activity in granulocyte-like cells, J Biol Chem 276 (2001) 33495-33503.

[8] I. Pessach, Z. Shmelzer, T.L. Leto, M.C. Dinauer, R. Levy, The C-terminal flavin domain of gp91phox bound to plasma membranes of granulocyte-like X-CGD PLB-985 cells is sufficient to anchor cytosolic oxidase components and support NADPH oxidase-associated diaphorase activity independent of cytosolic phospholipase A2 regulation, J Leukoc Biol 80 (2006) 630-639.

[9] M. Geiszt, J.B. Kopp, P. Varnai, T.L. Leto, Identification of renox, an NAD(P)H oxidase in kidney, Proc Natl Acad Sci U S A 97 (2000) 8010-8014.

[10] Y. Gorin, K. Block, J. Hernandez, B. Bhandari, B. Wagner, J.L. Barnes, H.E. Abboud, Nox4 NAD(P)H oxidase mediates hypertrophy and fibronectin expression in the diabetic kidney, J Biol Chem 280 (2005) 39616-39626.

[11] A. Shiose, J. Kuroda, K. Tsuruya, M. Hirai, H. Hirakata, S. Naito, M. Hattori, Y. Sakaki, H. Sumimoto, A novel superoxide-producing NAD(P)H oxidase in kidney, J Biol Chem 276 (2001) 1417-1423.

[12] J.K. Maranchie, Y. Zhan, Nox4 is critical for hypoxia-inducible factor 2-alpha transcriptional activity in von Hippel-Lindau-deficient renal cell carcinoma, Cancer Res 65 (2005) 9190-9193.

[13] G. Cheng, Z. Cao, X. Xu, E.G. van Meir, J.D. Lambeth, Homologs of gp91phox: cloning and tissue expression of Nox3, Nox4, and Nox5, Gene 269 (2001) 131-140.

[14] S.H. Ellmark, G.J. Dusting, M.N. Fui, N. Guzzo-Pernell, G.R. Drummond, The contribution of Nox4 to NADPH oxidase activity in mouse vascular smooth muscle, Cardiovasc Res 65 (2005) 495-504.

[15] K. Wingler, S. Wunsch, R. Kreutz, L. Rothermund, M. Paul, H.H. Schmidt, Upregulation of the vascular NAD(P)H-oxidase isoforms Nox1 and Nox4 by the renin-angiotensin system in vitro and in vivo, Free Radic Biol Med 31 (2001) 1456-1464.

[16] R.E. Clempus, D. Sorescu, A.E. Dikalova, L. Pounkova, P. Jo, G.P. Sorescu, H.H. Schmidt, B. Lassegue, K.K. Griendling, Nox4 is required for maintenance of the differentiated vascular smooth muscle cell phenotype, Arterioscler Thromb Vasc Biol 27 (2007) 42-48.

[17] R.M. Touyz, X. Chen, F. Tabet, G. Yao, G. He, M.T. Quinn, P.J. Pagano, E.L. Schiffrin, Expression of a functionally active gp91phox-containing neutrophil-type NAD(P)H oxidase in smooth muscle cells from human resistance arteries: regulation by angiotensin II, Circ Res 90 (2002) 1205-1213.

[18] T. Ago, T. Kitazono, H. Ooboshi, T. Iyama, Y.H. Han, J. Takada, M. Wakisaka, S. Ibayashi, H. Utsumi, M. Iida, Nox4 as the major catalytic component of an endothelial NAD(P)H oxidase, Circulation 109 (2004) 227-233.

[19] J. Kuroda, K. Nakagawa, T. Yamasaki, K. Nakamura, R. Takeya, F. Kuribayashi, S. Imajoh-Ohmi, K. Igarashi, Y. Shibata, K. Sueishi, H. Sumimoto, The superoxide-producing NAD(P)H oxidase Nox4 in the nucleus of human vascular endothelial cells, Genes Cells 10 (2005) 1139-1151.

[20] H.S. Park, D.K. Jin, S.M. Shin, M.K. Jang, N. Longo, J.W. Park, D.S. Bae, Y.S. Bae, Impaired generation of reactive oxygen species in leprechaunism through downregulation of Nox4, Diabetes 54 (2005) 3175-3181.

[21] A. Rossary, K. Arab, J.P. Steghens, Polyunsaturated fatty acids modulate Nox4 anion superoxide production in human fibroblasts, Biochem J 406 (2007) 77-83.

[22] J.T. Colston, S.D. de la Rosa, J.R. Strader, M.A. Anderson, G.L. Freeman, H2O2 activates Nox4 through PLA2-dependent arachidonic acid production in adult cardiac fibroblasts, FEBS Lett 579 (2005) 2533-2540.

[23] I. Cucoranu, R. Clempus, A. Dikalova, P.J. Phelan, S. Ariyan, S. Dikalov, D. Sorescu, NAD(P)H oxidase 4 mediates transforming growth factor-beta1-induced differentiation of cardiac fibroblasts into myofibroblasts, Circ Res 97 (2005) 900-907.

[24] W. Chamulitrat, W. Stremmel, T. Kawahara, K. Rokutan, H. Fujii, K. Wingler, H.H. Schmidt, R. Schmidt,

A constitutive NADPH oxidase-like system containing gp91phox homologs in human keratinocytes, J Invest Dermatol 122 (2004) 1000-1009.

[25] K. Mahadev, H. Motoshima, X. Wu, J.M. Ruddy, R.S. Arnold, G. Cheng, J.D. Lambeth, B.J. Goldstein, The NAD(P)H oxidase homolog Nox4 modulates insulin-stimulated generation of H2O2 and plays an integral role in insulin signal transduction, Mol Cell Biol 24 (2004) 1844-1854.

[26] S. Mouche, S.B. Mkaddem, W. Wang, M. Katic, Y.H. Tseng, S. Carnesecchi, K. Steger, M. Foti, C.A. Meier, P. Muzzin, C.R. Kahn, E. Ogier-Denis, I. Szanto, Reduced expression of the NADPH oxidase Nox4 is a hallmark of adipocyte differentiation, Biochim Biophys Acta 1773 (2007) 1015-1027.

[27] P. Vallet, Y. Charnay, K. Steger, E. Ogier-Denis, E. Kovari, F. Herrmann, J.P. Michel, I. Szanto, Neuronal expression of the NADPH oxidase Nox4, and its regulation in mouse experimental brain ischemia, Neuroscience 132 (2005) 233-238.

[28] X. Dai, X. Cao, D.L. Kreulen, Superoxide anion is elevated in sympathetic neurons in DOCA-salt hypertension via activation of NADPH oxidase, Am J Physiol Heart Circ Physiol 290 (2006) H1019-1026.

[29] C. Piccoli, R. Ria, R. Scrima, O. Cela, A. D'Aprile, D. Boffoli, F. Falzetti, A. Tabilio, N. Capitanio, Characterization of mitochondrial and extra-mitochondrial oxygen consuming reactions in human hematopoietic stem cells. Novel evidence of the occurrence of NAD(P)H oxidase activity, J Biol Chem 280 (2005) 26467-26476.

[30] T. Akasaki, Y. Ohya, J. Kuroda, K. Eto, I. Abe, H. Sumimoto, M. Iida, Increased expression of gp91phox homologues of NAD(P)H oxidase in the aortic media during chronic hypertension: involvement of the renin-angiotensin system, Hypertens Res 29 (2006) 813-820.

[31] M. Sedeek, R.L. Hebert, C.R. Kennedy, K.D. Burns, R.M. Touyz, Molecular mechanisms of hypertension: role of Nox family NADPH oxidases, Curr Opin Nephrol Hypertens 18 (2009) 122-127.

[32] T. Djordjevic, R.S. BelAiba, S. Bonello, J. Pfeilschifter, J. Hess, A. Gorlach, Human urotensin II is a novel activator of NADPH oxidase in human pulmonary artery smooth muscle cells, Arterioscler Thromb Vasc Biol 25 (2005) 519-525.

[33] D. Sorescu, D. Weiss, B. Lassegue, R.E. Clempus, K. Szocs, G.P. Sorescu, L. Valppu, M.T. Quinn, J.D. Lambeth, J.D. Vega, W.R. Taylor, K.K. Griendling, Superoxide production and expression of nox family proteins in human atherosclerosis, Circulation 105 (2002) 1429-1435.

[34] L. Grange, M.V. Nguyen, B. Lardy, M. Derouazi, Y. Campion, C. Trocme, M.H. Paclet, P. Gaudin, F. Morel, NAD(P)H oxidase activity of Nox4 in chondrocytes is both inducible and involved in collagenase expression, Antioxid Redox Signal 8 (2006) 1485-1496.

[35] B. Banfi, R.A. Clark, K. Steger, K.H. Krause, Two novel proteins activate superoxide generation by the NADPH oxidase Nox1, J Biol Chem 278 (2003) 3510-3513.

[36] R. Takeya, N. Ueno, K. Kami, M. Taura, M. Kohjima, T. Izaki, H. Nunoi, H. Sumimoto, Novel human homologues of p47phox and p67phox participate in activation of superoxide-producing NADPH oxidases, J Biol Chem 278 (2003) 25234-25246.

[37] M. Geiszt, K. Lekstrom, J. Witta, T.L. Leto, Proteins homologous to p47phox and p67phox support superoxide production by NAD(P)H oxidase 1 in colon epithelial cells, J Biol Chem 278 (2003) 20006-20012.

[38] K.D. Martyn, L.M. Frederick, K. von Loehneysen, M.C. Dinauer, U.G. Knaus, Functional analysis of Nox4 reveals unique characteristics compared to other NADPH oxidases, Cell Signal 18 (2006) 69-82.

[39] T. Kawahara, D. Ritsick, G. Cheng, J.D. Lambeth, Point mutations in the proline-rich region of p22phox

are dominant inhibitors of Nox1- and Nox2-dependent reactive oxygen generation, J Biol Chem 280 (2005) 31859-31869.
[40] L. Serrander, L. Cartier, K. Bedard, B. Banfi, B. Lardy, O. Plastre, A. Sienkiewicz, L. Forro, W. Schlegel, K.H. Krause, Nox4 activity is determined by mRNA levels and reveals a unique pattern of ROS generation, Biochem J 406 (2007) 105-114.
[41] L. Zhang, M.V. Nguyen, B. Lardy, A.J. Jesaitis, A. Grichine, F. Rousset, M. Talbot, M.H. Paclet, G. Qian, F. Morel, New insight into the Nox4 subcellular localization in HEK293 cells: first monoclonal antibodies against Nox4, Biochimie 93 (2011) 457-468.
[42] S. Audic, F. Lopez, J.M. Claverie, O. Poirot, C. Abergel, SAmBA: an interactive software for optimizing the design of biological macromolecules crystallization experiments, Proteins 29 (1997) 252-257.
[43] S. Berthier, M.H. Paclet, S. Lerouge, F. Roux, S. Vergnaud, A.W. Coleman, F. Morel, Changing the conformation state of cytochrome b558 initiates NADPH oxidase activation: MRP8/MRP14 regulation, J Biol Chem 278 (2003) 25499-25508.
[44] C.H. Han, Y. Nisimoto, S.H. Lee, E.T. Kim, J.D. Lambeth, Characterization of the flavoprotein domain of gp91phox which has NADPH diaphorase activity, J Biochem 129 (2001) 513-520.
[45] B. Marques, L. Liguori, M.H. Paclet, A. Villegas-Mendez, R. Rothe, F. Morel, J.L. Lenormand, Liposome-mediated cellular delivery of active gp91(phox), PLoS One 2 (2007) e856.
[46] Y. Nisimoto, H. Ogawa, K. Miyano, M. Tamura, Activation of the flavoprotein domain of gp91phox upon interaction with N-terminal p67phox (1-210) and the Rac complex, Biochemistry 43 (2004) 9567-9575.
[47] P. Goyal, N. Weissmann, F. Rose, F. Grimminger, H.J. Schafers, W. Seeger, J. Hanze, Identification of novel Nox4 splice variants with impact on ROS levels in A549 cells, Biochem Biophys Res Commun 329 (2005) 32-39.
[48] K. Wada, Y. Wada, F. Ishibashi, T. Gojobori, T. Ikemura, Codon usage tabulated from the GenBank genetic sequence data, Nucleic Acids Res 20 Suppl (1992) 2111-2118.
[49] R.A. Spanjaard, J. van Duin, Translation of the sequence AGG-AGG yields 50% ribosomal frameshift, Proc Natl Acad Sci U S A 85 (1988) 7967-7971.
[50] S. Varenne, C. Lazdunski, Effect of distribution of unfavourable codons on the maximum rate of gene expression by an heterologous organism, J Theor Biol 120 (1986) 99-110.
[51] B. Miroux, J.E. Walker, Over-production of proteins in Escherichia coli: mutant hosts that allow synthesis of some membrane proteins and globular proteins at high levels, J Mol Biol 260 (1996) 289-298.
[52] H. Otsuka-Murakami, Y. Nisimoto, Purification of an NADPH-dependent diaphorase from membrane of DMSO-induced differentiated human promyelocytic leukemia HL-60 cells, FEBS Lett 361 (1995) 206-210.
[53] A. Poinas, J. Gaillard, P. Vignais, J. Doussiere, Exploration of the diaphorase activity of neutrophil NADPH oxidase, Eur J Biochem 269 (2002) 1243-1252.
[54] R.K. Ambasta, P. Kumar, K.K. Griendling, H.H. Schmidt, R. Busse, R.P. Brandes, Direct interaction of the novel Nox proteins with p22phox is required for the formation of a functionally active NADPH oxidase, J Biol Chem 279 (2004) 45935-45941.
[55] Y. Nisimoto, H.M. Jackson, H. Ogawa, T. Kawahara, J.D. Lambeth, Constitutive NADPH-dependent electron transferase activity of the Nox4 dehydrogenase domain, Biochemistry 49 (2010) 2433-2442.
[56] H.M. Jackson, T. Kawahara, Y. Nisimoto, S.M. Smith, J.D. Lambeth, Nox4 B-loop creates an interface between the transmembrane and dehydrogenase domains, J Biol Chem 285 (2010) 10281-10290.

Application of a new manner to study the topology of the transmembrane heterodimer: Nox4 and p22phox (article 4).

Les protéines membranaires sont impliquées dans une large gamme de processus biologiques importants, mais les techniques disponibles pour caractériser leur positionnement dans la membrane sont limitées. En l'absence de données de cristallisation, seules des prédictions de séquence peuvent être utilisées: on connait peu de choses sur la topologie et les domaines fonctionnels de p22phox. Seules des analogies de séquence avec Nox2 peuvent permettre une approche topologique de Nox4.

Dans cette méthode que nous proposons, les protéines de fusion ubGFP sont utilisées comme des instruments pour obtenir des détails sur la topologie des protéines membranaires. Cela conduit à réaliser la fusion de deux séquences, l'ubiquitin-GFP (ubGFP) et le gène d'intérêt, qui sera ensuite exprimée dans les cellules.

La validité de cette approche a été confirmée en utilisant deux protéines membranaires présentant une topologie connue. Ensuite, la méthode a été appliquée à l'étude de la topologie de Nox4 et p22phox. Dans ce travail, la fluorescence de la GFP a été analysée par FACS et l'expression des protéines a été détectée par western blot.

My contribution to this work includes 1) the construction of plasmids encoding p22phox and Nox4 proteins, 2) the selection of stable transfected cells (HEK293-Nox2N131ubGFP cells, HEK293-Nox2N131GFP cells, HEK293- IL1R1ubGFP cells and HEK293- IL1R1GFP cells), 3) the validation of TDUFA method by flow cytometry and western blot on IL1R1, Nox2N131 and 4) the application of this method to get some preliminary topology information on Nox4 and p22 phox.

Article 4:

Application of a new manner to study the topology of the transmembrane heterodimer: Nox4 and p22phox

Application of a new manner to study the topology of the transmembrane heterodimer: Nox4 and p22phox

1 Introduction

Membrane proteins are involved in a wide range of important biological processes such as cell signaling, transport of membrane-impermeable molecules, cell-cell communication. Many of them are also the prime drug targets, and it has been estimated that more than half of all drugs currently on the market target are membrane proteins (Klabunde *et al.*, 2002). Despite the important role of topology in protein function, the techniques now available for characterizing the topological distribution of proteins of the cells are limited.

In the absence of crystallization data, the investigation of the membrane protein topology depends on the prediction according to their primary sequences. The predictions according to computational approaches examining the relative hydrophobicity of different polypeptide regions of a protein are not fully reliable, and different algorithms have led to different results (Wilkinson *et al.*, 1996). Moreover, such predictions often do not clarify whether the amino or carboxyl terminus of a protein faces the cytoplasm, lumen or cell exterior.

Neutrophil cytochrome b558 is a membrane heterodimer composed of Nox2 (gp91phox) and p22phox. This is the catalytic center of the phagocyte NADPH oxidase complex responsible for the production of reactive oxygen species in response to inflammatory stimuli (Vignais, 2002; Nauseef, 2008). The p22phox subunit has 2 major functions. It binds and stabilizes Nox proteins, and serves as a membrane anchor for cytosolic regulatory factors. It was recently shown that p22phox also associates with Nox1, Nox3 and Nox4 (Ambasta *et al.*, 2004; Ueno *et al.*, 2005), suggesting a central role of p22phox in the cellular production of reactive oxygen species.

Until now, the topology and functional domains within p22phox are not clearly characterized. p22phox was proposed to contain 2–4 membrane-spanning segments according to the primary sequence analysis by computational methods, while by using specific monoclonal antibodies against p22phox and “peptide walking”, p22phox was proposed to contain 2 or 4 transmembrane helix (Leto *et al.*, 1994; Dahan *et al.*, 2002; Taylor *et al.*, 2004; Groemping *et al.*, 2005).

NADPH oxidase Nox4 shares ~39% identity to Nox2, p22phox is the only component necessary for its activity. Little is known at the molecular level, and there were no related reports on the topology of Nox4. The topology information of Nox4 only comes from the computational analysis of Nox4 sequence and the comparison with Nox2.

To get more topology information, we developed a rapid and straightforward manner: TDUFA (Topological Determination by Ubiquitin Fusion Assay). In this method, ubGFP fusion proteins are used as tools to obtain details of membrane protein topology. It requires the construction of a fusion between ubiquitin-GFP (ubGFP) coding sequence and the gene of interest, which is then expressed in cells.

2 Materials and methods

2.1 Materials

DMEM, fetal bovine serum, neomycin (G418, geneticin) were purchased from GIBCO; ECL Western Blotting Detection reagents were purchased from Amersham Biosciences; complete mini EDTA-free protease inhibitor EASYpack, leupeptin, pepstatin, TLCK were purchased from Roche; GFP mAb was purchased from Santa Cruz; saponin was purchased from SIGMA; Goat anti-Mouse IgG-HRP was purchased from GE healthcare; HiPerFect Transfection Reagent was purchased from QIAGEN; MassRuler DNA Marker was purchased from Euromedex.

2.2 Cell culture

HEK293 cells stable tansfected with different plasmids (table 3) were cultured in DMEM containing 4.5g/L glucose and 0.11g/L sodium pyruvate, supplemented with 10% (v/v) fetal bovine serum and 100units/ml penicillin and 100μg/ml streptomycin and 2mM glutamine at 37°C in air with 5% CO_2. Selecting antibiotics, neomycin (500μg/ml) was used.

2.3 Stable transfection of mammalian expression plasmids

5×10^5 HEK293 cells were seeded in 6-well plates and allowed to grow for 24h to reach a 70% confluence in 2ml of culture medium. The cells were transfected with 3μg of vectors according to the manufacturing protocol (JetPEI, Polyplus transfection). After 24h, stable transfected cells were selected with 500μg/ml geneticin for 3 weeks before analysis.

2.4 Flow cytometry

Cells were suspended in PBS (10^7/ml) and incubated with or without 0.01% saponin for 3min on ice. After centrifugation, supernatant was collected and stored for further use. Meanwhile, cells were washed twice and resuspended in PBS. GFP fuorescence intensity (FL1) of the cells was measured on a FACScalibur

(Becton Dickinson) cytometer.

Fluorescently Tagged Proteins	**Abbreviation**
Nox2(1-131)GFP	Nox2N131GFP
Nox2(1-131)ubGFP	Nox2N131ubGFP
IL1R1GFP	IL1R1GFP
IL1R1ubGFP	IL1R1ubGFP
Nox4(1-578)GFP	Nox4FLGFP
Nox4(1-46)GFP	Nox4N46GFP
Nox4(1-98)GFP	Nox4N98GFP
Nox4(1-144)GFP	Nox4N144GFP
Nox4(1-341)GFP	Nox4N341GFP
Nox4(1-578)ubGFP	Nox4FLubGFP
Nox4(1-46)ubGFP	Nox4N46ubGFP
Nox4(1-98)ubGFP	Nox4N98ubGFP
Nox4(1-144)ubGFP	Nox4N144ubGFP
Nox4(1-341)ubGFP	Nox4N341ubGFP
p22(1-195)GFP	p22FLGFP
p22(1-36)GFP	p22N36GFP
p22(1-63)GFP	p22N63GFP
p22(1-110)GFP	p22N110GFP
p22(1-143)GFP	p22N143GFP
p22(1-195)ubGFP	p22FLubGFP
p22(1-36)ubGFP	p22N36ubGFP
p22(1-63)ubGFP	p22N63ubGFP
p22(1-110)ubGFP	p22N110ubGFP
p22(1-143)ubGFP	p22N143ubGFP

Table 3. Abbreviated nomenclature of the fluorescently tagged proteins used in this study

2.5 SDS/PAGE and Western Blotting

Cells (10^8 cells/ml) were suspended ml in PBS containing 2μM leupeptin, 2μM pepstatin, 10μM TLCK, complete mini EDTA-free protease inhibitor. The cells were fractionated after sonication 3×10s at 4°C and 40W using a Branson sonifier. The homogenate was centrifuged at 1,000 g for 15 min at 4°C to remove unbroken cells and nuclei. The post-nuclearsupernatant was centrifuged at 200,000 g for 1 h at 4°C. This high-speed centifugation supernatant was referred to as the cytosol, and the pellet consisting of crude membranes was suspended in the same buffer (The method of detection of Nox4N341GFP and Nox4GFP expression by western blot was the same as the method in article (Zhang *et al.*, 2010)).

The supernatant collected in flow cytometry, membrane or cytosol fractions were loaded on a 10% SDS-PAGE and electro-transferred to nitrocellulose, as previously described. Immunodetection was performed using primary monoclonal antibodies against GFP (dilution 1:1000). The immune complexes were detected with a secondary antibody combined with peroxidase. The bound peroxidase activity was detected using ECL reagents.

3 Results

3.1 Establishment of the TDUFA technique

In developing TDUFA to determine membrane protein topology, we attached the ubiquitin-GFP (ubGFP) protein to the C terminus of a protein of interest. Subsequently, cells expressing the fusion protein were exposed to saponin to permeabilize the plasma membrane. In eukaryotic cells, there are a variety of deubiquitinating enzymes (DUBs) which could hydrolyze ester bond at the C terminus of ub (Larsen *et al.*, 1998; Rytkönen *et al.*, 2007). As shown in Figure 17, if the C terminus of the protein faces the cytoplasm (Figure. 17A), ester bond between ubiquitin and GFP will be broken by DUBs, then its fluorescence signal should be lost. Conversely, if the C terminus of the protein faces the cell exterior or lumen of the compartment (Figure. 17B), its fluorescence should be persist. Given these potential outcomes, we could deduce the membrane orientation of transmembrane segments to determine membrane protein topology.

(A.)

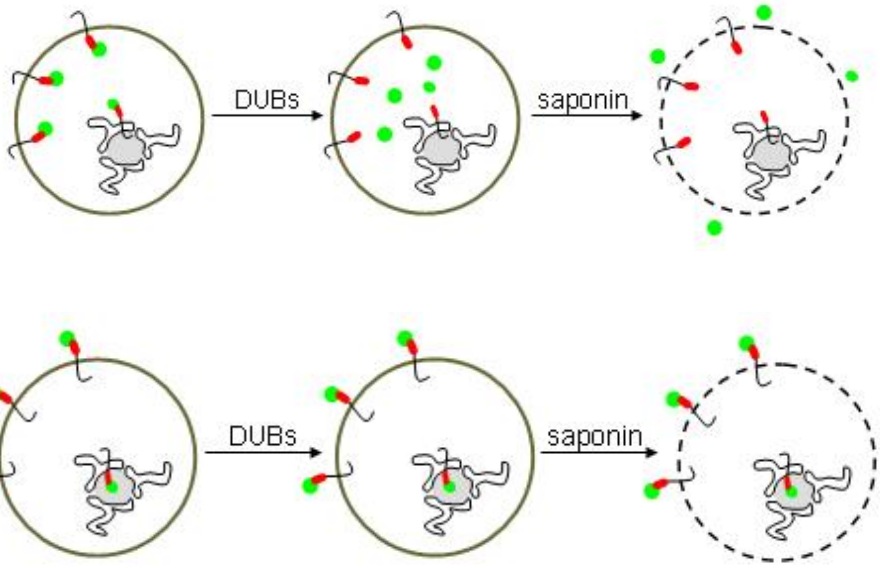

Figure 17. Cartoon of TDUFA (Topological Determination by Ubiquitin Fusion Assay) technique *DUBs: deubiquitinating enzymes "● " indicates ubiquitin; "● " indicates eGFP （This cartoon was designed by Chuong）*

Saponin is a mild and widely used detergent that extracts cholesterol from membranes. Since different cholesterol concentrations are found in various cellular membranes, saponin can be used at very low concentrations (below 0.02%) to selectively permeabilize only a few membrane compartments of mammalian cells (e.g. the plasma membrane but not the endoplasmic reticulum) (Wassler *et al.*, 1987). In a preliminary experiment a saponin concentration of 0.01% was determined.

3.2 TDUFA reveal the topology of the protein IL1R1 and Nox2N131

As proof-of-principle, we used TDUF assay to test whether it could reveal the membrane topology of IL1R1, a single transmembrane protein with its C terminus facing the cytoplasm and Nox2N131, a transmembrane proteins with its C terminus facing the cell exterior (Campion *et al.*, 2007). We constructed two versions of tagged IL1R and Nox2N131 respectively and transfected them in cells: one with ub-GFP attached to the C terminus of IL1R and Nox2N131, and the other with GFP attached to the C terminus of IL1R and Nox2N131 which is used as a negative control.

To determine whether TDUF assay could provide results consistent with the known membrane topology of the constructs, Cells expressing IL1R1ubGFP or Nox2N131ubGFP were incubating with or without 0.01% saponin for 3min on ice. After centrifugation, supernatant was collected and GFP expression in the

supernatant was analyzed by western blot using GFP mAb. Meanwhile, GFP fluorescence intensity (FL1) of the cells was measured on a FACScalibur (Becton Dickinson) cytometer. As in Figure 18A and B, fluorescence from IL1R1ubGFP quickly decreased, suggesting that ubGFP moiety on IL1R1 faces the cytoplasm. By contrast, fluorescence associated with Nox2N131ubGFP did not change during the treatment, suggesting its ubGFP moiety faces the cell exterior or lumen. Meanwhile, as the negative control, fluorescence of IL1R1GFP or Nox2N131GFP did not change too. These results are consistent with the analysis of GFP expression in the supernatant. As shown in Figure 18C, GFP expression is detected only in the supernatant from IL1R1ubGFP.

Then, we corroborated these results by separating the cytosol and crude membrane fraction, and measured the GFP expression in the two fractions by western blot. As in figure 18D, GFP alone was detected in the cytosol fraction of IL1R1ubGFP. Due to the low transfection efficiency and probably technique problems, we did not detect the expression of IL1R1GFP, Nox2N131GFP and Nox2N131ubGFP in crude membrane fraction. These results need further experiments.

Based on these results, we could say that TDUF assay functioned properly in revealing the membrane topology.

(A).

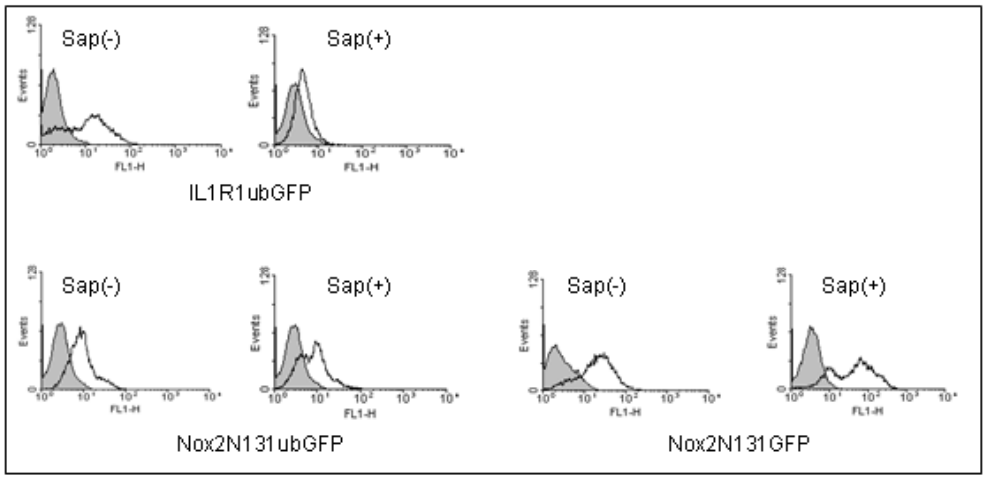

(B).

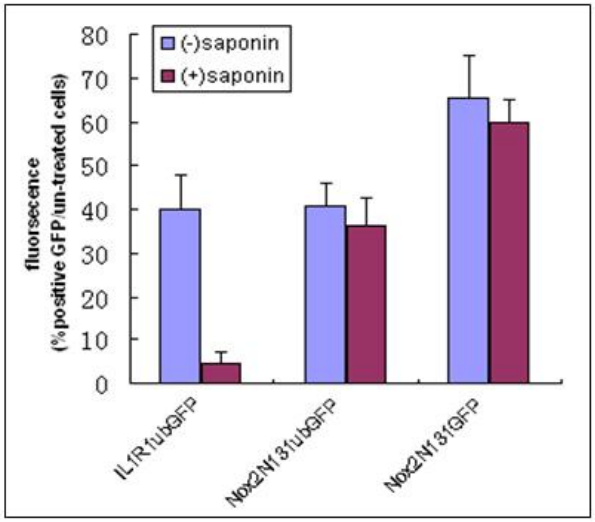

(C).

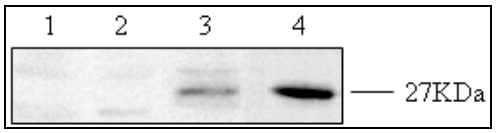

(D).

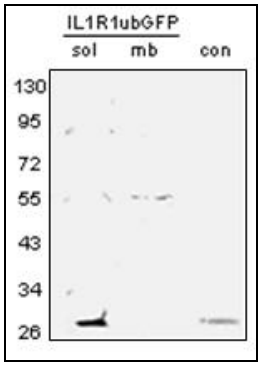

Figure 18. TDUFA reveal the topology of the protein IL1R1 and Nox2N131. *A, Flow cytometry analysis of GFP fluorescence of cells treated with or without saponin (white area). For each kind of stable transfected cells, left panel was cells untreated with saponin and right panel was cells treated with saponin, gray area indicates wide type HEK293 cells; B, GFP fluorescence of cells treated with or without saponin by FACS were shown in column diagram; C, western blot of GFP expression in the supernatant of cells treated with saponin; 1: HEK293-Nox2N131ubGFP cells, 2: HEK293-Nox2N131GFP cells, 3: HEK293-IL1R1ubGFP cells, 4: control eGFP; D, western blot of GFP expression in the cytosolic (sol) and membrane (mb) fraction of HEK293-IL1R1ubGFP cells. HEK293 cells stable transfected with eGFP was used as a positive control.*

3.3 Membrane topology of Nox4 by the TDUFA approach

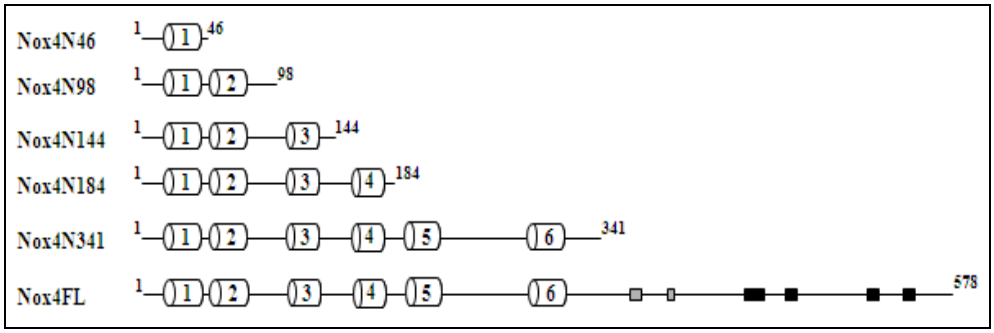

Figure 19. Schematic of the truncated protein Nox4

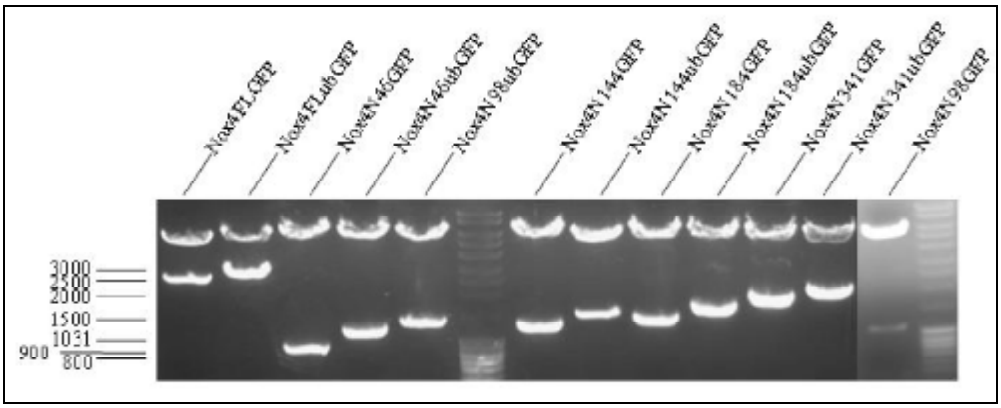

Figure 20. Restriction enzyme digestion analysis of full length and C-terminal-deleted derivatives Nox4 recombinant plasmids (double digested by KpnI/ApaI)

Next, we used TDUF assay to reveal the topology of Nox4. We attached the ubiquitin-GFP (ubGFP) protein or GFP protein to the C terminus of full length and C-terminal-deleted derivatives Nox4 recombinant proteins (Figure. 19). The results of digestion analysis with restriction enzymes are shown in Figure 20. GFP fluorescence of HEK293 cells expressing different Nox4 fusion protein were measured before and after permeabilizing cells with saponin. As seen in Figure 21A and B, fluorescence from Nox4FLubGFP, Nox4N341ubGFP and Nox4N98ubGFP quickly decreased, suggesting that ubGFP moiety on Nox4FL, Nox4N341 and Nox4N98 faces the cytoplasm. Meanwhile, as the negative control, fluorescence of Nox4FLGFP and Nox4N341GFP did not change. By contrast, fluorescence associated with Nox4N46ubGFP and Nox4N144ubGFP did not change during the treatment, suggesting its ubGFP moiety faces the cell exterior or lumen. These results are consistent with the analysis of GFP expression in the supernatant. As shown in Figure 21C, GFP expression is detected only in the supernatant from Nox4FLubGFP, Nox4N341ubGFP and Nox4N98ubGFP.

(A).

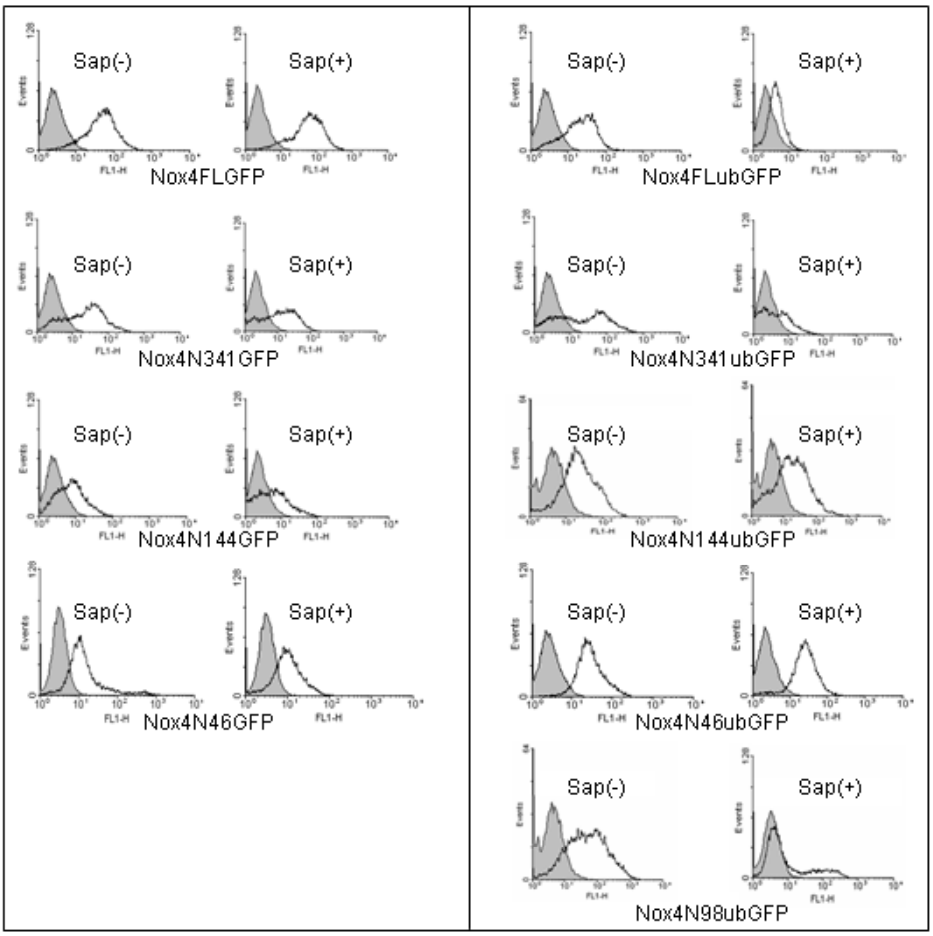
Sap(-)
Sap(+)
Nox4FLGFP
Nox4FLubGFP
Nox4N341GFP
Nox4N341ubGFP
Nox4N144GFP
Nox4N144ubGFP
Nox4N46GFP
Nox4N46ubGFP
Nox4N98ubGFP

(B).

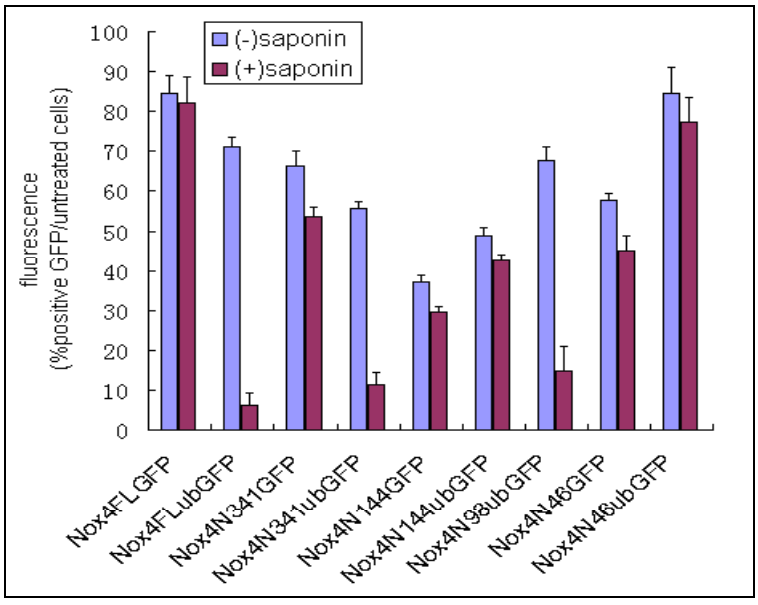
(-)saponin
(+)saponin
fluorescence
(%positive GFP/untreated cells)
100
90
80
70
60
50
40
30
20
10
0
Nox4FLGFP
Nox4FLubGFP
Nox4N341GFP
Nox4N341ubGFP
Nox4N144GFP
Nox4N144ubGFP
Nox4N98ubGFP
Nox4N46GFP
Nox4N46ubGFP

(C).

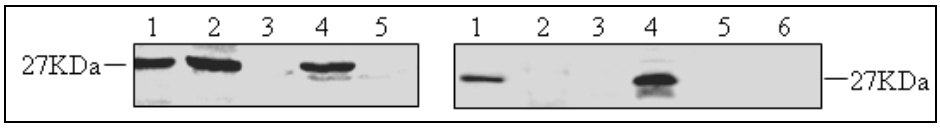

(D).

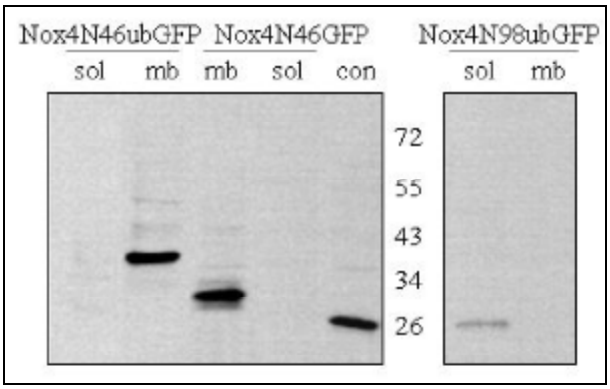

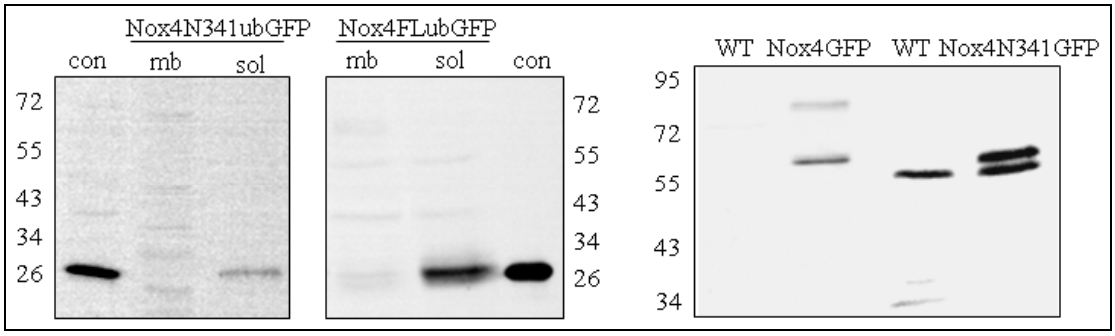

Figure 21. TDUFA reveal the topology of Nox4. *A, Flow cytometry analysis of GFP fluorescence of cells treated with or without saponin (white area). For each kind of stable transfected cells, left panel was cells untreated with saponin and right panel was cells treated with saponin, gray area indicates wide type HEK293 cells; B, GFP fluorescence of cells treated with or without saponin by FACS were shown in column diagram; C, western blot of GFP expression in the supernatant of cells treated with saponin; left panel: 1: control eGFP, 2: HEK293-Nox4FLubGFP cells, 3: HEK293-Nox4FLGFP cells, 4: HEK293-Nox4N341ubGFP cells, 5: HEK293-Nox4N341GFP cells; right panel: 1: control eGFP, 2: HEK293-Nox4N144ubGFP cells, 3: HEK293-Nox4N144GFP cells, 4: HEK293-Nox4N98ub cells，5: HEK293-Nox4N46ubGFP cells, 6: HEK293-Nox4N46GFP cells; D, western blot of GFP expression in the cytosolic (sol) and membrane (mb) fraction of HEK293 cells stable transfected with full length and different C-terminal-deleted derivatives of Nox4. WT: HEK293 wide type cell; HEK293 cells stable transfected with eGFP was used as a positive control.*

These results were also confirmed by using cytosol and crude membrane fractions, and measuring the GFP expression by western blot. As in figure 21D, GFP alone was detected in the cytosol fraction of

Nox4FLubGFP, Nox4N341ubGFP and Nox4N98ubGFP. As the negative control, the expression of Nox4FLGFP and Nox4N341GF protein was detected as their predicted size by GFP mAb. While the expression of Nox4N46ubGFP protein was detected as its predicted size in the crude membrane fraction. Due to the low transfection efficiency and probably technique problems, we did not detect the expression of Nox4N144ubGFP and Nox4N144GFP, in the cytosol fraction or crude membrane fraction. Thus, this part needs to be continued.

3.4 Membrane topology of p22phox by the TDUFA approach

Then, TDUF assay was used to reveal the topology of p22phox. As shown in Figure 22, ubiquitin-GFP (ubGFP) protein or GFP protein was attached to the C terminus of full length and C-terminal-deleted derivatives of p22phox recombinant proteins. The digestion analysis of these constructs with restriction enzyme was shown in Figure 23. GFP fluorescence of HEK293 cells expressing different p22phox fusion protein were measured before and after permeabilization with saponin. As seen in Figure 24A and B, decreased fluorescence from p22FLubGFP, p22N143ubGFP, p22N63ubGFP, and p22N36ubGFP suggested that ubGFP moiety on p22FL, p22N143, p22N63 and p22N36 faces the cytoplasm. As the negative control, fluorescence of p22FLGFP, p22N143GFP, p22N63GFP, and p22N36GFP did not show difference. These results are consistent with the analysis of GFP expression in the supernatant from these different constructs shown in Figure 24C.

Then, these results were confirmed by measuring the GFP expression in cytosol and crude membrane fractions of HEK293 cells transfected with different p22phox constructs by western blot. As in figure 24D, GFP alone was detected in the cytosol fraction of p22FLubGFP, p22N143ubGFP. As the negative control, the expression of p22FLGFP and p22N143GFP protein was detected as their predicted size by GFP mAb. Due to the low transfection efficiency and time, we did not get results for p22N36 and p22N63.

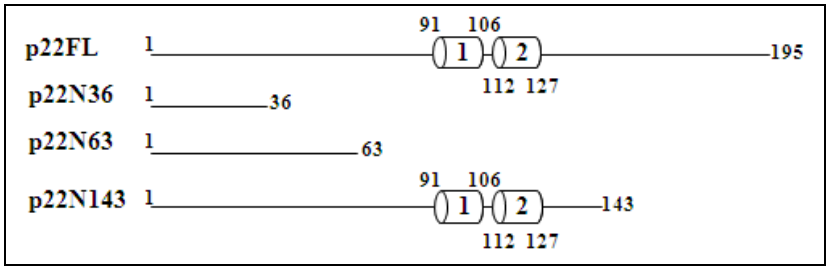

Figure 22. Schematic of the truncated protein p22phox

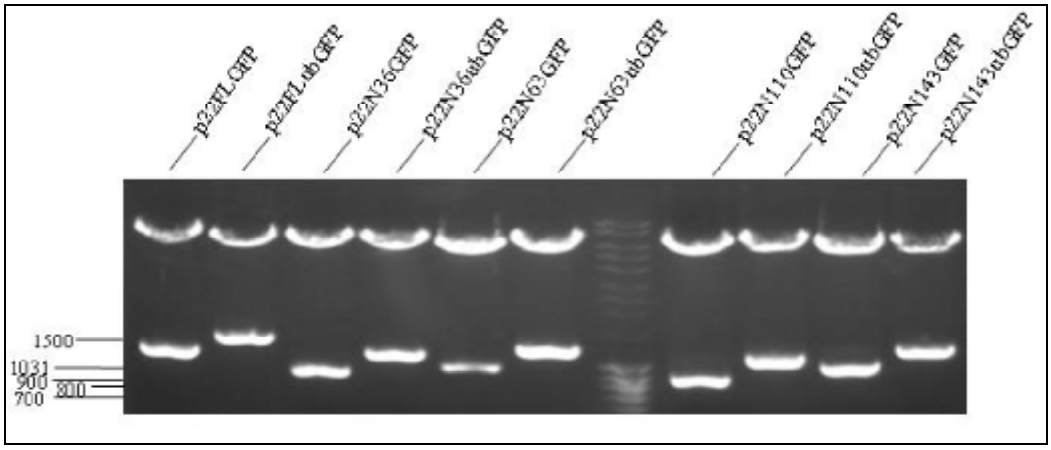

Figure 23. Restriction enzyme digestion analysis of full length and C-terminal-deleted derivatives p22phox recombinant plasmids (double digested by KpnI/ApaI)

(A).

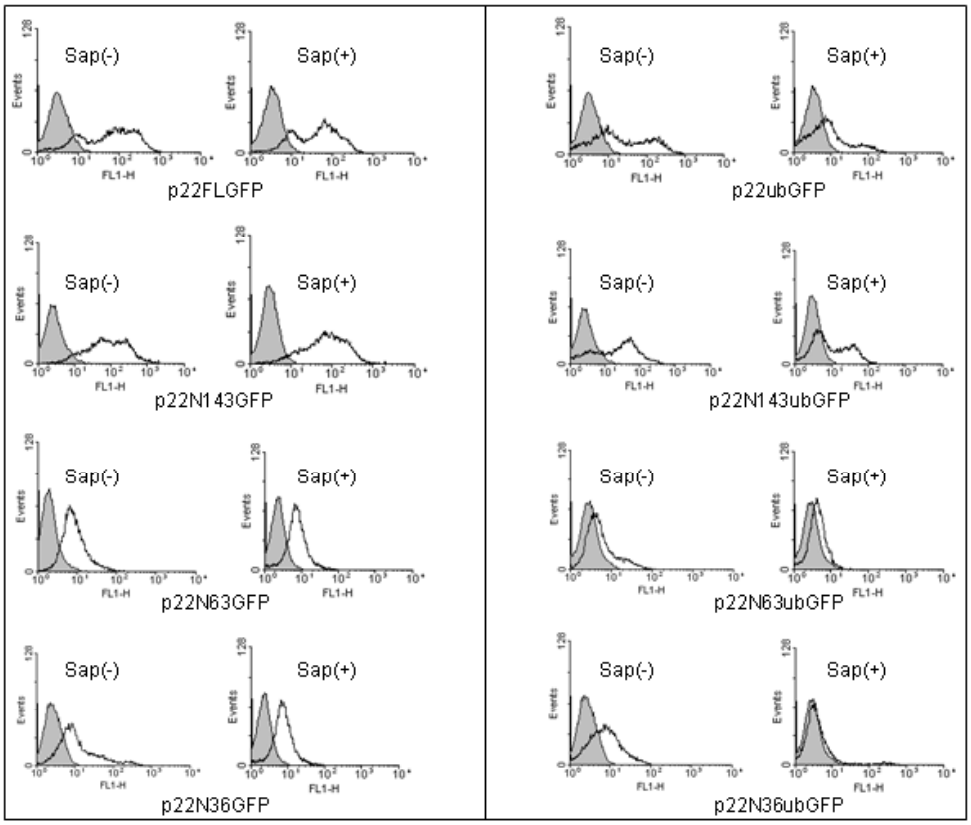

(B).

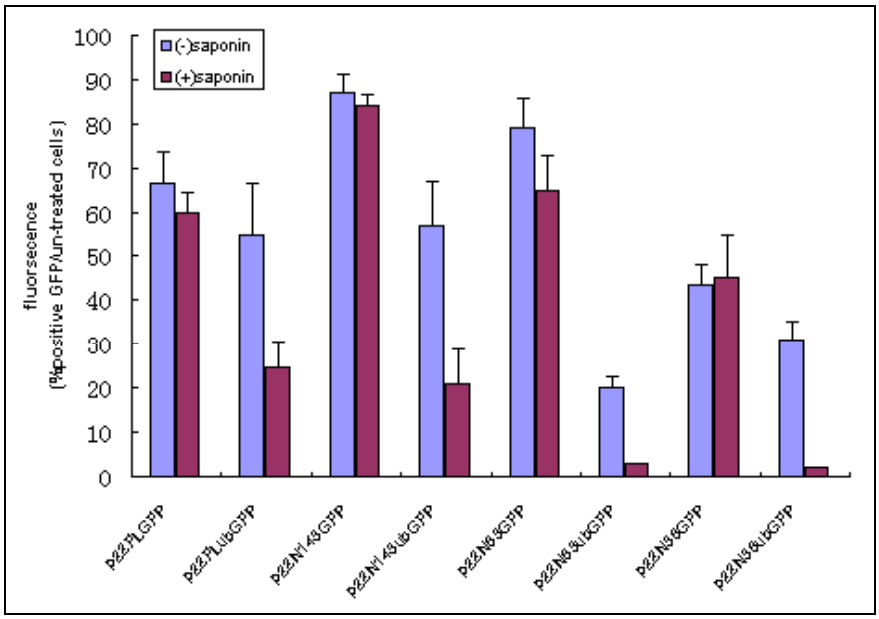

(C).

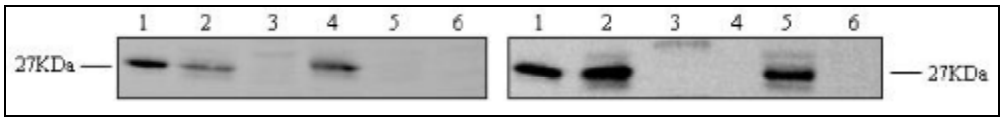

(D).

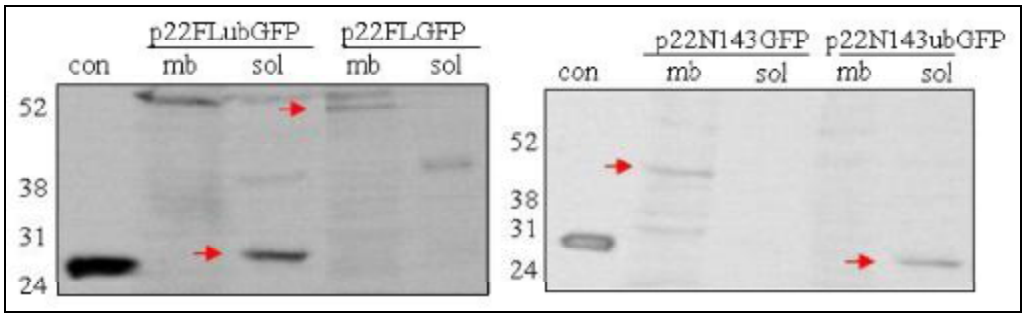

Figure 24. TDUFA reveal the topology of p22phox. *A, Flow cytometry analysis of GFP fluorescence of cells treated with or without saponin (white area). For each kind of stable transfected cells, left panel was cells untreated with saponin and right panel was cells treated with saponin, gray area indicates wide type HEK293 cells; B, GFP fluorescence of cells treated with or without saponin by FACS were shown in column diagram; C, western blot of GFP expression in the supernatant of cells treated with saponin; left panel: 1: control eGFP, 2: HEK293-p22FLubGFP cells, 3: HEK293-p22FLGFP cells, 4: HEK293-p22N143ubGFP cells, 5: HEK293-p22N143GFP cells, 6: HEK293 cells; right panel: 1: control eGFP, 2: HEK293-p22N36ubGFP cells, 3: HEK293-p22N36GFP cells, 4: HEK293 cells, 5: HEK293-p22N63ubGFP cells, 6: HEK293-p22N63GFP cells; D, western blot of GFP expression in the cytosolic (sol) and membrane (mb) fraction of HEK293 cells stable transfected with full length and different C-terminal-deleted derivatives of p22phox. HEK293 cells stable transfected with eGFP was used as a positive control.*

4 Discussion

Membrane protein has a unique structural characterization involved in many basic and important cell biological functions, such as solute transport and signalling across the membrane. To understand the cellular function of a protein, it is therefore crucial to know its membrane topology. At present, some theoretical and experimental methods have been used to study the topology of membrane proteins, such as using the relative hydrophobicity of amino acid side chain of a protein in order to establish a topology model of a membrane protein. But different algorithms have led to different results, therefore requiring certain of experimental methods to test and verify them, such as limited proteolysis (Wilkinson *et al.*, 1996), glycosylation mapping (Chang *et al.*, 1994) and cysteine substitution (Giraudat *et al.*, 1985; Bogdanov *et al.*, 2005) have been used. These approaches often require substantial investments of time and effort.

The topology information of Nox4 only comes from the computational analysis of Nox4 sequence and the comparison with Nox2. Until now, no studies have been reported to investigate the topology of Nox4 directly.

Sequence analysis by computational methods suggests that p22phox contains two to four hydrophobic regions that may comprise TM α helices. Although its topology structure cannot reach a consensus in the absence of crystallization data, the weight of evidence favors a two transmembrane structure with both the NH_2 terminus and the COOH terminus facing the cytoplasm (Imajoh-Ohmi *et al.*, 1992; Burritt *et al.*, 1998; Taylor *et al.*, 2004). Based on peptide walking, Dahan et al. proposed a four transmembrane topology model. In this model, one transmembrane domain is proposed to extend from residue 10 to 50 which is interrupted by an extracellular domain from residue 30 to 36. Another transmembrane domain is proposed to extend from residue 92 to 110 and is interrupted by an extracellular domain, the limits of which remain unknown. The cytosolic tail is proposed to start at residue 111(Dahan *et al.*, 2002). However, characterization of monoclonal antibodies to the p22phox proposed a two transmembrane topology model which also assigned membrane-spanning segments to the predominantly hydrophobic region of p22phox, comprised of residues 91–126 (Taylor *et al.*, 2004).

TDUFA method described here provides a new approach for determining protein topology in cells. It does not require large quantities of target proteins. Besides, the use of GFP chimeras in the TDUFA does not need appropriate and available antibodies that are required in protein topology assays relying upon site-specific immunoreactivity (Canfield *et al.*, 1993). In rare cases, the addition of GFP or ubGFP could interfere proper functioning and localization of the fusion protein, which needs to be considered and

addressed.

Preliminary results obtained by TDUFA method suggested that p22phox has 2 transmembrane domains, C terminal of p22FL, p22N143, p22N63, and p22N36 faces the cytoplasm. Nox4 has 6 transmembrane domains, the C-terminus of Nox4FL, Nox4N341 and Nox4N98 face the cytoplasm while the C-terminus of Nox4N46, Nox4N144 faces the cell exterior or lumen. These preliminary results need further experiments.

Through the mutation analysis of Nox4 and p22phox, two Nox4 mutants, Nox4-GT (304-305) insert and Nox4-del 4aa (575-578), partially functional in ROS production did not up-regulate p22phox levels (Martyn *et al.*, 2006). This provided evidence that these two mutations were in regions of Nox4 that either directly, or indirectly, impacted endogenous p22phox; and the N-terminal amino acids 6-11 of p22phox is essential, whereas the C terminus (amino acids 130-195) is dispensable for Nox4 activity (von Lohneysen *et al.*, 2008).

Information about the topology of Nox4 and p22phox will be helpful to characterize the interaction domain of p22phox and Nox4 involved in the NADPH oxidase activity and their localization. In the following study, we could use these different p22phox and Nox4 truncated proteins to study the interaction between Nox4 and p22phox.

5 References

Ambasta, R. K., P. Kumar, K. K. Griendling, H. H. Schmidt, R. Busse and R. P. Brandes (2004). Direct interaction of the novel Nox proteins with p22phox is required for the formation of a functionally active NADPH oxidase. *J Biol Chem* **279**(44): 45935-45941.

Bogdanov, M., W. Zhang, J. Xie and W. Dowhan (2005). Transmembrane protein topology mapping by the substituted cysteine accessibility method (SCAM(TM)): application to lipid-specific membrane protein topogenesis. *Methods* **36**(2): 148-171.

Burritt, J. B., S. C. Busse, D. Gizachew, D. W. Siemsen, M. T. Quinn, C. W. Bond, E. A. Dratz and A. J. Jesaitis (1998). Antibody imprint of a membrane protein surface. Phagocyte flavocytochrome b. *J Biol Chem* **273**(38): 24847-24852.

Campion, Y., M. H. Paclet, A. J. Jesaitis, B. Marques, A. Grichine, S. Berthier, J. L. Lenormand, B. Lardy, M. J. Stasia and F. Morel (2007). New insights into the membrane topology of the phagocyte NADPH oxidase: characterization of an anti-gp91-phox conformational monoclonal antibody. *Biochimie* **89**(9): 1145-1158.

Canfield, V. A. and R. Levenson (1993). Transmembrane organization of the Na,K-ATPase determined by epitope addition. *Biochemistry* **32**(50): 13782-13786.

Chang, X. B., Y. X. Hou, T. J. Jensen and J. R. Riordan (1994). Mapping of cystic fibrosis transmembrane conductance regulator membrane topology by glycosylation site insertion. *J Biol Chem* **269**(28): 18572-18575.

Dahan, I., I. Issaeva, Y. Gorzalczany, N. Sigal, M. Hirshberg and E. Pick (2002). Mapping of functional domains in the p22(phox) subunit of flavocytochrome b(559) participating in the assembly of the NADPH oxidase complex by "peptide walking". *J Biol Chem* **277**(10): 8421-8432.

Giraudat, J., C. Montecucco, R. Bisson and J. P. Changeux (1985). Transmembrane topology of acetylcholine receptor subunits probed with photoreactive phospholipids. *Biochemistry* **24**(13): 3121-3127.

Groemping, Y. and K. Rittinger (2005). Activation and assembly of the NADPH oxidase: a structural perspective. *Biochem J* **386**(Pt 3): 401-416.

Imajoh-Ohmi, S., K. Tokita, H. Ochiai, M. Nakamura and S. Kanegasaki (1992). Topology of cytochrome b558 in neutrophil membrane analyzed by anti-peptide antibodies and proteolysis. *J Biol Chem* **267**(1): 180-184.

Klabunde, T. and G. Hessler (2002). Drug design strategies for targeting G-protein-coupled receptors. *Chembiochem* **3**(10): 928-944

Leto, T. L., A. G. Adams and I. de Mendez (1994). Assembly of the phagocyte NADPH oxidase: binding of Src homology 3 domains to proline-rich targets. *Proc Natl Acad Sci U S A* **91**(22): 10650-10654.

Martyn, K. D., L. M. Frederick, K. von Loehneysen, M. C. Dinauer and U. G. Knaus (2006). Functional analysis of Nox4 reveals unique characteristics compared to other NADPH oxidases. *Cell Signal* **18**(1): 69-82.

Nauseef, W. M. (2008). Biological roles for the Nox family NADPH oxidases. *J Biol Chem* **283**(25): 16961-16965.

Taylor, R. M., J. B. Burritt, D. Baniulis, T. R. Foubert, C. I. Lord, M. C. Dinauer, C. A. Parkos and A. J. Jesaitis (2004). Site-specific inhibitors of NADPH oxidase activity and structural probes of flavocytochrome b: characterization of six monoclonal antibodies to the p22phox subunit. *J Immunol* **173**(12): 7349-7357.

Ueno, N., R. Takeya, K. Miyano, H. Kikuchi and H. Sumimoto (2005). The NADPH oxidase Nox3 constitutively produces superoxide in a p22phox-dependent manner: its regulation by oxidase organizers and activators. *J Biol Chem* **280**(24): 23328-23339.

Vignais, P. V. (2002). The superoxide-generating NADPH oxidase: structural aspects and activation mechanism. *Cell Mol Life Sci* **59**(9): 1428-1459.

von Lohneysen, K., D. Noack, A. J. Jesaitis, M. C. Dinauer and U. G. Knaus (2008). Mutational analysis reveals distinct features of the Nox4-p22 phox complex. *J Biol Chem* **283**(50): 35273-35282.

Wassler, M., I. Jonasson, R. Persson and E. Fries (1987). Differential permeabilization of membranes by saponin treatment of isolated rat hepatocytes. Release of secretory proteins. *Biochem J* **247**(2): 407-415.

Wilkinson, B. M., A. J. Critchley and C. J. Stirling (1996). Determination of the transmembrane topology of yeast Sec61p, an essential component of the endoplasmic reticulum translocation complex. *J Biol Chem* **271**(41): 25590-25597.

Part 3: Discussion and perspectives

En Français

La NADPH oxydase, Nox4, appartient à la famille des Nox qui sont directement impliquées dans la production des espèces réactives de l'oxygène en transférant un électron à l'oxygène moléculaire. Tous les membres de la famille des Nox partagent une infrastructure commune: en N-terminale, 6 domaines transmembranaires et en C-terminale, les sites de liaison du FAD et du NADPH. Deux hèmes non-identiques sont coordonnés sur la 3ème et la 5ème hélice alpha par 2 paires de résidus His. Nox2 est le propotype de la famille des Nox et une source bien étudiée pour la production de ROS. Malgré sa distribution large dans les tissus, Nox4 est encore mal comprise. Contrairement aux autres Nox, Nox4 montre un caractère unique: son activité est constitutive; elle est mesurée en l'absence d'une quelconque stimulation des cellules et n'exige pas la présence des facteurs cytosoliques nécessaires à Nox2. La plupart des études rapportent que Nox4 génère H_2O_2. Par ailleurs, la production de ROS générés par Nox4 est associée à différentes pathologies inflammatoires et dans le vieillissement. L'étude de la structure de Nox4 en lien avec sa fonction devrait permettre de comprendre son fonctionnement et d'identifier de nouvelles cibles thérapeutiques pour la prévention et le traitement des maladies en rapport avec les ROS.

Les anticorps monoclonaux spécifiques de Nox4

La compréhension du rôle de Nox4 dans la production des espèces réactives de l'oxygène et du mécanisme de régulation de l'activité oxydase a été entravée par l'absence d'anticorps monoclonaux spécifiques qui sont également des outils essentiels pour apporter des preuves directes à des modèles de topologie et identifier les caractéristiques structurelles de l'hétérodimère avec p22phox. Dans cette étude (Zhang *et al.*, 2010), pour la première fois, cinq anticorps monoclonaux spécifiques de Nox4 ont été générés et caractérisés. Parmi ces anticorps monoclonaux, 3 d'entre eux, 8E9, 6B11 et 5F9, reconnaissent la protéine Nox4 native dans le cortex rénal humain et après surexpression dans les lignée cellulaire HEK293 et C20/A4, chondrocytes humains. La taille théorique de Nox4 est 66.9kDa (Shiose *et al.*, 2001). On a pu montrer que ces anticorps marquent deux types de proteine/peptide correspondant à un poids moleculaire de 75-80kDa et de 55-65kDa dans les cellules exprimant Nox4 endogène et/ou surexprimant Nox4 (Hilenski *et al.*, 2004; Kawahara *et al.*, 2005; Martyn *et al.*, 2006). Ces différences de poids moléculaire et la présence dans la molécule de Nox4 de quatre sites de N-glycosylation, pourraient suggérer que Nox4 est glycosylée, bien que

le traitement avec la N-glycosidase F soit sans effets (Shiose *et al.*, 2001). Quant à nous, Nox4 a été détectée en utilisant deux lignées cellulaires à la taille de 58kDa, avec une bande à 31kDa qui représente très probablement un fragment clivé. Ces contradictions entre les masses moléculaires calculées et apparentes ont été observées pour d'autres membres de la famille de Nox: Nox5 est révélé à 70kDa, plutôt que 82kDa, taille prédite; la forme déglycosylée de Nox2, 55kDa, est active. Le précurseur de Nox2 est à 65kDa; Nox1 fonctionne à 55-60kDa plutôt que 65kDa prédit (Serrander *et al.*, 2007). On peut imaginer que ces différences puissent provenir de la structure de ces protéines qui présente un pI 9.0 pour Nox1; pI 8,9 pour Nox2; pI 9.0 pour Nox5 et pI 8.96 pour Nox4 (Lametsch *et al.*, 2000). Dans le cortex rénal, la taille de Nox4 proposée est de 68kDa (Gorin *et al.*, 2005; Hecker *et al.*, 2009). Cette différence de taille de Nox4 suggère aussi un état de glycosylation ou de dégradation dans les tissus qui peut ne pas être le même. Le processus de dégradation de Nox4 peut dépendre des modalités de stockage et de congélation/décongélation lors de l'homogénéisation des cellules et de l'extraction des protéines. Dans notre étude, nous avons mis l'accent sur la grande sensibilité de Nox4 à la température et sur la nécessité d'ajouter des anti-protéases, mais aussi du vanadate et de l'acide okadaic qui inhibe les phosphatases; par ailleurs, le protocole de solubilisation en SDS doit être effectué à 4°C.

Localisation subcellulaire de Nox4

Les ROS sont produits dans une grande variété de contextes biologiques, tant physiologique que pathologique et dans presque tous les tissus et les organes des organismes multicellulaires (Bedard *et al.*, 2007). Bien que les protéines Nox représentent les principales sources non-mitochondriales de ROS, l'identification de la protéine Nox4 dans un tissu particulier est difficile compte tenu d'un manque d'outils sûrs pour l'analyse. Par exemple, alors que plusieurs anticorps polyclonaux et monoclonaux sont bien caractérisés contre Nox2 et largement utilisés, il n'existe pas actuellement de sondes immunochimiques spécifiques de Nox3 et Nox4. Les études de localisation tissulaire reposent sur la détection des ARNm et non sur la protéine, ou indirectement sur l'identification de p22phox, comme un marqueur de Nox1–4 (Nauseef, 2008).

Nox4 a été détecté dans plusieurs compartiments subcellulaires: dans les cellules transfectées, réticulum endoplasmique (Martyn *et al.*, 2006; Chen *et al.*, 2008) ou membrane plasmique (Lee *et al.*, 2006; von Lohneysen *et al.*, 2008). Dans les cellules endothéliales et les cellules musculaires lisses, la localisation de Nox4 est nucléaire; dans les cellules musculaires lisses vasculaires, une localisation près de foyers d'adhésion

focale a été proposée. De plus, dans les cellules somatiques, Nox4 a été détectée dans les mitochondries (Block *et al.*, 2009). Ces résultats contradictoires peuvent être la conséquence de partenaires de Nox4 non encore identifiés à l'image de ce qui est rapporté avec Poldip2 dans les cellules musculaires lisses. Ces difficultés peuvent être aussi liées à la surexpression de Nox4 membranaire mais aussi à l'absence de spécificité des anticorps utilisés, dirigés contre Nox4. Enfin cette localisation subcellulaire peut dépendre de l'état fonctionnel ou pathologique des cellules (Weyemi *et al.*, 2010). Dans les cellules musculaires lisses vasculaires, Nox4 situé au niveau des fibres d'adhésion focale change de localisation pendant la differentiation (Clempus *et al.*, 2007). Dans cette étude, les résultats d'immunochimie obtenus avec les nouveaux anticorps monoclonaux, ont montré que Nox4 est détectable non seulement dans le réticulum endoplasmique mais aussi dans la membrane plasmique.

Caractéristique des ROS dépendant de Nox4

En raison de la similitude avec Nox2 et compte tenu du transfert d'un seul électron au niveau de l'hème, toutes les oxydases Nox devraient produire essentiellement O_2^- (Bedard et al., 2007). En fait, si Nox1, Nox2, Nox3 et Nox5 synthétisent O_2^-, la plupart des études ont montré que H_2O_2 est la principale source de ROS dépendant de Nox4; H_2O_2 est détecté à l'extérieur des cellules (Chen *et al.*, 2008; Hecker *et al.*, 2009) mais dans les hépatocytes, on met en évidence O_2^- (Boudreau *et al.*, 2009). Dans certaines cellules, bien que Nox4 soit localisé à la membrane plasmique, de façon inattendue, c'est H_2O_2 qui est détecté (von Lohneysen *et al.*, 2010). Il a été suggéré que la formation de H_2O_2 par Nox4 puisse être la conséquence de sa localisation subcellulaire ou encore puisse s'expliquer par un système de détection défectueux. L'analyse de mutations (Helmcke *et al.*, 2009), les sondes intracellulaires pour la détection des ROS (Serrander *et al.*, 2007) et les études de surexpression dans les cellules ont démontré que le type de ROS produit par Nox4 ne dépend pas de sa localisation subcellulaire.

Les Duox produisent aussi H_2O_2 (Geiszt *et al.*, 2003; Forteza *et al.*, 2005) mais le type de ROS généré ne semble pas dépendre de l'état de maturation (Ameziane-El-Hassani *et al.*, 2005). On a observé, une relocalisation du complexe Duox/Duoxa à partir du réticulum endoplasmique au niveau de la membrane plasmique (Morand *et al.*, 2009), mais on ne sait pas quel est l'impact sur les ROS produits. Ces mécanismes pourraient expliquer la formation de H_2O_2 par Nox4. La colocalisation de Nox4 avec la superoxyde dismutase SOD1 a été suggérée; elle pourrait accélèrer la dismutation de O_2^- en H_2O_2 (von Lohneysen *et al.*, 2008).

La boucle E de Nox4 présente une caractéristique essentielle en terme de structure pour la formation de H_2O_2 (Takac *et al.* 2011). Les modifications de certains résidus amino-acides conduisent l'enzyme à produire O_2^-. Comparativement à d'autres Nox, la boucle E de Nox4 est beaucoup plus longue. Elle pourrait présenter une structure capable de ralentir la sortie de O_2^- et/ou de H_2O_2 à partir de son site de formation au niveau de l'hème, en permettant d'accumuler et d'accélérer la dismutation spontanée compte tenu de l'augmentation de la concentration locale de superoxyde. En outre, les cystéines Cys226 et Cys270 pourraient former un pont disulfure permettant de stabiliser une telle structure. Cette hypothèse a été appuyée par les expériences réalisées avec l'anticorps monoclonal 8E9. L'autre mécanisme qui propose une dismutation de O_2^- en H_2O_2 reste à démontrer mais dans les deux processus, histidines et cysteines pourraient jouer un rôle important. Contrairement à Nox1 ou Nox2, la boucle E de Nox4 contient une histidine H222 hautement conservé. D'une façon intéressante, la mutation de His222 ou Cys226 de Nox4 dans la séquence THPPGC conduit à la formation de O_2^-. La présence de deux prolines dans cette séquence pourrait en modifier la structure secondaire, la Cys226 se retrouvant à proximité de His222. His222 dans la boucle E pourrait servir de donneur de proton pour l'anion O_2^- et accélérer sa dismutation spontanée en H_2O_2.

Nox4 et l'activité diaphorase

Dans l'article (Takac *et al.* 2011), la formation de H_2O_2 est montrée comme étant une propriété intrinsèque de Nox4. Structurellement, les enzymes produisant H_2O_2 sont différents de ceux qui synthétisent O_2^- et la xanthine oxidase est l'un des rares exemples capable de générer les deux types de ROS (Nishino *et al.*, 2008). Un mutant de la xanthine oxydase qui conduit à l'augmentation de la synthèse de O_2^- et à la diminition de celle de H_2O_2 a montré que la formation de H_2O_2 se produit en effet habituellement sur les sites FAD et n'exige pas la présence d'un hème dans les protéines Nox (Asai *et al.*, 2007). Les hémoprotéines en revanche produisent O_2^-. Ainsi, H_2O_2 pourrait être formé par Nox4 au niveau du site FAD. Mais l'expression isolée du site catalytique de Nox4 conduit à la formation d'un domaine de type « flavodéshydrogénase » qui reste capable de réduire le cytochrome c ainsi que plusieurs accepteurs d'électron (Nisimoto *et al.*, 2010) et ne forme pas H_2O_2 directement.

Le mécanisme de transfert d'électrons est bien documenté pour la protéine Nox2. L'activité diaphorase correspond au transfert d'électrons jusqu'au FAD, centre redox qui se trouve dans le domaine cytosolique de Nox2 du côté C terminale. Peu d'études existent sur l'activité diaphorase de Nox4. La pré-incubation des lysats

totaux des cellules avec les anticorps monoclonaux, 6B11 ou 5F9, conduit à une inhibition modérée mais significative de l'activité de Nox4, ce qui indique qu'ils interagissent avec une région importante pour le transfert d'électrons. Ce résultat suggère que la queue cytosolique de Nox4 pourrait être responsable de son activité constitutive ce qui a été également proposé par (Nisimoto *et al.*, 2010). L'étude fonctionnelle de Nox4 exige la production de protéine soluble ce qui n'a été réalisé pour aucune des Nox à l'exception de Nox2 (Marques *et al.*, 2007). Pour bien comprendre la propriété de transfert électronique de Nox4, les protéines Nox4 tronquées solubles et actives ont été produites par deux approches optimisées (in vitro RTS et l'induction bactérienne) ce qui a permis d'étudier l'activité diaphorase. Contrairement à Nox2, dans ce travail (Nguyen *et al.* 2011), l'activité diaphorase de Nox4Aqc (AA: 309-578) est constitutive et l'addition de facteurs cytosoliques n'améliore pas cette activité (Han *et al.*, 2001; Nisimoto *et al.*, 2004; Marques *et al.*, 2007). Ce résultat est en accord avec l'observation de (Nisimoto *et al.*, 2010), selon lequel le domaine deshydrogénase de Nox4 est actif constitutivement.

Les informations sur la topologie de Nox4 et p22phox

Les ROS régulent le comportement des cellules en tant que outils de signalisation; une expression et une activation anormales de Nox4 sont associées au développement tumoral et pourraient être impliquées dans de nombreuses autres pathologies inflammatoires ou du vieillissement.

Les membranes cellulaires sont de véritables barrières permettant de séparer différents environnements cellulaires et compartiments sub-cellulaires. Les protéines membranaires comme les Nox doivent adopter des orientations appropriées pour communiquer avec leurs partenaires d'interaction respectifs et être actives. Pour comprendre la fonction des Nox qui sont des protéines transmembranaires, dans les cellules, il est essentiel d'analyser leur topologie au sein de la membrane. L'étude de l'hydrophobicité de ces protéines et les différents algorithmes obtenus nécessitent des vérifications par protéolyse limitée (Wilkinson *et al.*, 1996), cartographie de glycosylation (Chang *et al.*, 1994) ou la substitution des cysteines (Giraudat *et al.*, 1985; Bogdanov *et al.*, 2005) ; ces approches exigeant bien souvent des investissements considérables en temps et en effort.

L'ARNm de p22phox est largement exprimé dans les tissus fœtaux et adultes (Cheng *et al.*, 2001) et dans les lignées cellulaires (Parkos *et al.*, 1988). Son expression est nécessaire à la fonction de Nox1, Nox2, Nox3, et Nox4 (Kawahara *et al.*, 2005; Martyn *et al.*, 2006). La structure de p22phox contiendrait 2-4 segments

transmembranaires selon l'analyse de la séquence primaire obtenue par des méthodes de calcul. Mais sa topologie ne résulte pas d'un consensus en l'absence de données de cristallisation. Des résultats suggèrent une structure à deux passages transmembranaires avec les extrémités NH_2 terminale et COOH terminale du côté cytoplasmique (Imajoh-Ohmi ***et al.***, 1992; Burritt ***et al.***, 1998; Taylor ***et al.***, 2004).

Actuellement, la topographie et la structure de Nox4 sont suggérées à partir des études sur Nox2 et la prédiction de courbes d'hydropathie de Nox4. Puisque p22phox est le seul partenaire reconnu pour interagir avec Nox4, il est nécessaire d'étudier de manière conjointe la topologie de Nox4 et celle de p22phox.

La méthode de «Topological Determination by Ubiquitin Fusion Assay » TDUFA, décrite ici fournit une approche nouvelle, originale, permettant de déterminer la topologie des protéines membranaires dans les cellules.

Le travail encore très préliminaire, présenté et réalisé avec Nox4 et p22phox par cette approche, a permis de montrer que les extrémités C-terminale de p22FL, p22N143, p22N63 et de p22N36 font face au cytoplasme. Par ailleurs, pour ce qui concerne Nox4 et ses 6 domaines transmembranaires, les extrémités en C-terminale de Nox4FL, Nox4N341 et Nox4N98 sont orientées du côté intracellulaire alors que le domaine en C-terminale de Nox4N46, Nox4N144 fait face au milieu extracellulaire.

Différents mutants de Nox4, Nox4-GT (304-305) insert et Nox4-del 4aa (575-578), partiellement fonctionnels en terme de production de ROS ont apporté l'évidence que les régions de Nox4 mutées avaient un impact direct ou indirect sur p22phox endogène (Martyn ***et al.***, 2006); par ailleurs, les acides aminés en N-terminale 6-11 de p22phox sont essentiels, alors que le domaine en C-terminale (AA: 130-195) ne sont pas nécessaires pour l'activité de Nox4 (von Lohneysen ***et al.***, 2008).

Perspective

Une production excessive de ROS peut endommager les tissus sains de l'environnement. L'expression et l'activation anormales de Nox4 peuvent induire tumorigenèse, angiogenèse tumorale (Xia ***et al.***, 2007), et être associées à l'apparition et au développement d'autres pathologies, comme l'hypertension (Akasaki ***et al.***, 2006; Sedeek ***et al.***, 2009), l'athérosclérose (Sorescu ***et al.***, 2002), l'arthrose (Grange ***et al.***, 2006), etc. L'inhibition de la NADPH oxydase Nox4 pourrait donc être bénéfique chez les patients souffrant de tels désordres. Aucun inhibiteur spécifique de Nox4 n'a encore été identifié. Les anticorps monoclonaux, 5F9 et 6B11 qui diminuent de manière significative l'activité de Nox4 pourraient, à partir des connaissances relatives aux épitopes

marqués, ouvrir une voie pour l'identification de telles molécules et pour une approche de thérapie. Trois anticorps monoclonaux présentent des propriétés distinctes et spécifiques: 8E9 reconnaît un epitope sur la dernière boucle extracellular de Nox4 (^{222}H-E^{241}). L'alignement des séquences d' amino acides des Nox 1-5 a révélé que la boucle E de Nox4 possède 28 acides aminés de plus que la boucle E des autres Nox; l'anticorps monoclonal 8E9 qui marque une région de cette boucle, devrait être une sonde précieuse pour repérer Nox4 chez ces patients.

Contrairement à Nox2, p22phox est le seul partenaire connu qui interagit avec Nox4 (Ambasta *et al.*, 2004; Martyn *et al.*, 2006). Récemment, Poldip2 a été associé au fonctionnement de Nox4/p22phox dans les VSMC (Lyle *et al.*, 2009); Poldip2 a même été présenté comme un régulateur positif de Nox4. Les perspectives d'isolement de Nox4 feront appel aux anticorps monoclonaux notamment, 8E9, 5F9 et 6B11 récemment caractérisés et permettront peut-être d'identifier de nouveaux partenaires voire de confirmer le rôle proposé pour Poldip2.

Une approche d'étude de la topologie membranaire de Nox4 et p22phox a été abordée par la methode TDUFA. Il est en effet utile de caractériser les domaines d'interaction de p22phox et Nox4 impliqués dans l'activité de la NADPH oxydase et leur localisation. Pour poursuivre ce travail, nous nous proposons d'utiliser les différentes constructions de Nox4 et p22phox recombinates protéines tronquées ou natives pour étudier l'interaction entre Nox4 et p22phox en associant des approches immunologiques et structurales à une étude fonctionnelle.

L'activité constitutive de Nox4 illustre pour la première fois un modèle de structure active des Nox. L'anticorps 5F9 ne permet pas de détecter Nox4 sur la membrane plasmique. Les résultats de « phage display » suggèrent que 5F9 interagit avec la région (^{392}D-F^{398}). Par conséquent, l'étude par mutagenèse dirigée de cette région devrait permettre de mieux comprendre son rôle dans la structure active de Nox4.

Une analyse structure/fonction de la NADPH oxydase Nox4, devrait donc bénéficier (i) d'une approche immunochimique à l'aide des anticorps monoclonaux que nous avons caractérisés mais dont les épitopes pour certains d'entre eux (mAcs 8E9 et 6B11) restent à être déterminés, (ii) de l'étude de la topologie membranaire de Nox4 proposée par la methode TDUFA et aussi (iii) des différentes constructions de Nox4 recombinant, protéine native ou tronquée, qui ont été generées dans notre laboratoire à cet effet.

In English

NADPH oxidase, Nox4, belongs to the Nox family which could generate reactive oxygen species by transferring an electron to molecular oxygen. All Nox members share highly conserved structural features: the N-terminal 6 predicted transmembrane domains that contain four conserved histidine residues located in the third and fifth transmembrane domain and the C-terminal domain containing binding sites for FAD and NADPH. Nox2 is the propotype of the Nox family and a well studied characterized source for ROS production. Despite its wide distribution in tissues, Nox4 is still poorly understood. Unlike the other Noxes, Nox4 shows some unique characters: it is constitutively active without the need for cell stimulation and does not require the cytosolic factors; most studies report that Nox4 generates H_2O_2, etc. Nox4 involving ROS has been proposed to be implicated in several pathologies. Thus, the study structure/function and regulation of the activity of Nox4 will provide new ideas and new drug targets for the effective prevention and treatment of clinical diseases related with ROS.

Monoclonal antibodies specific to Nox4

Understanding of the role of Nox4 in the production of reactive oxygen species and of regulation mechanism of oxidase activity has been hindered by the lack of specific monoclonal antibodies which are also essential tools to provide direct evidence to topology models and to identify structural features of heterodimer with p22phox.

In this study (Zhang *et al.*, 2010), five monoclonal antibodies specific to Nox4 were raised for the first time. Among these mAbs, 3 of them, 8E9, 6B11 and 5F9, could recognize native overexpressed Nox4 protein in human kidney cortex and HEK293 cell lines and chondrocytes cell line. The theoretical size of Nox4 is 66.9kDa (expasy, proteomic server), as shown for the first time by Shiose et al (Shiose *et al.*, 2001). It has been reported that Nox4 antibodies recognize two kinds of bands: one of 75-80kDa and a second of 55-65kDa from endogenous Nox4 expressing cells and/or Nox4-overexpressing cells (Hilenski *et al.*, 2004; Kawahara *et al.*, 2005; Martyn *et al.*, 2006). The fact that two molecular masses are detected and that Nox4 contains four putative N-glycosylation sites might suggest that Nox4 is glycosylated, although treatment with N-glycosidase F failed to reduce the protein to a single band (Shiose *et al.*, 2001). As for us, Nox4 was detected using two different cell lines (HEK293 over expressing Nox4GFP and the tet-induction model HEK 293 T-Rex Nox4) at the size of 58kDa. Also a small band of 31kDa observed with Nox4 mAbs most likely represents a cleaved

fragment. Discrepancies between calculated and apparent molecular masses have been observed for other members of Nox family: Nox5 runs 70kDa, rather than the predicted 82kDa; the de-glycosolated form of Nox2 runs at 55kDa, rather than the predicted 65kDa, and Nox1 runs at 55-60kDa rather than the predicted 65kDa (Serrander *et al.*, 2007). The reason for this discrepancy is not known, but it has been proposed that this phenomenon may result from the basic nature of these proteins (pI 9.0 for Nox1; pI 8.9 for Nox2; pI 9.0 for Nox5 and pI 8.96 for Nox4) (Lametsch *et al*., 2000). 68kDa is the size of Nox4 detected in kidney cortex, which has also been reported by (Gorin *et al.*, 2005; Hecker *et al.*, 2009). The difference of size of Nox4 might suggest that the protein is more glycosylated in the tissues or less degraded. The degradation process of Nox4 may depend on the modalities of storage and freezing and thawing, and on the procedure of cell homogenization and protein extraction. In our study, we emphasized the great sensitivity of Nox4 to the temperature and the necessary addition to sample fraction not only of an anti-protease cocktail but also of vanadate and okadaic acid reagents that inhibit phosphatases; moreover the SDS solubilisation procedure has to be carried out at 4°C.

Subcellular localization of Nox4

ROS are generated in a wide variety of biological contexts, both physiological and pathophysiological, and in nearly all tissues and organs of multicellular organisms (Bedard *et al.*, 2007). Although Nox proteins represent the major non-mitochondrial sources of ROS, identification of the specific Nox protein(s) responsible for ROS production in a particular tissue or organ system has been undermined by limited availability of reliable tools for robust analysis. For example, whereas several well characterized antibodies against Nox2 are widely used, no such immunochemical probes exist at this time for Nox3. Antibodies for other non-phagocyte Nox proteins are variably or incompletely characterized and nonspecific. Tissue localization studies have relied on detection of mRNA and not protein, or the identification of p22phox, as a surrogate marker for Nox1–4 (Nauseef, 2008).

Nox4 has been detected in several cellular compartments: in transfected cells, Nox4 was localized in the ER (Martyn *et al.*, 2006; Chen *et al.*, 2008) or plasma membrane (Lee *et al.*, 2006; von Lohneysen *et al.*, 2008); in endothelial cells (Kuroda *et al.*, 2005) and smooth muscle cells (Hilenski *et al.*, 2004), the localization of Nox4 was reported within the nucleus; in vascular smooth muscle cells, a localization close to focal adhesion was reported. Moreover, in somatic cells, Nox4 was detected in mitochondria (Block *et al.*,

2009). It is uncertain whether these contradicting findings are a consequence of so-far unknown partner of Nox4 changing the localization of Nox4 or of potential problems arising from the overexpression of a membrane protein per se or of the specificity of the different Nox4 antibodies used. It is also possible that the localization of Nox4 changes with the functional or pathological state of the cells (Weyemi *et al.*, 2010). In fact, in vascular smooth muscle cells, Nox4 relocates from focal adhesions to stress fibers during differentiation (Clempus *et al.*, 2007). This also reflects the cell-specific targeting of Nox4 or the different specificity of Nox4 antibodies (Goettsch *et al.*, 2009). In this study, immunochemistry results with these new mAbs showed that Nox4 was detected not only in the ER but also in the plasma membrane.

Characteristic of Nox4 dependent ROS

Due to the similarity to Nox2 and the obligate 1-electron transfer from heme iron, all Nox NADPH oxidases should primarily produce O_2^- (Bedard *et al.*, 2007). In fact, Nox1, Nox2, Nox3 and Nox5 produce primarily O_2^-. Most studies showed that H_2O_2 is the principal source of Nox4 dependent ROS detected outside of cells (Chen *et al.*, 2008; Hecker *et al.*, 2009), although it has been reported that O_2^- is synthesized in the extra cellular medium of hepatocytes (Boudreau *et al.*, 2009). However Nox4 in some cells resides in part in the plasma membrane, but unexpectedly still produces H_2O_2 without any detectable O_2^- (von Lohneysen *et al.*, 2010). Therefore, The H_2O_2 formation by Nox4 was thought as a consequence of its intracellular location or some artefact of the detection system. Mutation analysis (Helmcke *et al.*, 2009), intracellular probes for ROS detection (Serrander *et al.*, 2007) and comparative expression studies in cells exhibiting different localizations of Nox4 however demonstrated that the type of ROS produce by the enzyme is independent of its localization. This suggests that Nox NADPH oxidases can directly release either O_2^- or H_2O_2 and that this feature is dependent on structural properties of the individual Nox enzyme.

Duox enzymes also generate H_2O_2 (Geiszt *et al.*, 2003; Forteza *et al.*, 2005) and the type of ROS generated appears to depend on the maturation state of the Duoxes (Ameziane-El-Hassani *et al.*, 2005). This process also involves relocalization of the Duox/Duoxa complex from the endoplasmic reticulum to the plasma membrane (Morand *et al.*, 2009), but it is not clear whether localization impacts the observed reduced oxygen species. These mechanisms could also account for the H_2O_2 formation of Nox4. But there is not study reported about the partners such as p22phox or p22phox-interacting protein Poldip2 alters the type of ROS formed by Nox4. It has also been suggested that Nox4 might colocalize with SOD1 and therefore accelerate

the O_2^- dismutation to H_2O_2 (von Lohneysen *et al.*, 2008).

In a collaborative study (Takac *et al.* 2011), we identified the extended E-loop of the protein as an essential structural feature for the intrinsic H_2O_2 formation by Nox4 and alterations of the loop switch Nox4 from H_2O_2 into a O_2^- producing enzyme. Compare to other Nox members, Nox4 shows significantly increased length of the extended E-loop. Therefore, the E-loop might form a physical structure that slows the egress of O_2^- and/or $HO_2^\cdot$ from its site of formation at the heme, allowing it to accumulate and accelerating the spontaneous dismutation by virtue of increasing the local concentration of superoxide. Furthermore, the cysteines Cys226 and Cys270 might form a disulfide bridge to stabilize such a structure. This presumption was also supported by a mAb 8E9 binding to the E-loop, since it was able to decrease H_2O_2 to the same extent as an extracytoplasmic crosslinking agent which should also interfere with the structure of the E-loop.

Another possible mechanism is that this enzyme might have endogenous SOD activity or it acts as a dioxygenase and directly forms H_2O_2. For both processes histidines and cysteines could be important. Unlike to Nox1 or Nox2, the E-loop of Nox4 contains a highly conserved histidine H222. Interestingly, mutation of His222 or Cys226 of Nox4 embedded in the sequence THPPGC switched Nox4 from H_2O_2 to O_2^- formation. Given that the two prolines in this sequence should force a 90 degree deviation in the secondary structure of the sequence, the Cys226 is likely to be in close proximity to His222 and therefore might contribute to metal coordination. Besides, histidine might also directly accelerate the formation of H_2O_2 in the absence of a metal. This amino acid is frequently involved in enzyme catalysis, where it acts as a proton donor (Holliday *et al.*, 2009). The reported rate constant for the process is $\sim 1\times10^8$ $M^{-1}s^{-1}$, seven orders of magnitude higher than the spontaneous dismutation rate for two superoxide anions (Behar *et al.*, 1970; Marklund, 1976). Thus, His222 in the E-Loop might also serve as a proton donor for a superoxide anion to form the perhydroxyl radical, which would accelerate spontaneous O_2^- dismutation by many orders of magnitude.

Nox4 and diaphorase activity

In article (Takac *et al.* 2011), H_2O_2 formation is showed to be the intrinsic property of Nox4. Structurally, H_2O_2 to O_2^- forming enzymes are usually quite different and xanthine oxidase is one of the few examples of an enzyme capable of producing both types of ROS (Nishino *et al.*, 2008). A mutant of xanthine oxidase with increased O_2^- and decreased H_2O_2 formation showed that H_2O_2 formation indeed usually occurs at FAD sites and does not require the heme present in the Nox proteins (Asai *et al.*, 2007). Heme proteins in contrast

produce $O_2^{\cdot}$. Thus, H_2O_2 formation by Nox4 might occur at the FAD site. But expression of the isolated dehydrogenase domain of Nox4 demonstrated that this domain of Nox4 is able to reduce cytochrome c and several dye electron acceptors (Nisimoto *et al.*, 2010) but does not form H_2O_2 directly.

The mechanism of electron transfer is well documented for the Nox2 protein. Diaphorase activity is the electron transfer from FAD to redox center and is located at the cytosolic tail of Nox2. Few studies exist regarding the diaphorase activity of Nox4. Pre-incubation of total lysates of tet-induced T-REx™ Nox4 cells with either mAb 6B11 or mAb 5F9 leads to a moderated but significant inhibition of Nox4 activity, indicating that they interact with a region important for the electron transfer. This result also suggested that cytosolic tail of Nox4 could be responsible for its constitutive activity. Functional study of Nox4 requires the production of soluble protein which has not been achieved for any Nox except Nox2 (Marques *et al.*, 2007). To well understand the electronic transfer property of Nox4, soluble and active Nox4 truncated proteins were produced by two optimized approaches (in vitro RTS and bacterial induction) and the diaphorase activity was studied. Unlike Nox2, in this work (Nguyen *et al.* 2011) the diaphorase activity of Nox4Aqc (AA: 309-578) was shown to be constitutive and the addition of cytosolic extract did not enhance its activity (Han *et al.*, 2001; Nisimoto *et al.*, 2004; Marques *et al.*, 2007). This result is consistent with the observation that Nox4 displays a constitutive activity by cell-free system (Nisimoto *et al.*, 2010).

Topology information on Nox4 and p22phox

ROS generated by Nox4 can regulate cell behaviour as a signal molecule. The abnormal expression and activation of Nox4 may induce tumorigenesis and be involved in many other diseases.

Cellular membranes act as barriers and scaffolds to separate different cellular environments. Consequently, it is important for membrane proteins like Nox proteins to adopt appropriate orientations to communicate with their respective interacting partners. Membrane protein has a unique structural characterization involved in many basic and important cell biological functions, such as solute transport and signalling across the membrane. In the current drug development, membrane proteins also make for ~70% of current drug targets (Drews, 2000; Kiefer, 2003).

To understand the cellular function of Nox which are membrane proteins, it is therefore crucial to know its membrane topology. At present, some theoretical and experimental methods have been used to study the topology of membrane proteins, such as using the relative hydrophobicity of amino acid side chain of a

protein in order to establish a topology model of a membrane protein. But different algorithms have led to different results, therefore requiring certain of experimental methods to test and verify them, such as limited proteolysis (Wilkinson *et al.*, 1996), glycosylation mapping (Chang *et al.*, 1994) and cysteine substitution (Giraudat *et al.*, 1985; Bogdanov *et al.*, 2005) have been used. These approaches often require substantial investments of time and effort.

The mRNA for p22phox is widely expressed in both fetal and adult tissues (Cheng *et al.*, 2001) and in cell lines (Parkos *et al.*, 1988). Its expression is involved in the function of the activity of Nox1, Nox2, Nox3, and Nox4 (Kawahara *et al.*, 2005; Martyn *et al.*, 2006). p22phox was proposed to contain 2–4 membrane-spanning segments according to the primary sequence analysis by computational methods. But its topology structure cannot reach a consensus in the absence of crystallization data. However, the weight of evidence favors a two transmembrane structure with both the NH_2 terminus and the COOH terminus facing the cytoplasm (Imajoh-Ohmi *et al.*, 1992; Burritt *et al.*, 1998; Taylor *et al.*, 2004).

Currently, the topography and structure of Nox4 is derived from studies on Nox2 and hydropathy plots prediction of Nox4. Since p22phox is the only known partner that interacts with Nox4, it is necessary to study the topology of Nox4 and p22phox.

TDUFA method described here provides a new and original approach for determining protein topology in cells. It does not require large quantities of target proteins. Besides, the use of GFP chimeras in the TDUFA does not need appropriate and available antibodies that are required in protein topology assays relying upon site-specific immunoreactivity (Canfield *et al.*, 1993). In rare cases, the addition of GFP or ubGFP could interfere proper functioning and localization of the fusion protein, which needs to be considered and addressed.

To learn more about the topology of Nox4 and p22phox, this method was first verified by using two membrane proteins IL1R1 and Nox2N131. Therefore, it was further used to study the topology of Nox4 and p22phox. Preliminary results obtained by TDUFA method suggested that C terminal of p22FL, p22N143, p22N63, and p22N36 faces the cytoplasm. Nox4 has 6 transmembrane domains, the C-terminus of Nox4FL, Nox4N341 and Nox4N98 face the cytoplasm while the C-terminus of Nox4N46, Nox4N144 faces the cell exterior or lumen.

Through the mutation analysis of Nox4 and p22phox, two Nox4 mutants, Nox4-GT (304-305) insert and Nox4-del 4aa (575-578), partially functional in ROS production did not up-regulate p22phox levels (Martyn *et al.*, 2006). This provided evidence that these two mutations were in regions of Nox4 that either directly, or

indirectly, impacted endogenous p22phox; and the N-terminal amino acids 6-11 of p22phox is essential, whereas the C terminus (amino acids 130-195) is dispensable for Nox4 activity (von Lohneysen *et al.*, 2008).

Perspectives

Excessive ROS production can damage healthy bystander tissues. The abnormal expression and activation of Nox4 may induce tumorigenesis, tumor angiogenesis (Xia *et al.*, 2007), and be related with the occurrence and development of other diseases, such as hypertension (Akasaki *et al.*, 2006; Sedeek *et al.*, 2009), atherosclerosis (Sorescu *et al.*, 2002), osteoarthritis (Grange *et al.*, 2006), etc. Pharmacological NADPH oxidase inhibition might therefore be beneficial in patient with these disorders. No specific inhibitors for Nox4 have so far been identified. As mAb 5F9 and mAb 6B11 significantly decreased the Nox4 activity, they will be helpful in identifying specific inhibitors of Nox4 activity.

Three mAbs display distinct and specific properties. mAb 8E9 recognizes an epitope on the last extracellular loop of Nox4 (^{222}H-E^{241}). As the alignment of the AA sequences of Nox1-5 revealed that the E-loop of Nox4 is 28 amino acids longer than the loop of other Noxs, mAb 8E9 which marks a region of this loop should be a valuable probe to identify Nox4 in these patients.

Unlike Nox2, p22phox is the only known partner that interacts with Nox4 (Ambasta *et al.*, 2004; Martyn *et al.*, 2006). Recently, (Lyle *et al.*, 2009) reported in VSMC the association of Poldip2 with heterodimer Nox4/p22phox and Poldip2 was introduced as a positive regulator of Nox4. With these new monoclonal antibodies, the isolation of Nox4 may help to find out additional partners such as Poldip2 as a complex from HEK293 cells and to confirm the proposed role of Poldip2. Monoclonal antibodies developed against Nox4 described in this study will be powerful tools for a structure/function relationship investigation.

The constitutive activity of Nox4 shows for the first time a model of active structure of Nox. mAb 5F9 could not detect Nox4 at the plasma membrane. Phage display epitope mapping suggested that mAb 5F9 interacts with (^{392}D-F^{398}) region of Nox4. Three possibilities could explain such a result: (i) Nox4 may change its conformation once transferred to the plasma membrane and therefore could hide the epitope of 5F9; (ii) additional Nox4 partner such as Poldip 2 (Lyle *et al.*, 2009) which influence Nox4 subcellular localization in VSMC may bind to this epitope region; (iii) the permeabilization process could alter the epitope of 5F9. Therefore, mutagenesis study in this region is necessary for further understanding its role in the localization and activity of Nox4. More work is necessary to further determine the specific epitope of mAbs 8E9 and

6B11.

An analysis of structure / function of NADPH oxidase Nox4 will benefit (i) an immunochemical approach using monoclonal antibodies we have characterized, but the epitopes mAb 8E9 and 6B11 are to be determined; (ii) to study the membrane topology of Nox4 by the proposed method TDUFA and also (iii) different constructs of Nox4 recombinant proteins, native or truncated, which were generated in our laboratory.

Reference

A

Abo, A., E. Pick, A. Hall, N. Totty, C. G. Teahan and A. W. Segal (1991). Activation of the NADPH oxidase involves the small GTP-binding protein p21rac1. *Nature* **353**(6345): 668-670.

Ago, T., T. Kitazono, H. Ooboshi, T. Iyama, Y. H. Han, J. Takada, M. Wakisaka, S. Ibayashi, H. Utsumi and M. Iida (2004). Nox4 as the major catalytic component of an endothelial NAD(P)H oxidase. *Circulation* **109**(2): 227-233.

Ago, T., J. Kuroda, J. Pain, C. Fu, H. Li and J. Sadoshima (2010). Upregulation of Nox4 by hypertrophic stimuli promotes apoptosis and mitochondrial dysfunction in cardiac myocytes. *Circ Res* **106**(7): 1253-1264.

Akasaki, T., Y. Ohya, J. Kuroda, K. Eto, I. Abe, H. Sumimoto and M. Iida (2006). Increased expression of gp91phox homologues of NAD(P)H oxidase in the aortic media during chronic hypertension: involvement of the renin-angiotensin system. *Hypertens Res* **29**(10): 813-820.

Ambasta, R. K., P. Kumar, K. K. Griendling, H. H. Schmidt, R. Busse and R. P. Brandes (2004). Direct interaction of the novel Nox proteins with p22phox is required for the formation of a functionally active NADPH oxidase. *J Biol Chem* **279**(44): 45935-45941.

Ameziane-El-Hassani, R., S. Morand, J. L. Boucher, Y. M. Frapart, D. Apostolou, D. Agnandji, S. Gnidehou, R. Ohayon, M. S. Noel-Hudson, J. Francon, K. Lalaoui, A. Virion and C. Dupuy (2005). Dual oxidase-2 has an intrinsic Ca2+-dependent H2O2-generating activity. *J Biol Chem* **280**(34): 30046-30054.

Arakawa, N., M. Katsuyama, K. Matsuno, N. Urao, Y. Tabuchi, M. Okigaki, H. Matsubara and C. Yabe-Nishimura (2006). Novel transcripts of Nox1 are regulated by alternative promoters and expressed under phenotypic modulation of vascular smooth muscle cells. *Biochem J* **398**(2): 303-310.

Arnold, R. S., J. Shi, E. Murad, A. M. Whalen, C. Q. Sun, R. Polavarapu, S. Parthasarathy, J. A. Petros and J. D. Lambeth (2001). Hydrogen peroxide mediates the cell growth and transformation caused by the mitogenic oxidase Nox1. *Proc Natl Acad Sci U S A* **98**(10): 5550-5555.

Asai, R., T. Nishino, T. Matsumura, K. Okamoto, K. Igarashi and E. F. Pai (2007). Two mutations convert mammalian xanthine oxidoreductase to highly superoxide-productive xanthine oxidase. *J Biochem* **141**(4): 525-534.

Audic, S., F. Lopez, J. M. Claverie, O. Poirot and C. Abergel (1997). SAmBA: an interactive software for optimizing the design of biological macromolecules crystallization experiments. *Proteins* **29**(2): 252-257.

Azimi, P. H., J. G. Bodenbender, R. L. Hintz and S. B. Kontras (1968). Chronic granulomatous disease in three female siblings. *JAMA* **206**(13): 2865-2870.

Babior, B. M. (1999). NADPH Oxidase: An Update. *Blood* **93**(5): 1464-1476.

Babior, B. M., J. T. Curnutte and B. S. Kipnes (1975). Pyridine nucleotide-dependent superoxide production by a cell-free system from human granulocytes. *J Clin Invest* **56**(4): 1035-1042.

Babior, B. M., R. S. Kipnes and J. T. Curnutte (1973). Biological defense mechanisms. The production by leukocytes

of superoxide, a potential bactericidal agent. *J Clin Invest* **52**(3): 741-744.

Balaban, R. S., S. Nemoto and T. Finkel (2005). Mitochondria, oxidants, and aging. *Cell* **120**(4): 483-495.

Baldridge, C. W. and R. W. Gerard (1932). The extra respiration of phagocytosis. *AJP - Legacy* **103**(1): 235-236.

Banfi, B., R. A. Clark, K. Steger and K. H. Krause (2003). Two novel proteins activate superoxide generation by the NADPH oxidase NOX1. *J Biol Chem* **278**(6): 3510-3513.

Banfi, B., B. Malgrange, J. Knisz, K. Steger, M. Dubois-Dauphin and K. H. Krause (2004). NOX3, a superoxide-generating NADPH oxidase of the inner ear. *J Biol Chem* **279**(44): 46065-46072.

Banfi, B., A. Maturana, S. Jaconi, S. Arnaudeau, T. Laforge, B. Sinha, E. Ligeti, N. Demaurex and K. H. Krause (2000). A mammalian H+ channel generated through alternative splicing of the NADPH oxidase homolog NOH-1. *Science* **287**(5450): 138-142.

Banfi, B., G. Molnar, A. Maturana, K. Steger, B. Hegedus, N. Demaurex and K. H. Krause (2001). A Ca(2+)-activated NADPH oxidase in testis, spleen, and lymph nodes. *J Biol Chem* **276**(40): 37594-37601.

Banfi, B., F. Tirone, I. Durussel, J. Knisz, P. Moskwa, G. Z. Molnar, K. H. Krause and J. A. Cox (2004). Mechanism of Ca2+ activation of the NADPH oxidase 5 (NOX5). *J Biol Chem* **279**(18): 18583-18591.

Beckman, K. B. and B. N. Ames (1998). The free radical theory of aging matures. *Physiol Rev* **78**(2): 547-581.

Bedard, K. and K. H. Krause (2007). The NOX family of ROS-generating NADPH oxidases: physiology and pathophysiology. *Physiol Rev* **87**(1): 245-313.

Behar, D., G. Czapski, J. Rabani, L. M. Dorfman and H. A. Schwarz (1970). Acid dissociation constant and decay kinetics of the perhydroxyl radical. *The Journal of Physical Chemistry* **74**(17): 3209-3213.

BelAiba, R. S., T. Djordjevic, A. Petry, K. Diemer, S. Bonello, B. Banfi, J. Hess, A. Pogrebniak, C. Bickel and A. Gorlach (2007). NOX5 variants are functionally active in endothelial cells. *Free Radic Biol Med* **42**(4): 446-459.

Benedyk, M., C. Sopalla, W. Nacken, G. Bode, H. Melkonyan, B. Banfi and C. Kerkhoff (2007). HaCaT keratinocytes overexpressing the S100 proteins S100A8 and S100A9 show increased NADPH oxidase and NF-kappaB activities. *J Invest Dermatol* **127**(8): 2001-2011.

Berendes, H., R. A. Bridges and R. A. Good (1957). A fatal granulomatous disease of childhood; the clinical study of a new syndrome. *Minn Med* **40**: 309-312.

Berthier, S., M. H. Paclet, S. Lerouge, F. Roux, S. Vergnaud, A. W. Coleman and F. Morel (2003). Changing the conformation state of cytochrome b558 initiates NADPH oxidase activation: MRP8/MRP14 regulation. *J Biol Chem* **278**(28): 25499-25508.

Biberstine-Kinkade, K. J., F. R. DeLeo, R. I. Epstein, B. A. LeRoy, W. M. Nauseef and M. C. Dinauer (2001). Heme-ligating histidines in flavocytochrome b(558): identification of specific histidines in gp91(phox). *J Biol Chem* **276**(33): 31105-31112.

Biberstine-Kinkade, K. J., L. Yu and M. C. Dinauer (1999). Mutagenesis of an arginine- and lysine-rich domain in the gp91(phox) subunit of the phagocyte NADPH-oxidase flavocytochrome b558. *J Biol Chem* **274**(15): 10451-10457.

Block, K., Y. Gorin and H. E. Abboud (2009). Subcellular localization of Nox4 and regulation in diabetes. *Proc Natl Acad Sci U S A* **106**(34): 14385-14390.

Block, K., Y. Gorin, P. Hoover, P. Williams, T. Chelmicki, R. A. Clark, T. Yoneda and H. E. Abboud (2007). NAD(P)H oxidases regulate HIF-2alpha protein expression. *J Biol Chem* **282**(11): 8019-8026.

Bogdanov, M., W. Zhang, J. Xie and W. Dowhan (2005). Transmembrane protein topology mapping by the substituted cysteine accessibility method (SCAM(TM)): application to lipid-specific membrane protein topogenesis. *Methods* **36**(2): 148-171.

Borregaard, N., J. M. Heiple, E. R. Simons and R. A. Clark (1983). Subcellular localization of the b-cytochrome component of the human neutrophil microbicidal oxidase: translocation during activation. *J Cell Biol* **97**(1): 52-61.

Boudreau, H. E., S. U. Emerson, A. Korzeniowska, M. A. Jendrysik and T. L. Leto (2009). Hepatitis C virus (HCV) proteins induce NADPH oxidase 4 expression in a transforming growth factor beta-dependent manner: a new contributor to HCV-induced oxidative stress. *J Virol* **83**(24): 12934-12946.

Brand, M. D., C. Affourtit, T. C. Esteves, K. Green, A. J. Lambert, S. Miwa, J. L. Pakay and N. Parker (2004). Mitochondrial superoxide: production, biological effects, and activation of uncoupling proteins. *Free Radic Biol Med* **37**(6): 755-767.

Brar, S. S., Z. Corbin, T. P. Kennedy, R. Hemendinger, L. Thornton, B. Bommarius, R. S. Arnold, A. R. Whorton, A. B. Sturrock, T. P. Huecksteadt, M. T. Quinn, K. Krenitsky, K. G. Ardie, J. D. Lambeth and J. R. Hoidal (2003). NOX5 NAD(P)H oxidase regulates growth and apoptosis in DU 145 prostate cancer cells. *Am J Physiol Cell Physiol* **285**(2): C353-369.

Brar, S. S., T. P. Kennedy, A. B. Sturrock, T. P. Huecksteadt, M. T. Quinn, A. R. Whorton and J. R. Hoidal (2002). An NAD(P)H oxidase regulates growth and transcription in melanoma cells. *Am J Physiol Cell Physiol* **282**(6): C1212-1224.

Bridges, R. A., H. Berendes and R. A. Good (1959). A fatal granulomatous disease of childhood; the clinical, pathological, and laboratory features of a new syndrome. *AMA J Dis Child* **97**(4): 387-408.

Bromberg, Y. and E. Pick (1985). Activation of NADPH-dependent superoxide production in a cell-free system by sodium dodecyl sulfate. *J Biol Chem* **260**(25): 13539-13545.

Brown, D. I. and K. K. Griendling (2009). Nox proteins in signal transduction. *Free Radic Biol Med* **47**(9): 1239-1253.

Browning, J. A. and R. J. Wilkins (2002). The effect of intracellular alkalinisation on intracellular Ca(2+) homeostasis in a human chondrocyte cell line. *Pflugers Arch* **444**(6): 744-751.

Burritt, J. B., S. C. Busse, D. Gizachew, D. W. Siemsen, M. T. Quinn, C. W. Bond, E. A. Dratz and A. J. Jesaitis (1998). Antibody imprint of a membrane protein surface. Phagocyte flavocytochrome b. *J Biol Chem* **273**(38): 24847-24852.

Burritt, J. B., F. R. DeLeo, C. L. McDonald, J. R. Prigge, M. C. Dinauer, M. Nakamura, W. M. Nauseef and A. J. Jesaitis (2001). Phage display epitope mapping of human neutrophil flavocytochrome b558. Identification of two juxtaposed extracellular domains. *J Biol Chem* **276**(3): 2053-2061.

Burritt, J. B., T. R. Foubert, D. Baniulis, C. I. Lord, R. M. Taylor, J. S. Mills, T. D. Baughan, D. Roos, C. A. Parkos and A. J. Jesaitis (2003). Functional epitope on human neutrophil flavocytochrome b558. *J Immunol* **170**(12): 6082-6089.

Cadenas, E. and K. J. A. Davies (2000). Mitochondrial free radical generation, oxidative stress, and aging. *Free Radical Biology and Medicine* **29**(3-4): 222-230.

Campion, Y., M. H. Paclet, A. J. Jesaitis, B. Marques, A. Grichine, S. Berthier, J. L. Lenormand, B. Lardy, M. J. Stasia and F. Morel (2007). New insights into the membrane topology of the phagocyte NADPH oxidase: characterization of an anti-gp91-phox conformational monoclonal antibody. *Biochimie* **89**(9): 1145-1158.

Canfield, V. A. and R. Levenson (1993). Transmembrane organization of the Na,K-ATPase determined by epitope addition. *Biochemistry* **32**(50): 13782-13786.

Carrichon, L., A. Picciocchi, F. Debeurme, F. Defendi, S. Beaumel, A. J. Jesaitis, M. C. Dagher and M. J. Stasia (2010). Characterization of superoxide overproduction by the D-Loop(Nox4)-Nox2 cytochrome b(558) in phagocytes-Differential sensitivity to calcium and phosphorylation events. *Biochim Biophys Acta*.

Chamulitrat, W., W. Stremmel, T. Kawahara, K. Rokutan, H. Fujii, K. Wingler, H. H. Schmidt and R. Schmidt (2004). A constitutive NADPH oxidase-like system containing gp91phox homologs in human keratinocytes. *J Invest Dermatol* **122**(4): 1000-1009.

Chang, X. B., Y. X. Hou, T. J. Jensen and J. R. Riordan (1994). Mapping of cystic fibrosis transmembrane conductance regulator membrane topology by glycosylation site insertion. *J Biol Chem* **269**(28): 18572-18575.

Chen, K., M. T. Kirber, H. Xiao, Y. Yang and J. F. Keaney, Jr. (2008). Regulation of ROS signal transduction by NADPH oxidase 4 localization. *J Cell Biol* **181**(7): 1129-1139.

Cheng, G., Z. Cao, X. Xu, E. G. van Meir and J. D. Lambeth (2001). Homologs of gp91phox: cloning and tissue expression of Nox3, Nox4, and Nox5. *Gene* **269**(1-2): 131-140.

Cheng, G., B. A. Diebold, Y. Hughes and J. D. Lambeth (2006). Nox1-dependent reactive oxygen generation is regulated by Rac1. *J Biol Chem* **281**(26): 17718-17726.

Cheng, G. and J. D. Lambeth (2004). NOXO1, regulation of lipid binding, localization, and activation of Nox1 by the Phox homology (PX) domain. *J Biol Chem* **279**(6): 4737-4742.

Cheng, G., D. Ritsick and J. D. Lambeth (2004). Nox3 regulation by NOXO1, p47phox, and p67phox. *J Biol Chem* **279**(33): 34250-34255.

Chiarugi, P. and P. Cirri (2003). Redox regulation of protein tyrosine phosphatases during receptor tyrosine kinase signal transduction. *Trends in Biochemical Sciences* **28**(9): 509-514.

Chiarugi, P. and T. Fiaschi (2007). Redox signalling in anchorage-dependent cell growth. *Cellular Signalling* **19**(4):

672-682.

Clempus, R. E., D. Sorescu, A. E. Dikalova, L. Pounkova, P. Jo, G. P. Sorescu, B. Lassegue and K. K. Griendling (2007). Nox4 Is Required for Maintenance of the Differentiated Vascular Smooth Muscle Cell Phenotype. *Arteriosclerosis, Thrombosis, and Vascular Biology* **27**(1): 42-48.

Clempus, R. E., D. Sorescu, A. E. Dikalova, L. Pounkova, P. Jo, G. P. Sorescu, H. H. Schmidt, B. Lassegue and K. K. Griendling (2007). Nox4 is required for maintenance of the differentiated vascular smooth muscle cell phenotype. *Arterioscler Thromb Vasc Biol* **27**(1): 42-48.

Colston, J. T., S. D. de la Rosa, J. R. Strader, M. A. Anderson and G. L. Freeman (2005). H2O2 activates Nox4 through PLA2-dependent arachidonic acid production in adult cardiac fibroblasts. *FEBS Lett* **579**(11): 2533-2540.

Commoner, B., J. Townsend and G. E. Pake (1954). Free radicals in biological materials. *Nature* **174**(4432): 689-691.

Cross, A. R. (2000). p40(phox) Participates in the activation of NADPH oxidase by increasing the affinity of p47(phox) for flavocytochrome b(558). *Biochem J* **349**(Pt 1): 113-117.

Cross, A. R. and A. W. Segal (2004). The NADPH oxidase of professional phagocytes--prototype of the NOX electron transport chain systems. *Biochim Biophys Acta* **1657**(1): 1-22.

Cross, A. R. and A. W. Segal (2004). The NADPH oxidase of professional phagocytes--prototype of the NOX electron transport chain systems. *Biochimica et Biophysica Acta (BBA) - Bioenergetics* **1657**(1): 1-22.

Cucoranu, I., R. Clempus, A. Dikalova, P. J. Phelan, S. Ariyan, S. Dikalov and D. Sorescu (2005). NAD(P)H oxidase 4 mediates transforming growth factor-beta1-induced differentiation of cardiac fibroblasts into myofibroblasts. *Circ Res* **97**(9): 900-907.

Cui, X. L., D. Brockman, B. Campos and L. Myatt (2006). Expression of NADPH oxidase isoform 1 (Nox1) in human placenta: involvement in preeclampsia. *Placenta* **27**(4-5): 422-431.

D'Autreaux, B. and M. B. Toledano (2007). ROS as signalling molecules: mechanisms that generate specificity in ROS homeostasis. *Nat Rev Mol Cell Biol* **8**(10): 813-824.

Dahan, I., I. Issaeva, Y. Gorzalczany, N. Sigal, M. Hirshberg and E. Pick (2002). Mapping of functional domains in the p22(phox) subunit of flavocytochrome b(559) participating in the assembly of the NADPH oxidase complex by "peptide walking". *J Biol Chem* **277**(10): 8421-8432.

Dai, X., X. Cao and D. L. Kreulen (2006). Superoxide anion is elevated in sympathetic neurons in DOCA-salt hypertension via activation of NADPH oxidase. *Am J Physiol Heart Circ Physiol* **290**(3): H1019-1026.

Daiyasu, H. and H. Toh (2000). Molecular evolution of the myeloperoxidase family. *J Mol Evol* **51**(5): 433-445.

De Deken, X., D. Wang, J. E. Dumont and F. Miot (2002). Characterization of ThOX proteins as components of the thyroid H(2)O(2)-generating system. *Exp Cell Res* **273**(2): 187-196.

De Deken, X., D. Wang, M. C. Many, S. Costagliola, F. Libert, G. Vassart, J. E. Dumont and F. Miot (2000). Cloning of two human thyroid cDNAs encoding new members of the NADPH oxidase family. *J Biol Chem* **275**(30):

23227-23233.

de Mochel, N. S., S. Seronello, S. H. Wang, C. Ito, J. X. Zheng, T. J. Liang, J. D. Lambeth and J. Choi (2010). Hepatocyte NAD(P)H oxidases as an endogenous source of reactive oxygen species during hepatitis C virus infection. *Hepatology* **52**(1): 47-59.

DeLeo, F. R., J. B. Burritt, L. Yu, A. J. Jesaitis, M. C. Dinauer and W. M. Nauseef (2000). Processing and maturation of flavocytochrome b558 include incorporation of heme as a prerequisite for heterodimer assembly. *J Biol Chem* **275**(18): 13986-13993.

DeLeo, F. R., L. Yu, J. B. Burritt, L. R. Loetterle, C. W. Bond, A. J. Jesaitis and M. T. Quinn (1995). Mapping sites of interaction of p47-phox and flavocytochrome b with random-sequence peptide phage display libraries. *Proc Natl Acad Sci U S A* **92**(15): 7110-7114.

Dhaunsi, G. S., M. K. Paintlia, J. Kaur and R. B. Turner (2004). NADPH oxidase in human lung fibroblasts. *J Biomed Sci* **11**(5): 617-622.

Diebold, B. A. and G. M. Bokoch (2001). Molecular basis for Rac2 regulation of phagocyte NADPH oxidase. *Nat Immunol* **2**(3): 211-215.

Dinauer, M. C., E. A. Pierce, G. A. Bruns, J. T. Curnutte and S. H. Orkin (1990). Human neutrophil cytochrome b light chain (p22-phox). Gene structure, chromosomal location, and mutations in cytochrome-negative autosomal recessive chronic granulomatous disease. *J Clin Invest* **86**(5): 1729-1737.

Djordjevic, T., R. S. BelAiba, S. Bonello, J. Pfeilschifter, J. Hess and A. Gorlach (2005). Human urotensin II is a novel activator of NADPH oxidase in human pulmonary artery smooth muscle cells. *Arterioscler Thromb Vasc Biol* **25**(3): 519-525.

Doussiere, J., G. Buzenet and P. V. Vignais (1995). Photoaffinity labeling and photoinactivation of the O2(-)-generating oxidase of neutrophils by an azido derivative of FAD. *Biochemistry* **34**(5): 1760-1770.

Doussiere, J., F. Laporte and P. V. Vignais (1986). Photolabeling of a O2-. generating protein in bovine polymorphonuclear neutrophils by an arylazido NADP+ analog. *Biochem Biophys Res Commun* **139**(1): 85-93.

Drews, J. (2000). Drug discovery: a historical perspective. *Science* **287**(5460): 1960-1964.

Droge, W. (2002). Free Radicals in the Physiological Control of Cell Function. *Physiological Reviews* **82**(1): 47-95.

Dupuy, C., R. Ohayon, A. Valent, M. S. Noel-Hudson, D. Deme and A. Virion (1999). Purification of a novel flavoprotein involved in the thyroid NADPH oxidase. Cloning of the porcine and human cdnas. *J Biol Chem* **274**(52): 37265-37269.

Edderkaoui, M., P. Hong, E. C. Vaquero, J. K. Lee, L. Fischer, H. Friess, M. W. Buchler, M. M. Lerch, S. J. Pandol and A. S. Gukovskaya (2005). Extracellular matrix stimulates reactive oxygen species production and increases pancreatic cancer cell survival through 5-lipoxygenase and NADPH oxidase. *Am J Physiol Gastrointest Liver Physiol* **289**(6): G1137-1147.

Edens, W. A., L. Sharling, G. Cheng, R. Shapira, J. M. Kinkade, T. Lee, H. A. Edens, X. Tang, C. Sullards, D. B.

Flaherty, G. M. Benian and J. D. Lambeth (2001). Tyrosine cross-linking of extracellular matrix is catalyzed by Duox, a multidomain oxidase/peroxidase with homology to the phagocyte oxidase subunit gp91phox. *J Cell Biol* **154**(4): 879-891.

el Benna, J., L. P. Faust and B. M. Babior (1994). The phosphorylation of the respiratory burst oxidase component p47phox during neutrophil activation. Phosphorylation of sites recognized by protein kinase C and by proline-directed kinases. *J Biol Chem* **269**(38): 23431-23436.

Ellmark, S. H., G. J. Dusting, M. N. Fui, N. Guzzo-Pernell and G. R. Drummond (2005). The contribution of Nox4 to NADPH oxidase activity in mouse vascular smooth muscle. *Cardiovasc Res* **65**(2): 495-504.

Etoh, T., T. Inoguchi, M. Kakimoto, N. Sonoda, K. Kobayashi, J. Kuroda, H. Sumimoto and H. Nawata (2003). Increased expression of NAD(P)H oxidase subunits, NOX4 and p22phox, in the kidney of streptozotocin-induced diabetic rats and its reversibity by interventive insulin treatment. *Diabetologia* **46**(10): 1428-1437.

Finan, P., Y. Shimizu, I. Gout, J. Hsuan, O. Truong, C. Butcher, P. Bennett, M. D. Waterfield and S. Kellie (1994). An SH3 domain and proline-rich sequence mediate an interaction between two components of the phagocyte NADPH oxidase complex. *J Biol Chem* **269**(19): 13752-13755.

Finger, F., C. Schörle, S. Soder, A. Zien, M. B. Goldring and T. Aigner (2004). Phenotypic Characterization of Human Chondrocyte Cell Line C-20/A4: A Comparison between Monolayer and Alginate Suspension Culture. *Cells Tissues Organs* **178**(2): 65-77.

Forteza, R., M. Salathe, F. Miot and G. E. Conner (2005). Regulated hydrogen peroxide production by Duox in human airway epithelial cells. *Am J Respir Cell Mol Biol* **32**(5): 462-469.

Geiszt, M., J. B. Kopp, P. Varnai and T. L. Leto (2000). Identification of renox, an NAD(P)H oxidase in kidney. *Proc Natl Acad Sci U S A* **97**(14): 8010-8014.

Geiszt, M., K. Lekstrom, S. Brenner, S. M. Hewitt, R. Dana, H. L. Malech and T. L. Leto (2003). NAD(P)H oxidase 1, a product of differentiated colon epithelial cells, can partially replace glycoprotein 91phox in the regulated production of superoxide by phagocytes. *J Immunol* **171**(1): 299-306.

Geiszt, M., K. Lekstrom and T. L. Leto (2004). Analysis of mRNA transcripts from the NAD(P)H oxidase 1 (Nox1) gene. Evidence against production of the NADPH oxidase homolog-1 short (NOH-1S) transcript variant. *J Biol Chem* **279**(49): 51661-51668.

Geiszt, M., K. Lekstrom, J. Witta and T. L. Leto (2003). Proteins homologous to p47phox and p67phox support superoxide production by NAD(P)H oxidase 1 in colon epithelial cells. *J Biol Chem* **278**(22): 20006-20012.

Geiszt, M. and T. L. Leto (2004). The Nox family of NAD(P)H oxidases: host defense and beyond. *J Biol Chem* **279**(50): 51715-51718.

Geiszt, M., J. Witta, J. Baffi, K. Lekstrom and T. L. Leto (2003). Dual oxidases represent novel hydrogen peroxide sources supporting mucosal surface host defense. *FASEB J* **17**(11): 1502-1504.

Genestra, M. (2007). Oxyl radicals, redox-sensitive signalling cascades and antioxidants. *Cell Signal* **19**(9): 1807-1819.

Genova, M. L., M. M. Pich, A. Biondi, A. Bernacchia, A. Falasca, C. Bovina, G. Formiggini, G. Parenti Castelli and G. Lenaz (2003). Mitochondrial production of oxygen radical species and the role of Coenzyme Q as an antioxidant. *Exp Biol Med (Maywood)* **228**(5): 506-513.

Gerald, D., E. Berra, Y. M. Frapart, D. A. Chan, A. J. Giaccia, D. Mansuy, J. Pouyssegur, M. Yaniv and F. Mechta-Grigoriou (2004). JunD reduces tumor angiogenesis by protecting cells from oxidative stress. *Cell* **118**(6): 781-794.

Gerson, C., J. Sabater, M. Scuri, A. Torbati, R. Coffey, J. W. Abraham, I. Lauredo, R. Forteza, A. Wanner, M. Salathe, W. M. Abraham and G. E. Conner (2000). The lactoperoxidase system functions in bacterial clearance of airways. *Am J Respir Cell Mol Biol* **22**(6): 665-671.

Giraudat, J., C. Montecucco, R. Bisson and J. P. Changeux (1985). Transmembrane topology of acetylcholine receptor subunits probed with photoreactive phospholipids. *Biochemistry* **24**(13): 3121-3127.

Goettsch, C., W. Goettsch, G. Muller, J. Seebach, H. J. Schnittler and H. Morawietz (2009). Nox4 overexpression activates reactive oxygen species and p38 MAPK in human endothelial cells. *Biochem Biophys Res Commun.*

Goettsch, C., W. Goettsch, G. Muller, J. Seebach, H. J. Schnittler and H. Morawietz (2009). Nox4 overexpression activates reactive oxygen species and p38 MAPK in human endothelial cells. *Biochem Biophys Res Commun* **380**(2): 355-360.

Gonzalez, F. J. (2005). Role of cytochromes P450 in chemical toxicity and oxidative stress: studies with CYP2E1. *Mutat Res* **569**(1-2): 101-110.

Gorin, Y., K. Block, J. Hernandez, B. Bhandari, B. Wagner, J. L. Barnes and H. E. Abboud (2005). Nox4 NAD(P)H oxidase mediates hypertrophy and fibronectin expression in the diabetic kidney. *J Biol Chem* **280**(47): 39616-39626.

Gorin, Y., J. M. Ricono, N. H. Kim, B. Bhandari, G. G. Choudhury and H. E. Abboud (2003). Nox4 mediates angiotensin II-induced activation of Akt/protein kinase B in mesangial cells. *Am J Physiol Renal Physiol* **285**(2): F219-229.

Gottlieb, R. A. (2003). Cytochrome P450: major player in reperfusion injury. *Arch Biochem Biophys* **420**(2): 262-267.

Govindarajan, B., J. E. Sligh, B. J. Vincent, M. Li, J. A. Canter, B. J. Nickoloff, R. J. Rodenburg, J. A. Smeitink, L. Oberley, Y. Zhang, J. Slingerland, R. S. Arnold, J. D. Lambeth, C. Cohen, L. Hilenski, K. Griendling, M. Martinez-Diez, J. M. Cuezva and J. L. Arbiser (2007). Overexpression of Akt converts radial growth melanoma to vertical growth melanoma. *J Clin Invest* **117**(3): 719-729.

Goyal, P., N. Weissmann, F. Rose, F. Grimminger, H. J. Schafers, W. Seeger and J. Hanze (2005). Identification of novel Nox4 splice variants with impact on ROS levels in A549 cells. *Biochem Biophys Res Commun* **329**(1): 32-39.

Graham, F. L., J. Smiley, W. C. Russell and R. Nairn (1977). Characteristics of a human cell line transformed by DNA from human adenovirus type 5. *J Gen Virol* **36**(1): 59-74.

Grange, L., M. V. Nguyen, B. Lardy, M. Derouazi, Y. Campion, C. Trocme, M. H. Paclet, P. Gaudin and F. Morel (2006). NAD(P)H oxidase activity of Nox4 in chondrocytes is both inducible and involved in collagenase expression.

Antioxid Redox Signal **8**(9-10): 1485-1496.

Grasberger, H. and S. Refetoff (2006). Identification of the maturation factor for dual oxidase. Evolution of an eukaryotic operon equivalent. *J Biol Chem* **281**(27): 18269-18272.

Griendling, K. K., D. Sorescu, B. Lassegue and M. Ushio-Fukai (2000). Modulation of protein kinase activity and gene expression by reactive oxygen species and their role in vascular physiology and pathophysiology. *Arterioscler Thromb Vasc Biol* **20**(10): 2175-2183.

Grizot, S., F. Fieschi, M. C. Dagher and E. Pebay-Peyroula (2001). The active N-terminal region of p67phox. Structure at 1.8 A resolution and biochemical characterizations of the A128V mutant implicated in chronic granulomatous disease. *J Biol Chem* **276**(24): 21627-21631.

Groemping, Y., K. Lapouge, S. J. Smerdon and K. Rittinger (2003). Molecular basis of phosphorylation-induced activation of the NADPH oxidase. *Cell* **113**(3): 343-355.

Groemping, Y. and K. Rittinger (2005). Activation and assembly of the NADPH oxidase: a structural perspective. *Biochem J* **386**(Pt 3): 401-416.

Ha, E. M., C. T. Oh, Y. S. Bae and W. J. Lee (2005). A direct role for dual oxidase in Drosophila gut immunity. *Science* **310**(5749): 847-850.

Hadj-Slimane, R., Y. Lepelletier, N. Lopez, C. Garbay and F. Raynaud (2007). Short interfering RNA (siRNA), a novel therapeutic tool acting on angiogenesis. *Biochimie* **89**(10): 1234-1244.

Han, C. H., J. L. Freeman, T. Lee, S. A. Motalebi and J. D. Lambeth (1998). Regulation of the neutrophil respiratory burst oxidase. Identification of an activation domain in p67(phox). *J Biol Chem* **273**(27): 16663-16668.

Han, C. H., Y. Nisimoto, S. H. Lee, E. T. Kim and J. D. Lambeth (2001). Characterization of the flavoprotein domain of gp91phox which has NADPH diaphorase activity. *J Biochem* **129**(4): 513-520.

Harman, D. (1956). Aging: a theory based on free radical and radiation chemistry. *J Gerontol* **11**(3): 298-300.

Harper, A. M., M. F. Chaplin and A. W. Segal (1985). Cytochrome b-245 from human neutrophils is a glycoprotein. *Biochem J* **227**(3): 783-788.

Harper, A. M., M. J. Dunne and A. W. Segal (1984). Purification of cytochrome b-245 from human neutrophils. *Biochem J* **219**(2): 519-527.

Harper, R. W., C. Xu, K. Soucek, H. Setiadi and J. P. Eiserich (2005). A reappraisal of the genomic organization of human Nox1 and its splice variants. *Arch Biochem Biophys* **435**(2): 323-330.

Harrison, R. (2004). Physiological roles of xanthine oxidoreductase. *Drug Metab Rev* **36**(2): 363-375.

Hattori, H. (1961). Studies on the labile, stable Nadi oxidase and peroxidase staining reactions in the isolated particles of horse granulocyte. *Nagoya J Med Sci* **23**: 362-378.

Hecker, L., R. Vittal, T. Jones, R. Jagirdar, T. R. Luckhardt, J. C. Horowitz, S. Pennathur, F. J. Martinez and V. J.

Thannickal (2009). NADPH oxidase-4 mediates myofibroblast activation and fibrogenic responses to lung injury. *Nat Med* **15**(9): 1077-1081.

Heidari, Y., A. M. Shah and C. Gove (2004). NOX-2S is a new member of the NOX family of NADPH oxidases. *Gene* **335**: 133-140.

Helmcke, I., S. Heumuller, R. Tikkanen, K. Schroder and R. P. Brandes (2009). Identification of structural elements in Nox1 and Nox4 controlling localization and activity. *Antioxid Redox Signal* **11**(6): 1279-1287.

Heyneman, R. A. and R. E. Vercauteren (1984). Activation of a NADPH oxidase from horse polymorphonuclear leukocytes in a cell-free system. *J Leukoc Biol* **36**(6): 751-759.

Hilenski, L. L., R. E. Clempus, M. T. Quinn, J. D. Lambeth and K. K. Griendling (2004). Distinct subcellular localizations of Nox1 and Nox4 in vascular smooth muscle cells. *Arterioscler Thromb Vasc Biol* **24**(4): 677-683.

Hoidal, J. R., S. S. Brar, A. B. Sturrock, K. A. Sanders, B. Dinger, S. Fidone and T. P. Kennedy (2003). The role of endogenous NADPH oxidases in airway and pulmonary vascular smooth muscle function. *Antioxid Redox Signal* **5**(6): 751-758.

Holliday, G. L., J. B. Mitchell and J. M. Thornton (2009). Understanding the functional roles of amino acid residues in enzyme catalysis. *J Mol Biol* **390**(3): 560-577.

Hu, T., S. P. Ramachandrarao, S. Siva, C. Valancius, Y. Zhu, K. Mahadev, I. Toh, B. J. Goldstein, M. Woolkalis and K. Sharma (2005). Reactive oxygen species production via NADPH oxidase mediates TGF-beta-induced cytoskeletal alterations in endothelial cells. *Am J Physiol Renal Physiol* **289**(4): F816-825.

Huang, J., N. D. Hitt and M. E. Kleinberg (1995). Stoichiometry of p22-phox and gp91-phox in phagocyte cytochrome b558. *Biochemistry* **34**(51): 16753-16757.

Imajoh-Ohmi, S., K. Tokita, H. Ochiai, M. Nakamura and S. Kanegasaki (1992). Topology of cytochrome b558 in neutrophil membrane analyzed by anti-peptide antibodies and proteolysis. *J Biol Chem* **267**(1): 180-184.

Inanami, O., J. L. Johnson, J. K. McAdara, J. E. Benna, L. R. Faust, P. E. Newburger and B. M. Babior (1998). Activation of the leukocyte NADPH oxidase by phorbol ester requires the phosphorylation of p47PHOX on serine 303 or 304. *J Biol Chem* **273**(16): 9539-9543.

Inoguchi, T., T. Sonta, H. Tsubouchi, T. Etoh, M. Kakimoto, N. Sonoda, N. Sato, N. Sekiguchi, K. Kobayashi, H. Sumimoto, H. Utsumi and H. Nawata (2003). Protein kinase C-dependent increase in reactive oxygen species (ROS) production in vascular tissues of diabetes: role of vascular NAD(P)H oxidase. *J Am Soc Nephrol* **14**(8 Suppl 3): S227-232.

Irani, K., Y. Xia, J. L. Zweier, S. J. Sollott, C. J. Der, E. R. Fearon, M. Sundaresan, T. Finkel and P. J. Goldschmidt-Clermont (1997). Mitogenic signaling mediated by oxidants in Ras-transformed fibroblasts. *Science* **275**(5306): 1649-1652.

Ismail, S., A. Sturrock, P. Wu, B. Cahill, K. Norman, T. Huecksteadt, K. Sanders, T. Kennedy and J. Hoidal (2009). NOX4 mediates hypoxia-induced proliferation of human pulmonary artery smooth muscle cells: the role of autocrine

production of transforming growth factor-{beta}1 and insulin-like growth factor binding protein-3. *Am J Physiol Lung Cell Mol Physiol* **296**(3): L489-499.

Iyer, G. Y. N., M. F. Islam and J. H. Quastel (1961). Biochemical Aspects of Phagocytosis. *Nature* **192**(4802): 535-541.

Jackson, H. M., T. Kawahara, Y. Nisimoto, S. M. Smith and J. D. Lambeth (2010). Nox4 B-loop creates an interface between the transmembrane and dehydrogenase domains. *J Biol Chem* **285**(14): 10281-10290.

Janiszewski, M., L. R. Lopes, A. O. Carmo, M. A. Pedro, R. P. Brandes, C. X. Santos and F. R. Laurindo (2005). Regulation of NAD(P)H oxidase by associated protein disulfide isomerase in vascular smooth muscle cells. *J Biol Chem* **280**(49): 40813-40819.

Jaulmes, A., P. Sansilvestri-Morel, G. Rolland-Valognes, F. Bernhardt, R. Gaertner, B. P. Lockhart, A. Cordi, M. Wierzbicki, A. Rupin and T. J. Verbeuren (2009). Nox4 mediates the expression of plasminogen activator inhibitor-1 via p38 MAPK pathway in cultured human endothelial cells. *Thromb Res* **124**(4): 439-446.

Jezek, P. and L. Hlavata (2005). Mitochondria in homeostasis of reactive oxygen species in cell, tissues, and organism. *Int J Biochem Cell Biol* **37**(12): 2478-2503.

Kanofsky, J. R. (1989). Singlet oxygen production by biological systems. *Chem Biol Interact* **70**(1-2): 1-28.

Katsuyama, M., H. Hirai, K. Iwata, M. Ibi, K. Matsuno, M. Matsumoto and C. Yabe-Nishimura (2011). Sp3 transcription factor is crucial for transcriptional activation of the human NOX4 gene. *FEBS J* **278**(6): 964-972.

Kawahara, T., Y. Kuwano, S. Teshima-Kondo, R. Takeya, H. Sumimoto, K. Kishi, S. Tsunawaki, T. Hirayama and K. Rokutan (2004). Role of nicotinamide adenine dinucleotide phosphate oxidase 1 in oxidative burst response to Toll-like receptor 5 signaling in large intestinal epithelial cells. *J Immunol* **172**(5): 3051-3058.

Kawahara, T., D. Ritsick, G. Cheng and J. D. Lambeth (2005). Point mutations in the proline-rich region of p22phox are dominant inhibitors of Nox1- and Nox2-dependent reactive oxygen generation. *J Biol Chem* **280**(36): 31859-31869.

Kawahara, T., S. Teshima, A. Oka, T. Sugiyama, K. Kishi and K. Rokutan (2001). Type I Helicobacter pylori lipopolysaccharide stimulates toll-like receptor 4 and activates mitogen oxidase 1 in gastric pit cells. *Infect Immun* **69**(7): 4382-4389.

Kiefer, H. (2003). In vitro folding of alpha-helical membrane proteins. *Biochim Biophys Acta* **1610**(1): 57-62.

Kikuchi, H., M. Hikage, H. Miyashita and M. Fukumoto (2000). NADPH oxidase subunit, gp91(phox) homologue, preferentially expressed in human colon epithelial cells. *Gene* **254**(1-2): 237-243.

Klabunde, T. and G. Hessler (2002). Drug design strategies for targeting G-protein-coupled receptors. *Chembiochem* **3**(10): 928-944.

Klebanoff, S. J. (1970). Myeloperoxidase: contribution to the microbicidal activity of intact leukocytes. *Science* **169**(950): 1095-1097.

Knaus, U. G., P. G. Heyworth, T. Evans, J. T. Curnutte and G. M. Bokoch (1991). Regulation of phagocyte oxygen radical production by the GTP-binding protein Rac 2. *Science* **254**(5037): 1512-1515.

Koga, H., H. Terasawa, H. Nunoi, K. Takeshige, F. Inagaki and H. Sumimoto (1999). Tetratricopeptide repeat (TPR) motifs of p67(phox) participate in interaction with the small GTPase Rac and activation of the phagocyte NADPH oxidase. *J Biol Chem* **274**(35): 25051-25060.

Krause, K. H. (2004). Tissue distribution and putative physiological function of NOX family NADPH oxidases. *Jpn J Infect Dis* **57**(5): S28-29.

Kreck, M. L., J. L. Freeman, A. Abo and J. D. Lambeth (1996). Membrane association of Rac is required for high activity of the respiratory burst oxidase. *Biochemistry* **35**(49): 15683-15692.

Kuribayashi, F., H. Nunoi, K. Wakamatsu, S. Tsunawaki, K. Sato, T. Ito and H. Sumimoto (2002). The adaptor protein p40(phox) as a positive regulator of the superoxide-producing phagocyte oxidase. *EMBO J* **21**(23): 6312-6320.

Kuroda, J., T. Ago, S. Matsushima, P. Zhai, M. D. Schneider and J. Sadoshima (2010). NADPH oxidase 4 (Nox4) is a major source of oxidative stress in the failing heart. *Proc Natl Acad Sci U S A* **107**(35): 15565-15570.

Kuroda, J., K. Nakagawa, T. Yamasaki, K. Nakamura, R. Takeya, F. Kuribayashi, S. Imajoh-Ohmi, K. Igarashi, Y. Shibata, K. Sueishi and H. Sumimoto (2005). The superoxide-producing NAD(P)H oxidase Nox4 in the nucleus of human vascular endothelial cells. *Genes Cells* **10**(12): 1139-1151.

Lambeth, J. D. (2000). Regulation of the phagocyte respiratory burst oxidase by protein interactions. *J. Biochem. Mol. Biol*. **33**: 427–439.

Lambeth, J. D. (2004). NOX enzymes and the biology of reactive oxygen. *Nat Rev Immunol* **4**(3): 181-189.

Lambeth, J. D. (2007). Nox enzymes, ROS, and chronic disease: An example of antagonistic pleiotropy. *Free Radical Biology and Medicine* **43**(3): 332-347.

Lametsch, R., J. T. Rasmussen, L. B. Johnsen, S. Purup, K. Sejrsen, T. E. Petersen and C. W. Heegaard (2000). Structural characterization of the fibroblast growth factor-binding protein purified from bovine prepartum mammary gland secretion. *J Biol Chem* **275**(26): 19469-19474.

Lapouge, K., S. J. Smith, Y. Groemping and K. Rittinger (2002). Architecture of the p40-p47-p67phox complex in the resting state of the NADPH oxidase. A central role for p67phox. *J Biol Chem* **277**(12): 10121-10128.

Lapouge, K., S. J. Smith, P. A. Walker, S. J. Gamblin, S. J. Smerdon and K. Rittinger (2000). Structure of the TPR domain of p67phox in complex with Rac.GTP. *Mol Cell* **6**(4): 899-907.

Lardy, B., M. Bof, L. Aubry, M. H. Paclet, F. Morel, M. Satre and G. Klein (2005). NADPH oxidase homologs are required for normal cell differentiation and morphogenesis in Dictyostelium discoideum. *Biochim Biophys Acta* **1744**(2): 199-212.

Larsen, C. N., B. A. Krantz and K. D. Wilkinson (1998). Substrate specificity of deubiquitinating enzymes: ubiquitin C-terminal hydrolases. *Biochemistry* **37**(10): 3358-3368.

Lassegue, B. and K. K. Griendling (2010). NADPH oxidases: functions and pathologies in the vasculature. *Arterioscler Thromb Vasc Biol* **30**(4): 653-661.

Lee, H. S., S. J. Millward-Sadler, M. O. Wright, G. Nuki and D. M. Salter (2000). Integrin and mechanosensitive ion channel-dependent tyrosine phosphorylation of focal adhesion proteins and beta-catenin in human articular chondrocytes after mechanical stimulation. *J Bone Miner Res* **15**(8): 1501-1509.

Lee, N. K., Y. G. Choi, J. Y. Baik, S. Y. Han, D. W. Jeong, Y. S. Bae, N. Kim and S. Y. Lee (2005). A crucial role for reactive oxygen species in RANKL-induced osteoclast differentiation. *Blood* **106**(3): 852-859.

Lee, Y. M., B. J. Kim, Y. S. Chun, I. So, H. Choi, M. S. Kim and J. W. Park (2006). NOX4 as an oxygen sensor to regulate TASK-1 activity. *Cell Signal* **18**(4): 499-507.

Leto, T. L., A. G. Adams and I. de Mendez (1994). Assembly of the phagocyte NADPH oxidase: binding of Src homology 3 domains to proline-rich targets. *Proc Natl Acad Sci U S A* **91**(22): 10650-10654.

Leusen, J. H., B. G. Bolscher, P. M. Hilarius, R. S. Weening, W. Kaulfersch, R. A. Seger, D. Roos and A. J. Verhoeven (1994). 156Pro-->Gln substitution in the light chain of cytochrome b558 of the human NADPH oxidase (p22-phox) leads to defective translocation of the cytosolic proteins p47-phox and p67-phox. *J Exp Med* **180**(6): 2329-2334.

Leusen, J. H., K. Fluiter, P. M. Hilarius, D. Roos, A. J. Verhoeven and B. G. Bolscher (1995). Interactions between the cytosolic components p47phox and p67phox of the human neutrophil NADPH oxidase that are not required for activation in the cell-free system. *J Biol Chem* **270**(19): 11216-11221.

Li, J. M. and A. M. Shah (2002). Intracellular localization and preassembly of the NADPH oxidase complex in cultured endothelial cells. *J Biol Chem* **277**(22): 19952-19960.

Liu, L., E. M. Rodriguez-Belmonte, N. Mazloum, B. Xie and M. Y. Lee (2003). Identification of a novel protein, PDIP38, that interacts with the p50 subunit of DNA polymerase delta and proliferating cell nuclear antigen. *J Biol Chem* **278**(12): 10041-10047.

Liu, R. M., J. Choi, J. H. Wu, K. A. Gaston Pravia, K. M. Lewis, J. D. Brand, N. S. Mochel, D. M. Krzywanski, J. D. Lambeth, J. S. Hagood, H. J. Forman, V. J. Thannickal and E. M. Postlethwait (2010). Oxidative modification of nuclear mitogen-activated protein kinase phosphatase 1 is involved in transforming growth factor beta1-induced expression of plasminogen activator inhibitor 1 in fibroblasts. *J Biol Chem* **285**(21): 16239-16247.

Lyle, A. N., N. N. Deshpande, Y. Taniyama, B. Seidel-Rogol, L. Pounkova, P. Du, C. Papaharalambus, B. Lassegue and K. K. Griendling (2009). Poldip2, a novel regulator of Nox4 and cytoskeletal integrity in vascular smooth muscle cells. *Circ Res* **105**(3): 249-259.

Mahadev, K., H. Motoshima, X. Wu, J. M. Ruddy, R. S. Arnold, G. Cheng, J. D. Lambeth and B. J. Goldstein (2004). The NAD(P)H oxidase homolog Nox4 modulates insulin-stimulated generation of H2O2 and plays an integral role in insulin signal transduction. *Mol Cell Biol* **24**(5): 1844-1854.

Maranchie, J. K. and Y. Zhan (2005). Nox4 is critical for hypoxia-inducible factor 2-alpha transcriptional activity in von Hippel-Lindau-deficient renal cell carcinoma. *Cancer Res* **65**(20): 9190-9193.

Marklund, S. (1976). Spectrophotometric study of spontaneous disproportionation of superoxide anion radical and sensitive direct assay for superoxide dismutase. *J Biol Chem* **251**(23): 7504-7507.

Marques, B., L. Liguori, M. H. Paclet, A. Villegas-Mendez, R. Rothe, F. Morel and J. L. Lenormand (2007). Liposome-mediated cellular delivery of active gp91(phox). *PLoS One* **2**(9): e856.

Martyn, K. D., L. M. Frederick, K. von Loehneysen, M. C. Dinauer and U. G. Knaus (2006). Functional analysis of Nox4 reveals unique characteristics compared to other NADPH oxidases. *Cell Signal* **18**(1): 69-82.

Maturana, A., S. Arnaudeau, S. Ryser, B. Banfi, J. P. Hossle, W. Schlegel, K. H. Krause and N. Demaurex (2001). Heme histidine ligands within gp91(phox) modulate proton conduction by the phagocyte NADPH oxidase. *J Biol Chem* **276**(32): 30277-30284.

Meier, B., A. R. Cross, J. T. Hancock, F. J. Kaup and O. T. Jones (1991). Identification of a superoxide-generating NADPH oxidase system in human fibroblasts. *Biochem J* **275 (Pt 1)**: 241-245.

Miller, F. J., Jr. (2009). NADPH oxidase 4: walking the walk with Poldip2. *Circ Res* **105**(3): 209-210.

Miroux, B. and J. E. Walker (1996). Over-production of proteins in Escherichia coli: mutant hosts that allow synthesis of some membrane proteins and globular proteins at high levels. *J Mol Biol* **260**(3): 289-298.

Miyano, K., N. Ueno, R. Takeya and H. Sumimoto (2006). Direct involvement of the small GTPase Rac in activation of the superoxide-producing NADPH oxidase Nox1. *J Biol Chem* **281**(31): 21857-21868.

Mizuki, K., K. Kadomatsu, K. Hata, T. Ito, Q. W. Fan, Y. Kage, Y. Fukumaki, Y. Sakaki, K. Takeshige and H. Sumimoto (1998). Functional modules and expression of mouse p40(phox) and p67(phox), SH3-domain-containing proteins involved in the phagocyte NADPH oxidase complex. *Eur J Biochem* **251**(3): 573-582.

Mizuno, T., K. Kaibuchi, S. Ando, T. Musha, K. Hiraoka, K. Takaishi, M. Asada, H. Nunoi, I. Matsuda and Y. Takai (1992). Regulation of the superoxide-generating NADPH oxidase by a small GTP-binding protein and its stimulatory and inhibitory GDP/GTP exchange proteins. *J Biol Chem* **267**(15): 10215-10218.

Mochizuki, T., S. Furuta, J. Mitsushita, W. H. Shang, M. Ito, Y. Yokoo, M. Yamaura, S. Ishizone, J. Nakayama, A. Konagai, K. Hirose, K. Kiyosawa and T. Kamata (2006). Inhibition of NADPH oxidase 4 activates apoptosis via the AKT/apoptosis signal-regulating kinase 1 pathway in pancreatic cancer PANC-1 cells. *Oncogene* **25**(26): 3699-3707.

Morand, S., T. Ueyama, S. Tsujibe, N. Saito, A. Korzeniowska and T. L. Leto (2009). Duox maturation factors form cell surface complexes with Duox affecting the specificity of reactive oxygen species generation. *FASEB J* **23**(4): 1205-1218.

Morel, F. (2007). [Molecular aspects of chronic granulomatous disease. "the NADPH oxidase complex"]. *Bull Acad Natl Med* **191**(2): 377-390; discussion 390-372.

Morel, F., J. Doussiere and P. V. Vignais (1991). The superoxide-generating oxidase of phagocytic cells. Physiological, molecular and pathological aspects. *Eur J Biochem* **201**(3): 523-546.

Moreno, J. C., H. Bikker, M. J. Kempers, A. S. van Trotsenburg, F. Baas, J. J. de Vijlder, T. Vulsma and C. Ris-Stalpers (2002). Inactivating mutations in the gene for thyroid oxidase 2 (THOX2) and congenital hypothyroidism. *N Engl J Med* **347**(2): 95-102.

Mouche, S., S. B. Mkaddem, W. Wang, M. Katic, Y.-H. Tseng, S. Carnesecchi, K. Steger, M. Foti, C. A. Meier, P.

Muzzin, C. R. Kahn, E. Ogier-Denis and I. Szanto (2007). Reduced expression of the NADPH oxidase NOX4 is a hallmark of adipocyte differentiation. *Biochimica et Biophysica Acta (BBA) - Molecular Cell Research* **1773**(7): 1015-1027.

Mouche, S., S. B. Mkaddem, W. Wang, M. Katic, Y. H. Tseng, S. Carnesecchi, K. Steger, M. Foti, C. A. Meier, P. Muzzin, C. R. Kahn, E. Ogier-Denis and I. Szanto (2007). Reduced expression of the NADPH oxidase NOX4 is a hallmark of adipocyte differentiation. *Biochim Biophys Acta* **1773**(7): 1015-1027.

Moulton, P. J., M. B. Goldring and J. T. Hancock (1998). NADPH oxidase of chondrocytes contains an isoform of the gp91phox subunit. *Biochem J* **329 (Pt 3)**: 449-451.

Nakamura, M., M. Murakami, T. Koga, Y. Tanaka and S. Minakami (1987). Monoclonal antibody 7D5 raised to cytochrome b558 of human neutrophils: immunocytochemical detection of the antigen in peripheral phagocytes of normal subjects, patients with chronic granulomatous disease, and their carrier mothers. *Blood* **69**(5): 1404-1408.

Nakamura, R., H. Sumimoto, K. Mizuki, K. Hata, T. Ago, S. Kitajima, K. Takeshige, Y. Sakaki and T. Ito (1998). The PC motif: a novel and evolutionarily conserved sequence involved in interaction between p40phox and p67phox, SH3 domain-containing cytosolic factors of the phagocyte NADPH oxidase. *Eur J Biochem* **251**(3): 583-589.

Nakano, Y., B. Banfi, A. J. Jesaitis, M. C. Dinauer, L. A. Allen and W. M. Nauseef (2007). Critical roles for p22phox in the structural maturation and subcellular targeting of Nox3. *Biochem J* **403**(1): 97-108.

Nathan, C. (2002). Immunology. Catalytic antibody bridges innate and adaptive immunity. *Science* **298**(5601): 2143-2144.

Nauseef, W. M. (2004). Assembly of the phagocyte NADPH oxidase. *Histochem Cell Biol* **122**(4): 277-291.

Nauseef, W. M. (2008). Biological roles for the NOX family NADPH oxidases. *J Biol Chem* **283**(25): 16961-16965.

Nauseef, W. M. (2008). Nox enzymes in immune cells. *Semin Immunopathol* **30**(3): 195-208.

Nishino, T., K. Okamoto, B. T. Eger and E. F. Pai (2008). Mammalian xanthine oxidoreductase - mechanism of transition from xanthine dehydrogenase to xanthine oxidase. *FEBS J* **275**(13): 3278-3289.

Nisimoto, Y., H. M. Jackson, H. Ogawa, T. Kawahara and J. D. Lambeth (2010). Constitutive NADPH-dependent electron transferase activity of the Nox4 dehydrogenase domain. *Biochemistry* **49**(11): 2433-2442.

Nisimoto, Y., S. Motalebi, C. H. Han and J. D. Lambeth (1999). The p67(phox) activation domain regulates electron flow from NADPH to flavin in flavocytochrome b(558). *J Biol Chem* **274**(33): 22999-23005.

Nisimoto, Y., H. Ogawa, K. Miyano and M. Tamura (2004). Activation of the flavoprotein domain of gp91phox upon interaction with N-terminal p67phox (1-210) and the Rac complex. *Biochemistry* **43**(29): 9567-9575.

Nisimoto, Y., H. Ogawa, K. Miyano and M. Tamura (2004). Activation of the Flavoprotein Domain of gp91phox upon Interaction with N-Terminal p67phox (1−210) and the Rac Complex. *Biochemistry* **43**(29): 9567-9575.

Novo, E. and M. Parola (2008). Redox mechanisms in hepatic chronic wound healing and fibrogenesis. *Fibrogenesis & Tissue Repair* **1**(1): 5.

Nunoi, H., D. Rotrosen, J. I. Gallin and H. L. Malech (1988). Two forms of autosomal chronic granulomatous disease lack distinct neutrophil cytosol factors. *Science* **242**(4883): 1298-1301.

Nuttall, M. E., D. P. Nadeau, P. W. Fisher, F. Wang, P. M. Keller, W. E. DeWolf, Jr., M. B. Goldring, A. M. Badger, D. Lee, M. A. Levy, M. Gowen and M. W. Lark (2000). Inhibition of caspase-3-like activity prevents apoptosis while retaining functionality of human chondrocytes in vitro. *J Orthop Res* **18**(3): 356-363.

Ohno, Y., E. S. Buescher, R. Roberts, J. A. Metcalf and J. I. Gallin (1986). Reevaluation of cytochrome b and flavin adenine dinucleotide in neutrophils from patients with chronic granulomatous disease and description of a family with probable autosomal recessive inheritance of cytochrome b deficiency. *Blood* **67**(4): 1132-1138.

Otsuka-Murakami, H. and Y. Nisimoto (1995). Purification of an NADPH-dependent diaphorase from membrane of DMSO-induced differentiated human promyelocytic leukemia HL-60 cells. *FEBS Lett* **361**(2-3): 206-210.

Ottaviani, A., E. Gilson and F. Magdinier (2008). Telomeric position effect: from the yeast paradigm to human pathologies? *Biochimie* **90**(1): 93-107.

Overmyer, K., M. Brosche and J. Kangasjarvi (2003). Reactive oxygen species and hormonal control of cell death. *Trends Plant Sci* **8**(7): 335-342.

Paclet, M.-H., L. M. Henderson, Y. Campion, F. Morel and M.-C. Dagher (2004). Localization of Nox2 N-terminus using polyclonal antipeptide antibodies. *Biochemical Journal* **382**(3): 981-986.

Paclet, M. H., S. Berthier, L. Kuhn, J. Garin and F. Morel (2007). Regulation of phagocyte NADPH oxidase activity: identification of two cytochrome b558 activation states. *FASEB J* **21**(4): 1244-1255.

Paclet, M. H., A. W. Coleman, S. Vergnaud and F. Morel (2000). P67-phox-mediated NADPH oxidase assembly: imaging of cytochrome b558 liposomes by atomic force microscopy. *Biochemistry* **39**(31): 9302-9310.

Paffenholz, R., R. A. Bergstrom, F. Pasutto, P. Wabnitz, R. J. Munroe, W. Jagla, U. Heinzmann, A. Marquardt, A. Bareiss, J. Laufs, A. Russ, G. Stumm, J. C. Schimenti and D. E. Bergstrom (2004). Vestibular defects in head-tilt mice result from mutations in Nox3, encoding an NADPH oxidase. *Genes Dev* **18**(5): 486-491.

Park, H. S., D. K. Jin, S. M. Shin, M. K. Jang, N. Longo, J. W. Park, D. S. Bae and Y. S. Bae (2005). Impaired generation of reactive oxygen species in leprechaunism through downregulation of Nox4. *Diabetes* **54**(11): 3175-3181.

Park, M. Y., S. Imajoh-Ohmi, H. Nunoi and S. Kanegasaki (1997). Synthetic peptides corresponding to various hydrophilic regions of the large subunit of cytochrome b558 inhibit superoxide generation in a cell-free system from neutrophils. *Biochem Biophys Res Commun* **234**(2): 531-536.

Parkos, C. A., R. A. Allen, C. G. Cochrane and A. J. Jesaitis (1987). Purified cytochrome b from human granulocyte plasma membrane is comprised of two polypeptides with relative molecular weights of 91,000 and 22,000. *J Clin Invest* **80**(3): 732-742.

Parkos, C. A., M. C. Dinauer, A. J. Jesaitis, S. H. Orkin and J. T. Curnutte (1989). Absence of both the 91kD and 22kD subunits of human neutrophil cytochrome b in two genetic forms of chronic granulomatous disease. *Blood* **73**(6): 1416-1420.

Parkos, C. A., M. C. Dinauer, L. E. Walker, R. A. Allen, A. J. Jesaitis and S. H. Orkin (1988). Primary structure and unique expression of the 22-kilodalton light chain of human neutrophil cytochrome b. *Proc Natl Acad Sci U S A* **85**(10): 3319-3323.

Pedruzzi, E., C. Guichard, V. Ollivier, F. Driss, M. Fay, C. Prunet, J. C. Marie, C. Pouzet, M. Samadi, C. Elbim, Y. O'Dowd, M. Bens, A. Vandewalle, M. A. Gougerot-Pocidalo, G. Lizard and E. Ogier-Denis (2004). NAD(P)H oxidase Nox-4 mediates 7-ketocholesterol-induced endoplasmic reticulum stress and apoptosis in human aortic smooth muscle cells. *Mol Cell Biol* **24**(24): 10703-10717.

Pessach, I., T. L. Leto, H. L. Malech and R. Levy (2001). Essential requirement of cytosolic phospholipase A(2) for stimulation of NADPH oxidase-associated diaphorase activity in granulocyte-like cells. *J Biol Chem* **276**(36): 33495-33503.

Pessach, I., Z. Shmelzer, T. L. Leto, M. C. Dinauer and R. Levy (2006). The C-terminal flavin domain of gp91phox bound to plasma membranes of granulocyte-like X-CGD PLB-985 cells is sufficient to anchor cytosolic oxidase components and support NADPH oxidase-associated diaphorase activity independent of cytosolic phospholipase A2 regulation. *J Leukoc Biol* **80**(3): 630-639.

Piccoli, C., R. Ria, R. Scrima, O. Cela, A. D'Aprile, D. Boffoli, F. Falzetti, A. Tabilio and N. Capitanio (2005). Characterization of mitochondrial and extra-mitochondrial oxygen consuming reactions in human hematopoietic stem cells. Novel evidence of the occurrence of NAD(P)H oxidase activity. *J Biol Chem* **280**(28): 26467-26476.

Pick, E., Y. Gorzalczany and S. Engel (1993). Role of the rac1 p21-GDP-dissociation inhibitor for rho heterodimer in the activation of the superoxide-forming NADPH oxidase of macrophages. *Eur J Biochem* **217**(1): 441-455.

Poinas, A., J. Gaillard, P. Vignais and J. Doussiere (2002). Exploration of the diaphorase activity of neutrophil NADPH oxidase. *Eur J Biochem* **269**(4): 1243-1252.

Pufe, T., V. Harde, W. Petersen, M. B. Goldring, B. Tillmann and R. Mentlein (2004). Vascular endothelial growth factor (VEGF) induces matrix metalloproteinase expression in immortalized chondrocytes. *J Pathol* **202**(3): 367-374.

Quie, P. G., J. G. White, B. Holmes and R. A. Good (1967). In vitro bactericidal capacity of human polymorphonuclear leukocytes: diminished activity in chronic granulomatous disease of childhood. *J Clin Invest* **46**(4): 668-679.

Quinn, M. T. and K. A. Gauss (2004). Structure and regulation of the neutrophil respiratory burst oxidase: comparison with nonphagocyte oxidases. *J Leukoc Biol* **76**(4): 760-781.

Raha, S. and B. H. Robinson (2000). Mitochondria, oxygen free radicals, disease and ageing. *Trends Biochem Sci* **25**(10): 502-508.

Rhee, S. G., T. S. Chang, Y. S. Bae, S. R. Lee and S. W. Kang (2003). Cellular regulation by hydrogen peroxide. *J Am Soc Nephrol* **14**(8 Suppl 3): S211-215.

Richardson, S., G. Neama, T. Phillips, S. Bell, S. D. Carter, K. H. Moley, J. F. Moley, S. J. Vannucci and A. Mobasheri (2003). Molecular characterization and partial cDNA cloning of facilitative glucose transporters expressed in human articular chondrocytes; stimulation of 2-deoxyglucose uptake by IGF-I and elevated MMP-2 secretion by glucose deprivation. *Osteoarthritis Cartilage* **11**(2): 92-101.

Rossary, A., K. Arab and J. P. Steghens (2007). Polyunsaturated fatty acids modulate NOX 4 anion superoxide production in human fibroblasts. *Biochem J* **406**(1): 77-83.

Rossi, F. and M. Zatti (1964). Biochemical aspects of phagocytosis in polymorphonuclear leucocytes. NADH and NADPH oxidation by the granules of resting and phagocytizing cells. *Experientia* **20**(1): 21-23.

Rotrosen, D., M. E. Kleinberg, H. Nunoi, T. Leto, J. I. Gallin and H. L. Malech (1990). Evidence for a functional cytoplasmic domain of phagocyte oxidase cytochrome b558. *J Biol Chem* **265**(15): 8745-8750.

Rotrosen, D., C. L. Yeung, T. L. Leto, H. L. Malech and C. H. Kwong (1992). Cytochrome b558: the flavin-binding component of the phagocyte NADPH oxidase. *Science* **256**(5062): 1459-1462.

Royer-Pokora, B., L. M. Kunkel, A. P. Monaco, S. C. Goff, P. E. Newburger, R. L. Baehner, F. S. Cole, J. T. Curnutte and S. H. Orkin (1986). Cloning the gene for an inherited human disorder--chronic granulomatous disease--on the basis of its chromosomal location. *Nature* **322**(6074): 32-38.

Rytkönen, A. and D. W. Holden (2007). Bacterial Interference of Ubiquitination and Deubiquitination. *Cell Host & Microbe* **1**(1): 13-22.

Sagi, M. and R. Fluhr (2006). Production of reactive oxygen species by plant NADPH oxidases. *Plant Physiol* **141**(2): 336-340.

Sampson, N., R. Koziel, C. Zenzmaier, L. Bubendorf, E. Plas, P. Jansen-Durr and P. Berger (2011). ROS Signaling by NOX4 Drives Fibroblast-to-Myofibroblast Differentiation in the Diseased Prostatic Stroma. *Mol Endocrinol* **25**(3): 503-513.

Sbarra, A. J. and M. L. Karnovsky (1959). The biochemical basis of phagocytosis. I. Metabolic changes during the ingestion of particles by polymorphonuclear leukocytes. *J Biol Chem* **234**(6): 1355-1362.

Schrader, M. and H. D. Fahimi (2004). Mammalian peroxisomes and reactive oxygen species. *Histochem Cell Biol* **122**(4): 383-393.

Sedeek, M., R. L. Hebert, C. R. Kennedy, K. D. Burns and R. M. Touyz (2009). Molecular mechanisms of hypertension: role of Nox family NADPH oxidases. *Curr Opin Nephrol Hypertens* **18**(2): 122-127.

Segal, A. W. (1987). Absence of both cytochrome b-245 subunits from neutrophils in X-linked chronic granulomatous disease. *Nature* **326**(6108): 88-91.

Segal, A. W. and O. T. Jones (1978). Novel cytochrome b system in phagocytic vacuoles of human granulocytes. *Nature* **276**(5687): 515-517.

Segal, A. W., O. T. Jones, D. Webster and A. C. Allison (1978). Absence of a newly described cytochrome b from neutrophils of patients with chronic granulomatous disease. *Lancet* **2**(8087): 446-449.

Segal, A. W., I. West, F. Wientjes, J. H. Nugent, A. J. Chavan, B. Haley, R. C. Garcia, H. Rosen and G. Scrace (1992). Cytochrome b-245 is a flavocytochrome containing FAD and the NADPH-binding site of the microbicidal oxidase of phagocytes. *Biochem J* **284 (Pt 3)**: 781-788.

Segal, B. H., T. L. Leto, J. I. Gallin, H. L. Malech and S. M. Holland (2000). Genetic, biochemical, and clinical features of chronic granulomatous disease. *Medicine (Baltimore)* **79**(3): 170-200.

Selvaraj, R. J. and A. J. Sbarra (1967). Role of the phagocyte in host-parasite interactions. 8. Effect of whole-body x-irradiation on nicotinamides, lysosomal enzymes and bactericidal activities of leukocytes during phagocytosis. *J Bacteriol* **94**(1): 149-156.

Serrander, L., L. Cartier, K. Bedard, B. Banfi, B. Lardy, O. Plastre, A. Sienkiewicz, L. Forro, W. Schlegel and K. H. Krause (2007). NOX4 activity is determined by mRNA levels and reveals a unique pattern of ROS generation. *Biochem J* **406**(1): 105-114.

Serrander, L., V. Jaquet, K. Bedard, O. Plastre, O. Hartley, S. Arnaudeau, N. Demaurex, W. Schlegel and K. H. Krause (2007). NOX5 is expressed at the plasma membrane and generates superoxide in response to protein kinase C activation. *Biochimie* **89**(9): 1159-1167.

Shinagawa, Y., C. Tanaka and A. Teraoka (1966). A new cytochrome in neurophilic granules of rabbit leucocyte. *J Biochem* **59**(6): 622-624.

Shiose, A., J. Kuroda, K. Tsuruya, M. Hirai, H. Hirakata, S. Naito, M. Hattori, Y. Sakaki and H. Sumimoto (2001). A novel superoxide-producing NAD(P)H oxidase in kidney. *J Biol Chem* **276**(2): 1417-1423.

Shiose, A. and H. Sumimoto (2000). Arachidonic acid and phosphorylation synergistically induce a conformational change of p47phox to activate the phagocyte NADPH oxidase. *J Biol Chem* **275**(18): 13793-13801.

Soberman, R. J. (2003). Series Introduction: The expanding network of redox signaling: new observations, complexities, and perspectives. *The Journal of Clinical Investigation* **111**(5): 571-574.

Someya, A., I. Nagaoka and T. Yamashita (1993). Purification of the 260 kDa cytosolic complex involved in the superoxide production of guinea pig neutrophils. *FEBS Lett* **330**(2): 215-218.

Sorescu, D., D. Weiss, B. Lassegue, R. E. Clempus, K. Szocs, G. P. Sorescu, L. Valppu, M. T. Quinn, J. D. Lambeth, J. D. Vega, W. R. Taylor and K. K. Griendling (2002). Superoxide production and expression of nox family proteins in human atherosclerosis. *Circulation* **105**(12): 1429-1435.

Spanjaard, R. A. and J. van Duin (1988). Translation of the sequence AGG-AGG yields 50% ribosomal frameshift. *Proc Natl Acad Sci U S A* **85**(21): 7967-7971.

Stasia, M. J., P. Bordigoni, C. Martel and F. Morel (2002). A novel and unusual case of chronic granulomatous disease in a child with a homozygous 36-bp deletion in the CYBA gene (A22(0)) leading to the activation of a cryptic splice site in intron 4. *Hum Genet* **110**(5): 444-450.

Sturrock, A., B. Cahill, K. Norman, T. P. Huecksteadt, K. Hill, K. Sanders, S. V. Karwande, J. C. Stringham, D. A. Bull, M. Gleich, T. P. Kennedy and J. R. Hoidal (2006). Transforming growth factor-beta1 induces Nox4 NAD(P)H oxidase and reactive oxygen species-dependent proliferation in human pulmonary artery smooth muscle cells. *Am J Physiol Lung Cell Mol Physiol* **290**(4): L661-L673.

Suh, Y. A., R. S. Arnold, B. Lassegue, J. Shi, X. Xu, D. Sorescu, A. B. Chung, K. K. Griendling and J. D. Lambeth

(1999). Cell transformation by the superoxide-generating oxidase Mox1. *Nature* **401**(6748): 79-82.

Sumimoto, H., K. Hata, K. Mizuki, T. Ito, Y. Kage, Y. Sakaki, Y. Fukumaki, M. Nakamura and K. Takeshige (1996). Assembly and activation of the phagocyte NADPH oxidase. Specific interaction of the N-terminal Src homology 3 domain of p47phox with p22phox is required for activation of the NADPH oxidase. *J Biol Chem* **271**(36): 22152-22158.

Sumimoto, H., Y. Kage, H. Nunoi, H. Sasaki, T. Nose, Y. Fukumaki, M. Ohno, S. Minakami and K. Takeshige (1994). Role of Src homology 3 domains in assembly and activation of the phagocyte NADPH oxidase. *Proc Natl Acad Sci U S A* **91**(12): 5345-5349.

Sumimoto, H., K. Miyano and R. Takeya (2005). Molecular composition and regulation of the Nox family NAD(P)H oxidases. *Biochem Biophys Res Commun* **338**(1): 677-686.

Sumimoto, H., N. Sakamoto, M. Nozaki, Y. Sakaki, K. Takeshige and S. Minakami (1992). Cytochrome b558, a component of the phagocyte NADPH oxidase, is a flavoprotein. *Biochem Biophys Res Commun* **186**(3): 1368-1375.

Sundaresan, M., Z. X. Yu, V. J. Ferrans, K. Irani and T. Finkel (1995). Requirement for generation of H2O2 for platelet-derived growth factor signal transduction. *Science* **270**(5234): 296-299.

Szanto, I., L. Rubbia-Brandt, P. Kiss, K. Steger, B. Banfi, E. Kovari, F. Herrmann, A. Hadengue and K. H. Krause (2005). Expression of NOX1, a superoxide-generating NADPH oxidase, in colon cancer and inflammatory bowel disease. *J Pathol* **207**(2): 164-176.

Szatrowski, T. P. and C. F. Nathan (1991). Production of large amounts of hydrogen peroxide by human tumor cells. *Cancer Res* **51**(3): 794-798.

Szocs, K., B. Lassegue, D. Sorescu, L. L. Hilenski, L. Valppu, T. L. Couse, J. N. Wilcox, M. T. Quinn, J. D. Lambeth and K. K. Griendling (2002). Upregulation of Nox-based NAD(P)H oxidases in restenosis after carotid injury. *Arterioscler Thromb Vasc Biol* **22**(1): 21-27.

Takac, I., K. Schröder, L. Zhang, B. Lardy, N. Anilkumar, J.D. Lambeth, A.M. Shah, F. Morel, R.P. Brandes (2011). The E-loop is involved in the hydrogen peroxide formation of Nox4. *J Biol Chem* **286**(15):13304-13313.

Takeya, R., N. Ueno, K. Kami, M. Taura, M. Kohjima, T. Izaki, H. Nunoi and H. Sumimoto (2003). Novel human homologues of p47phox and p67phox participate in activation of superoxide-producing NADPH oxidases. *J Biol Chem* **278**(27): 25234-25246.

Taylor, R. M., J. B. Burritt, D. Baniulis, T. R. Foubert, C. I. Lord, M. C. Dinauer, C. A. Parkos and A. J. Jesaitis (2004). Site-specific inhibitors of NADPH oxidase activity and structural probes of flavocytochrome b: characterization of six monoclonal antibodies to the p22phox subunit. *J Immunol* **173**(12): 7349-7357.

Teahan, C., P. Rowe, P. Parker, N. Totty and A. W. Segal (1987). The X-linked chronic granulomatous disease gene codes for the beta-chain of cytochrome b-245. *Nature* **327**(6124): 720-721.

Tejada-Simon, M. V., F. Serrano, L. E. Villasana, B. I. Kanterewicz, G. Y. Wu, M. T. Quinn and E. Klann (2005). Synaptic localization of a functional NADPH oxidase in the mouse hippocampus. *Mol Cell Neurosci* **29**(1): 97-106.

Thannickal, V. J. and B. L. Fanburg (2000). Reactive oxygen species in cell signaling. *AJP - Lung Cellular and Molecular Physiology* **279**(6): L1005-1028.

Thrasher, A. J., N. H. Keep, F. Wientjes and A. W. Segal (1994). Chronic granulomatous disease. *Biochim Biophys Acta* **1227**(1-2): 1-24.

Tirone, F., L. Radu, C. T. Craescu and J. A. Cox (2010). Identification of the binding site for the regulatory calcium-binding domain in the catalytic domain of NOX5. *Biochemistry* **49**(4): 761-771.

Torres, M. A. and J. L. Dangl (2005). Functions of the respiratory burst oxidase in biotic interactions, abiotic stress and development. *Curr Opin Plant Biol* **8**(4): 397-403.

Touyz, R. M., X. Chen, F. Tabet, G. Yao, G. He, M. T. Quinn, P. J. Pagano and E. L. Schiffrin (2002). Expression of a functionally active gp91phox-containing neutrophil-type NAD(P)H oxidase in smooth muscle cells from human resistance arteries: regulation by angiotensin II. *Circ Res* **90**(11): 1205-1213.

Tsunawaki, S., H. Mizunari, M. Nagata, O. Tatsuzawa and T. Kuratsuji (1994). A novel cytosolic component, p40phox, of respiratory burst oxidase associates with p67phox and is absent in patients with chronic granulomatous disease who lack p67phox. *Biochem Biophys Res Commun* **199**(3): 1378-1387.

Ueno, N., R. Takeya, K. Miyano, H. Kikuchi and H. Sumimoto (2005). The NADPH oxidase Nox3 constitutively produces superoxide in a p22phox-dependent manner: its regulation by oxidase organizers and activators. *J Biol Chem* **280**(24): 23328-23339.

Ueyama, T., M. Geiszt and T. L. Leto (2006). Involvement of Rac1 in activation of multicomponent Nox1- and Nox3-based NADPH oxidases. *Mol Cell Biol* **26**(6): 2160-2174.

Vallet, P., Y. Charnay, K. Steger, E. Ogier-Denis, E. Kovari, F. Herrmann, J. P. Michel and I. Szanto (2005). Neuronal expression of the NADPH oxidase NOX4, and its regulation in mouse experimental brain ischemia. *Neuroscience* **132**(2): 233-238.

Van Buul, J. D., M. Fernandez-Borja, E. C. Anthony and P. L. Hordijk (2005). Expression and localization of NOX2 and NOX4 in primary human endothelial cells. *Antioxid Redox Signal* **7**(3-4): 308-317.

Vaquero, E. C., M. Edderkaoui, S. J. Pandol, I. Gukovsky and A. S. Gukovskaya (2004). Reactive oxygen species produced by NAD(P)H oxidase inhibit apoptosis in pancreatic cancer cells. *J Biol Chem* **279**(33): 34643-34654.

Varenne, S. and C. Lazdunski (1986). Effect of distribution of unfavourable codons on the maximum rate of gene expression by an heterologous organism. *J Theor Biol* **120**(1): 99-110.

Vignais, P. V. (2002). The superoxide-generating NADPH oxidase: structural aspects and activation mechanism. *Cell Mol Life Sci* **59**(9): 1428-1459.

Volpp, B. D., W. M. Nauseef and R. A. Clark (1988). Two cytosolic neutrophil oxidase components absent in autosomal chronic granulomatous disease. *Science* **242**(4883): 1295-1297.

von Lohneysen, K., D. Noack, A. J. Jesaitis, M. C. Dinauer and U. G. Knaus (2008). Mutational analysis reveals distinct features of the Nox4-p22 phox complex. *J Biol Chem* **283**(50): 35273-35282.

von Lohneysen, K., D. Noack, M. R. Wood, J. S. Friedman and U. G. Knaus (2010). Structural insights into Nox4 and Nox2: motifs involved in function and cellular localization. *Mol Cell Biol* **30**(4): 961-975.

Wada, K., Y. Wada, F. Ishibashi, T. Gojobori and T. Ikemura (1992). Codon usage tabulated from the GenBank genetic sequence data. *Nucleic Acids Res* **20 Suppl**: 2111-2118.

Wallach, T. M. and A. W. Segal (1997). Analysis of glycosylation sites on gp91phox, the flavocytochrome of the NADPH oxidase, by site-directed mutagenesis and translation in vitro. *Biochem J* **321 (Pt 3)**: 583-585.

Wang, D., X. De Deken, M. Milenkovic, Y. Song, I. Pirson, J. E. Dumont and F. Miot (2005). Identification of a novel partner of duox: EFP1, a thioredoxin-related protein. *J Biol Chem* **280**(4): 3096-3103.

Warburg, O. (1908). Beobachtungen über die Oxydationsprozesse im Seeigelei. *Hoppe-Seyler´s Zeitschrift für physiologische Chemie* **57**(1-2): 1-16.

Wassler, M., I. Jonasson, R. Persson and E. Fries (1987). Differential permeabilization of membranes by saponin treatment of isolated rat hepatocytes. Release of secretory proteins. *Biochem J* **247**(2): 407-415.

Wentworth, P., Jr., J. E. McDunn, A. D. Wentworth, C. Takeuchi, J. Nieva, T. Jones, C. Bautista, J. M. Ruedi, A. Gutierrez, K. D. Janda, B. M. Babior, A. Eschenmoser and R. A. Lerner (2002). Evidence for antibody-catalyzed ozone formation in bacterial killing and inflammation. *Science* **298**(5601): 2195-2199.

Weyemi, U., B. Caillou, M. Talbot, R. Ameziane-El-Hassani, L. Lacroix, O. Lagent-Chevallier, A. Al Ghuzlan, D. Roos, J. M. Bidart, A. Virion, M. Schlumberger and C. Dupuy (2010). Intracellular expression of reactive oxygen species-generating NADPH oxidase NOX4 in normal and cancer thyroid tissues. *Endocr Relat Cancer* **17**(1): 27-37.

Wientjes, F. B., J. J. Hsuan, N. F. Totty and A. W. Segal (1993). p40phox, a third cytosolic component of the activation complex of the NADPH oxidase to contain src homology 3 domains. *Biochem J* **296 (Pt 3)**: 557-561.

Wilkinson, B. M., A. J. Critchley and C. J. Stirling (1996). Determination of the transmembrane topology of yeast Sec61p, an essential component of the endoplasmic reticulum translocation complex. *J Biol Chem* **271**(41): 25590-25597.

Wingler, K., S. Wunsch, R. Kreutz, L. Rothermund, M. Paul and H. H. Schmidt (2001). Upregulation of the vascular NAD(P)H-oxidase isoforms Nox1 and Nox4 by the renin-angiotensin system in vitro and in vivo. *Free Radic Biol Med* **31**(11): 1456-1464.

Xia, C., Q. Meng, L. Z. Liu, Y. Rojanasakul, X. R. Wang and B. H. Jiang (2007). Reactive oxygen species regulate angiogenesis and tumor growth through vascular endothelial growth factor. *Cancer Res* **67**(22): 10823-10830.

Xiao, Q., Z. Luo, A. E. Pepe, A. Margariti, L. Zeng and Q. Xu (2009). Embryonic stem cell differentiation into smooth muscle cells is mediated by Nox4-produced H2O2. *Am J Physiol Cell Physiol* **296**(4): C711-723.

Yamamoto, A., K. Kami, R. Takeya and H. Sumimoto (2007). Interaction between the SH3 domains and C-terminal proline-rich region in NADPH oxidase organizer 1 (Noxo1). *Biochem Biophys Res Commun* **352**(2): 560-565.

Yamauchi, A., L. Yu, A. J. Potgens, F. Kuribayashi, H. Nunoi, S. Kanegasaki, D. Roos, H. L. Malech, M. C. Dinauer and M. Nakamura (2001). Location of the epitope for 7D5, a monoclonal antibody raised against human

flavocytochrome b558, to the extracellular peptide portion of primate gp91phox. *Microbiol Immunol* **45**(3): 249-257.

Yang, S., P. Madyastha, S. Bingel, W. Ries and L. Key (2001). A new superoxide-generating oxidase in murine osteoclasts. *J Biol Chem* **276**(8): 5452-5458.

Yang, S., Y. Zhang, W. Ries and L. Key (2004). Expression of Nox4 in osteoclasts. *J Cell Biochem* **92**(2): 238-248.

Yu, L., F. R. DeLeo, K. J. Biberstine-Kinkade, J. Renee, W. M. Nauseef and M. C. Dinauer (1999). Biosynthesis of flavocytochrome b558 . gp91(phox) is synthesized as a 65-kDa precursor (p65) in the endoplasmic reticulum. *J Biol Chem* **274**(7): 4364-4369.

Yuzawa, S., K. Ogura, M. Horiuchi, N. N. Suzuki, Y. Fujioka, M. Kataoka, H. Sumimoto and F. Inagaki (2004). Solution structure of the tandem Src homology 3 domains of p47phox in an autoinhibited form. *J Biol Chem* **279**(28): 29752-29760.

Yuzawa, S., N. N. Suzuki, Y. Fujioka, K. Ogura, H. Sumimoto and F. Inagaki (2004). A molecular mechanism for autoinhibition of the tandem SH3 domains of p47phox, the regulatory subunit of the phagocyte NADPH oxidase. *Genes Cells* **9**(5): 443-456.

Zhang, L., M. V. Nguyen, B. Lardy, A. J. Jesaitis, A. Grichine, F. Rousset, M. Talbot, M. H. Paclet, G. Qian and F. Morel (2011). New insight into the Nox4 subcellular localization in HEK293 cells: first monoclonal antibodies against Nox4. *Biochimie* **93**(3): 457-468.

Zhang, M., A. C. Brewer, K. Schroder, C. X. Santos, D. J. Grieve, M. Wang, N. Anilkumar, B. Yu, X. Dong, S. J. Walker, R. P. Brandes and A. M. Shah (2010). NADPH oxidase-4 mediates protection against chronic load-induced stress in mouse hearts by enhancing angiogenesis. *Proc Natl Acad Sci U S A* **107**(42): 18121-18126.

Zhu, Y., C. C. Marchal, A. J. Casbon, N. Stull, K. von Lohneysen, U. G. Knaus, A. J. Jesaitis, S. McCormick, W. M. Nauseef and M. C. Dinauer (2006). Deletion mutagenesis of p22phox subunit of flavocytochrome b558: identification of regions critical for gp91phox maturation and NADPH oxidase activity. *J Biol Chem* **281**(41): 30336-30346.

Annex

Publication list

Zhang, L., M. V. Nguyen, B. Lardy, A. J. Jesaitis, A. Grichine, F. Rousset, M. Talbot, M. H. Paclet, G. Qian and F. Morel (2010). New insight into the Nox4 subcellular localization in HEK293 cells: First monoclonal antibodies against Nox4. *Biochimie* **93**(3):457-468.

Takac, I., K. Schröder, L. Zhang, B. Lardy, N. Anilkumar, J.D. Lambeth, A.M. Shah, F. Morel, R.P. Brandes (2011). The E-loop is involved in the hydrogen peroxide formation of Nox4. *J Biol Chem* **286**(15):13304-13313.

Chuong Nguyen, Leilei Zhang, Nicolas Mouz, Jean Luc Lenormand, Bernard Lardy, and Françoise Morel. Nox4 cytosolic domain generates a constitutive diaphorase activity. (submitted to BBRC)

Nguyen, M.V., B. Lardy, L. Zhang, Y. Campion, L. Serrander, K.H. Krause and F. Morel. Quinone compounds regulate Nox4 NADPH oxidase activity. (submission June 2011)

Conferences & presentations

Zhang L, Nguyen MV, Lardy B, Jesaitis AJ, Grichine A, Rousset F, Morel F. New insight into Nox4 subcellular localization in HEK293 cells: First monoclonal antibodies against Nox4. (poster) Gordon Research Conference. Nox Family NADPH Oxidases. Switzerland. 2009-06

Zhang L, Lardy B, Nguyen MV, Rousset F, A. J. Jesaitis, Morel F. Localisation subcellulaire de l'oxydase Nox4 (abstract) Journée De La Recherche Médicale, Grenoble, France

Zhang L, Lardy B, Nguyen MV, Rousset F and Morel F. Validation des premiers anticorps monoclonaux dirigés contre l'oxydase Nox4: outils essentiels d'analyse structurale et immunochimique d'une protéine. (abstract) Journée De La Recherche Médicale, Grenoble, France, 2009-04

Zhang L, Nguyen MV, Lardy B, and Morel F. Subcellular localization of Nox4 in HEK293 TREx^{TM} Nox4 cells: characterization of new monoclonal antibodies. (Oral presentation), NADPH oxidase club, Paris, France, 2009-05

Rousset F, Lardy B, Zhang L, Grange L, Morel F. Effet de la chondroitine sulfate sur les chondrocytes humains stimulés par l'IL1β. (abstract) Journée De La Recherche Médicale, Grenoble, France, 2009-04

Nguyen MV, Lardy B., Zhang L, Grange L, Serrander L, Krause KH, and Morel F. Quinone Compounds Regulate Nox4 NADPH Oxidase Activity in HEK293E. (poster) Gordon Research Conference Nox Family NADPH Oxidases, New London, USA

Résumé en Français

La NADPH oxydase, Nox4, appartient à la famille des Nox qui génèrent les espèces radicalaires de l'oxygène, ROS, en transférant un électron à l'oxygène moléculaire. Malgré sa large distribution dans les tissus, Nox4 est encore mal comprise. Contrairement aux autres Nox, Nox4 est unique par son activité constitutive et sa capacité à former H_2O_2. Les ROS sont des espèces bactéricides dans les phagocytes et des outils de signalisation dans les cellules non phagocytaires en étant associés à de nombreuses pathologies inflammatoires et du vieillissement. Une étude de la structure en lien avec la fonction de Nox4 permettra de mettre l'accent sur un mécanisme de fonctionnement et sur de nouvelles cibles thérapeutiques.

5 nouveaux anticorps monoclonaux ont été générés contre une construction recombinante tronquée (AA: 206-578) de Nox4. La spécificité de 3 anticorps monoclonaux (8E9, 5F9, 6B11) a été confirmée par western blot dans les cellules HEK293 transfectées et le cortex de rein humain. L'anticorps 8E9 est le seul à permettre un marquage des cellules TRex-Nox4 sans perméabilisation par FACS.

La localisation subcellulaire a été étudiée dans les cellules HEK293. L'immunofluorescence confocale a montré que Nox4 est localisée dans la zone périnucléaire et le réticulum endoplasmique. La microscopie TIRF a confirmé sa présence dans la membrane plasmique. Un phénomène intéressant est que 5F9 ne détecte pas Nox4 à la membrane plasmique. L'épitope de 8E9 reconnaît une région sur la dernière boucle E extracellulaire de Nox4 (^{222}H-E^{241}), tandis que les anticorps monoclonaux, 6B11 et 5F9 marquent respectivement les régions 6B11 (^{389}S-P^{416}) et 5F9 (^{392}D-F^{398}). Par ailleurs, seuls 5F9 et 6B11 inhibent l'activité de Nox4, ce qui suggère que les deux régions marquées par ces ACm sont impliquées dans le transfert d'électrons.

Une étude ciblée sur la boucle E de Nox4 a permis de montrer que le changement de 2 cystéines modifie la nature des ROS générés par Nox4 avec la production de O_2^- au lieu de H_2O_2. O_2^- est mis en évidence par la formation de peroxynitrite en présence de NO. Par ailleurs l'ACm 8E9 diminue la production de H_2O_2 dans les cellules COS7 qui expriment Nox4 à la membrane plasmique alors que celle de O_2^- est augmentée. Des constructions recombinantes de Nox4 (native ou tronquée) ont été générées par induction bactérienne, *E.Coli*, et par un système de transcription/traduction (RTS). Les protéines correspondantes, solubles, ont été produites à grande échelle et l'activité diaphorase mesurée; cette activité est constitutive. L'étude de la topologie membranaire de Nox4 et p22phox a été abordée en préparant des protéines de fusion avec l'ubiquitine marquée à la GFP. Cette méthode, TDUFA, particulièrement originale, devrait permettre d'appréhender la topologie de l'hétérodimère Nox4/p22phox, actif.

Mots clés: Nox4, anticorps monoclonaux, la localisation subcellulaire, H_2O_2, l'activité diaphorase, topologie